Lewis M. Fraas

Low-Cost Solar Electric Power

Springer

Low-Cost Solar Electric Power

www.TechnicalBooksPDF.com

Lewis M. Fraas

Low-Cost Solar Electric Power

Springer

www.TechnicalBooksPDF.com

Lewis M. Fraas
JX Crystals Inc.
Bellevue, WA
USA

ISBN 978-3-319-07529-7 ISBN 978-3-319-07530-3 (eBook)
DOI 10.1007/978-3-319-07530-3
Springer Cham Heidelberg New York Dordrecht London

Library of Congress Control Number: 2014940920

© Springer International Publishing Switzerland 2014
This work is subject to copyright. All rights are reserved by the Publisher, whether the whole or part of the material is concerned, specifically the rights of translation, reprinting, reuse of illustrations, recitation, broadcasting, reproduction on microfilms or in any other physical way, and transmission or information storage and retrieval, electronic adaptation, computer software, or by similar or dissimilar methodology now known or hereafter developed. Exempted from this legal reservation are brief excerpts in connection with reviews or scholarly analysis or material supplied specifically for the purpose of being entered and executed on a computer system, for exclusive use by the purchaser of the work. Duplication of this publication or parts thereof is permitted only under the provisions of the Copyright Law of the Publisher's location, in its current version, and permission for use must always be obtained from Springer. Permissions for use may be obtained through RightsLink at the Copyright Clearance Center. Violations are liable to prosecution under the respective Copyright Law.
The use of general descriptive names, registered names, trademarks, service marks, etc. in this publication does not imply, even in the absence of a specific statement, that such names are exempt from the relevant protective laws and regulations and therefore free for general use.
While the advice and information in this book are believed to be true and accurate at the date of publication, neither the authors nor the editors nor the publisher can accept any legal responsibility for any errors or omissions that may be made. The publisher makes no warranty, express or implied, with respect to the material contained herein.

Printed on acid-free paper

Springer is part of Springer Science+Business Media (www.springer.com)

www.TechnicalBooksPDF.com



This photograph shows a 300 kW solar cell field near Shanghai China designed and installed by the authors company in 2008. The largest solar field in operation at the end of 2013 is one thousand times larger at 300 MW. In 2018, there will be multiple GW sized solar fields in operation around the world

www.TechnicalBooksPDF.com

Foreword

This latest solar cell technology book by Lewis Fraas is a rich resource of understanding, explanation, and simplification of developments to date as well as analysis of future opportunities. It is based on a deep history of Dr. Fraas' pioneering contributions to the field, his extensive experience working on and helping resolved key challenges, as well as his visionary projections of where we can go in the future.

Chapter 1 crisply summarizes the over 175 years of history it has taken to go from the first scientific observation of the photovoltaic effect until the modern era of economic conversion of sunlight into electricity on a large scale. He details all the key scientific and engineering developments and struggles over the almost 200 years it has taken to come this far.

Chapter 2 explains the amazing growth in the market for solar cells since the start of the twenty-first century to become a cost-effective way to provide large amounts of electricity at competitive prices to not only help address the energy shortage problem but also the related problems of global warming and air pollution.

Chapter 3 illustrates his unique and crisp skill of surveying the complex field of all solar cell technologies to explain why we are where we are now and what the opportunities are for the future many of which are currently being overlooked. Chapter 4 presents the most eloquent, accurate but non-mathematical description of the quantum mechanics of semiconductors I have ever seen. This makes underlying key scientific concepts more accessible to those without a deep theoretical physics background.

Chapter 5 is one of the most amazing. It makes dramatically clear what China's planned investment commitments have done to Japan's and the US's free-market-based solar cell industries with Germany's just barely hanging on. It is just the Sputnik versus Vanguard space rocket and satellites development process revisited once again. The catch up in space was not the US free market system but the planned and substantial investment by the US military. Eventually, the free market system has won out by 2014 with commercial space rockets just now becoming the most practical solutions soon expected to dominate. However Sputnik 1 was launched in 1957. One can just imagine the military risks—ballistic missiles, etc.—of the intervening 60 or so years had the US waited until the free-market approach eventually won.

www.TechnicalBooksPDF.com

There are present national and international interests in energy strategy, energy security, and energy independence, if not in global warming and pollution, that warrant wisely planned early investments well beyond just what a free market system can initially generate, particularly if the end result can become economically competitive. Many of the US-led pioneering technical innovations have come from the planned, largely military or NASA funded developments like commercial jet airliners, integrated circuits for electronics, the Internet, satellites, or landing men-on-the-moon not to mention infrastructure like the US Interstate Highway system.

Chapter 6 is a very nice, even handed, balanced, and brief treatment of thin films. The CdTe thin film solar cell modules have played a key role in leading the reduction of solar module prices below $2/W but eventually their inherently limited efficiency has proved problematic.

Chapter 7 provides a good introduction to the advantages of concentrated sunlight solar cell systems. Chapter 8 is a totally fascinating, compelling, and very personal description of the development of solar cells with 40 % efficiencies.

Chapter 9 is an excellent description of solar photovoltaics in the larger context of large-scale electric power generation. Particularly striking is the description of the potential of the vehicle-to-grid storage approach that makes the combination of solar and wind a truly reliable displacement for coal, oil, natural gas, and even nuclear utility power generation.

Chapter 10 is a delightfully novel presentation of how concentrated sunlight can provide lighting and some electricity generation whose future development should be interesting to follow. Chapter 11 was very useful for me to begin to understand for the first time some of the important elements and potential advantages of thermophotovoltaics.

Chapter 12 is perhaps the most visionary of all the chapters in its explanation of many of the complex details of how solar mirrors in space could provide one of the future's most promising advances in low-cost solar electric power.

Los Altos, CA Larry Partain

www.TechnicalBooksPDF.com

Preface

The 1973 Arab oil embargo with its associated gas lines was the first energy shock for the US. This led to President Gerald Ford launching a government funded program dedicated to US energy independence. This energy independence program was continued under President Jimmy Carter with an emphasis on renewable nonpolluting energy sources such as solar and wind. In 1975, Solar Technology International was formed in California to bring silicon solar cells down from space for terrestrial applications.

In a solar cell, sunlight is converted directly into electric power, the most valuable form of energy. This is a very elegant option with two outstanding advantages.

- There are no moving parts and semiconductor devices have almost no need for maintenance.
- No fuel is necessary eliminating almost all negative environmental impacts.

By 1980, Solar Technology International was the first to manufacture 1 MW of terrestrial solar modules per year. However, unfortunately, while President Carter had installed solar panels on the White House rooftop, President Ronald Reagan then removed them in 1980 and launched a new unspoken energy policy for the US where the US would defend access to the oil in the Middle East with military action if necessary. The first Middle East oil war eventually followed in 1991 when Iraq invaded Kuwait.

Meanwhile there was a Green Movement in Germany, Japan, and the US with homeowners buying terrestrial solar modules for off grid and grid connected applications. By 1999, terrestrial solar modules generating 1 GW of electricity were in operation around the world.

By the end of 2012, 100 GW of solar electric power had been installed around the world using solar cells including now large utility central power stations. We are now in the middle of a solar revolution. Chapter 1 herein recites the history of this solar cell revolution noting not just the history of the scientific cell and module research innovations but also noting the important roles played in policy and financial investments made by different governments at different times during this revolution up to today.

www.TechnicalBooksPDF.com

The arguments in favor of renewable energy are described in Chap. 2 with a discussion of Peak Oil and even the potential of a natural gas bubble over the next 5–10 years. Climate change is obvious with evidence of the glaciers melting and environment impacts such as Super Storm Sandy and Typhoon Haiyan. For evidence of pollution from coal, one only needs to look at the pictures of haze in Beijing and Shanghai on the TV news.

The technical aspects of solar cells are presented in Chaps. 3 and 4. Chapter 3 discusses the various types of solar cells and modules and systems and their production status today and Chap. 4 describes how solar cells work and emphasizes the importance of single crystal semiconductors for achieving high cell efficiencies.

The dominant solar cell module in the market today is the crystalline silicon (c-Si) solar module. That core technology is described in detail in Chap. 5. Installed system prices for that c-Si technology have now fallen to $2.50 per W and are continuing to fall. There are clear technical paths for continued cost reductions.

A dream for over 30 years now has been the idea that noncrystalline thin film cells will lead to even lower installed solar residential and utility system prices. Unfortunately, for scientific reasons explained in Chap. 4, this dream has not turned into reality because the conversion efficiencies of noncrystalline thin film cells are limited. Nevertheless, there have been outstanding achievements in this field. I have been using an Eco-Drive wristwatch as well as a simple calculator for years now powered by amorphous silicon photovoltaic cells. There has also been another outstanding spinoff application of amorphous silicon semiconductor devices as large area Field Effect Transistor drive circuits for liquid crystal displays. These displays are in our I-Pads, Cell phones, flat screen, TV and computer screens. This technology is described in Chap. 6. This is an example of two interacting revolutions in solar cells and displays.

Chapters 1–6 in this book describe an unstoppable solar cell revolution that is already well underway. The second half of this book describes things that are technically possible but still will require political will and financing to come to full completion.

One path for cost reduction for solar utility systems is by the use of concentrated sunlight systems. The idea is that optical elements like mirrors and plastic or glass lenses are cheaper as large area collectors than single crystal cells and that they can be used to dilute the cost of still higher efficiency solar cells at the focus of these optical elements. This Concentrating PhotoVoltaic (CPV) technology can take one of two forms with either low concentrating systems (LCPV) using 24 % efficient silicon cells or with high concentration systems (HCPV) using 44 % efficient multijunction cells. These concepts are described in Chap. 7. SunPower Corp. is having notable success with the LCPV concept with a recent announcement of an

www.TechnicalBooksPDF.com

order for 70 MW of solar electric power. Chapter 8 tells the story of the development of the 40 % efficient multijunction solar cell from this author's point of view.

As noted in Chap. 1 and 2, there has been a continuing debate between the oil, gas, coal, and nuclear main stream energy groups, the incumbency, and the renewable energy advocates, the insurgency. The incumbency group has been very strong in the US as evidenced by the second Iraq war in 2003 and the unfortunate fact that the US lost its initial leading position in c-Si PV to China in 2005. The criticism by the incumbency has been that renewable energy is too expensive. This argument is now losing ground, as the first eight chapters of this book hopefully illustrate.

The incumbency argument is now shifting to the statement that solar and wind are both too intermittent. Energy storage is a solution to this problem and is already being implemented. However, there is potential help from a second ongoing revolution, the introduction of electric vehicles (EVs) as commute vehicles replacing gasoline powered cars. EVs are driven approximately 2 h to work and back each day. For the remaining 22 h, they are either sitting in a parking lot at work or they are in the home garage. Solar and/or wind can be used to charge their batteries at work and then those batteries can be used to power the home appliances at night. This vehicle to grid idea is described in Chap. 9.

While the US lost its position in PV manufacturing to China, there is still innovation going on in the US and Europe. As described in Chaps. 10 and 11, PV cells can also be used in multiple hybrid applications. For example, infrared sensitive PV cells or Thermo Photo Voltaic (TPV) cells can be used to convert infrared thermal energy from glowing objects into electricity in cogeneration applications. Natural gas heated glowing ceramic elements in home heating furnaces in cold climates can be used in homes to generate heat and electricity with 90 % conversion efficiencies. In addition, these IR cells can capture radiation from glowing steel billets in steel mills to generate electricity reducing the amount of coal burned in China.

A last very imaginative augmentation of solar energy is described in Chap. 12. This application is another example of potential interactions between two ongoing revolutions with surprising potential benefits. One of the challenges that solar energy faces is associated with the fact that solar energy is limited to daytime hours. A Space Power Satellite (SPS) capable of providing solar electric power economically for 24 h per day has been a dream for decades. However, the SPS concept is very complex since it assumes multiple energy conversion steps and includes specially constructed ground microwave receiver stations. In Chap. 12, an alternative is described. A constellation of 10 km diameter mirror arrays in a sun synchronous orbit at an altitude of 1,000 km deflecting sunbeams down to terrestrial solar power fields at dawn and dusk can provide 3 additional hours in the morning and another 3 additional hours in the evening. The key is that larger and larger terrestrial solar fields, photovoltaic or trough concentrated solar power, are

www.TechnicalBooksPDF.com

already being built all around the world. Mirrors deflecting sunbeams down to earth is a much simpler concept. A surprising convergence of two technologies under development is now possible, i.e., lower cost access to space and the ongoing construction of larger and larger solar power fields. If this concept is implemented in the future, the hours of solar electricity production in sunny PV fields around the world can be potentially increased to 14 h per day with an increase in the solar field capacity factor to 58 % and a reduction in the cost of renewable pollution-free solar electricity to below 6 cents per kWh.

The second half of this book describes some exciting possibilities. An outstanding problem has been access to financing for these new ideas. The money in the hands of the financial community has tended to favor the status quo incumbency energy technologies (as most recently, "fracking," for example). Hopefully the young and older educated readers of this book will find the new ideas presented here intriguing enough to work for the political will and financing to make them become a reality. We can all strive for a peaceful bright and sunny energy future.

March 2014 Dr. Lewis M. Fraas

www.TechnicalBooksPDF.com

Contents

1 History of Solar Cell Development 1
The Discovery Years 1
Theoretical Foundation 1
The First Single Crystal Silicon Solar Cell 2
Enthusiastic Support for PV in USA and New PV Devices 2
USA Abandons Renewable Energy and Energy Independence 4
International Support and Volume Production at Low Cost 7
References 11

2 The Solar PV Market Today and the Need for Non-polluting Solar Energy 13
The Age of Hydrocarbon Fuels 13
Peak Oil 15
Global Warming 16
The Arguments for Solar Energy 19
Reason #1: Lower-Cost Solar Electricity 21
Reason #2: Rising Oil and Natural Gas Prices 22
Reason #3: War, Weapons of Mass Destruction, and the Moral Argument for Solar 22
Solar PV Cells and Markets 24
Solar PV Economics 25
Future Opportunities for PV Technology Improvements 28
References 29

3 Types of Photovoltaic Cells 31
Introduction 31
Types of Solar Cells and Modules 34
Cells in High Volume Production Today 35
The Future and High Efficiency Solar Cells 38
Conclusions 41
References 42

www.TechnicalBooksPDF.com

4 Fundamentals of PV and the Importance of Single Crystals 45
Electrons in Atoms as Waves and the Periodic Table of the Elements 45
Semiconductors as Crystals 47
Junctions and Diodes 51
Solar Cell Band Diagrams and Power Curves 52
High Efficiency and Multijunction Solar Cells 53
Types of Solar Cells and Cost Trades 57
The Importance of Single Crystals 59
References 61

5 Terrestrial Silicon Solar Cells Today 63
References 71

6 The Dream of Thin Film PV 73
References 79

7 Introduction to Concentrated Sunlight Solar Cell Systems 81
Introduction 81
Why Track the Sun? 82
Single-Axis Tracking Systems 85
Two-Axis Tracking Systems 87
Revolutionary Space Sun Tracking Concepts 88
Conclusions 93
References 94

8 The Story of the 40 % Efficient Multijunction Solar Cell 97
Introduction 97
A Personal History of Multijunction or Multicolor Solar Cells 98
History Continued: Epitaxy and Monolithic Multijunction Cells 101
History Continued: New Infrared Sensitive GaSb Cell and the 35 % Efficient GaAs/GaSb Stacked Cell 103
Different Designs for Different Applications 107
Recent Developments in Concentrator Modules: Germany and Japan Bring Multicolor Cells Down to Earth 112
Recent Developments in Concentrator Modules: The Cassegrain PV Module 112
Conclusion 114
References 114

9 Solar PV in a Larger Electric Power Context 117
Fuels for Electric Power 117
Solar Electricity is Cost Competitive 117
Intermittency and Energy Storage 119
Vehicle to Grid 121

www.TechnicalBooksPDF.com

The Vehicle to Grid Concept . . . 123
Vehicle to Grid Opportunity in California . . . 124
References . . . 126

10 Infrared Photovoltaics (IR PV) for Combined Solar Lighting and Electricity for Buildings . . . 127
Concept of Concentrated and Piped Sunlight for Indoor Illumination . . . 127
Oak Ridge National Lab Coalition . . . 128
ORNL Concept and Economic Potential . . . 128
ORNL Demonstration Prototype . . . 132
Design, Fabrication, and Performance for the Infrared PV Array . . . 132
References . . . 134

11 Thermophotovoltaics Using Infrared Sensitive Cells . . . 135
The TPV Concept . . . 136
TPV Historical Background . . . 136
TPV Key Components and Requirements . . . 137
TPV Applications . . . 138
The Midnight Sun™ TPV Stove . . . 140
Lightweight TPV Battery Replacement . . . 142
Portable TPV Battery Concept . . . 143
Industrial Applications for TPV . . . 151
Single Cell Demonstration . . . 157
Conclusions . . . 158
References . . . 158

12 Sunbeams from Space Mirrors for Terrestrial PV . . . 159
Introduction . . . 160
Mirror Array Constellation Concept . . . 160
Ground Solar Farms Around the World . . . 164
What About Global Warming? . . . 165
Mirror Satellite Design . . . 167
Economics . . . 170
Mirror Constellation Development Roadmap . . . 170
Conclusions . . . 172
References . . . 173

Appendix: Calculations Related to Table 12.1 and Global Warming . . . 175

Author Biography . . . 177

Index . . . 179

www.TechnicalBooksPDF.com

Chapter 1
History of Solar Cell Development

It has been 175 years since 1839 when Alexandre Edmond Becquerel observed the photovoltaic (PV) effect via an electrode in a conductive solution exposed to light [1]. It is instructive to look at the history of PV cells [2] since that time because there are lessons to be learned that can provide guidance for the future development of PV cells.

The Discovery Years

This 175 year history can be divided into six time periods beginning with the discovery years from 1839 to 1904. Table 1.1 gives the most significant events during this first period. In 1877, Adams and Day observed the PV effect in solidified selenium [3] and in 1904, Hallwachs made a semiconductor-junction solar cell with copper and copper oxide. However, this period was just a discovery period without any real understanding of the science behind the operation of these first PV devices.

Theoretical Foundation

A theoretical foundation for PV device operation and potential improvements was formulated in the second phase of the history of PV in the period from 1905 to 1950 as summarized in Table 1.2. Key events in this period were Einstein's photon theory [4], the adaptation of the Czochralski crystal growth method for single crystal silicon and germanium growth [5] and the development of band theory for high purity single crystal semiconductors [6, 7]. The PV cell theory developed emphasized the importance of high purity single crystal semiconductors for high efficiency solar cells. This theoretical foundation will be reviewed in Chap. 4 in this book. These developments laid the foundations for the third phase of PV device development.

L. M. Fraas, *Low-Cost Solar Electric Power*, DOI: 10.1007/978-3-319-07530-3_1,

© Springer International Publishing Switzerland 2014

www.TechnicalBooksPDF.com

Table 1.1 1800–1904: Discovery years

1839—Alexandre Edmond Becquerel observes the photovoltaic effect via an electrode in a conductive solution exposed to light [1]
1877—W.G. Adams and R.E. Day observed the photovoltaic effect in solidified selenium, and published a paper on the selenium cell [3]. 'The action of light on selenium', in "Proceedings of the Royal Society", A25, 113
1883—Charles Fritts develops a solar cell using selenium on a thin layer of gold to form a device giving less than 1 % efficiency
1904—Wilhelm Hallwachs makes a semiconductor-junction solar cell (copper and copper oxide)

Table 1.2 1905–1950: Scientific foundation

1905—Albert Einstein publishes a paper explaining the photoelectric effect on a quantum basis [4]
1918—Jan Czochralski, a Polish scientist, produces a method to grow single crystals of metal. Decades later, the method is adapted to produce single-crystal silicon
1928—F. Bloch develops band theory based on single crystal periodic lattice [5]
1931—A. H. Wilson develops theory of high purity semiconductor [6]
1948—Gordon Teal and John Little adapt the Czochralski method of crystal growth to produce single-crystalline germanium and, later, silicon [7]

The First Single Crystal Silicon Solar Cell

Table 1.3 summarizes the events between 1950 and 1959 leading to the practical silicon single-crystal PV device. The key events were the Bell Lab's announcement of the Silicon solar cell [8] in 1954 with the Pearson, Chapin, and Fuller patent in 1957 for the 8 % efficient Silicon solar cell [9]. The foundation was now laid for the development of a variety of markets for PV as will be discussed in more detail in Chaps. 2 and 3 herein.

Enthusiastic Support for PV in USA and New PV Devices

The next three phases of PV development can best be divided according to the political climate of the time. The 4th phase of PV history from 1960 to 1980 was defined by enthusiastic support in the US for PV solar cells first for applications on space satellites and then for initial terrestrial applications. Table 1.4 shows the timeline for significant events in this period.

This period began with the success of the first Telstar communication satellite [10] launched in 1962 and powered by silicon solar cells as shown in Fig. 1.1a. Then in the 1970s, silicon cells were evolved for use in terrestrial installations. Figure 1.1b shows a typical terrestrial silicon solar cell today. The present author began working in the solar field in 1973. This was the year of the Arab oil embargo [11] and the first gas lines in the US.

www.TechnicalBooksPDF.com

Table 1.3 1950–1959: First practical device demonstration

1950—Bell labs produce solar cells for space activities
1953—Gerald Pearson begins research into lithium-silicon photovoltaic cells
1954—Bell labs announces the invention of the first modern silicon solar cell [8]. These cells have about 6 % efficiency. The New York Times forecasts that solar cells will eventually lead to a source of "limitless energy of the sun"
1955—Western electric licences commercial solar cell technologies. Hoffman electronics-semiconductor division creates a 2 % efficient commercial solar cell for $25/cell or $1,785/Watt
1957—AT&T assignors (Gerald L. Pearson, Daryl M. Chapin, and Calvin S. Fuller) receive patent US2780765, "*Solar Energy Converting Apparatus*" [9]. They refer to it as the "solar battery". Hoffman electronics creates an 8 % efficient solar cell
1958—T. Mandelkorn, U.S. Signal Corps Laboratories, creates n-on-p silicon solar cells, which are more resistant to radiation damage and are better suited for space. Hoffman Electronics creates 9 % efficient solar cells. Vanguard I, the first solar powered satellite, was launched with a 0.1 W, 100 cm^2 solar panel
1959—Hoffman electronics creates a 10 % efficient commercial solar cell, and introduces the use of a grid contact, reducing the cell's resistance

Table 1.4 1960–1980: US enthusiastic support and new PV devices

1960—Hoffman electronics creates a 14 % efficient solar cell
1961—"Solar Energy in the Developing World" conference is held by the *United Nations*
1962—The *Telstar* communications satellite is powered by solar cells [10]
1967—*Soyuz 1* is the first *manned* spacecraft to be powered by solar cells
1970—First highly effective *GaAs heterostructure* solar cells are created by *Zhores Alferov* and his team in the *USSR* [12]
1971—*Salyut 1* is powered by solar cells
1972—Hovel and Woodall at IBM demonstrate AlGaAs/GaAs solar cell with 18–20 % efficiency [13]
1973—*Skylab* is powered by solar cells
1975—First JPL flat solar array block buy to transition silicon PV from space to terrestrial applications
1976—David Carlson and Christopher Wronski of RCA laboratories create first amorphous silicon PV cells, which have an efficiency of 1.1 % [16]
1977—The *Solar Energy Research Institute* is established at *Golden, Colorado*
1977—President *Jimmy Carter* installs *solar panels* on the *White House* and promotes incentives for solar energy systems
1977—The world production of photovoltaic cells exceeded 500 kW
1978—First amorphous silicon solar-powered calculator [17]
Late 1970—the "*Energy Crisis*" [11]; groundswell of public interest in solar energy use: *photovoltaic* and active and passive solar, including in architecture and off-grid buildings and home sites
1978—L. Fraas and R. Knechtli describe the InGaP/GaInAs/Ge triple junction concentrator cell predicting 40 % efficiency at 300 suns concentration [14]
1978—US public utilities regulation act (PURPA) passed [18]

www.TechnicalBooksPDF.com

Another key event was the beginning of the US government sponsored JPL block buys of silicon PV arrays in 1975 for terrestrial system development and durability testing. This followed the first middle-east oil embargo [11] in 1973. Both Presidents Ford and Carter championed US Energy Independence. President Carter installed solar panels on the White House in 1977.

There were several new technical successes in this period including the demonstration of 20 % efficiency single crystals AlGaAs/GaAs solar cells for space [12, 13]. These cells were shown to be more radiation resistant than silicon cells [14]. Also, Fraas and Knechtli described theoretically the InGaP/GaInAs/Ge triple junction concentrator) cell predicting 40 % efficiency [15]. The idea of very high efficiency solar cells in combination with concentrated sunlight will be the subject of Chaps. 7 and 8 in this book.

Deviating from the single crystal theory foundation for solar cells, Carlson and Wronski fabricated the first amorphous silicon solar cell in 1976 [16]. While the conversion efficiency was low, the ability to add voltages in monolithic structures led to the amorphous silicon powered calculator in 1978 powered by room light [17]. This was the demonstration of a non solar PV device. While solar PV was a motivation for amorphous silicon development, amorphous silicon has found huge markets outside of the solar arena with the biggest being for flat screen LCD televisions. While non crystalline film application are not strictly PV, a lot of effort and money has been committed to non crystalline PV devices and the positive benefits of that effort will be described here in Chap. 6.

This 4th period in the history of PV development ended with the passage of the US Public Utility Regulation Act (PURPA) in 1978 [18]. This was important because it assisted with the development of PV in the next historical period.

USA Abandons Renewable Energy and Energy Independence

The political climate in the 5th period from 1980 to 2000 shifted from enthusiastic support for Energy Independence to a de-emphasis on Energy Independence and a commitment beginning with President Reagan to an emphasis on protecting the oil supply from the middle-east with the US military as necessary. This led to a slowing of solar PV development in the US with no major demonstration projects in the US between 1980 and 2000. President Reagan removed the solar panels from the white hose in 1986. Table 1.5 shows some of the major events during this period.

The DOE Solar Energy Research Institute (SERI) was renamed the National Renewable Energy Lab (NREL)) in 1991. SERI and NREL spent most of their R&D funds on non crystalline thin film solar cells with little tangible results. Most of the US government funded PV cell advances in this period even at NREL related to space cells. The InGaP/GaAs two junction monolithic cell was

www.TechnicalBooksPDF.com

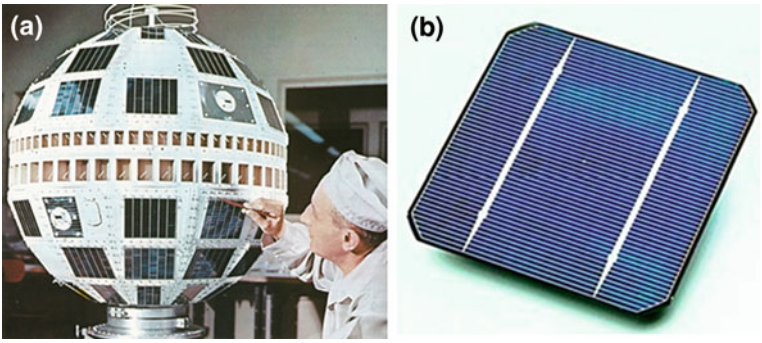


Fig. 1.1 **a** Telstar satellite [10], **b** typical silicon solar cell or photovoltaic (PV) cell [1]

Table 1.5 1980–2000: Slowed development phase

1981—First concentrating PV system using Fresnel lenses goes into operation with 350 kW funded by US and Saudi Arabia SOLERAS project
1983—Worldwide photovoltaic production exceeds 21.3 megawatts, and sales exceed $250 million
1985—20 % efficient silicon cells are created by the *Centre for Photovoltaic Engineering* at the *University of New South Wales*
1986—President *Ronald Reagan* removes solar panels from the White House
1990—L. Fraas, J. Gee, K. Emery, et al. describe the 35 % efficient two-chip stack GaAs/GaSb concentrator solar cell [20]
1991—President *George H. W. Bush* directs the *U.S. Department of Energy* to establish the *National Renewable Energy Laboratory* (transferring the existing solar energy research institute)
1992—Kuryla, Fraas, and Bigger report 25 % efficient CPV module using GaAs/GaSb stacked cell circuit [21]
1993—The *National Renewable Energy Laboratory*'s *Solar Energy Research Facility* is established
1994—NREL develops a GaInP/GaAs two-terminal concentrator cell (180 suns) which becomes the first monolithic two Junction solar cell to exceed 30 % conversion efficiency [19]
1998—Demonstration of first ThermoPhotoVoltaic heat and electricity co-generation MidnightSun™ Stove by JX Crystals Inc [23]

developed for space with the 30 % CPV cell being a spin off for terrestrial applications [19].

Fraas et al. with funding from NASA and the DOD demonstrated the GaAs/GaSb 35 % efficient stacked cell for concentrator) applications in 1990 [20]. Then Kuryla, Fraas, and Bigger with IR&D funding from Boeing reported a 25 % efficient CPV module with a GaAs/GaSb stacked Cell circuit. This 25 % efficiency was measured in outdoor sunlight at the STAR test facility in Arizona [21]. Figure 1.2 shows a photo of a similar CPV module fabricated for a Photovoltaic Advanced Space Power flight. This CPV PASP + module was tested successfully in space in 1994 [22].

www.TechnicalBooksPDF.com

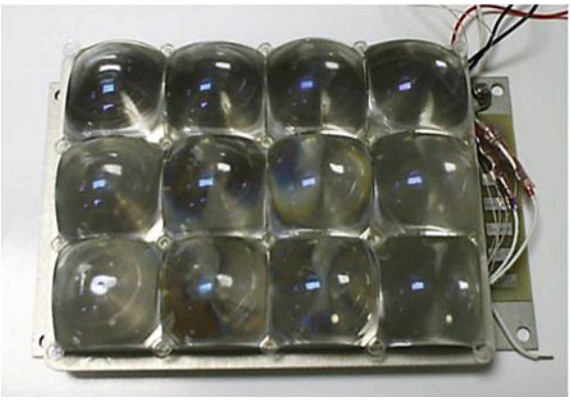


Fig. 1.2 Photograph of PV advanced space power (PASP +) module fabricated at Boeing using GaAs/GaSb stacked two-junction cells and flown in space by NASA in 1994 [22]

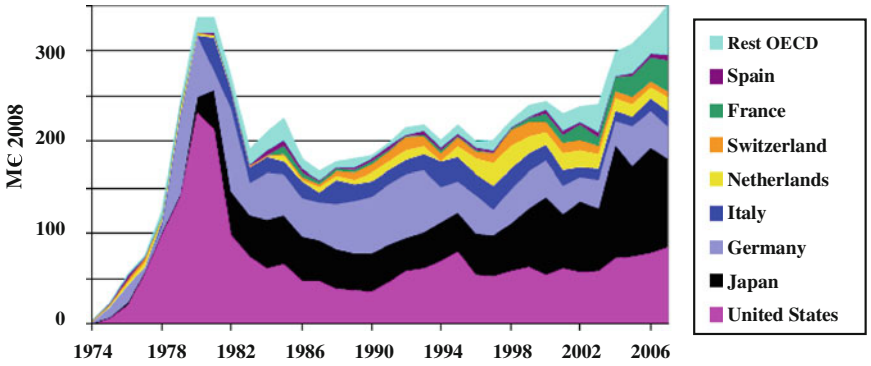


Fig. 1.3 Annual public funding in PV by OECD countries from 1974 to 2008 [24]. US R&D funding fell steeply in 1980 and R&D support for PV passed over to Japan and Germany. Annual funding levels fell from over 300 to 200 million Euros and did not reach 300 million again until 2003

Also in 1998, Fraas et al. at JX Crystals Inc with internal funding developed the first ThermoPhotoVoltaic product, the MidnightSun™ Stove [23]. GaSb infrared cells are used in TPV to generate electricity for combined heat and power applications. Here again, one encounters non-solar IR PV cells in an application that works day and night. TPV will be the subject of Chap. 11 in this book.

During this period, PV development funding passed over to Japan and Germany as shown in Fig. 1.3 [24].

www.TechnicalBooksPDF.com

Table 1.6 2000—Present: International support and new opportunities

2000—Germany's renewable energy sources act creates Feed-In-Tariff (FIT) for solar [25]
2001—Suntech power founded in China [26]
2002—Amonix and Arizona public service install 175 kW high concentration (HCPV) utility system at Prescott AZ (Chap. 7)
2004—K. Araki et al. demonstrate 28 % efficient CPV module [30]
2004—SunPower corp first manufacturing facility (Fab 1) making 20 % A-300 cells comes online in the Philippines and the company's first utility-scale power plant comes online in Bavaria (Chap. 5)
2006—Polysilicon use in photovoltaics exceeds all other polysilicon use for the first time
2006—L. Fraas et al. demonstrate 33 % efficient dual focus HCPV module (Chap. 7)
2006—New world record achieved in solar cell technology—new solar cell breaks the "40 % efficient" sunlight-to-electricity barrier (Chap. 8)
2007—Construction of *Nellis Solar Power Plant*, a 15 MW PPA installation using SunPower corp modules
2010—President *Barack Obama* orders installation of additional solar panels and a solar hot water heater at the *White House* [10]
2011—Fast-growing factories in China push manufacturing costs down to about $1.25 per watt for silicon photovoltaic modules. Installations double worldwide [27]
2011—Solyndra investment fiasco based on CIGS technology severely slows solar in US
2013—Amonix demonstrates a 35.9 % efficient HCPV module (Chap. 7)
2013—Fraas proposes mirrors in space in dawn dusk sun synchronous orbit deflecting sunlight down to terrestrial solar farms in early morning and evening hours (Chap. 12)
2013—Cumulated world wide solar PV installations passes 100 GW [27]

International Support and Volume Production at Low Cost

The 6th and final historical period from 2000 until the present is characterized by a shift to international participation in PV cell deployment with the US playing primarily an R&D role. Table 1.6 presents the key events in this period. Germany, China, and Japan are dominant in this period. This period begins with the German Renewable Energy Sources Act [25] which creates a Solar Feed-In-Tariff or FIT which creates a solar market in Europe. Suntech Power [26] is then formed in China in 2001 and this begins a period of commitment to solar manufacturing with government subsidies and low cost labor in China. Cumulative solar PV installed capacity world wide then grows from 1 GW in 2002 to 134 GW in the beginning of 2014 [27]. The silicon solar PV cell is now established as the dominant cell. This is phenomenal growth which continues today. See Fig. 1.4.

The PURPA in the US [18] and the German FIT [25] created good market conditions and this along with the technical innovations over the years and the Chinese government's investment in solar PV module manufacturing allowed for the solar PV module market expansion shown in Fig. 1.4 along with module and installed system continuous price reductions as shown in Figs. 1.5 and 1.6. Prices for both modules and systems have been consistently dropping year after year in both Germany and the US. However, note that the installed system pries are lower

www.TechnicalBooksPDF.com

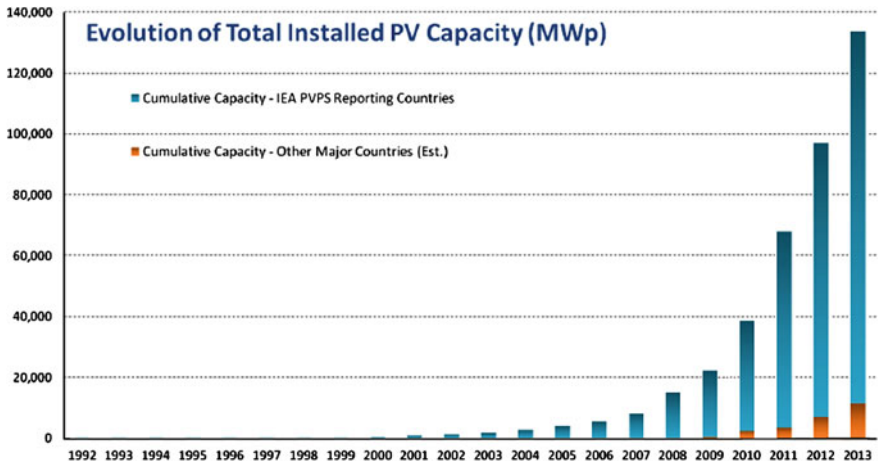


Fig. 1.4 Evolution of total PV installed capacity from 1992 to 2013 [27]—in MW

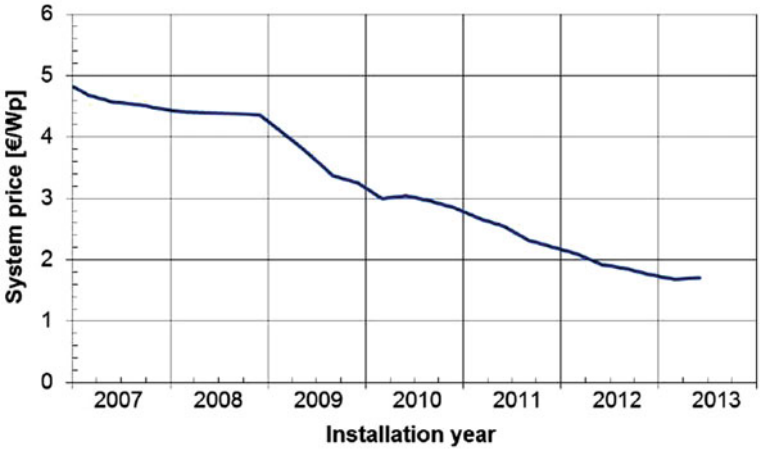


Fig. 1.5 Average end customer price (*net system price*) in Germany [28] for installed rooftop plants with rated power of up to 10 kWp, data from (BSW)

in Germany in 2013 at $2.35 per W (correcting Euro to $) than for similar systems in the US at $4 per W. This difference will be discussed in Chap. 2. In any case, installed system prices are consistently dropping and there are opportunities for continued improvements as will be discussed in subsequent chapters herein. Figure 1.7 shows photographs of large solar PV systems in operation today.

www.TechnicalBooksPDF.com

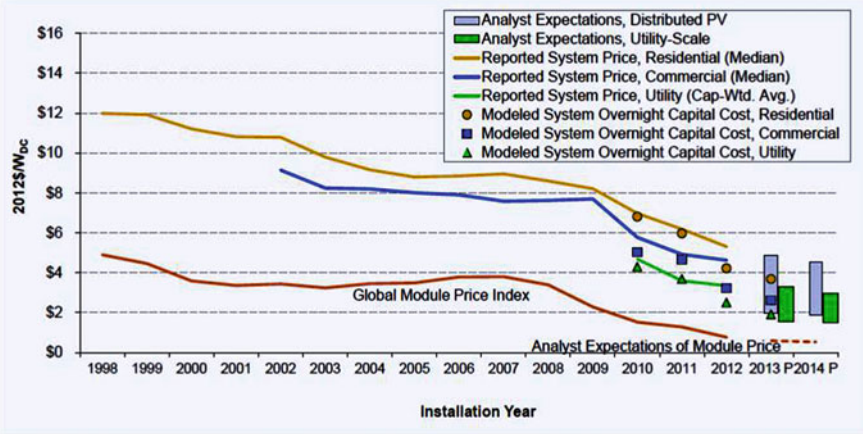


Fig. 1.6 Reported, *bottom-up*, and analyst-projected average U.S. PV system prices over time [29]

However, there are some indications of new opportunities as well as some pitfalls indicated in Table 1.6. Concentrator)PV (CPV) development is an opportunity because of the higher module efficiencies. In 2004, K. Araki from Japan demonstrated the 28 % efficient module [30] shown in Fig. 1.8. Note the resemblance to the CPV module in Fig. 1.2. CPV module efficiencies are continuing to rise with the most recent module efficiency at 35.9 % as will be discussed more here in Chap. 7. CPV obviously represents a future opportunity for development potentially leading to lower cost solar electric power.

However, Table 1.6 also highlights some pitfalls. For example, note the Solyndra disaster in 2011 associated with CIGS thin film technology. After 50 years of development, the efficiencies for non crystalline thin film modules are still well below 15 %. In this authors opinion, it is not wise to continue emphasizing the development of non crystalline thin film solar PV modules. Higher efficiency will be a key to lower cost along with extending the hours of operation beyond the traditional terrestrial sunlight hours. Ideas will be presented in Chap. 12 related to solar power from space.

This chapter has been a review of the history of PV cell development. There is a lot more to cover in the following chapters.

www.TechnicalBooksPDF.com



Fig. 1.7 Large solar PV fields in operation today [27]

www.TechnicalBooksPDF.com

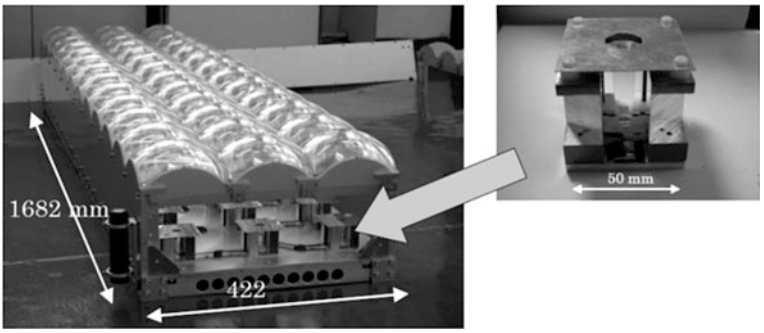


Fig. 1.8 Domed Fresnel lens terrestrial 28 % efficient 200 W CPV module [30] Photovoltaics (PV)

References

1. E. Becquerel, Mémoire sur les effets électriques produits sous l'influence des rayons solaires. Comptes Rendus **9**, 561–567 (Issue date: 7 May 1935) (1839)
2. http://en.wikipedia.org/wiki/Timeline_of_solar_cells
3. W.G. Adams, R.E. Day, The action of light on selenium. Proc R Soc **A25**, 113 (1877)
4. A. Einstein, On the quantum theory of radiation. Physikalische Zeitschrift **18** (1917)
5. D.C. Brock, *Useless no more*, ed. by K. Gordon Teal, Germanium, and Single-Crystal Transistors. Chemical Heritage Newsmagazine (Chemical Heritage Foundation, Spring) vol. 24, no. 1. Accessed 21 Jan 2008 (2006)
6. F. Bloch, Z. Phys **52**, 555 (1928)
7. A.H. Wilson, Proc. Roy. Soc. A, **133**, 458; **134**, 277 (1931)
8. D.M. Chapin, C.S. Fuller, G.L. Pearson, A new silicon p-n junction photocell for converting solar radiation into electrical power. J. Appl. Phys. **25**(5), 676–677 (1954). doi:10.1063/1.1721711
9. G.L. Pearson, D.M. Chapin, C.S. Fuller, (AT&T) Receive patent US2780765, *Solar Energy Converting Apparatus* (1957)
10. US Patent Office. http://en.wikipedia.org/wiki/Telstar
11. http://en.wikipedia.org/wiki/1973_oil_crisis
12. Z.I. Alferov, V.M. Andreev, M.B. Kagan, I.I. Protasov, V.G. Trofim, 'Solar-energy converters based on p-n AlxGa12xAs-GaAs heterojunctions, Fiz. Tekh. Poluprovodn. **4**, 2378 (Sov. Phys. Semicond. 4, 2047 (1971)) (1970)
13. H.J. Hovel, J.M. Woodall, High efficiency AlGaAs-GaAs solar cells. Appl. Phys. Lett. **21**, 379–381 (1972)
14. R. Loo, R. Knechtli, S. Kamath et al., in *Electron and Proton Degradation in AlGaAs-GaAs Solar Cells*. 13th IEEE Photovoltaic Specialist Conference, vol. 562 (1978)
15. L.M. Fraas, R.C. Knechtli, in *Design of High Efficiency Monolithic Stacked Multijunction Solar Cells*. 13th IEEE Photovoltaic Specialist Conference, vol. 886 (1978)
16. D.E. Carlson, C.R. Wronski, Amorphous silicon solar cell. Appl. Phys. Lett. **28**, 671 (1976)
17. http://www.vintagecalculators.com/html/calculator_time-line.html
18. http://en.wikipedia.org/wiki/Public_Utility_Regulatory_Policies_Act
19. Friedman D et al., Prog. Photovolt.: Res. Appl. **3**, 47–50 (1995)
20. F. Lewis, A. James, G. James, E. Keith et al., *Over 35 % Efficient GaAs/GaSb Stacked Concentrator Cell Assemblies for Terrestrial Applications*, 21st IEEE PV Specialist Conference, p. 190 (1990)

www.TechnicalBooksPDF.com

21. http://ntrs.nasa.gov/archive/nasa/casi.ntrs.nasa.gov/19930018773.pdf
22. http://www.ionbeamoptics.com/pdf/SSU_9-17-07.pdf
23. F. Lewis, B. Russ, H. She, Y. Shi-Zhong, G. Sean, K. Jason, A. James, L. David, D. Bert, Commercial GaSb cell and circuit development for the Midnight Sun® TPV stove. AIP Conf. Proc. **460**(1), 480–487 (1999). doi:10.1063/1.57830
24. http://www.qcells.com/uploads/tx_abdownloads/files/17_RESEARCH_AND_DEVELOPMENT_Paper_02.pdf
25. http://en.wikipedia.org/wiki/German_Renewable_Energy_Act
26. http://en.wikipedia.org/wiki/Suntech_Power
27. PVPS_report_-_A_Snapshot_of_Global_PV_-_1992-2013_-_final_3.pdf. http://en.wikipedia.org/wiki/Agua_Caliente_Solar_Project
28. _MAR_19_Recent_Facts_about_PV_in_Germany—Final.docx26.03.14
29. https://haiti-now.org/wp-content/uploads/2013/08/Photovoltaic-System-Pricing-Trends-2013.pdf
30. K. Araki et al., A 28 % Efficient, 400 X & 200 WP Concentrator …, www.physics.usyd.edu.au/app/solar/…/pdf/19thEUPV_5BV_2_20.pdf

www.TechnicalBooksPDF.com

Chapter 2
The Solar PV Market Today and the Need for Non-polluting Solar Energy

In Chap. 1, it was noted that installed solar PV systems prices have now dropped to approximately $4 per W in the US. What does that mean in terms of cents per kWh and how does that compare with the costs of other ways of generating electricity? The US Department of Energy (DOE) Energy Information Agency (EIA) published a projection for 2017, for the costs of the various forms of generating electricity as shown in Table 2.1 [1].

It is interesting that there is a row for carbon capture and sequestration, which already suggests a bias in favor of hydrocarbon fuels since this technology does not yet exist. Nevertheless, let us explore the solar PV predictions. The range is from 12.2 cents per kWh ($122 per MWh) to 24.6 cents per kWh. How does one relate installed system price in $ per W to Levelized Cost of Electricity (LCOE) in cents per kWh? The following is a simple intuitive way of connecting these numbers. One needs the number of annual hours of solar energy in kWh/m2/year and as well as the PV technology efficiency. The following is a simple example calculation. If the PV module efficiency is 20 %, then for a solar intensity of 1 kW/m^2, 1 kW of solar PV will require 5 m^2 of module area. That 1 kW will cost $4,000 at $4 per W installed. Next one needs a map of solar intensity as for example in Fig. 2.1 for the US.

Notice from this map that most of California has a solar resource of over 2,000 kWh/m^2 per year. This means that at 10 cents per kWh, 1 kW of installed PV will produce revenue of $200 per year and it will require 20 years for an investment payback. However, at 20 cents per kWh, the payback time will be 10 years. In either case, the PV modules are warranted to last for 25 years.

The Age of Hydrocarbon Fuels

We now live in the age of energy from hydrocarbon fuels. Oil has certainly changed our lives to the extent that the energy in one barrel of oil equates to approximately 25,000 h of human labor or 12.5 years at 40 h per week [3].

L. M. Fraas, *Low-Cost Solar Electric Power*, DOI: 10.1007/978-3-319-07530-3_2,

© Springer International Publishing Switzerland 2014

www.TechnicalBooksPDF.com

Table 2.1 Projected costs for electricity from various fuel sources for 2017 [1]

Plant type	Range for total system levelized costs (2010 USD/MWh)		
	Minimum	Average	Maximum
Conventional coal	90.1	99.6	116.3
Advanced coal	103.9	112.2	126.1
Advanced coal with CCS	129.6	140.7	162.4
Natural gas fired			
Conventional combined cycle	61.8	68.6	88.1
Advanced combined cycle	58.9	65.5	83.3
Advanced CC with CCS	82.8	92.8	110.9
Conventional combustion turbine	94.6	132.0	164.1
Advanced combustion turbine	80.4	105.3	133.0
Advanced nuclear	108.4	112.7	120.1
Geothermal	85.0	99.6	113.9
Biomass	101.5	120.2	142.8
Wind	78.2	96.8	114.1
Solar PV	122.2	156.9	245.6
Solar thermal	182.7	251.0	400.7
Hydro [16]	57.8	88.9	147.6

O&M = operation and maintenance. *CC* = combined cycle. *CCS* = carbon capture and sequestration. *PV* = photovoltaics. *GHG* = greenhouse gas

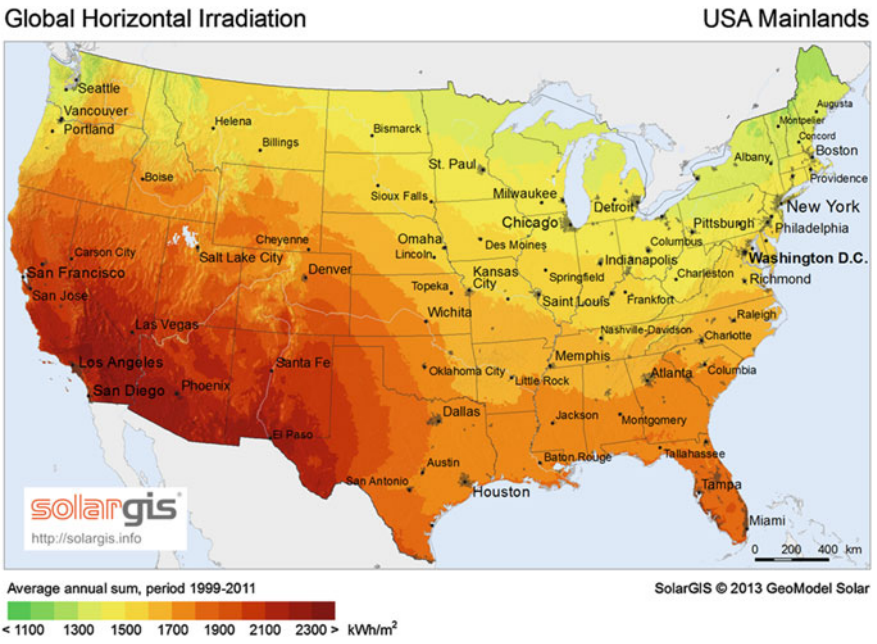


Fig. 2.1 Solar radiation map for US [2]

www.TechnicalBooksPDF.com

Hydrocarbon fuels include oil, natural gas, and coal. Of these, oil is the most apparent in our lives in that we depend on gasoline for transportation and we are very aware of gasoline prices at the pump.

Peak Oil

Oil has revolutionized our means of transportation. However, economically recoverable oil reserves are finite. In 1956, the geologist M. King Hubbert predicted that U. S. oil production would peak in the early 1970s. Almost everyone, inside and outside the oil industry rejected Hubbert's analysis. The controversy raged until 1970, when the U. S. production of crude oil started to fall. Hubbert was right. Around 1995, several analysts began applying Hubbert's method to world oil production, and most of them estimated that the peak year for world oil would be between 2004 and 2008. These analyses were reported in some of the most widely circulated sources [4]: Nature, Science, and Scientific American. The oil price hit $147 per barrel in July 2008. However, this price fell with the beginning of the great recession. While the great recession was attributed to subprime mortgage defaults, higher gasoline prices may have contributed to some of the stress on mortgage payments. Nevertheless, the oil industry denied that peak oil might be approaching.

Figure 2.2 presents data and a projection for the US DOE EIA for World's Liquid Fuel Supply. It shows that the World's Liquid Fuel Supply has been level at around 83 million barrels per day since 2008. It also shows a developing decline in known production sources starting in about 2015 [5]. One can be optimistic that unidentified sources might fill the developing gap between supply and demand.

However, many doubt that new liquid fuel sources will be found to fill this gap. For example, Olivier Rech, at one time responsible for petroleum issues at the International Energy Agency has said "The production of oil has already been on a plateau since 2005 at around 82 mb/d (NB: with biofuels and coal-to-liquid, it is approximate 88 mb/d for all liquid fuels). It appears to me impossible to go much higher. Since demand is still on an increasing trajectory (unless, possibly, the economic crisis engulfs the emerging economies), I expect to see the first tensions arising between 2013 and 2015. Afterwards, in my view, we will have to face a decline of the production of all forms of liquid fuels somewhere between 2015 and 2020" [6].

Why is peak oil relevant to a discussion of Solar PV? Solar PV is not going to replace oil for transportation in the near term. However, Solar PV could in the longer term provide electricity for electric car batteries. This will be discussed further in Chap. 9.

Jeremy Leggett has written a recent book entitled, *Energy of Nations*, where he talks about an ongoing energy debate between an Incumbency and an Insurgency [3]. The Incumbency comes from the Oil, Natural Gas, Coal, Nuclear, and Financial sectors and the Insurgency is the Solar and Renewable Energy sector. He

www.TechnicalBooksPDF.com

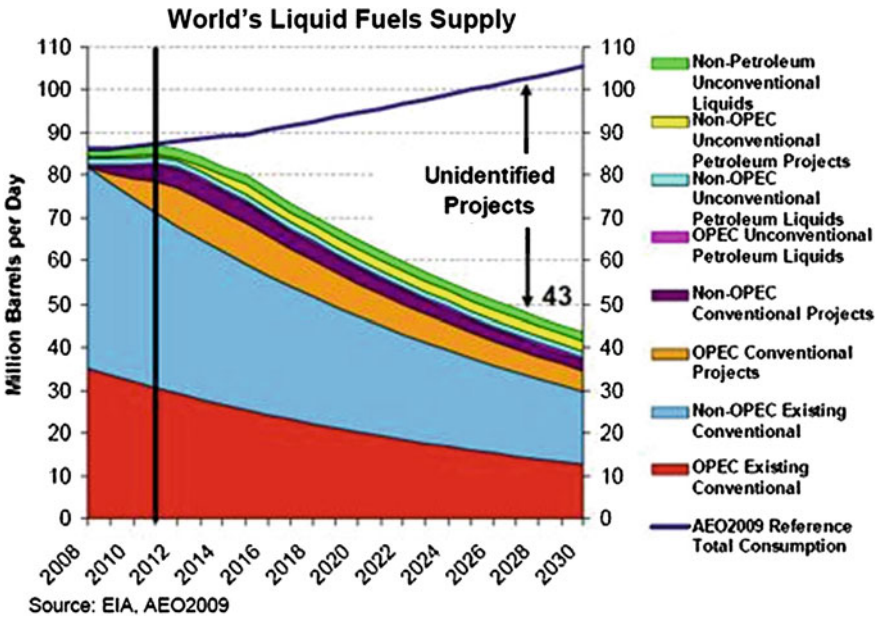


Fig. 2.2 EIA projection for liquid fuels supply [5]

argues that the money is now flowing to the Incumbency, but when there is an obvious decline in Liquid Fuel supply, there will be a shift in Context or mindset and money will then start to flow to Solar and the renewable energy sector.

Global Warming

Meanwhile, there is another driving force in favor of renewable energy and that is global warming or climate change. This is happening more slowly and again denied by the Incumbency. However, the evidence for climate change is abundant. The burning of hydrocarbon fuels is generating CO_2 in the atmosphere and that is producing a greenhouse effect trapping radiant heat by the atmosphere, thereby slowly increasing the earth's average temperature. Figure 2.3 shows the evidence for increasing CO_2 over time [7].

The dominant fuel burned in both the US and China for generating electricity is coal. It generates both particulates and lots of CO_2. In December of 2013, smog from burning coal in China severely limited visibility in both Beijing and Shanghai. Figure 2.4 shows a photograph of Shanghai on a typical smoggy day.

In spite of the denials from the Incumbency, there is ample evidence of global warming. For example, Fig. 2.5 shows that the Arctic Sea Ice is melting.

www.TechnicalBooksPDF.com

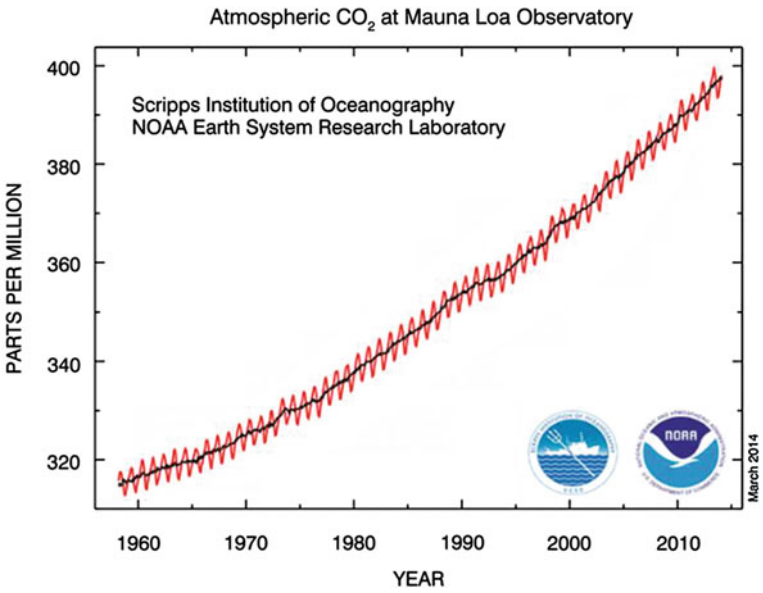


Fig. 2.3 Measured CO_2 levels in the atmosphere [7]



Fig. 2.4 Shanghai Dec 3, 2013

There are also recent weather events that should serve as warnings. For example, Superstorm Sandy at the end of 2012, caused $62 billion in damages and led to the flooding of the New York subway system. Then in 2013, Typhoon Haiyan pictured in Fig. 2.6 killed 6,000 people with more than 12 million people

www.TechnicalBooksPDF.com

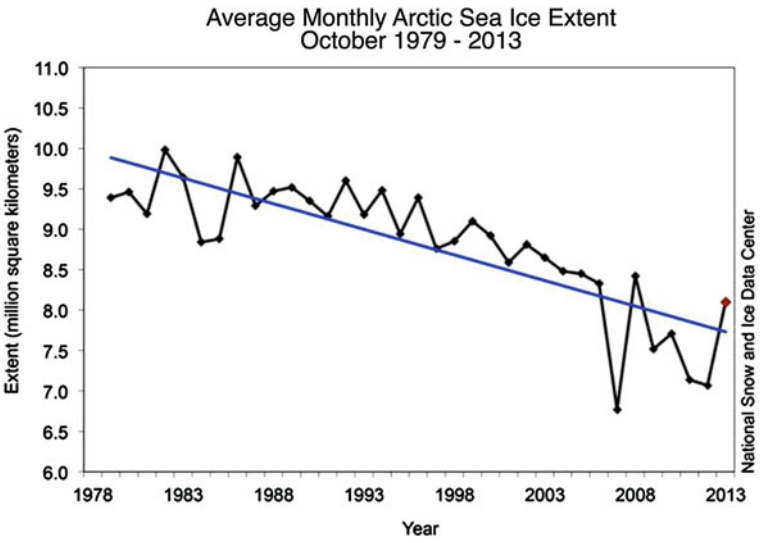


Fig. 2.5 Satellite photos show that the arctic sea ice is melting [8]

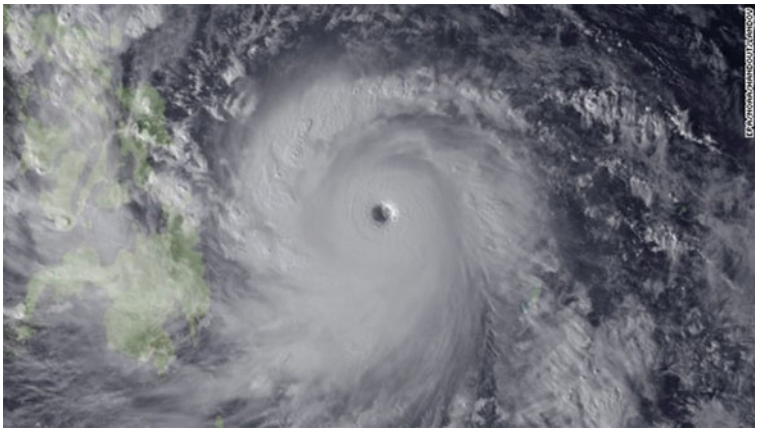


Fig. 2.6 Photograph of Typhoon Haiyan taken from the international space station [9]

affected by the monster typhoon. It left behind catastrophic scenes of destruction and despair when it made landfall in the Philippines.

So, the relevant question here is: What can be done to survive a decrease in oil supply and global warming? The obvious answer is a shift to renewable energy. Unfortunately, the Incumbency is still dominant. Figures 2.7 and 2.8 show what may well happen by continuing to burn hydrocarbons with business as usual [10]. Representative Carbon Pathways (RCP) have been modeled based on the amount of hydrocarbon burning in the future and the effect of thermal energy trapped by

www.TechnicalBooksPDF.com

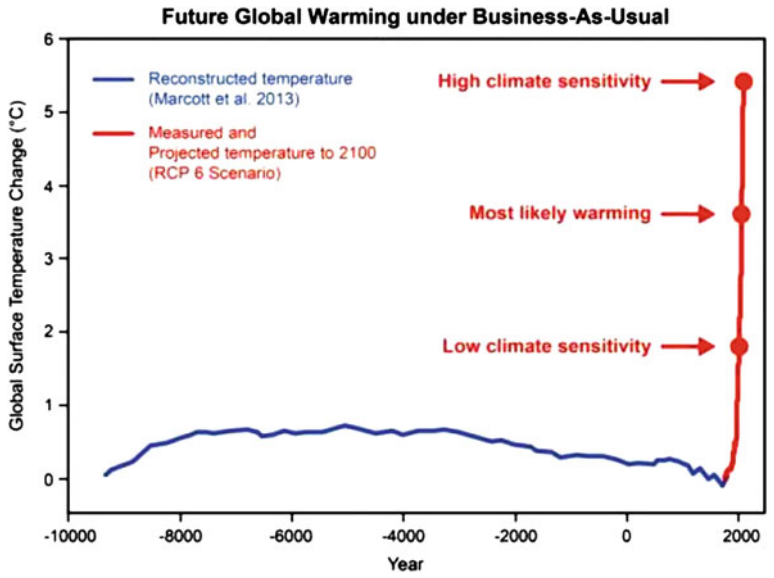


Fig. 2.7 Predicted global surface temperature change by 2,100 for the RCP-6 scenario. Representative concentration pathways (RCPs). Specify radiation forcings at this interval—3, 4.5, 6 W/m^2 plus the big one at 8.5 W/m^2 (*the* 3 W/m^2 *scenario actually peaks earlier at* 3 W/m^2 *and declines to* 2.6 W/m^2 by 2100)

the accumulated CO_2. For example, RCP-6 implies that the earth warming from CO_2 will be increased by 6 W/cm^2.

Most recently, there has been a news media promotion for shale oil and natural gas. The incumbency is now claiming that the Shale Gas boom will last for 100 years. However, there are critics. Bill Powers in his book entitled *Cold, Hungry and in the Dark: Exploding the Natural Gas Supply Myth* argues that the Shale gas supply will peak in 2015 or soon thereafter [11]. In any case, it is true that Natural Gas is the least polluting of the hydrocarbon fuels and will be complementary with solar PV in the next decade.

The Arguments for Solar Energy

My group at Boeing first demonstrated the 35 % solar cell 24 years ago in 1989. It then took another 17 years before there was funding to incorporate this cell with optics into a 33 % efficient concentrating PV module. Why did it take so long? When I wrote my first book, *Path to Affordable Solar Electric Power and The 35 % Efficient Solar Cell*, in 2004 [12], I made a plea for a US Apollo program to launch solar energy.

www.TechnicalBooksPDF.com

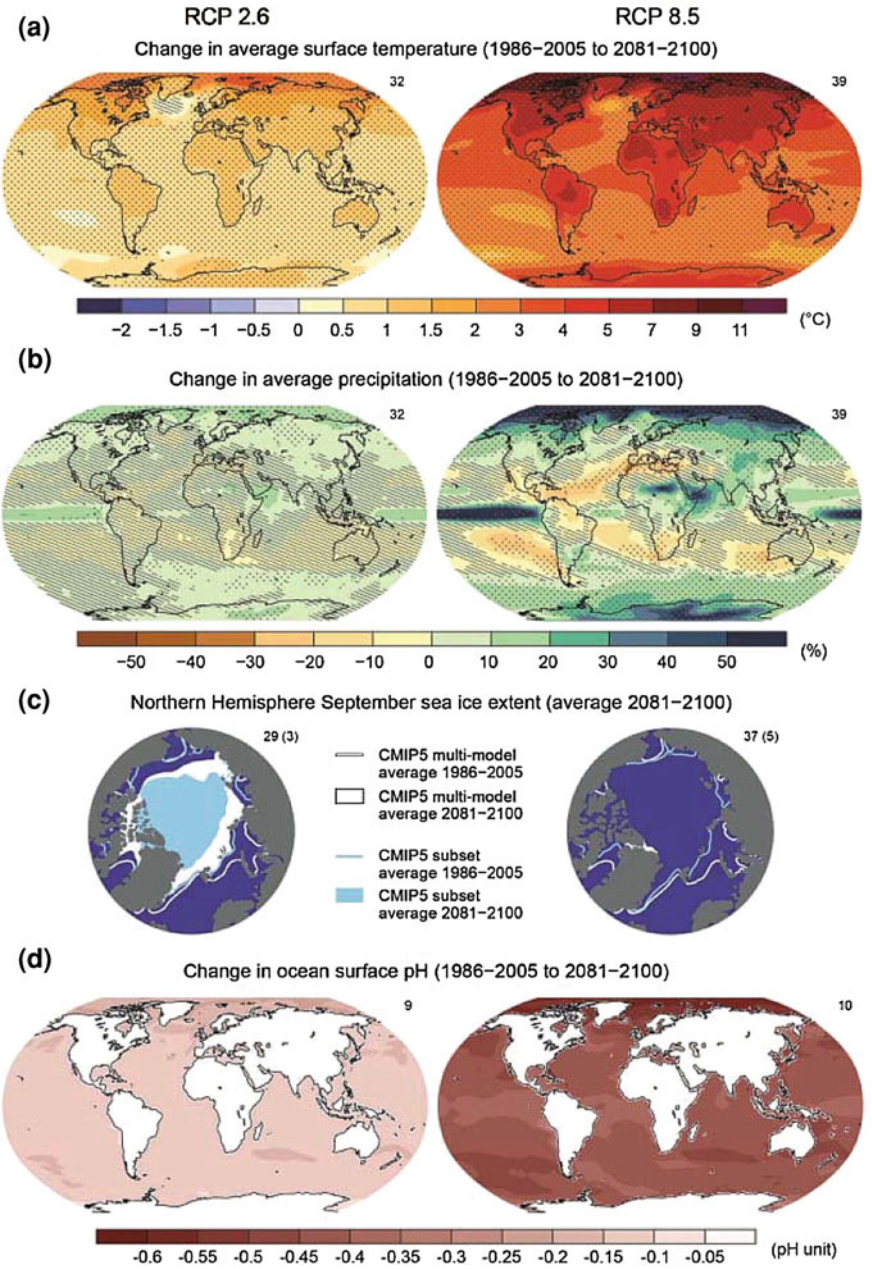


Fig. 2.8 Predicted global changes [10] between approximately 2000 and 2100 for the RCP 2.5 and RCP 8.5 cases. **a** Change in average surface temperature (1986–2005 to 2081–2100), **b** change in average precipitation (1986–2005 to 2081–2100), **c** Northern Hemisphere september sea ice extent (average 2081–2100), **d** change in ocean surface pH (1986–2005 to 2081–2100)

www.TechnicalBooksPDF.com

At that time, I asked: "Who is going to commercialize solar energy?" I noted: "It is not the American oil companies given that they can obtain low-cost oil from the Middle East secured by the American military. It is probably not the defense industry given that their charter is to develop weapon systems. It is probably not the electric utilities as they are very conservative and it may not be in their interest for the homeowner to generate his own power." I noted that while I had hoped that it could be small business, I had discovered that small business do not have access to the financial resources to play in the energy game. This game requires hundreds of millions to billions of dollars in order to play.

My plea in 2004 was not answered by the US government and as I noted in Table 6 in Chap. 1, the focus for solar PV shifted away from the US to Europe and China after 2001. China actually provided the billions of dollars required for manufacturing to launch silicon PV modules.

I am writing this book to make two strong statements: First, solar energy can become a mainstream source of energy over the next 10 years. And second, I would like to see the US re-establish a serious national program to develop alternative energy. There are still opportunities in PV for innovations leading to still lower costs as I will describe in Chaps. 7–12 in this book.

Why do I make these statements? I have three sets of reasons. My thinking has evolved through my career and so, I have to tell you a little about myself. I am a US scientist and I have been working on solar cells as well as other semiconductor devices for the last 40 years. I have worked with major defense contractors on space solar cells (Hughes from 1973 to 1978 and Boeing from 1986 to 1992) and at a major oil company on terrestrial solar cells (Chevron from 1978 to 1986). For the last 20 years, I have been president of JX Crystals Inc., a small solar cell research company.

In the following, I enumerate my reasons for advocating a larger national solar energy program now.

Reason #1: Lower-Cost Solar Electricity

Since I have spent my career in industry, I have learned that my first argument should be that solar cells can generate electricity at cost competitive rates with respect to other sources of electricity. This is because today's commercial solar cells produce electricity in sunny locations at rates of around 15 cents per kWh. However, advanced solar cells have been demonstrated that are twice as efficient as today's commercial cells. My group at Boeing demonstrated a solar cell in 1989, with 32 % efficiency as measured by NASA. This is the efficiency for space. Subsequently, it was shown that these cells can be operated here on earth with an efficiency of 35 % [13]. Higher cell efficiencies will bring down costs. Besides efficiency improvements, still other cost reductions are possible. Glass or plastic lenses or aluminum mirrors can be used to concentrate sunlight onto efficient solar cells. These collector materials are cheaper than single crystal semiconductor

www.TechnicalBooksPDF.com

material. Cost reductions can also come by tracking the sun, thereby producing more kilowatt-hours (kWh) per kW installed. Implementing these cost reductions in high volume production can bring solar electric costs down below 10 cents per kWh. However, very large investments are required to integrate these cells into CPV systems and manufacture these cells and systems in quantities sufficient to bring down prices. The issue of the cost of solar electricity is a complex subject that will be treated in detail in the chapters throughout this book.

Reason #2: Rising Oil and Natural Gas Prices

My second reason relates to the fact that our oil and natural gas resources are being depleted. The consequence of this "Impending World Oil Shortage" is that electricity prices are going to be rising probably abruptly within the next 5–10 years. Add to this the possibility that global warming may lead to a carbon tax when the costs of weather disasters and increased insurance costs are finally added to the costs of burning hydrocarbon fuels. This affects the economics of solar electricity as solar modules based on semiconductor devices will last for 25 years or longer. Today's cost competition assumptions for solar usually assume a short-term payback and nonescalating energy prices.

Reason #3: War, Weapons of Mass Destruction, and the Moral Argument for Solar

When one thinks about conventional electric power production, one thinks about oil, natural gas, nuclear, and coal as fuel sources. The incumbency does not include Solar on this list. However, these conventional fuel sources have hidden unintended costs.

For example, nuclear fuels are coupled with nuclear waste management and nuclear weapons. Then nuclear waste and nuclear weapons are coupled with the cost of homeland security and our fear of weapons of mass destruction. There are hidden costs involved in attempting to guarantee that nuclear materials do not find their way into the hands of terrorists.

As another example of hidden costs, our dependence on oil from the Middle East has linked us unavoidably with terrorists from the Middle East. We have now fought two wars in the Middle East to secure our oil supply.

In contrast to the unintended costs just enumerated, let us look at solar energy. Solar is inevitable on the larger scale of time. Solar energy is really already a primary energy source through wind and hydroelectricity. Solar energy generated our coal, oil, and natural gas via photosynthesis a hundred million years ago. Solar cells are very much more efficient than plants at converting sunlight to useful energy. Finally, solar energy is benign and will benefit the whole world.

www.TechnicalBooksPDF.com

My problem is that I have watched our US energy policy over the last 30 years and independent of political party, our national energy policy de facto has simply been to guarantee the oil supply from the Middle East with our military as necessary. It is now time for a shift in policy.

This then brings me to my moral argument for solar energy. It is clear that oil and natural gas are resources being depleted. If we do nothing and allow these resources to become more and more scarce, we will be fighting future wars over these scarce resources. If on the other hand, we decide to invest in solar energy, we can decrease or eliminate our dependence on foreign oil.

We can make solar electric power generating arrays for the western US economically using automation. Automation is ideal for solar arrays and automation is what has allowed high American productivity. Then, we could even export solar power arrays to the Middle East and developing world in exchange for cash to buy oil. The present problem with this scenario is that automating solar array production will require very large investments.

So where are we now? Over the last 35 years since 1989, I have seen massive government funding to make 30 % efficient solar cells, the primary power source for spy satellites and I have seen the same semiconductor materials used in large numbers of weapon systems. As president of a small company, I have looked for funding to bring the 35 % solar cell to the terrestrial market place. However, there has been little interest in peaceful applications.

At the same time, I have learned that the amount of investment required to make an impact in the energy field is massive. The energy business is a multi-billion-dollar business. This book outlines a path to cost competitive solar electric power, but argues that major government commitment and cooperation with industry is needed to bring solar electricity into the mainstream in the US. While the investment support required is larger than small entrepreneurs can handle, it is small compared to the cost of war and terrorism.

Let us pause for a moment to put the current US government support for photovoltaic (PV) or solar cell development into perspective. The US DOE budget for solar energy in 2014 is $350 million to be divided between universities and government labs and the whole US solar industry. Most of this funding is going to universities and government labs. Meanwhile, the Chinese government is spending $2.1 billion in 2013 in subsidies to Chinese Solar Companies. The Chinese solar companies are using Si module technology initially developed in the US. Let me put these costs into a larger context. The cost of a new 1 GW electric power plant is roughly $1 billion. The cost of the Iraq & Afghanistan wars is estimated to be between $4 and $6 trillion. The cost of the Manhattan Atomic Bomb Project was $20 billion for the effort between 1940 and 1945[12]. Finally, the five-decade-plus bill for the U.S. nuclear weapons enterprise up to 2004 was $5.5 trillion, in 1996 dollars.

Over the next 20 years, solar electricity is inevitable. Building on U.S. discoveries, solar electric industries are now being expanded outside the U.S. through foreign government support. It is hoped that this book will awaken informed interest in the US.

www.TechnicalBooksPDF.com

I would like to see the US government set us on a path for a peaceful future. We will need the knowledge to make intelligent choices. I want the US to be remembered 100 years from now as the country that put a man on the moon and did constructive things and not as the strong military power that built the atomic bomb and took whatever it needed through wars.

At this point, some readers will object to my plea for government support and, in fact, this is a difficult issue that will require intelligent and careful implementation. My point here is that the Iraqi war has told us that time is running out. My message in this book is that there are already proven technical paths to affordable solar electric power. The problem is moving these innovations into commercially viable systems, qualification testing these systems, and then moving from small-scale production into automated high volume production. The magnitude of funding required for these early tasks is too large for private investors to handle without government commitment and cooperation. In this regard, government needs to actually help small businesses and investors and not just feed government labs and universities with long-term searches for miraculous future breakthroughs.

Solar PV Cells and Markets

There are a large number of PV cell types and a large variety of PV cell markets. Let us begin with the markets for the terrestrial Silicon solar cell planar module. The silicon solar cell planar module represents 80 % of the terrestrial market. All the terrestrial solar cell types will be discussed in Chaps. 3 and 5 will discuss the c-Si cell and module technology in more detail. This market began with off-grid cabins in the 1970s, but then spread to grid connected residential with PURPA in the 1980s. Grid-connected commercial installations with hundreds of kWs then began in the 1990s. Finally, after 2005, the utilities began to install systems with 10–100 MW sizes.

Today's terrestrial solar market is divided into three sectors with residential PV systems being generally less than 10 kW in size, commercial systems being in the 100 kW to 2 MW range, and utility systems being in the over 2–500 MW size today. In the future, a solar market segment with systems of 1 GW and larger should be expected.

Figure 2.9 summarizes the terrestrial solar PV market as of the end of 2013. Accumulated solar PV installed power hit 134 GW. However, the US fraction of this accumulated total was only 13 GW or 10 % of this total [14]. The message here in Leggett's terminology is that the US is the home of the incumbency. However, there is a small indication that a shift may be underway. In 2013, the total new PV capacity hit 35 GW worldwide with 5 GW of new capacity for solar in the US. The US share is then increasing to 14 %. However, China installed 12 GW in 2013 [15].

www.TechnicalBooksPDF.com

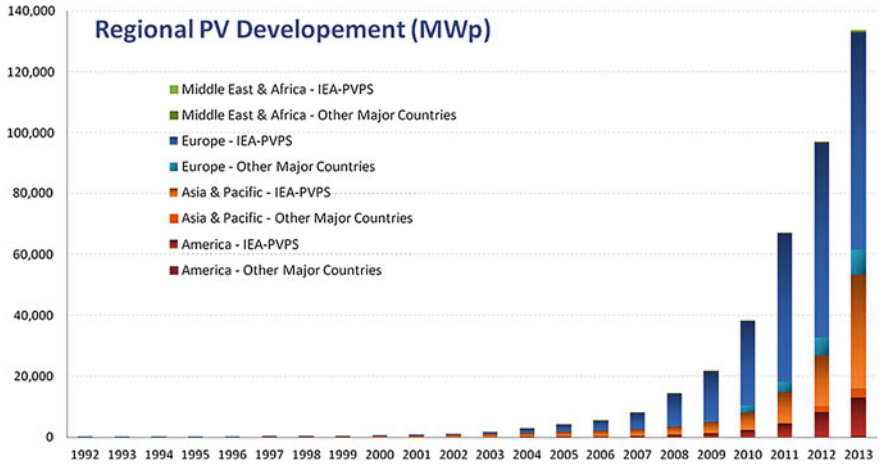


Fig. 2.9 PV development by region [14]

Solar PV Economics

The solar community often talks about module costs in $ per W. A Watt is a unit of power. However, it is now more relevant to talk about installed system power costs in $ per W instead of just module cost. It is even more important to talk about the LCOE in cents per kWh. A kWh is a measure of energy. The Electric Power Research Institute (EPRI) presented an important equation for calculating the LCOE for solar cell electricity systems [16]. This equation is repeated in Fig. 2.10 below along with nine important input variables required in order to calculate a numerical value for the LCOE. This equation is more precise than the simple qualitative intuitive example presented at the beginning of this chapter. The nine variable in Fig. 2.10 are important because they highlight the fact that vertical integration and cooperation is required amongst a large number of diverse groups in order to bring down the price of solar electricity in terms of cents per kWh.

For example, emphasizing low-cost modules is just the C_m term in the LCOE equation. The module supports, field wiring, and installation costs can be higher when the module efficiency is low because more modules need to be installed. This is the C_b term in this equation. The sunlight, S, available at the location is certainly important. Following the sun by tracking the modules will increase the number of hours per year of operation, which is the h_a term. Increasing the annual hours of operation will reduce the impact of the inverter cost, C_i. Note also that the cost of the hardware and installation are not the only costs. The projects have to be financed by the banks and this is the finance, F, term. Government permitting is also required and this can cause delays increasing costs and this is part of the project specific overhead, r, term. Finally, the system will need some maintenance over time.

www.TechnicalBooksPDF.com

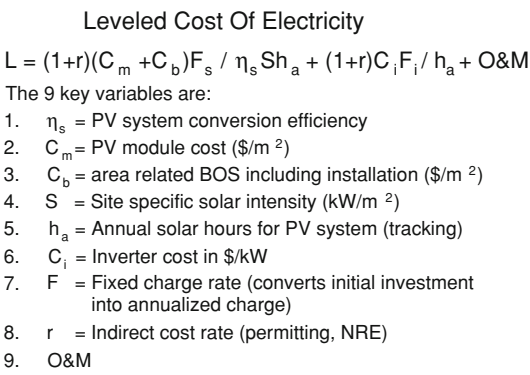


Fig. 2.10 EPRI equation for calculating the levelized cost of electricity [16]

Figure 2.11 provides information on solar power system costs in $ per W from a DOE study [17]. Referring to the equation in Fig. 2.10, this study presents results for

$$(1 + \mathbf{r})(\mathbf{C_m} + \mathbf{C_b} + \mathbf{C_i})\mathbf{F}.$$

Notice from this figure that the system cost is being doubled relative to the hardware cost by the permitting and financing terms, r & F. One might describe these as soft costs or, perhaps as some penalties associated with Leggett's Context imposed by the Incumbency.

The penalty associated with soft costs is significantly lower in Germany.

Installed PV system costs have been steadily falling. Starting in 2008, supply exploded as new manufacturing capacity was built. From 2008 to 2012, 80 % of the decline in total system cost was a result of falling module prices. The costs of nonmodule hardware also declined slightly, including "soft costs" like marketing, customer acquisition, design, installation, permitting, and inspection. But they did not fall as rapidly as module costs.

Whereas module prices declined as a result of global market factors—particularly the rapid buildup of supply in China, and strong feed-in tariff (FIT) incentives ensuring demand in Europe—reducing soft costs will require public policy changes aimed at removing market barriers and accelerating deployment.

Soft costs are the main reason why small residential PV systems installed in 2012, cost far less in Germany, Italy, and Australia than they did in the United States. Excluding sales or VAT taxes, Germany's median installed system price ($2.60/watt) was half the U.S. price ($5.20/watt). Unsurprisingly, residential system size has increased as prices fell. The median system size in 1998 was 2.4 kW; by 2012, it had grown to 5.2 kW.

The cost difference is even more pronounced with larger systems. Utility-scale systems in Germany were quoted at $1.90/watt in 2012, while they were installed for $4.50/watt in the U.S.

www.TechnicalBooksPDF.com

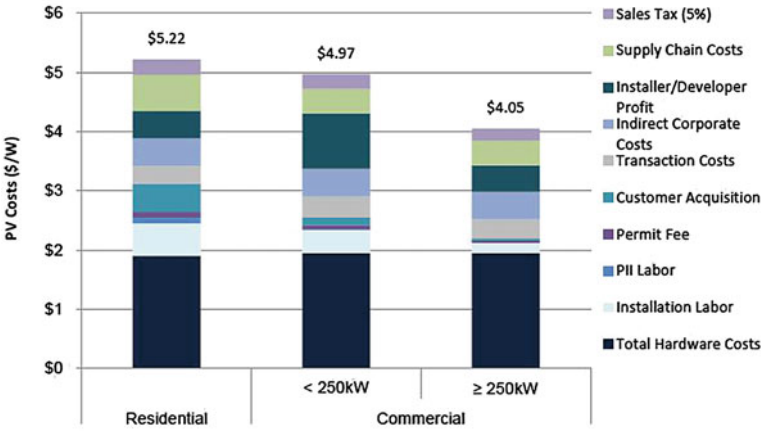


Fig. 2.11 Total US PV system price, by sector and system size (*first half of* 2012). Opportunities for PV improvements [17]

Maintaining the growth of the U.S. PV industry depends on continuing cost reductions, and that depends on significantly reducing soft costs. How can that be done? A LBNL report [18] found that soft costs for residential PV in Germany are just 19 % of those in the U.S. Why?

First, it costs about one-tenth as much to acquire a customer in Germany. That is primarily because Germany has a national FIT and the U.S. does not.

Second, costs for permitting, interconnection, and inspection in Germany are also nearly one-tenth of those in the U.S. Part of that is because it takes much less time: about 5.2 h per system in Germany, versus 22.6 h in the U.S. It takes an extraordinary amount of labor to create extremely burdensome, redundant, and oftentimes totally unnecessary permit packages to satisfy the requirements of building and planning authorities, which are different in every little town and county. The best way to reduce those costs is to standardize building and planning requirements for PV systems nationwide, and make it as easy and as cheap as possible to pull a permit. Local authorities should follow the example of Lancaster California where mayor Rex Parris directed city staff to clear away obstacles in the building and planning approval process to encourage the growth of PV. Contractors can now pull a simple permit for a residential solar system in Lancaster in 15 min, over the counter, for just $61.

Third, it's vital to cut the cost of installation labor. It takes almost twice as long to install a system in the U.S. as it does in Germany, partly because German installers rarely use the roof-penetrating mounting systems that are usually required in U.S. building codes. U.S. wiring practices should also be harmonized and standardized to reduce the amount of time installers have to spend trying to satisfy nitpicky and unnecessary requirements in certain jurisdictions.

www.TechnicalBooksPDF.com

Fourth, we should exempt solar PV systems from state sales taxes. Those taxes accounted for a median $0.21/watt in the U.S. in 2011, whereas in Germany, residential solar systems are exempt from revenue, sales, or value-added taxes.

Finally, U.S. markets could be more open to competition in installation labor. Too many customers (particularly tax-exempt entities) are subject to restrictions requiring them to use union labor, or to allow only electrical contractors with certain licenses to install solar systems. Liberalizing installation rules could cut prices further.

The U.S. solar industry needs policymakers, regulators, code jockeys (electrical, building, and planning), and elected officials to step up and keep its growth momentum going.

Future Opportunities for PV Technology Improvements

Referring to Fig. 2.9, worldwide solar PV is growing dramatically. Solar PV in the US is finally growing even more dramatically up by 35 % in 2013 relative to 2012. To date, solar PV consists principally of planar silicon PV modules. However, there are some exciting PV developments on the horizon as will be described in this book.

Chapter 7 herein will describe a very exciting development involving highly-efficient solar cells with lens technology, or so-called concentrator photovoltaics (CPV). This new technology is just getting established in the market, and has a growth rate exceeding several hundred percent per year. It is already competitive, but still has great potential to become even cheaper. In the San Diego area, where there is a factory producing these types of cells, a 300 MW solar plant is being planned.

However, a problem for solar PV is that it just functions when the sun is shining during the day. However, Chap. 11 herein describes a nonsolar PV option where man-made heat sources can be used to generate infrared radiation where infrared sensitive PV cells can be used to generate electricity day and night. Thermo-PhotoVoltaics or TPV can be used for generating heat and electricity in residential furnaces for small distributed systems. In other words, solar PV cells can be placed on the home's roof for electricity during the day and IR PV cells in the home furnace can be used for heat and electricity at night and on cold winter days. TPV can also be used to convert waste heat in industrial systems into electricity as, for example, in steel mills.

Finally, there is the dream of using solar cells to generate electricity 24 h per day with Space Power Satellites. This idea is explored in Chap. 12 of this book. A more economic variation on this idea is to deploy mirror in space in a low earth–sun synchronous orbit to deflect sunbeams down to GW sized solar farms distribute in sunny locations around the world. While this option does not provide solar energy 24 h per day, it can extend the sunlight hours at the GW sites into the early morning and evening hours reducing the cost of solar electricity to below 6 cents per kWh.

www.TechnicalBooksPDF.com

References

1. Energy Information Administration, Annual energy outlook 2012. June 2012, DOE/EIA-0383 (2012)
2. SolarGIS: Free solar radiation maps download page—GHI *solargis.info/doc/71*
3. Jeremy Leggett Energy of Nations
4. Hubbert's Peak, The Peak https://www.princeton.edu/hubbert/the-peak.html Princeton University
5. http://www.postpeakliving.com/peak-oil-primer
6. http://www.theoildrum.com/node/8797
7. http://thinkprogress.org/climate/2014/04/09/3424704/carbon-dioxide-highest-level/
8. Late summer Arctic sea ice extent has decreased substantially since the satellite data record began in 1979, and has been particularly low over the past seven summers. Credit: National Snow and Ice Data Center
9. Sheena McKenzie, for CNN, and Fionnuala Sweeney, CNN "Astronaut Karen Nyberg captures Typhoon Haiyan from space" updated 6:00 AM EST, Fri 22 November 2013
10. http://futuristablog.com/ scientists-prediction-climate-change-business-usual-versus-alternative-futures/
11. Bill Powers, Cold, Hungry and in the Dark: Exploding the Natural Gas Supply Myth (2013)
12. L. Fraas, Path to Affordable Solar Electric Power and The 35 % Efficient Solar Cell, JX Crystals (2004)
13. L. Fraas, J. Avery, J. Gee, K. Emery et. al., in *Over* 35 % *Efficient GaAs/GaSb Stacked Concentrator Cell Assemblies for Terrestrial Applications*, 21st IEEE PV Specialist Conference, p. 190 (1990)
14. PVPS_report_-_A_Snapshot_of_Global_PV_-_1992-2013_-_final_3.pdf
15. http://about.bnef.com/press-releases/ chinas-12gw-solar-market-outstripped-all-expectations-in-2013/
16. L. Fraas, L. Partain (eds.), in *Solar Cells and Their Applications*, 2nd edn. (Wiley, New Jersey, 2010)
17. Benchmarking Non-Hardware Balance-of-System (Soft) Costs for U.S. Photovoltaic Systems, Using a Bottom-Up Approach and Installer Survey, 2nd edn. NREL/TP-6A20-60412 Oct 2013
18. http://emp.lbl.gov/sites/all/files/german-us-pv-price-ppt.pdf

www.TechnicalBooksPDF.com

Chapter 3
Types of Photovoltaic Cells

PV cells can be categorized according to application, cell material and structure, and cost within the system application context. The three application areas are terrestrial solar, space solar, and non-solar. For example, Thermophotovoltaics (TPV) systems use man-made infrared energy sources at night. The three alternative cell structures are large crystallite silicon cells (mono- and multi-crystal Si), small grain size, or amorphous thin film cells (CdTe, CIGS, and a-Si), and very high efficiency high power density cells (InGaP.GaInAs/Ge multi junction cells and GaSb IR cells) . Cell and module cost are very dependent on production scale and cell conversion efficiency is very important at the system level. Silicon cells are now dominant in the residential terrestrial solar arena. Thin film cells have intrinsic efficiency limitations because of their non-crystalline nature and have been loosing market share to silicon. Multijunction solar cells now have conversion efficiencies over 40 %, but must be integrated into more complicated Concentrator PV sunlight systems (CPV). CPV is very promising for lower cost solar electricity for utility systems in sunny locations at the 100 MW scale, but still require production volume and component supply-chain integration. Infrared sensitive TPV cells can be used at night and in cold climates in residential furnaces for combined heat and power (CHP) complimenting solar modules on the home rooftop.

Introduction

In 1839, Edmond Becquerel discovered the photovoltaic (PV) effect. He found that two different brass plates immersed in a liquid produced a continuous current when illuminated with sunlight. We now believe that he had made a copper-cuprous oxide thin film solar cell. Later in the 1870s, Willoughby Smith, W. G. Adams, and R. E. Day discovered a photovoltaic effect in selenium [1]. However, the conversion efficiencies of both the thin film cuprous oxide and amorphous selenium solar cells were less than 1 %.

L. M. Fraas, *Low-Cost Solar Electric Power*, DOI: 10.1007/978-3-319-07530-3_3,

© Springer International Publishing Switzerland 2014

www.TechnicalBooksPDF.com

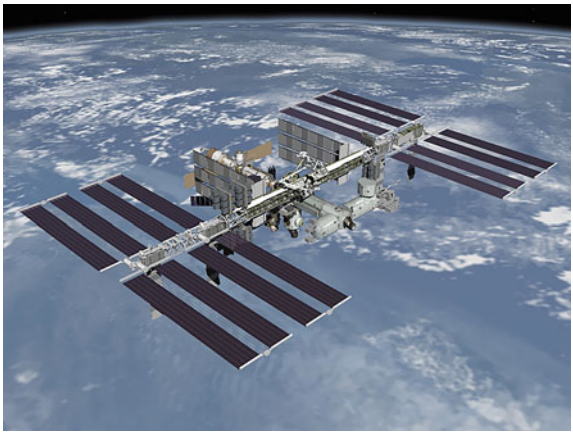


Fig. 3.1 International space station silicon solar arrays generate from 84 to 120 kW

Around 75 years passed while quantum mechanics was discovered, the importance of single crystal semiconductors was recognized, and p/n junction behavior was explained [2]. By 1954, Chapin et al. at Bell Labs had discovered, invented and demonstrated the silicon single crystal solar cell with 6 % efficiency [3]. Over a few following years, researchers brought the silicon solar cell efficiency up to 15 %. The timing was fortunate because Sputnik was launched in 1957 and solar cells were the perfect light weight low maintenance remote electric power source. Today, as shown in Fig. 3.1, silicon solar cells are being used to power the space station.

The solar cell industry remained small until the first Arab oil embargo in 1973. Up until that time, the solar cell industry established a firm foothold with low level but consistent cell and array production and performance. During those first 20 years, reliability was the driver and cost was not as important. After 1973, the flat plate silicon module was brought down to earth and modified for weather resistance.

Also after 1973, in order to realize a dream of a major contribution to our electric power needs here on Earth, cost became a major driver of a large research effort in the US. There were three schools of thought. The first group argued that the single crystal silicon cells developed for space could be made low-cost by clever manufacturing innovations and economies of scale.

The second group argued that single crystals silicon cells are like gem stones and will always be intrinsically too expensive and therefore, non-crystalline thin film cells were needed. This led to a major research effort in the US on Cadmium Telluride (CdTe), Copper Indium Gallium di-Selluride (CIGS), and amorphous Silicon (a-Si) thin film solar cells. A third group argued that single crystals were necessary for high-efficiency conversion and that the low cost large area solar energy collection function could be managed with low cost optical lenses or mirrors. This effort has led to 35 % efficient dual junction single crystal cells like the Gallium Arsenide /Gallium Antimonide (GaAs/GaSb) mechanically stacked

www.TechnicalBooksPDF.com

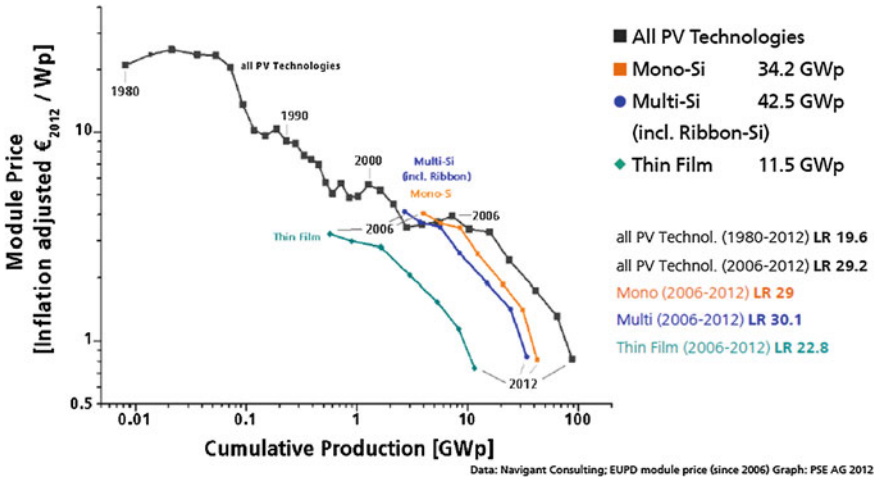


Fig. 3.2 Price learning curve by PV technology: cumulative production up to 2012



Fig. 3.3 A 300 kW silicon module solar system operating in China and designed by JX Crystals Inc

cell and the 40 % efficient three-junction Indium Gallium Phosphide /Indium Gallium Arsenide /Germanium (GaInP/InGaAs/Ge) monolithic cell.

Now in 2013, 40 years later, the laws of physics and volume manufacturing have provided some interesting answers. As shown in Fig. 3.2, volume production has indeed been very important and silicon modules are still dominant in the terrestrial arena with module cost now below a dollar per Watt [4]. Notice that silicon module production accounts for 87 % of the total installed PV capacity as of the end of 2012. In 2013, cumulative worldwide installed PV production capacity hit 100 GW.

Figure 3.3 shows a representative installation of Si Modules in a field near Shanghai in China.

www.TechnicalBooksPDF.com

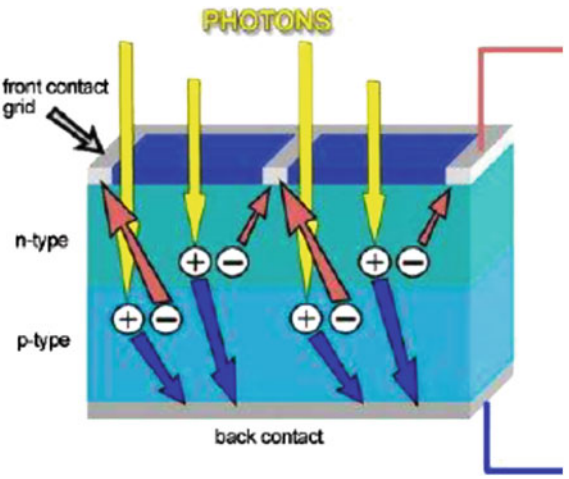


Fig. 3.4 N /P junction solar cell with metal grid on *top*

Types of Solar Cells and Modules

There are three types of terrestrial solar cells and associated modules today. The planar crystalline silicon module dominates the market today. This cell's structure is shown in Fig. 3.4.

As shown in Fig. 3.5, the silicon module fabrication starts with the growth of a single crystal ingot. That ingot is then cut into wafers and the cells are fabricated via a diffusion process. Individual cells are then assembled into modules.

Silicon modules today are assembled using automated equipment.

The second type of solar cell and module is the thin film module. This concept is superficially very attractive. Since single crystal material is expensive, why not replace it with inexpensive thin films? This brings to mind paint but unfortunately, while paint is cheap, it does not produce electricity. The problem with this approach is that destroying the crystallinity destroys the performance. The conversion efficiency drops dramatically. Thin film modules can be made with CdTe, $CuInGaSe_2$ (CIGS), or amorphous silicon. There are a large number of possible process used in fabricating thin film modules, but they are generally based on roll-to-roll processing. An example schematic process for fabricating CIGS cells is shown in Fig. 3.6.

The difficulty with both crystalline silicon and thin film planar modules is that one tries to obtain both low cost and high efficiency with the same element. There is an alternate approach, using concentrated sunlight referred to as Concentrator PV or CPV. This approach separates the two requirements of low cost and high performance into two separate elements. The single crystal cells are the high efficiency converters used sparingly, while mirrors or lenses are used to concentrate the sunlight onto the cells. The aluminum mirrors (or alternately glass or plastic lenses) are inexpensive. High efficiency multijunction solar cells represent

www.TechnicalBooksPDF.com

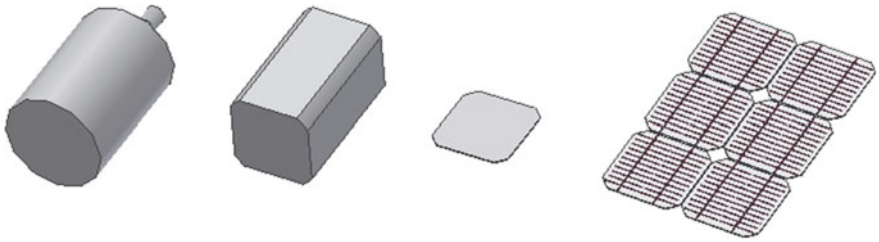


Fig. 3.5 Standard silicon single crystal module fabrication crystal to ingot to wafer to module

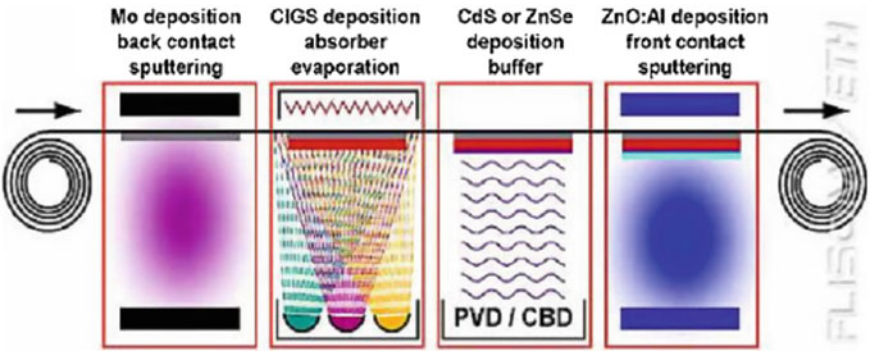


Fig. 3.6 Simplified CIGS) cell fabrication schematic. In fact, there are four elements required with only three evaporation sources shown. Cheung—Berkeley http://www.inst.eecs.berkeley.edu/~ee143/fa10/lectures/Lec_26.pdf

a third class of terrestrial solar cells. They will be discussed in more detail later in this chapter.

It is also evident that both volume production and module conversion efficiency are very important drivers for future system level cost reduction. For these two reasons, this chapter now divides into first a discussion of the cells now in high volume production (Sect. 3.3), and then into a discussion of the promise of an exciting future when the high efficiency cells are integrated into systems and CPV systems are brought into high volume production (Sect. 3.4).

Cells in High Volume Production Today

Figure 3.7 provides an efficiency comparison for the various cell technologies in production today [4]. Best lab cell and best lab module efficiencies are shown. Notice that there are now two types of silicon technologies shown referred to as mono-Si and multi-Si with the mono-Si cells and module efficiencies being the highest for all types of cell technologies shown.

www.TechnicalBooksPDF.com

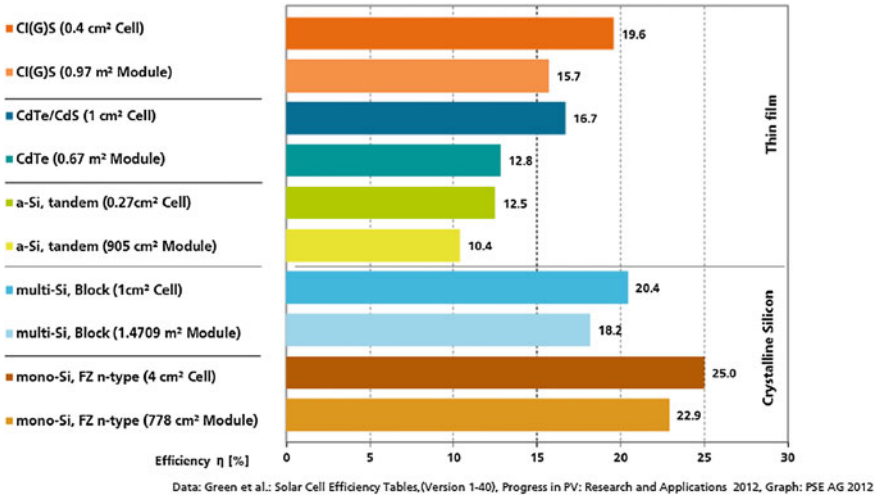


Fig. 3.7 Efficiency comparison for PV technologies now in production: best lab cells and best lab modules

What are multi-Si cells and modules? Figure 3.8 shows a picture of a multi-crystalline silicon cell. Notice the large crystallites. In the late 1970s, it was discovered that good cells could be made with multi-crystalline wafers as long as the crystal size is at least 20 times larger than the optical absorption length [5]. Only those excited state electrons within an optical absorption length from the crystal boundaries are lost. This is less than 5 % of the carriers. Today, the best multi-crystalline Si module efficiency is around 18 %, whereas the best single crystal Si module efficiency is around 23 %. In 2011, modules with multi-crystalline cells accounted for about 45 % of sales and modules with single crystal cells accounted for about 40 % of sales.

Referring again to Fig. 3.7, note that all of the thin film modules have substantially lower conversion efficiencies. The majority of thin film modules produced today are CdTe modules manufactured by First Solar. Figure 3.9 shows a photograph of some of these modules in a field installation [6].

What about the efficiency versus cost trade for thin film modules versus multi-Si modules? According to [7], the spot price on June 17, 2013 for thin film modules was $0.64 per W and for multi-Si modules, the spot price was $0.72 per W. So, thin film modules are in fact cheaper, but one also needs to consider the installed system price. The problem is the module efficiency. From Fig. 3.7, note that the CdTe module efficiency is only 12.8 %, whereas that of a multi-Si module is 18.2 %. The problem at the system level is the installation cost. Almost 50 % more module area is required for the CdTe thin film system. Furthermore, note from Fig. 3.7 that the CdTe thin film modules area of 0.67 m^2 is half the size of the multi-Si module area of 1.47 m^2. All this translates to more bolts, more labor, and more land required for the lower efficiency thin film modules. Another factor favoring efficiency is that residential rooftop area tends to be limited.

www.TechnicalBooksPDF.com



Fig. 3.8 A single polycrystalline silicon PV cell showing the cell grid lines and multi-crystals (*left*), and the installation of several modules on a home rooftop (*right*)



Fig. 3.9 First solar Inc CdTe thin film modules in a field installation in South Western USA, CstSte_Eldorado_0194_ SemprTIF (2011)

Nevertheless, there are niche applications for thin film cell technology. For example, a-Si cells are found in calculators. In this case, thin films have an advantage in being able to easily interconnect from cell to cell to add voltage as is shown in Fig. 3.10. There are also applications for a-Si technology in X-ray medical imaging and in liquid crystal displays [8] as will be discussed further in this book in Chap. 6. Thin film modules may also be useful in Building Integrated PV systems.

However, returning to the dream of low-cost solar electric power making a significant large scale contribution to the world's electric power needs, there is another problem for non-silicon thin film cell technology. As shown in Fig. 3.11, silicon is an abundant element, but tellurium is not [9]. Tellurium is about as abundant as gold and selenium is not much better. Eventually, this will also favor silicon modules.

www.TechnicalBooksPDF.com

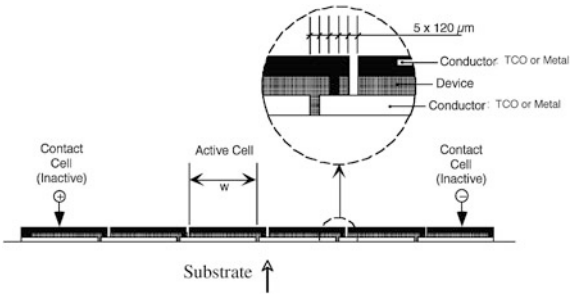


Fig. 3.10 Typical thin film cell monolithic integration scheme for thin film modules

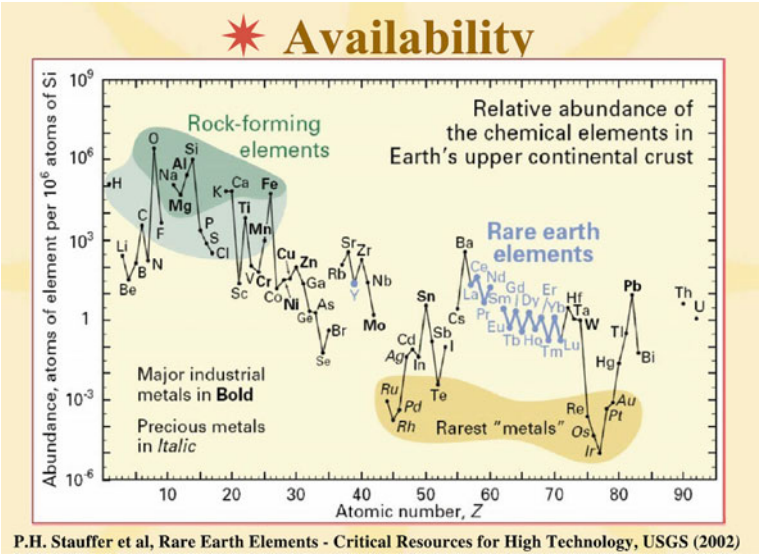


Fig. 3.11 Availability of the elements, Tellurium (Te) is as rare as gold (Au)

The Future and High Efficiency Solar Cells

As shown in Fig. 3.12, the InGaP/GaInAs/Ge 40 % efficient triple junction concentrator cell was first proposed theoretically by Fraas and Kinechtli [10]. This cell was proposed for terrestrial concentrator applications. However, the technology was not available at that time to fabricate it. So, Fraas et al. [11] proceeded to demonstrate in 1990 a 35 % efficient dual junction GaAs/GaSb cell as shown in Fig. 3.13 again with a focus on terrestrial concentrar system applications. While this 35 % cell then motivated funding for work on multijunction cells, work was first performed during the 1990s on demonstrating multijunction solar cells for space satellite applications.

www.TechnicalBooksPDF.com

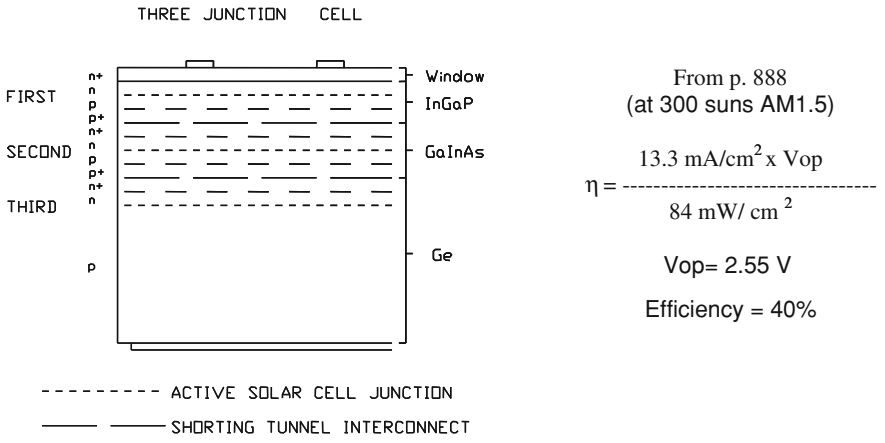


Fig. 3.12 Monolithic triple junction InGaP/GaInAs/Ge CPV cell (Fraas and Kinechtli, 13th IEEE PV Specialist Conference [10]). In 1978, cell efficiency of 40 % at 300 suns AM1.5 was predicted

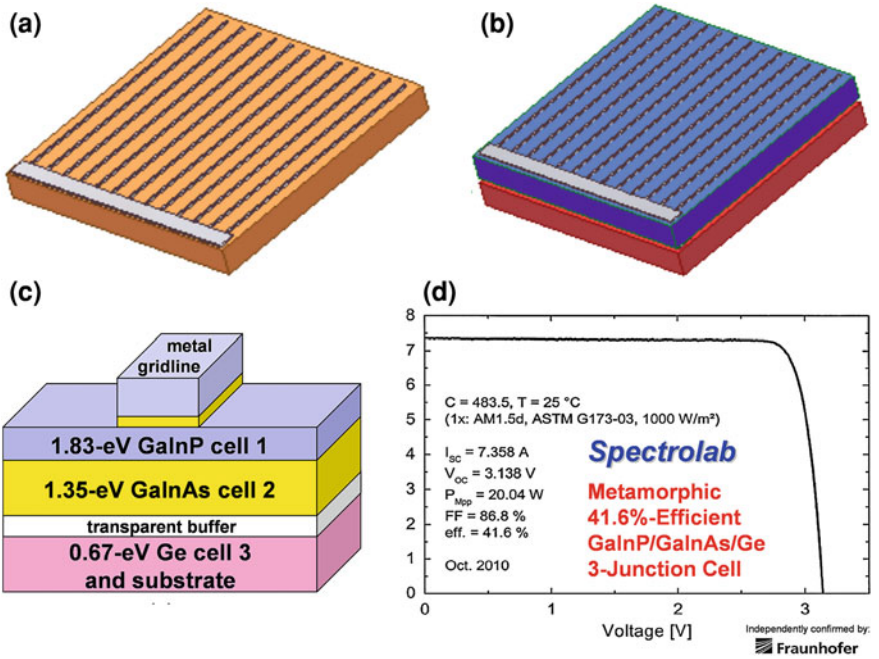


Fig. 3.13 **a** Single junction Si solar cell, **b** the 35 % GaAs/GaSb two junction cell first demonstrated in 1990 [11], **c** NREL and spectrolab three junction cell, **d** the experimental result [12] in 2012 confirmed the prediction made in 1978 [10]

www.TechnicalBooksPDF.com

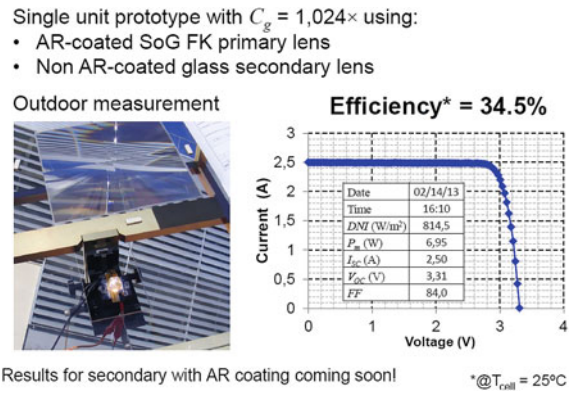


Fig. 3.14 A small 44 % triple junction cell is shown at the *left* in operation at the focus of a sunlight concentrating lens. The result including optical losses is the measured mini-module efficiency of 34.5 % shown at the *right*

Finally, during the first decade of this century, work shifted to cells for terrestrial concentrator systems. Spectrolab with funding from NREL then finally demonstrated in 2012 the InGaAs/GaInAs/Ge triple junction cell as proposed in 1978. The Spectrolab/NREL structure and test results are also shown in Fig. 3.13 [12].

Why did it take so long for the demonstration of a 40 % efficient concentrator cell? Part of the problem is the perceived complexity of CPV systems. More than just cells are now required as shown in Fig. 3.14. Lenses and sun trackers are now required and the systems need to be deployed in very sunny locations. Nevertheless, as shown in Fig. 3.14, cell efficiencies are still increasing now at 44 % [13] and headed higher. Module efficiencies are now at 34.5 % [13]. Because these high concentration PV (HCPV) systems require two axis trackers, they are most suited to large field installations in the 10–100 MW range. The problem for these systems is now component supply-chain management and system scale-up. Just imagine what economies of scale can do for HCPV system cost and the resultant cost of solar electric power.

So the cost of solar electric power now appears to be at the threshold as an economical mainstream electric power source. However, critics will then point out that solar energy is only available when the Sun is shining. There are responses to this criticism. For example, the GaSb infrared cell [14] invented for use in the dual junction CPV application is now available for use with man-made heat sources for distributed combined heat and power applications in homes as shown for the MidnightSun TPV Stove [15] in Fig. 3.15. This technology is called Thermophotovoltaics or TPV [16, 17]. TPV will be described further in Chap. 11. This technology is similar to CPV in that it also requires system integration with other components like burners and matched IR emitters [18, 19]. But again miracles will occur with cost reductions associated with economies of scale.

www.TechnicalBooksPDF.com



Fig. 3.15 JXC Midnight Sun™ TPV Stove co-generates 25,000 BTU per hour (7.25 kW) of heat and 100 W of electricity. JXC GaSb IR PV cells are key enabling elements for TPV

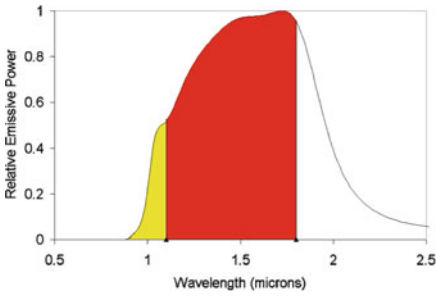


Fig. 3.16 With spectra from man-made heat source, GaSb IR cells respond in *red region* whereas standard silicon solar cell responds only in *yellow region*

Conclusions

The advantage of both planar thin film and planar Si modules is simplicity. This has made planar 1-sun modules popular for residential rooftop applications. In this arena, the efficiency advantage of large crystal size Si modules has made them preferable to the alternate thin film option. Both these 1-sun module options have also been used in large quantities in large field installations by both industrial and utility customers. In this large field installation arena, silicon has again dominated, but First Solar has also been successful because of their skill in marketing and access to financial resources.

While CPV cell efficiencies are now at 44 % and CPV module efficiencies are 1.5 times higher than the best planar modules (34.5/22.9 = 1.5), CPV systems still have some disadvantages. They are both more complex and therefore suited to large system applications and they are most suited to very sunny locations. Nevertheless, they are now being made and installed and tested at the 100 MW level.

www.TechnicalBooksPDF.com

It is odd to note that being most suited to sunny locations is a disadvantage, but this raises indirectly an important point. Government support for the development of solar PV to this point has been very important. It is said that the US invented and proved the Si cell and planar module technology, then Germany created the market through the feed-in-tariff program, and the Chinese invested in the manufacturing infrastructure to bring down the module costs. With this in mind, note that the solar resource in Germany is comparable to that of Alaska in the US. The South Western US has over twice the solar energy resource compared to that of Germany [20]. There is now a great opportunity for CPV in the US.

Unfortunately, the US government has had a policy of supporting military and space systems while ignoring the development of manufacturing in the commercial sector. Both high efficiency multijunction solar cell and TPV cell development demonstrate this point. The three junction cell was first developed for space and the development to date for the GaSb TPV cell has been from NASA, the US Army, and the US Navy. The fuel sources preferred to date have been either nuclear, or diesel, or jet fuel. There has not been any support for the development of TPV systems using the most useful residential fuels of propane or natural gas. The development of the MidnightSun TPV stove in Fig. 3.15 was done with JX Crystals internal funds. TPV could be very complimentary to solar for residential, commercial, and industrial applications (Fig. 3.16), but suffers from lack of investment in manufacturing scale up. TPV could also be important for the cogeneration of electricity in steel mills where hot steel is processed 24 h per day and 7 days a week. Based on annual steel production, this could translate into 10 GW of electric power production from the now wasted heat as steel billets cool.

Government support is still required to build the manufacturing infrastructure to scale up CPV. Once again, the high efficiency cell technology was initially demonstrated in the US. There is now an opportunity for the US government to support CPV system commercial manufacturing with a potential benefit to manufacturing jobs in the US and dramatic cost reductions for solar electric power world wide.

References

1. J. Perlin, *From Space to Earth, The Story of Solar Electricity* (AATEC Publications, Michigan, 1999)
2. L. Fraas, in *Solar Cells, Single Crystal Semiconductors, and High Efficiency*, Chap. 3, Solar Cells and Their Applications, 2nd edn. (Wiley, New Jersey, 2010)
3. D.M. Chapin, C.S. Fuller, G.L. Pearson, A new silicon p-n junction photocell for converting solar radiation into electrical power. J. Appl. Phys. **25**, 676 (1954)
4. Fraunhofer Institute for Solar Energy Systems ISE Photovoltaics Report (Freiburg), www.ise.fraunhofer.de/…/pdf-files/aktuelles/photovoltaics-report.pdf. Accessed 11 Dec 2012
5. H.C. Card, E.S. Yang, IEEE-TED **24**, 397 (1977)
6. First Solar, www.firstsolar.com/Press-Center/Media-Library
7. Mercom Capital Group, SOLAR_JUNE2013_MercomSolarReport24June2013.pdf

www.TechnicalBooksPDF.com

8. L. Fraas, L. *Partain Solar Cells and Their Applications*, Chs. 22–25, 2nd edn. (Wiley, New Jersey, 2010)
9. G.B. Haxel et al., in *Rare Earth Elements—Critical Resource for High Technology*, http://pubs.usgs.gov/fs/2002/fs087-02/ (2002). *Also* in *Cadmium Telluride: Advantages and Disadvantages*, www.solar-facts-and-advice.com/cadmium-telluride.html. Accessed 9 July 2013
10. L.M. Fraas, R.C. Knechtli, in *Design of High Efficiency Monolithic Stacked Multijunction Solar Cells*. 13th IEEE Photovoltaic Specialist Conference (Washington, DC, 1978), p. 886
11. L.M. Fraas, J. Avery, J. Gee et al., in *Over* 35 *% Efficient GaAs/GaSb Stacked Concentrator Cell Assemblies for Terrestrial Applications*. 21st IEEE PV Specialist Conference (Kissimmee, Florida, 1990), p. 190
12. R.R. King, D. Bhusari, D. Larrabee, X.-Q. Liu, E. Rehder, K. Edmondson, H. Cotal, R.K. Jones, J.H. Ermer, C.M. Fetzer, D.C. Law, N.H. Karam, Solar cell generations over 40 % efficiency, Paper Presented at 26th EU PVSEC, (Hamburg, Germany 2011), Progress in photovoltaics: research and applications, Prog. Photovolt: Res. Appl. (2012), Published online in Wiley Online Library (wileyonlinelibrary.com). doi: 10.1002/pip.1255
13. A. Jeff, S. Vijit, W. Mike, Y. Homan, in 44 *%-Efficiency Triple-Junction Solar Cells*. 9th International Conference on Concentrator Photovoltaic Systems ,Miyazaki, Japan, 15 April 2013
14. L.M. Fraas, J.E. Avery, P.E. Gruenbaum et al., in *Fundamental Characterization Studies of GaSb Solar Cells*, 22nd IEEE PV Specialist Conference, vol. 80 (1991)
15. L. Fraas et al., in *Commercial GaSb Cell and Circuit Development for the Midnight Sun® TPV Stove*, 4th NREL conference on thermophotovoltaic generation of electricity, AIP Conference Proceedings, vol. 460 (Denver, Colorado, 11–14 Oct 1998), pp. 480–487
16. T. Bauer, *Thermophotovoltaics: Basic Principles and Critical Aspects of System Design* (Springer, New York, 2011)
17. D. Chubb, *Fundamentals of TPV Energy Conversion* (Elsevier, New Jersey, 2007)
18. L.M. Fraas, J.E. Avery, H.X. Huang, R.U. Martinelli, Thermophotovoltaic system configurations and spectral control. Semicond. Sci. Technol. **18**, S165 (2003). doi:10.1088/0268-1242/18/5/305
19. L.M. Fraas, J.E. Avery, H.X. Huang, Thermophotovoltaic furnace–generator for the home using low bandgap GaSb cells. Semicond. Sci. Technol. **18**, S247 (2003). doi:10.1088/0268-1242/18/5/316
20. Solar resource, http://www.intellectualtakeout.org/library/chart-graph/photovoltaic-solar-resource-united-states-spain-germany

www.TechnicalBooksPDF.com

Chapter 4
Fundamentals of PV and the Importance of Single Crystals

There are several different types of solar cells made from materials ranging from single crystals to amorphous silicon. The goal here is to describe the different types of solar cells and their advantages and limitations. A fundamental description of the nature of semiconductors is presenting beginning with electrons in atoms as waves. The discussion of electrons as waves then leads to a description of semiconductors as single crystals. The theory of single crystal semiconductors is then used to describe how diodes and solar cells work. The effect of various defects in semiconductor materials on solar cell performance follows. Finally, a table of the performances to date of the various types of solar cells is presented. The reader will see that the performances enumerated are consistent with the simple concepts presented. More detailed descriptions of the various types of solar cells will follow in subsequent chapters. This chapter explains why high efficiency cells require good single crystal materials.

Electrons in Atoms as Waves and the Periodic Table of the Elements

The sun's rays are really electromagnetic waves with varying wavelengths. Electromagnetic radiation includes radio waves, microwaves, infrared, visible, and ultraviolet waves. When one thinks about longer wavelength radiation like radio waves, one always thinks about waves. However, for the shorter wavelengths associated with infrared and visible light, physicists start to talk about photons. A photon is like a particle or wavelet having a specific wavelength and energy. A photon is a quantum of energy or discrete packet of energy. Now, is radiation a wave or particle? The answer is both! This is the wave–particle duality, a subject called quantum mechanics [1], a subject normally taught in graduate school physics classes along with a lot of mathematics. Please don't be afraid. The key ideas can actually be described in simple non-mathematical terms and these ideas are important to the understanding of solar cells.

L. M. Fraas, *Low-Cost Solar Electric Power*, DOI: 10.1007/978-3-319-07530-3_4,

© Springer International Publishing Switzerland 2014

www.TechnicalBooksPDF.com

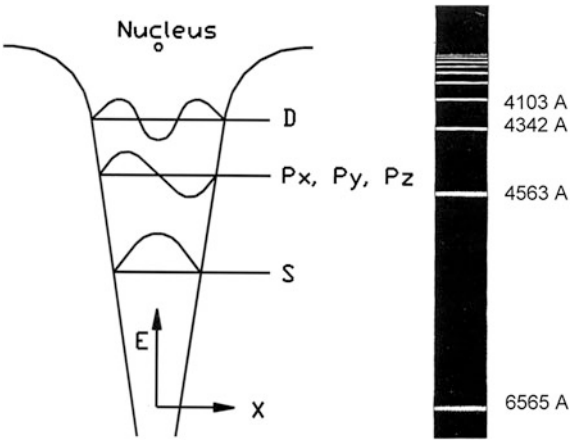


Fig. 4.1 *Left* potential well for electron around nucleus in atom with energy level *S*, *P*, and *D* wave functions. *Right* a spectral line sequence for hydrogen

While one normally thinks of electromagnetic radiation as waves, one generally thinks of electrons as particles circling an atomic nucleus just as planets circle the sun. However, an atom is really extremely small, so small that in crossing a human hair, one will pass by 2,00,000 atoms. Intuition based on everyday experience fails us at this small size. It turns out that electrons around atomic nuclei are described by wave functions. Here is the wave–particle duality again.

However, one can describe the rules that govern electrons in atoms and solids in fairly simple terms. In Fig. 4.1, we start with the simple hydrogen atom with a single negatively charged electron and a single positively charged proton [2]. The oppositely charged proton and electron attract each other and as they get closer and closer to each other, it is harder and harder to pull them apart. The electron is said to be in an energy-well or potential well as shown on the left of Fig. 4.1. The question is then: Can the electron collapse down and sit on the proton? The answer is no. How do we know this? We study the electromagnetic spectra emitted by atoms and we find discrete wavelengths and energies as shown on the right in Fig. 4.1. Not all energies are possible. How is this explained? Scientists hypothesize that the electron position is described by a wave function that then gives its probable position. Since one knows that the electron cannot be outside the potential well, one knows the wave functions have to be zero outside the well. Now, since we are talking about waves, we observe that the waves will have to have one, two, and three (etc.) nodes as is shown in the wells at the left in Fig. 4.1. For historical reasons, the state with one peak node is labeled S, and the states with two nodes are labeled Px, Py, and Pz. (X, Y, and Z are the three direction in 3 dimensional space.) The next rule is that electrons can have positive and negative spin and only one electron can occupy each state. So there will be two S states with opposite spins and two Px, two Py and two Pz states for a total of eight state configurations possible. This wave hypothesis has proven to be very successful as it explains atomic spectra and the periodic table of the elements [3] and all of chemistry.

www.TechnicalBooksPDF.com

The rule of eight including S and P orbitals explains the second and third rows of the periodic table. Table 4.1 is a summary of the important features of the periodic table including the common commercial semiconductor materials. The D level transition metals are not shown since they are not relevant here.

Semiconductors as Crystals

Why is it important to know about electrons as waves? The answer is that waves are intrinsically periodic as are the atom locations in single crystals. It is this periodicity that makes semiconductors special. Historically, the semiconductor revolution started 50 years ago with the discovery of the importance of high purity single crystals and the technology to obtain these high purity single crystals.

However, history is one thing but our goal here is to explain the reasons why single crystals are important to solar cells and to probe the question of how pure and how perfect do solar cell materials need to be. Most importantly, how are we going to make solar cells economical?

Before describing semiconductors, let us return to our periodic table and contrast the semiconductors with metals and insulators to see why semiconductors are special and why they are needed to make solar cells. To preview the answer, we note that in order to deliver electric power, a solar cell needs to generate both current and voltage. Generating current requires electron mobility and generating voltage requires a gap between electron energy states. Metals have electron mobility and insulators have gaps between energy states but only semiconductors have both.

The metals like sodium and magnesium are on the left in the periodic table. These atoms have only a few loosely bound electrons each and they can be tightly packed with up to twelve nearest neighbors. Because the atoms are closely packed, the potential energy well for a metal looks like a flat bottom well with the well bottom extending to the surfaces of the piece of metal. The metal surfaces form the energy barriers confining the electrons. Because this well is so large compared to one atom, all electron wave function wavelengths and energies are possible. Electrons are then free to move around in the metal but there are no energy gaps between energy states. Since the electrons hardly feel the metal atom core positions with the flat bottom potential well, crystallinity is not important to metallic properties.

The elements at the right of the periodic table like oxygen and chlorine have tightly bound electrons and are hungry to grab more. They readily form ionic compounds like salt (sodium chloride) and glass (silicon dioxide). The energy levels in these compounds are much like those of atoms in that the electrons only are excited between atomic energy states. There are gaps in energy but the electrons are not mobile. Crystallinity is not very important since electrons are localized on ions.

www.TechnicalBooksPDF.com

Table 4.1 Periodic table of the elements

I	II	III	IV	V	VI	VII	VIII
H Hydrogen							He Helium
Li Lithium	Be Berilium	B Boron	C Carbon	N Nitrogen	O Oxygen	F Fluorine	Ne Neon
Na Sodium	Mg Magnesium	Al Aluminum	Si Silicon	P Phosphorus	S Sulfur	Cl Chlorine	Ar Argon
		Ga Gallium	Ge German-ium	As Arsenic			
		In Indium		Sb Antimony			

www.TechnicalBooksPDF.com

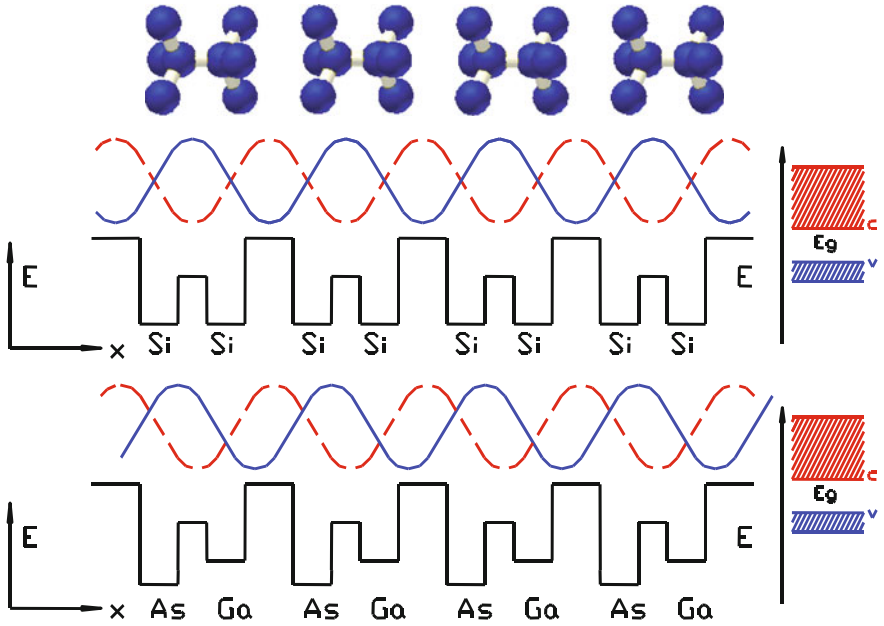


Fig. 4.2 *Top* tetrahedrally bonded silicon atoms in groups along cube diagonal in silicon crystal showing alternate bonded and non-bonded pairs. M*iddle* energy potential for top atom sequence with valence band bonding wave function as *solid line* and conduction band anti-bonding wave function as *dashed line*. *Bottom* the potential and wave functions for GaAs crystal

This brings us to the group IV elements like silicon. The structure of silicon in a silicon crystal is shown in Fig. 4.2. Silicon has 4 electrons and likes to form 4 tetrahedral bonds as shown. Looking at a row of silicon atoms along the diagonal in a silicon crystal, we see alternating bonded and non-bonded spaces between silicon atoms. The energy potential well profile for this row is shown in the middle of this figure along with two wave patterns, one drawn as a solid line and one drawn as a dashed line [3]. The peaks in the solid line wave pattern localize the electrons in the bonded regions with lower average energy potential. Meanwhile, the peaks in the dashed line wave pattern are localized in the non-bonded regions with higher average energy. However, both waves allow the electrons to be near any silicon pair in the crystal implying electron mobility throughout the crystal. Because of the periodic nature of the atomic positions in a single crystal, the wave functions allowed describing the electrons in a single crystal must have a corresponding wavelength. Thus the two types of states with bonding and anti-bonding electron locations between nearest silicon pairs or farthest silicon pairs are the only states allowed. There is an energy gap between these states because no other electron wave functions are allowed. The states representing the bonding states form what is called the valence band and the states representing the anti-bonding states form what is called the conduction band.

www.TechnicalBooksPDF.com

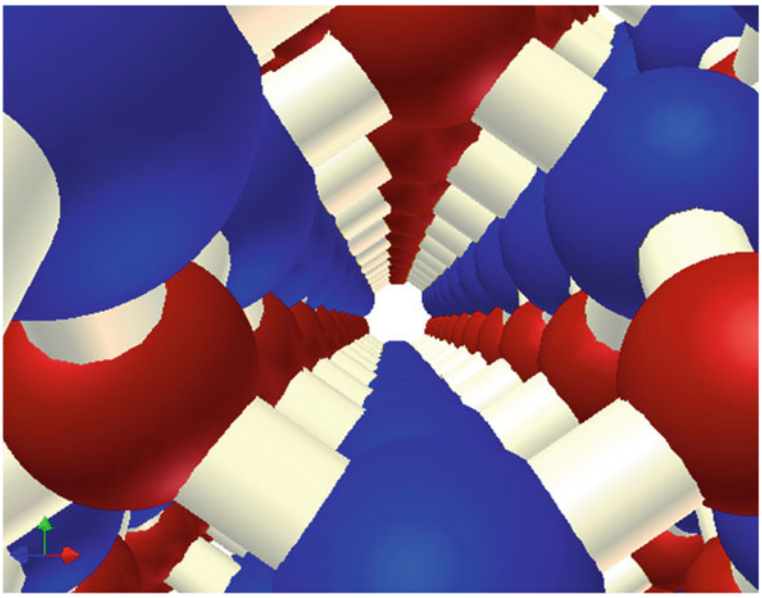


Fig. 4.3 A view of a channel open for conduction electron movement in a GaAs single crystal. *Small sphere* Gallium atom; *Large sphere* Arsenic atom; *White cylinders* valence bonds

Figure 4.2 also shows the energy potential and wave functions for a group III–V semiconductor. In this case, a group three (III) element like gallium can form tetrahedral bonds with a group five (V) element like arsenic where the result is the sharing of 4 electrons per atom as in silicon. The III–V's are a rich class of semiconductors.

It turns out that because of the crystal periodicity, there is both an energy gap and electron mobility in semiconductors. Figure 4.3 allows us to visualize this more easily.

In this figure, one can see both connected bonded regions and open channels in between. One can imagine electrons traveling in the bonded regions or separately in more energetic states in the open channels. Propagating electrons in the bonded region have energies in a valence band and propagating electrons in the open channels have energies in a conduction band. The separation between these regions provides the energy gap. Looking at Fig. 4.3, one can also imagine a large foreign atom or a crystal boundary or defect interfering with flow in the channels or a total disruption of the channels smearing the two sets of energy states into each other.

Figure 4.3 suggests intuitively that electrons will have higher mobility in single crystals than in amorphous or small crystal size thin films. This is in fact true quantitatively. Electron mobility is easily and routinely measured. The electron mobility in single crystal silicon is typically 1,500 cm^2/Vsec and in single crystal gallium arsenide, it is 4,500 cm^2/Vsec [4]. However, in amorphous silicon and

www.TechnicalBooksPDF.com

copper indium diselenide (CIS), two common thin film solar cell materials, it is only 4 cm^2/Vsec. This is a difference by a factor of 1,000 consistent with our intuitive expectations based on Fig. 4.3.

Junctions and Diodes

We have now established that carriers are mobile allowing current to flow in solar cells. How do we use an energy gap to create voltage. We need a P/N junction (P = Positive, N = Negative).

In the above description of electron movement in semiconductors, we need now to add that it is important to count electrons. If the semiconductor is very pure (a state we call intrinsic), then all of the bonding states will be occupied by electrons and there will be no electrons to move in the conduction band. Electrons can not move in the valence band either because there are no empty spaces to move to. Substituting a small number of phosphorus atoms for silicon atoms can rectify this problem (one in a million). Since phosphorus is from group V, it has one more electron than silicon. The resultant material is labeled N-type because the extra electrons are negatively charged.

Alternately, as a complement to our N-type material, we can substitute an aluminum atom for a silicon atom leaving the bonding or valence band one electron deficient because aluminum from group III has one less electron than a silicon atom. Now instead of thinking about a million electrons in the valence band, we talk about the missing electrons in the valence band. We call this a hole. It is like watching a bubble move in water. The hole has a positive charge and we call this material P-type.

Now what happens when N-type material and P-type material are brought together? The result is a P/N junction diode [4, 5] as shown in Fig. 4.4. The band edge diagrams at the bottom of this figure describe how a diode works. When the P region and N regions first come together, the electrons and holes from each side diffuse together eliminating each other leaving an electric field region in the junction. This happens until the valence band edge (v) in the P material almost lines up with the conduction band edge (c) in the N material as shown on the left in this figure. At this point, the free electrons and holes on both sides of the junction have the same energy as shown by the dashed horizontal line. This is the zero voltage band diagram (A). Now notice that there is an energy hill for electrons to climb in order to move from the N to P side of the junction. An applied voltage can either decrease this hill or energy barrier for forward bias (B) or increase it in reverse bias (C). If the hill is made small enough by a forward voltage about equal to two-thirds (67 %) of the band gap energy, eg, then current starts to flow. This corresponds to the knee in the diode current versus voltage curve shown at the top right in this figure. In reverse bias, no current flows because the barrier just gets bigger. Thus a diode is a rectifier allowing current flow in only one direction.

www.TechnicalBooksPDF.com

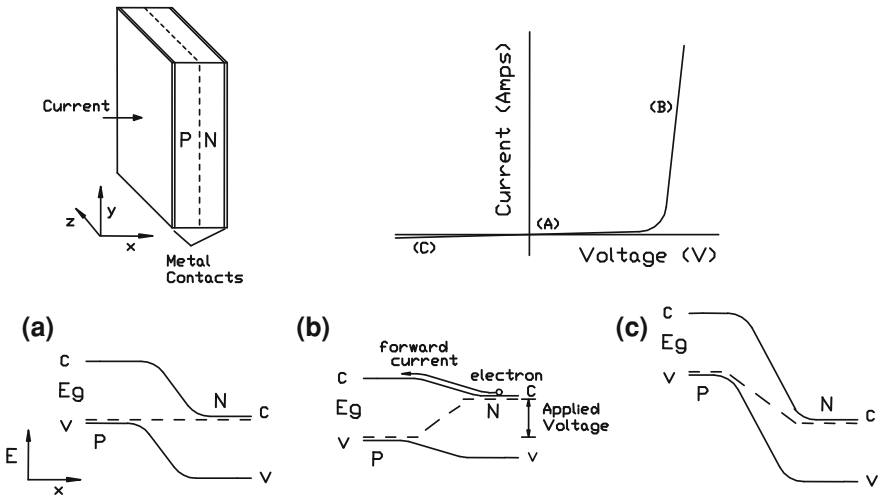


Fig. 4.4 *Upper left* P/N junction diode; *upper right* current versus voltage for P/N diode. *Lower left* conduction band minimum and valence band maximum positions through P/N junction at zero applied voltage. *Lower middle* forward voltage band diagram = reduced barrier for high current flow. *Lower right* reverse voltage = barrier blocks current flow

Solar Cell Band Diagrams and Power Curves

Referring now to Fig. 4.5, a solar cell is just a large P/N junction diode with a metal grid on its front side facing the sun. A solar cell converts the energy in sunrays to electric power. Now we shall refer to the sunrays as photons. In Fig. 4.5, the now familiar band edge diagrams are shown at the bottom. These band edge diagrams show how a solar cell works. First, a photon is absorbed exciting an electron from the ground state or valence band in the P material to an excited conduction band state. It is mobile in the conduction band and if it lives long enough in this excited state, it can diffuse to the junction and fall down the potential barrier to provide solar cell current.

Solar cell voltage performance in high efficiency devices is largely controlled by the semiconductor band gap, the recombination velocity of the potential well walls and the operating temperature. In most crystalline silicon solar cells and other lower performance crystalline and non-crystalline devices this potential well wall is an ohmic contact with a very high recombination velocity often approximated as infinity [6]. Such unprotected ohmic contact walls contribute to the solar cells' output voltages being increasingly below bandgap values. Fortunately the double heterostructures available for direct bandgap semiconductors allows for simultaneous achievement of ohmic contacts and low recombination velocity. This is particularly effective because of the close crystal lattice matching or perfection that can be achieved. This advantage becomes most dramatic when the incident sunlight is absorbed into 2 or 3 bands of different colors when solar cell junctions

www.TechnicalBooksPDF.com

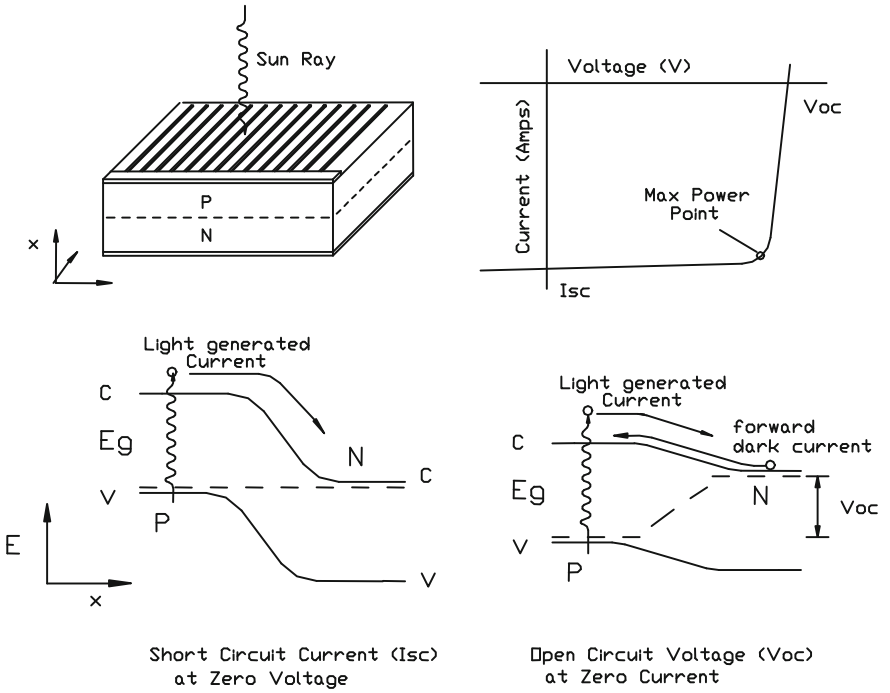


Fig. 4.5 *Upper left* P/N junction solar cell with metal grid on *top*. *lower left* photon absorption excites electron into conduction band. Electron then falls through junction potential. *Upper* and *lower right* current versus voltage *curve* for solar cell is diode I versus V *curve* moved *down* by light generated current

of different bandgaps are stacked one on top of each other. This stacking color separation works best in direct bandgap materials with sharp absorption edges. The gradual absorption band edges of indirect semiconductors like silicon interfere with efficient color separation. So far only stacked junction, direct bandgap semiconductor solar cells have shown dramatically higher efficiencies than the best single junction, single crystal silicon devices that have reduced areas of ohmic contacts.

High Efficiency and Multijunction Solar Cells

How efficient can a solar cell be and how do we achieve these high efficiencies? Theoretically, a solar cell efficiency of 70 % is possible. However, no one believes that, in practice, this can be achieved. Still, a 40 % efficient solar cell has been demonstrated and 50 % is probably an achievable target.

www.TechnicalBooksPDF.com

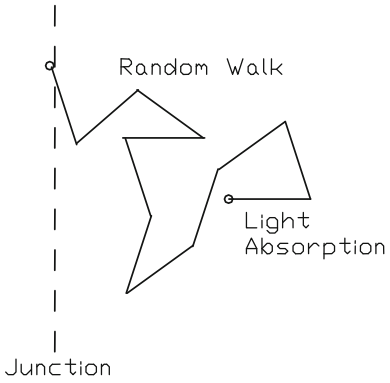


Fig. 4.6 A light generated carrier diffuses to the junction in a random walk sequence

What needs to be done to achieve high efficiencies is a more interesting question. In fundamental terms, three things need to be done. First, for each photon absorbed, the excited state carrier generated needs to last long enough to be collected at the junction. Second, while the sun's spectrum contains photons of different energies, the energy available in each photon must be used as wisely as possible. And third, the voltage a cell generates should be as close as possible to the bandgap energy. We will discuss each of these requirements in succession in the following paragraphs.

The first requirement of one electron collected for every photon absorbed implies single crystal material and high purity material. The measure of electrons collected per photon absorbed is called quantum efficiency. Anyway, Fig. 4.6 provides a semi-quantitative answer to the semiconductor purity question. To understand Fig. 4.6, let's go back to the crystal channels shown in Fig. 4.3. First, how far will an electron move through one of these crystal channels. The answer is about one hundred atomic spacings. This is because the atoms are not really stationary but are vibrating small distances around their home positions because they have thermal (heat) energy. This vibration energy is small, however, so that the excited electron does not return to the valence band but just gets deflected into another channel. We think of this deflection as a step in a random-walk diffusion problem. This brings us back to Fig. 4.6.

The next question is how far is the excited state carrier away from the junction? This depends on the photon absorption distance. This absorption distance depends on the material and the rules for photon absorption. Now we shall divert for a minute to the rules for photon absorption. This will be important because, as we will see, silicon is fundamentally different from the III–V semiconductors in its photoelectric properties.

Let's return quickly to the hydrogen atom in Fig. 4.1. A rule for photon absorption is that the wave functions involved have to have different symmetries. For example, note that the S and D wave functions are symmetric around the position of the nucleus while the P functions are anti-symmetric. Thus, absorption between S to P and P to D are allowed but S to D is not allowed. Now let's look at

www.TechnicalBooksPDF.com

the wave functions for silicon and gallium arsenide (GaAs) in Fig. 4.2. Note that both wave functions for silicon are symmetric around the point between two silicon atoms. This means that photon absorption in silicon is not allowed to first order. In GaAs, however, photon absorption is allowed.

So the photon absorption length in GaAs is about 10,000 atomic spaces. In reality, photons are also absorbed in silicon but in about 1,00,000 atomic spaces. This second order absorption in silicon results because of atomic thermal vibrations.

Now, we can return to the purity question and the random walk diffusion problem. Remember that a step length is about 100 atomic spaces. So a carrier in GaAs will be about 100 steps away from the junction and a carrier in silicon will be about 1,000 steps away. However, in a random walk problem, the number of steps required to move N steps away from the start is N x N steps. So the distance an excited electron must travel to the junction in GaAs will be 10,000 steps or 1 million (1,000,000) atomic spaces. If it were to see a large impurity in a channel on this path, it could return to the valence band and be lost. So the purity requirement for GaAs is about 1 part per million. The analogous argument for silicon suggests a purity requirement of 10 parts per billion. In fact, silicon solar cells lose performance given transition metal impurities in the range of several parts per billion. The above argument has been a little tedious but the goal is to impress the reader with this purity requirement. By analogy, it should also be clear that good single crystal quality without defects is as important as purity.

The above purity specification is routinely met in commercial single crystal silicon solar cells today as well as in various other single crystal silicon based devices that have revolutionized our lives over the last 50 years. While the reader is probably not aware of it, various single crystal III–V devices have penetrated our everyday lives as well in the last 10 years. As the above argument about the difference in photon absorption for GaAs versus silicon suggest, the III–V are often a better choice for photoelectric and optical-electronic applications. Referring to the periodic table, there are a large number of III–V materials available including GaAs, InP, InSb, and GaSb. Additionally, alloys of these materials are available including AlGaAs, GaAsP, InGaAsP, etc. This makes a large set of band gaps and electron mobilities available. Single crystal III–V devices can now be found in cell phones, satellite receivers, CD music players, CD-ROMs in personal computers, taillights in cars, traffic stoplights, and military weapon systems. Single crystal III–V devices are also key components in fiber optic phone communication and the internet.

In fact, the most efficient solar cells are made using III–V materials. This brings us back to our second requirement for making high efficiency solar cells. We need to use the energy in the sun's varied colored rays as efficiently as possible. A problem with sunlight is that the photons come in different colors with different associated energies. If we wanted to maximize the efficiency of a photodiode, we would illuminate it with only photons with a single energy with an energy equal to the bandgap energy, eg. Then if the crystal quality and purity were sufficient, all of the excited carriers would be collected at the junction with 67 % of the photon energy being delivered as a voltage. The energy conversion efficiency would be roughly 67 %.

www.TechnicalBooksPDF.com

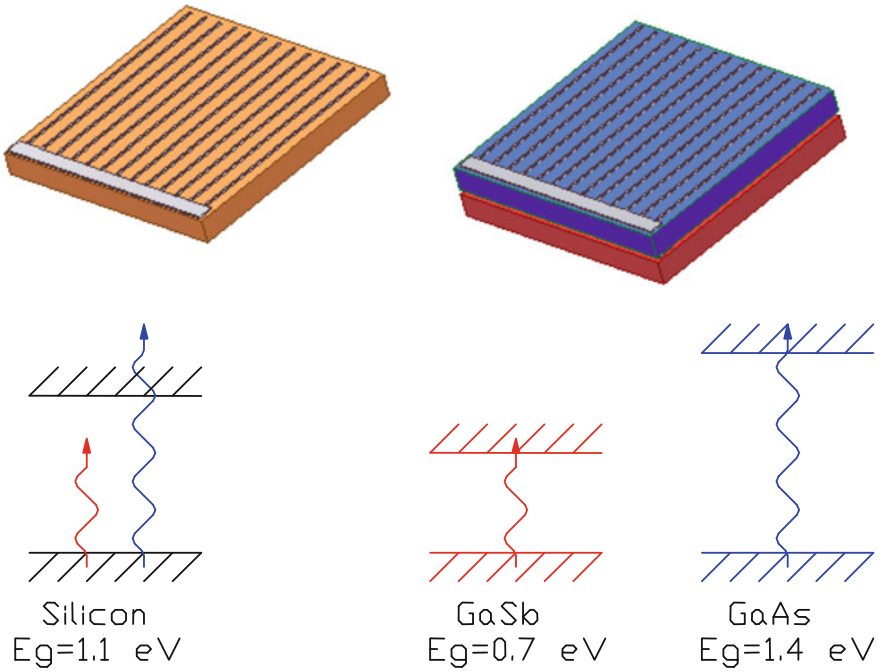


Fig. 4.7 *Left* for single junction solar cell, sunlight contains high energy photons with excess energy and low energy photons with too little energy. *Right* solar spectrum can be more efficiently utilized by stacking two different junctions together

However referring to Fig. 4.7, photons from the sun come with different energies. Some of the photons have too little energy to be absorbed and some of the photons have energy considerable in excess of the bandgap energy. For the sun's spectrum, this limits the single junction solar cell efficiency to less than 30 %. However, the III–V's offer a solution because various materials with various bandgap energies are available. Specifically, one can stack a visible light sensitive GaAs solar cell with metal grids on its front and back on an infrared sensitive GaSb solar cell to arrive at the two color or two junction solar cell shown at the right in Fig. 4.7. In this way, one absorbs the high-energy photons first in the top material generating a high voltage while the low energy photons pass through the top cell to be converted in the bottom cell. More photons are used and they are used more wisely. This then is the world record 35 % efficient GaAs/GaSb two color or two junction solar cell.

This brings us to the third way of increasing solar cell efficiency. For a given bandgap energy, we want to generate more voltage. Concentrating the sunlight onto the cell can do this. This is shown in Fig. 4.8. Sunlight can be concentrated using a lens as is shown at the left in this figure. The resulting currents versus voltage curves with and without a lens are shown at the right. As is customary for solar cells, the diode curves here have been flipped over. Note that the higher

www.TechnicalBooksPDF.com

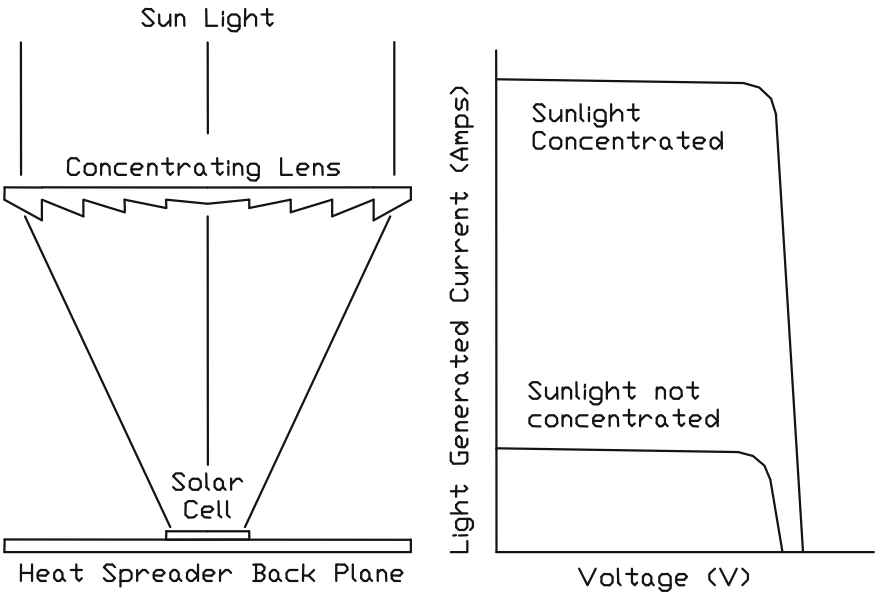


Fig. 4.8 Solar cells are more efficient with concentrated sunlight because both current and voltage increase

current concentrator cell has a higher efficiency. This is because the diode is being driven harder to a higher current and voltage. In other words, if the light level goes up by 10, the current also goes up by 10 but at the same time, the voltage also goes up. In practice, the open circuit voltage can go up from about two-thirds of eg to about three-quarters of eg under concentrated sunlight.

Types of Solar Cells and Cost Trades

The idea of producing cost competitive electric power using photovoltaic (PV) cells or solar cells in sunlight here on earth has been the dream of the PV community since the oil embargo in the early 1970s. In the decade of the 70s, three approaches to solving this problem were formulated.

The first approach, the planar crystalline silicon approach, was simply to bring down to earth the silicon solar panels used on satellites with straight forward improvements in manufacturing. In these planar modules, 90 % of the illuminated area is single crystal silicon cell area. This approach has come a long way in cost reduction with improvements like large grain size cast polycrystalline silicon ingots, screen-printed grid lines, and wire saws. This approach dominates the terrestrial solar cell market today.

www.TechnicalBooksPDF.com

Table 4.2 Types of solar cells and solar module efficiencies solar module efficiencies

Solar cell type	Module efficiency (Practical test conditions)(%)
Mono-crystalline silicon	19
Multi-crystalline silicon	15
Amorphous silicon thin film	9
Small grain size CIS thin film	10
Small grain size CdTe thin film	10
Single crystal silicon concentrator	24
Concentrator III-V	34

In the second approach, the thin-film PV approach, researchers observed that single crystals, like gemstones, are intrinsically expensive. Wouldn't it be nice if one could find a thin-film as cheap as paint that could produce electricity in sunlight. They dropped the single crystal cells in search of a thin-film cell material that would generate electricity inexpensively and efficiently. The problem they encounter is that the non-single-crystal materials have reduced cell conversion efficiencies. The National Renewable Energy Lab in the US has led the development of this PV technology.

In the third approach, the solar concentrator approach, researchers observed that one could concentrate the sunlight onto a small single crystal cell with an inexpensive lens or mirror and reduce the impact on cost of the single crystal gemstone. This approach is depicted in Fig. 4.8. It should be noted that this concentrator approach is most appropriate in sunny locations because the optics need to see the sun and track it in order to keep the sun focused on the cells. In this book, it is argued that this will be the lowest cost approach in the long term.

The status today of module efficiencies under outdoor sunlight measurement conditions is summarized in Table 4.2 for these three approaches. In this table for purposes of comparing these various different technologies, we summarize module efficiencies, not cell efficiencies where the modules are groups of cells wired together with a module solar collector area of at least 100 cm^2. This eliminates the odd small research scale single cell measurement. The first two rows in this table show typical efficiencies for planar large crystal size silicon solar cell modules. The efficiency of 19 % is for the case when the whole cell is single crystal. The second row efficiency is for the case when a cell has multiple crystals within its area but each crystal is at least 20 times larger than the optical absorption length. In this case, the module efficiency falls off slightly to 15 %. Planar modules based on single crystal silicon account for over 90 % of today's terrestrial commercial solar cell market. These modules will be discussed in more detail in Chap. 5.

The efficiency in the third row is for amorphous-silicon film cells. The module efficiencies in the next three rows are for various thin film options. The module efficiency for the amorphous silicon case is only 9 %.

The module efficiencies in the last two rows are for concentrator solar cell systems. These efficiencies are markedly higher than the others at over 20 % for

www.TechnicalBooksPDF.com

single crystal silicon cells and over 30 % for single crystal III–V multicolor cells. These efficiencies are much higher for the reasons described in the last section of this chapter and because using a lens or mirror concentrator allows one to separate the two apparently contradictory requirements for solar modules of lower cost and higher performance into two separate elements. With concentrators, the lens or mirror is the large area low cost collector whereas the small cells are the high efficiency converters. Given this separation of functions, the cells can cost more per unit area for higher performance but their small size relative to the lens area dilutes their cost impact on the total system cost. We shall describe these high power density photovoltaic concentrator cells in more detail in Chap. 7.

The standard operating condition efficiencies listed in Table 4.2 give useful first order estimates of performance in the field. However actual field performance of different cells types at different geographical locations vary substantially [7]. Field efficiency gives the most accurate comparisons. This is the AC power delivered in kWh/m^2 per year from a solar cell module divided by the sunlight energy striking that module as measured by an onsite periheliometer. Early estimates of concentrator field efficiencies gave higher efficiencies but somewhat lower than expected from Table 4.2 type of comparisons [8]. However concentrator systems are still in their early stages of development and their field performance is expected to improve with time and experience.

The Importance of Single Crystals

Given that 35 % efficient solar cells were demonstrated in 1989, why are they not commercially available in 2003. One of the reasons is that for the last 25 years, the solar R&D community has spent over 80 % of the available R&D funding on thin film solar cells. Why? One answer is that searching for a 20 % efficient low cost thin film solar cell is a very attractive dream. However in this chapter, we have talked about electrons as waves and semiconductors as crystals to convey the message that this dream is not well founded on scientific principles. In fact, in graduate school solid-state physics classes, the bandgap in semiconductors is rigorously derived based on the assumption of the perfect periodic single crystal lattice.

However, the importance of single crystals to semiconductor devices is not generally conveyed in a simple understandable way. It is certainly not knowledge available to funding sources or the financial community. Figure 4.9 is an attempt to rectify this situation by making an analogy between an electron traveling in a solid and a car traveling through a forest.

Organizing the atoms in single crystals is like removing the trees to make a road through a forest. Atoms out of place or atomic impurities are obstacles for the electron just like trees are obstacles for a car. Collisions with these obstacles force the electron (or the car) to lose energy. Efficiency is dramatically reduced. In any

www.TechnicalBooksPDF.com

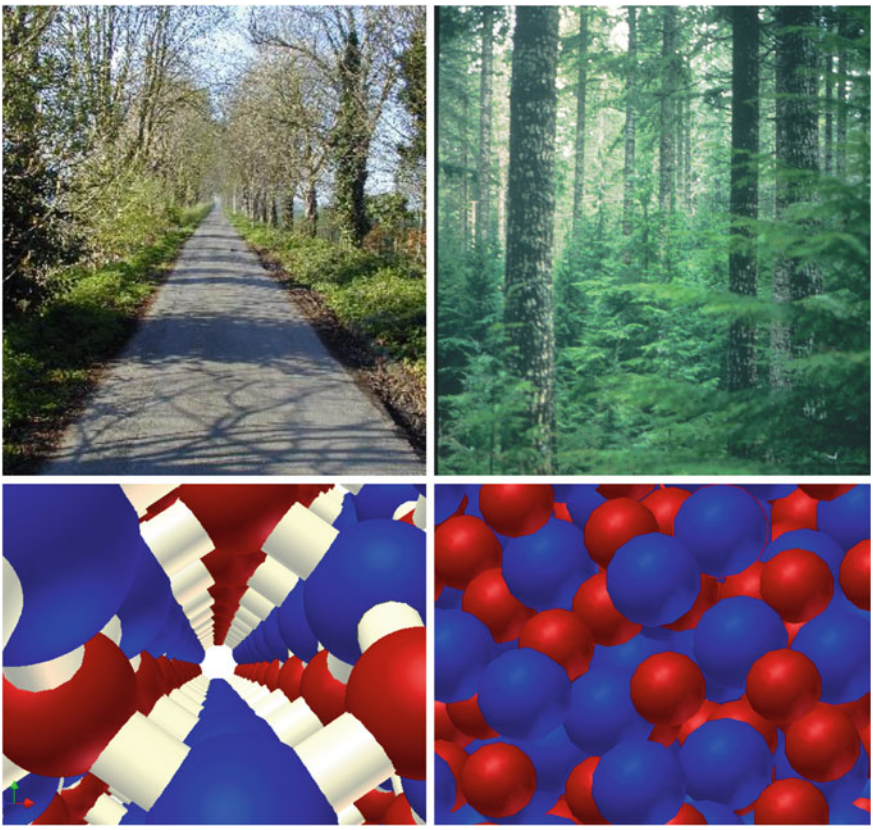


Fig. 4.9 Single crystal versus thin film solar cells "If you were a car driving through the national forest, or an electron passing through a solar cell, which path would you rather take?"

case after 25 years of effort on thin film solar cells, their module efficiencies are still low and they have not replaced the mainstream crystalline silicon module.

Concentrator solar cells are not yet main stream either. There are several reasons for this but it is not for lack of performance. The technology for solar concentrators is well founded on established scientific and engineering principles. One of the problems for concentrators is that a larger investment is required. Investment is required both for hardware like lenses and trackers as well as for new solar cell manufacturing facilities.

A problem faced by solar now is that the focus on non-crystalline thin films has robbed very limited resources from the solar concentrator alternative. The failure of thin film modules in the market place made investors think that all solar options are bad. Many still remember the SOLYNDRA failure which was a thin film technology (CIGS) failure [9]. A refocus of efforts on concentrators can reverse the

www.TechnicalBooksPDF.com

negative funding spiral with successes in the sunny southwestern US leading to ever expanding markets. Market sales can then support more R&D aimed toward longer-term dreams. Hopefully this chapter and this book will educate more of the public on the physics of solar cells so that investors and government decision makers can distinguish between the good and bad solar technology choices.

References

1. R.P. Feynman, R.B. Leighton, M. Sands, *The Feynman Lectures on Physics*, vol. 3—Quantum Mechanics, (Addison-Wesley, Reading, 1965)
2. R.P. Feynman, R.B. Leighton, M. Sands, *The Feynman Lectures on Physics*, vol. 3,—Chapter 19: "The Hydrogen Atom and the Periodic Table" (Addison–Wesley, Reading, 1965)
3. J. M. Ziman, *Principles of the Theory of Solids*, Chapter 3—"Electron States", (Cambridge University Press, Cambridge, 1964), pp. 72–74
4. S. M. Sze, *Physics of Semiconductor Devices*, (Wiley-Interscience, New York, 1969)
5. C. Kittel, *Introduction to Solid State Physics*, (Wiley, New York, 1967)
6. L. Partain, *Solar Cell Device Physics in Solar Cells and Their Applications*, eds. by L. Fraas, L. Partain (Wiley, Hoboken, 2010), p. 78
7. D. King, W. Boyson, J. Kratochvil, *Analysis of Factors Influencing the Annual Energy Production of Photovoltaic Systems,* Proceedings 37th Photovoltaic Specialists Conference Seattle, 2011, pp. 1356–1361
8. L. Fraas, L. Partain, *Summary, Conclusions and Recommendations in Solar Cells and Their Applications,* eds. by L. Fraas, L. Partain (Wiley, Hoboken, 2010), p. 594
9. http://en.wikipedia.org/wiki/Solyndra

www.TechnicalBooksPDF.com

Chapter 5
Terrestrial Silicon Solar Cells Today

The crystalline silicon solar cell and module dominate the terrestrial solar market today. While the silicon cell had been used in space since 1958, it was not brought down to earth for terrestrial applications until 1975 when Bill Yerkes left Spectrolab and formed Solar Technology International (STI) . The ownership of that pioneering company has changed hands several times, and it has now become SolarWorld [1]. STI developed the screen printed grid solar cell and the laminated glass module used by everybody today. Figure 5.1 shows a timeline for the terrestrial silicon module technology and market development. Figure 5.2 shows a photograph of a section of an early STI crystalline silicon (c-Si) module circa 1980.

Figure 5.3 shows photographs of today's evolved c-Si modules. A SolarWorld 14.9 % efficient module [2] is at the left with the best available Chinese 15.9 % efficient Yingli [3] module in the middle. These two modules are almost identical. The module at the right is a SunPower 19 % efficient module [4] with innovative higher efficiency c-Si cells.

While SolarWorld has definitely been a pioneer in the c-Si module technology and market development, in recent years, Chinese module manufacturers have taken market share and they now dominate the c-Si solar market as shown in Figs. 5.4 and 5.5.

As shown in Table 5.1, the reason that the Chinese module manufacturers have taken market share is because the Chinese government has given major financial support to the Chinese solar industry. Loans and Credit Agreements by Chinese Banks to Chinese solar companies in 2010 totaled $40.7 billion [5].

It is easy to understand why SolarWorld, the pioneering solar company, filed Anti-Dumping and Anti-Subsidy cases against China. What is involved here is a clash between the Western free enterprise model and the Chinese Government Industrial planning model. One can see both points of view here. The Chinese Government support model has advanced the world case for renewable energy but it has also been unfair to Western innovators like SolarWorld. Problems like this will continue but hopefully can be worked out amicably.

L. M. Fraas, *Low-Cost Solar Electric Power*, DOI: 10.1007/978-3-319-07530-3_5,

© Springer International Publishing Switzerland 2014

www.TechnicalBooksPDF.com

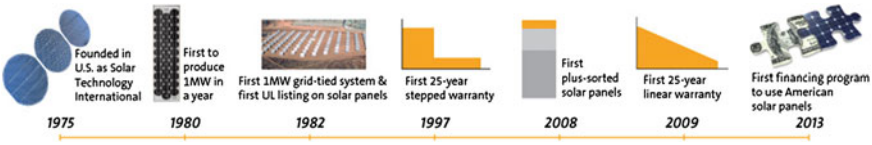


Fig. 5.1 Timeline of solar industry firsts at SolarWorld [1]

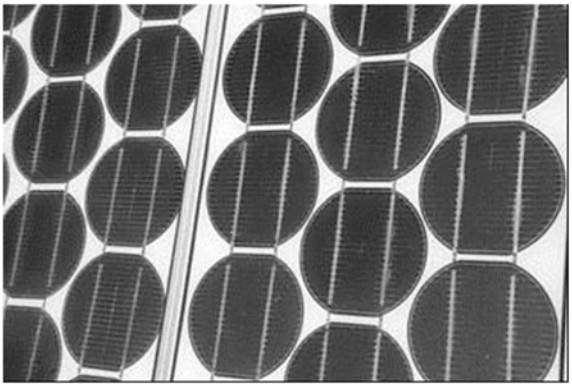


Fig. 5.2 Photo of 1980 STI solar panel (courtesy Jim Avery)

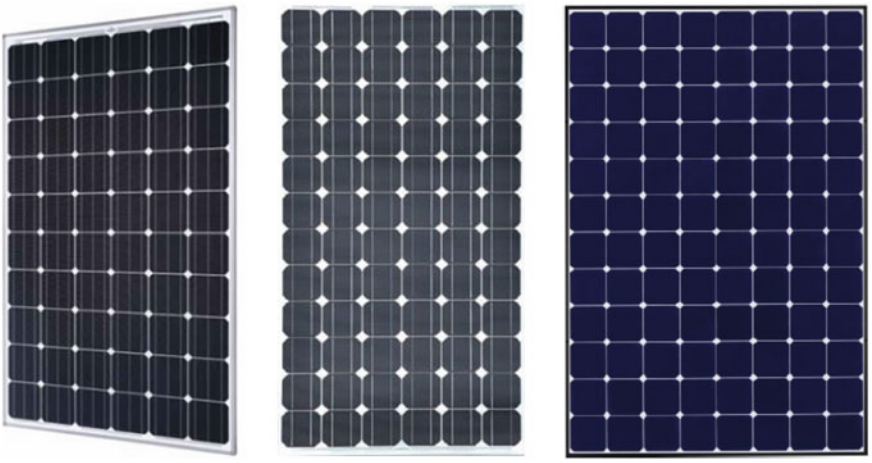


Fig. 5.3 C-Si modules with SolarWorld (*Left*), Yingli (*Middle*), and SunPower (*Right*)

Meanwhile, there are now multiple suppliers of c-Si modules at low cost and there are now multiple terrestrial applications for these modules as shown in Figs. 5.6 and 5.7.

www.TechnicalBooksPDF.com

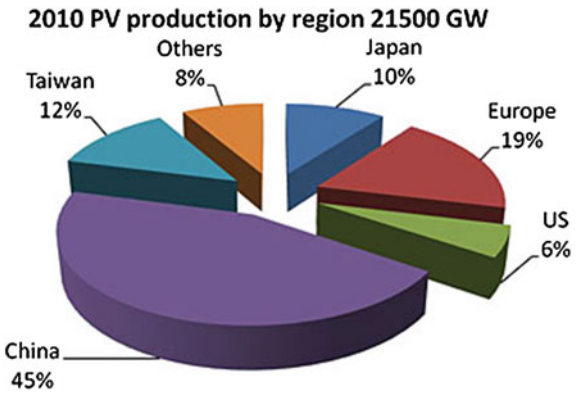


Fig. 5.4 PV production by region in 2010 [9]

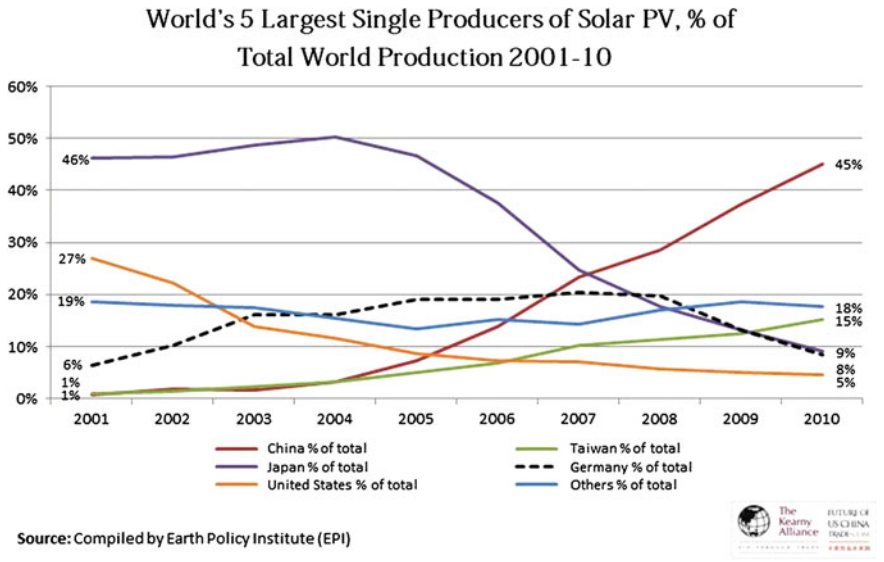


Fig. 5.5 China is capturing share in PV module manufacturing [10]

The modules shown in Figs. 5.6 and 5.7 are now a mass produced commodity. The module production processes subdivide into silicon wafer production steps followed by solar cell production steps followed by module assembly steps as shown in Fig. 5.8. Professor N. Cheung from UC Berkeley has posted an excellent presentation on Solar Cell Fabrication Technologies on the web [6]. This presentation is the source for Figs. 5.8, 5.9, 5.10, and 5.11.

www.TechnicalBooksPDF.com

Table 5.1 Loans and credit agreements involving chinese banks to chinese solar companies since Jan 2010

Company	Amount ($M)	Banks
China Sunergy	160	China Development Bank
Daqo New Energy	154	Bank of China
Hanwa SolarOne	1,000	Bank of China
Hanwa SolarOne	886	Bank of Shanghai
JA Solar	4,400	China Development Bank
Jinko Solar	7,600	Bank of China
LDK Solar	3,900	China Development Bank
Suntech	7,330	China Development Bank
Trina Solar	4,400	China Development Bank
Yingli Green Energy	179	China Citic Bank. Bank of China
Yingli Green Energy	5,300	China Development Bank
Yingli Green Energy	144	Bank of Communications
Yingli Green Energy	257	Bank of Communications
Total	40,709	

Source Mercom Capital Group, llc
All amounts miilions of dollars
[a] As of Sept. 26.2011



Fig. 5.6 SunPower modules on a home [11]

More detail on the wafer fabrication steps is shown in Fig. 5.9. Wafer fabrication subdivides into either crystal growth or ingot casting with the result being either single crystal wafers or large grain size polycrystalline wafers.

For either wafer case, the standard cell fabrication then begins involving a diffused step to create the P/N junction, an electric current collection grid fabrication step, an antireflection coating step, and a back contact metallization step as shown in Fig. 5.11.

www.TechnicalBooksPDF.com



Fig. 5.7 Partial view of 1.5 MW SunPower Oasis power block in 250 MW California Valley Solar Ranch project at San Luis Obispo, CA [12]

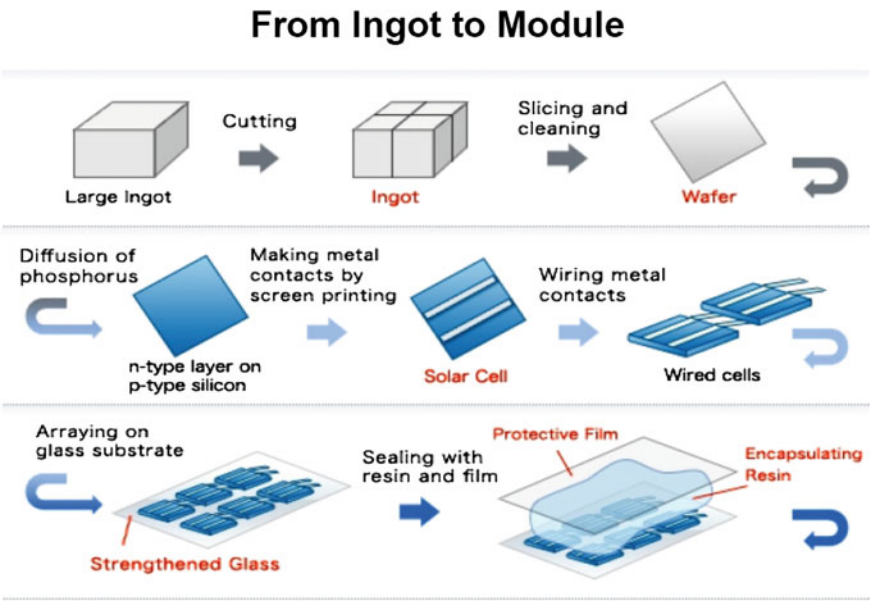


Fig. 5.8 c-Si solar cell and module fabrication [6]

www.TechnicalBooksPDF.com

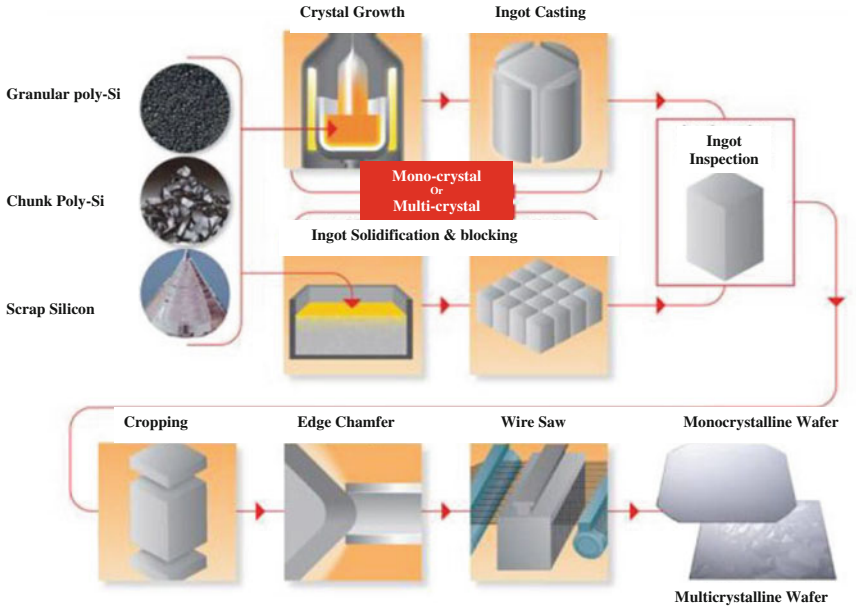


Fig. 5.9 There are two paths for Si wafer fabrication resulting in single crystal or multicrystalline wafers [6]

Once the cells are prepared, they are then wired together in series with soldered leads and laminated with glass into the final module. An advantage for China is that this can be done by hand with low-cost labor. Alternatively, it can be done with automated equipment as shown in Fig. 5.12.

So, c-Si module prices have dropped dramatically but what is now possible for the future? Today's modules made via the processes outlined in Figs. 5.9, 5.10 and 5.11 have efficiencies in the 15 % range. However, higher module efficiencies are possible using higher purity silicon feedstock and cell fabrication modifications. Cell efficiencies in the 22 % range are now available. One example is the HIT module described in the next chapter. Another example is the interdigitated-back-contact cell [7] made by SunPower shown in Fig. 5.12. Higher efficiency cells will produce more energy and reduce system costs provided that they are not too expensive themselves. However, there is a solution if the higher efficiency c-Si cells are more expensive in that one can break these cells into smaller cells and use lenses or mirrors to concentrate the sunlight as shown in Figs. 5.13 and 5.14. Figure 5.13 shows this concept for a 2× concentration and Fig. 5.14 shows SunPower's 7× sunlight concentration C7 system [8]. This is a very promising approach as discussed later in Chap. 7.

As shown in Fig. 5.15, SunPower believes that the C7 using their 24 % efficient c-Si cells will produce lower cost electricity (LCOE) than either the standard planar c-Si modules or any thin film PV module.

www.TechnicalBooksPDF.com

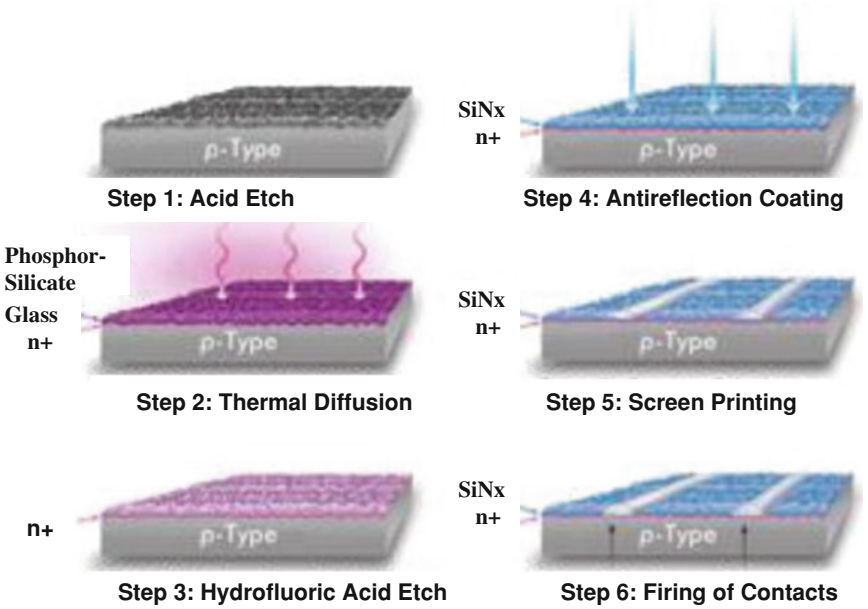


Fig. 5.10 Generic crystalline silicon cell processing using diffusion for junction formation and screen printing for front grid formation [6]

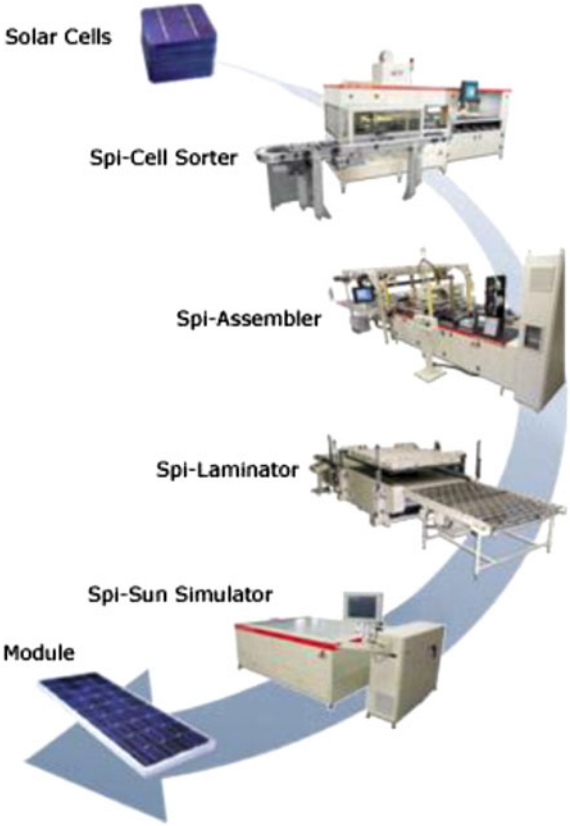


Fig. 5.11 Module packaging with automated equipment, *source* spire corporation

www.TechnicalBooksPDF.com

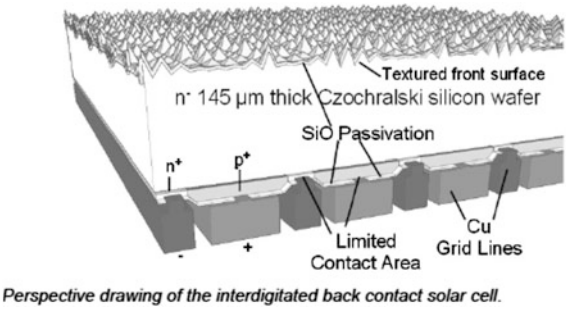


Fig. 5.12 Perspective drawing of the interdigitated back contact solar cell

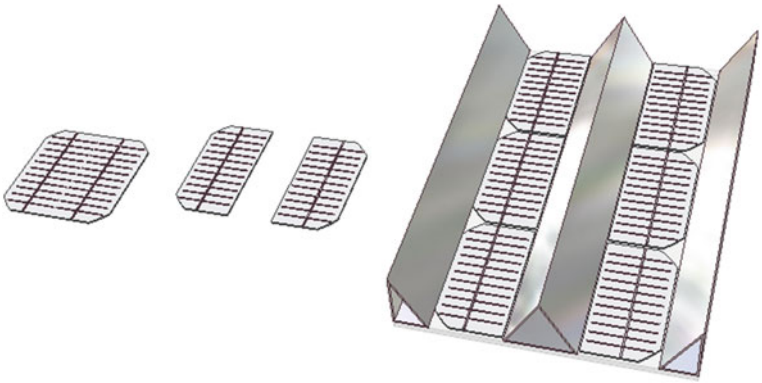


Fig. 5.13 Low concentration PV modules substitute lower cost mirrors for some of the expensive single crystal Si cell material



Fig. 5.14 SunPower C7 field installation [8]

www.TechnicalBooksPDF.com

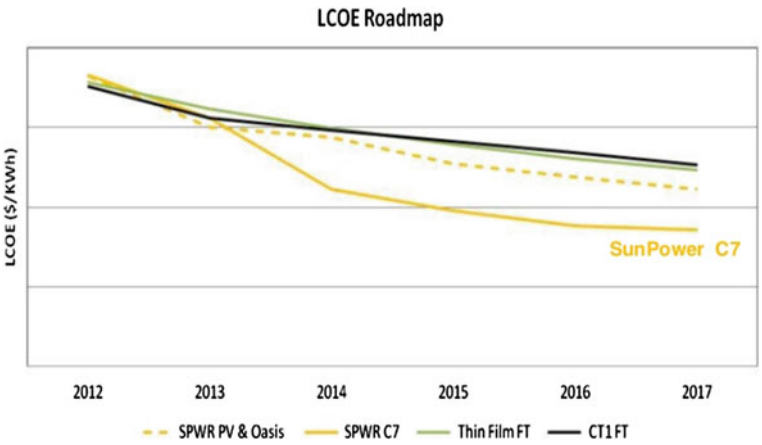


Fig. 5.15 SunPower believes that the LCOE for C7 solar fields will be lower than for planar c-Si or thin film solar systems [13]

References

1. http://www.solarworld-usa.com/about-solarworld/history-of-solar
2. http://www.solarworld-usa.com/～/media/www/files/datasheets/sunmodule-plus/sunmodule-solar-panel-250-mono-ds.pdf
3. http://www.yinglisolar.com/assets/uploads/products/downloads/2012_PANDA_60.pdf
4. http://us.sunpower.com/cs/Satellite?blobcol=urldata&blobheadername1=Content-Type&blobheadername2=Content-Disposition&blobheader
5. http://www.prosun.org/en/fair-competition/trade-distortions/subsidies.html 2/19/2014
6. http://www-inst.eecs.berkeley.edu/～ee143/fa10/lectures/Lec_26.pdf
7. L. Fraas L. Partain, *Solar Cells and Their Applications*, 2nd Edition, Ch 4, (Wiley, 2010)
8. http://www.solardaily.com/reports/SRP_and_SunPower_Dedicate_Completed_C7_Tracker_Solar_Power_System_at_ASU_Polytechnic_Campus_999.html
9. http://www.solarnovus.com/europes-role-in-the-worldwide-pv-market_N3570.html
10. http://en.wikipedia.org/wiki/List_of_photovoltaics_companies
11. http://gigaom.com/2012/08/08/sunpower-looks-to-solar-leases-as-a-bright-spot/
12. http://us.sunpower.com/power-plant/products-services/oasis-power-plant/;
13. http://www.slideshare.net/HitReach/sun-power-presentation?utm_source=slideshow02&utm_medium=ssemail&utm_campaign=share_slideshow

www.TechnicalBooksPDF.com

Chapter 6
The Dream of Thin Film PV

The Arab oil embargo in 1973 led to an interest in the US in energy independence. In order to realize a dream of a major contribution to our electric power needs here on earth from renewable solar energy, cost became a major driver of a large research effort for solar PV in the US. As noted in Chap. 3, there were three schools of thought. The first group argued that the single crystal silicon cells developed for space could be made low cost by clever manufacturing innovations and economies of scale.

The second group argued that single crystals silicon cells are like gem stones and will always be intrinsically too expensive and therefore, noncrystalline thin film cells were needed. This led to a major research effort in the US on Cadmium Telluride (CdTe), Copper Indium Gallium di-Selenide (CIGS), and amorphous Silicon (a-Si) thin film solar cells [1]. A third group argued that single crystals were necessary for high efficiency conversion and that the low cost large area solar energy collection function could be managed with low cost optical lenses or mirrors. This effort has led to 35 % efficient dual junction single crystal cells like the Gallium Arsenide/Gallium Antimonide (GaAs/GaSb) mechanically stacked cell [2] and the 40 % efficient three junction Indium Gallium Phosphide/Gallium Indium Arsenide/Germanium (InGaP/GaInAs/Ge) monolithic cell [3].

Now in 2014, 40 years later, the laws of physics and volume manufacturing have provided some interesting answers. We now know that volume production has indeed been very important and silicon modules are dominant in the terrestrial arena with module cost now below a dollar per Watt [4]. As shown in Fig. 6.1, the Silicon module production accounts for 90 % of the total installed PV capacity as of 2013 with thin film PV modules accounting for only about 10 % of the total [5].

Nevertheless, the story of a-Si solar cells is a very interesting story with some remarkable spinoff applications. In 1976, David Carlson and Christopher Wronski of RCA Laboratories created the first a-Si PV cells [6]. There followed a lot of work on understanding this material and developing methods of fabricating devices using this material. Today, while a-Si PV is not used for large-scale electric power generation, it is used by almost everybody in calculators [7] and solar watches [8] as shown in Fig. 6.2. The first solar-powered calculator [7] was introduced in 1978.

L. M. Fraas, *Low-Cost Solar Electric Power*, DOI: 10.1007/978-3-319-07530-3_6,

© Springer International Publishing Switzerland 2014

www.TechnicalBooksPDF.com

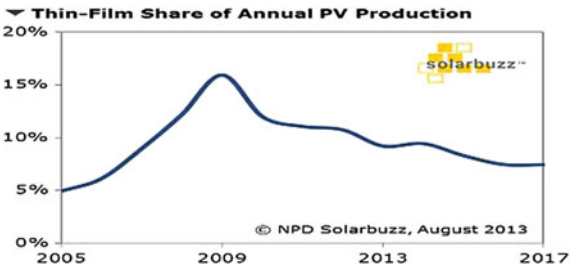


Fig. 6.1 Thin film PV module market share of annual PV production [5]



Fig. 6.2 Photographs of first solar powered calculator [7] and today's Eco-Drive [8] solar powered watch

Figure 6.3 shows the a-Si device structure [9].

Figure 6.4 shows several smaller a-Si modules [9] including the small 5 cell series connected monolithic circuit shown at the bottom right for use in powering calculators and the round circuit in the bottom middle for powering watches. These circuits illustrate the advantage of thin film PV in that cell voltages can be added through monolithic cell interconnections [1]. This concept is illustrated in Fig. 6.5.

This ability to monolithically interconnect a large number of devices on a large area sheet of glass has led to the much more economically successful application of amorphous thin film silicon for displays such as the liquid crystal display (LCD) using thin film transistor (TFT) drive circuits. The three key historical innovations for a-Si PV and TFT LCDs all occurred in the late 1970s. First in 1975, researchers at Hughes Research Lab [10] demonstrated a "Reflective Direct-View and Projection Display Using Twisted-Nematic Liquid Crystal Cells" as shown in Fig. 6.6. Then in 1976, Carlson and Wronski [6] demonstrated the a-Si PV cell shown in Fig. 6.3. The last key was the demonstration of the a-Si TFT structure in 1979 by LeCombre et al. [11] as shown [12] in Fig. 6.7.

www.TechnicalBooksPDF.com

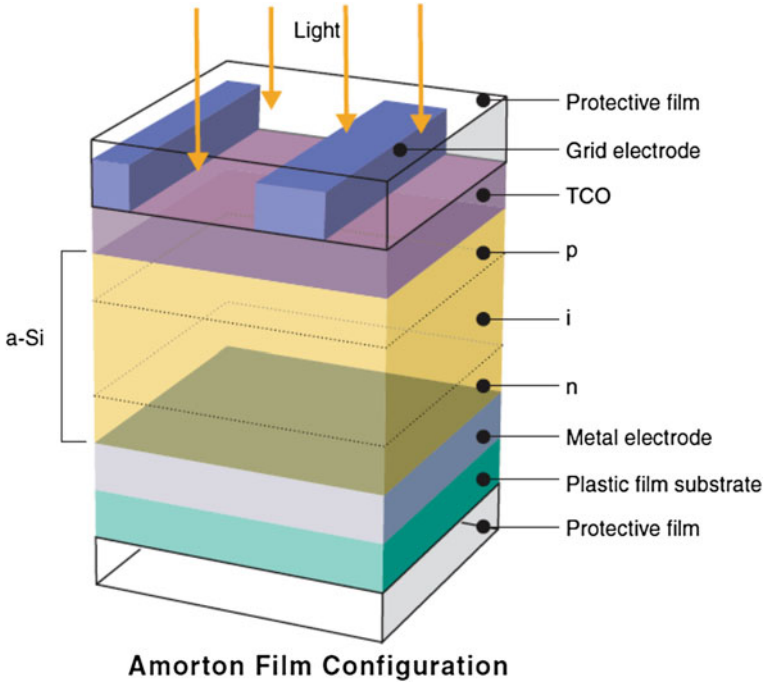


Fig. 6.3 Amorphous silicon solar cell device structure [9]

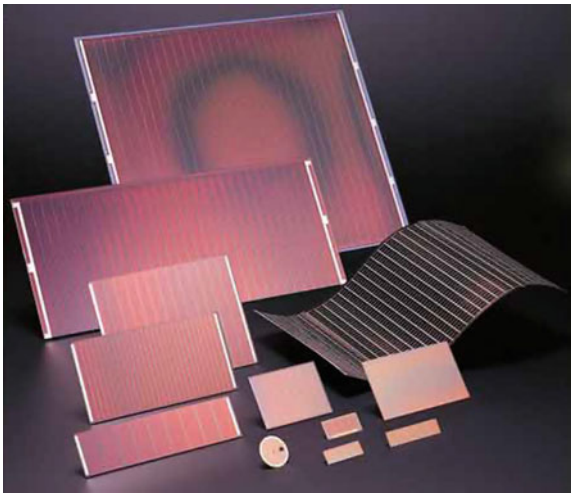


Fig. 6.4 The a-Si PV technology is adaptable to a large number of circuit configurations as illustrated here. This photo is from the Sanyo Amorton product brochure [9]

The LCD and TFT innovations were combined with the technology for monolithically integrating a-Si devices to result in the LCD TFT technology [13] shown in Fig. 6.8.

www.TechnicalBooksPDF.com

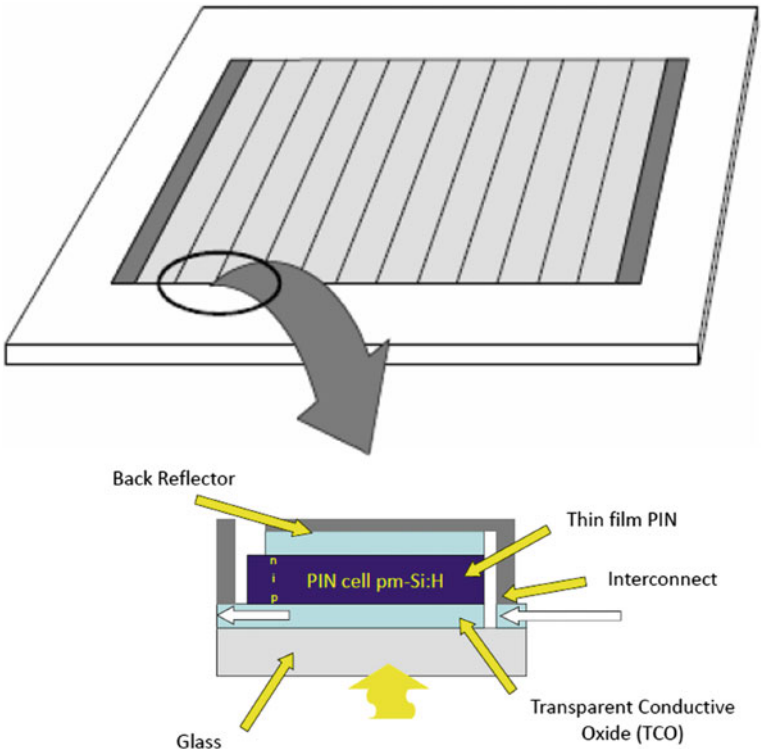


Fig. 6.5 A complete a-Si:H PV panel consists of multiple cells produced on a single substrate in series with interconnections done through a series of scribing, masking, and deposition steps

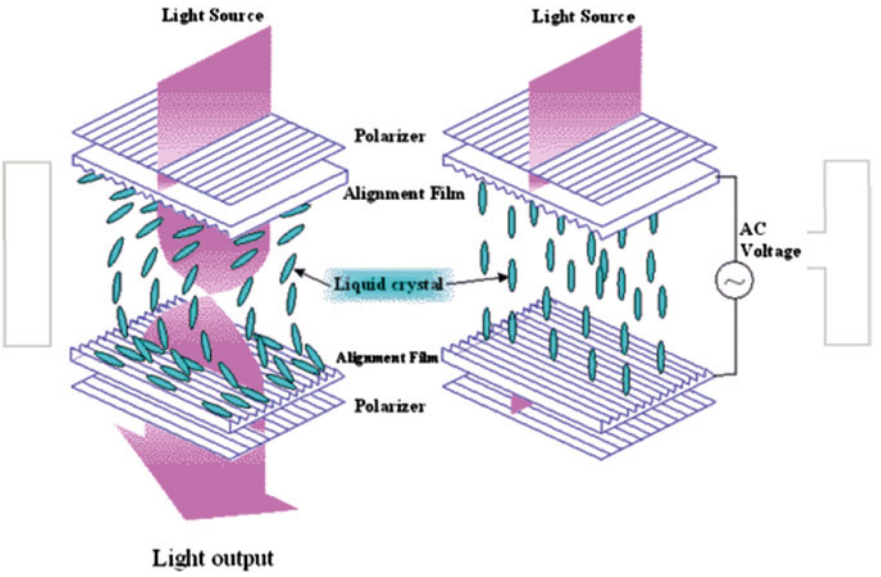


Fig. 6.6 Liquid crystal display concept [10]

www.TechnicalBooksPDF.com

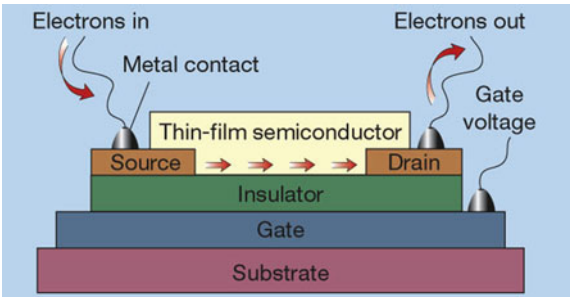


Fig. 6.7 Thin film field effect transistor [12]

In the mid-1980s, small size a-Si:H TFT LCDs, e.g. 5-inch displays were available for games and instruments [13]. In the late-1980s, the Hosiden Company supplied black and white TFT LCD panels to Apple Computers. However, the first large-area, color TFT LCDs, i.e., the 10.4-inch VGA (640 × 480 resolution) panels, were mass produced by DTI (Display Technology Inc.), which was a joint venture of IBM and Toshiba. Today, we all have flat screen TVs and computer monitors as shown for example in Fig. 6.9 [13].

It is interesting to see how technologies can interact resulting in different applications. So, why has a-Si been successful in displays but not for large-scale electric power generation? The answer is in the economics. A 40-inch flat screen TV sells for about $400 with profit margin included. Its area is about 4,450 sq cm. A 10 % efficient a-Si solar panel will produce about 1 W per 100 sq cm. So the a-Si PV panel with an area similar to the 40 inch TV would produce 44 W but if sold at $0.5 per W, it would have to sell for $22. This explains why a-Si is used predominately in displays.

The conclusion from the above is that PV module conversion efficiency is very important. This is why M. Tanaka et al. from Sanyo, the maker of the a-Si PV modules shown in Fig. 6.4, invented the HIT Si solar cell [14, 15] shown in Fig. 6.10. By applying a-Si layers on the front and back of a single crystal Si wafer, Sanyo was able to demonstrate [14, 15] a solar cell efficiency of 22 %.

Solar PV module conversion efficiency is very important because there are other constraints for electric power generation. For a large utility PV field, there are balance-of-system (BOS) costs such as land, module support structures, and installation labor costs such that a very low cost 10 % module is not good enough to pay these BOS costs. For residential solar systems, the rooftop area is limited and so higher efficiency systems provide more power. These are the reasons that First Solar, the supplier of CdTe thin film modules and the largest thin film solar module provider in 2009, does not provide thin film PV modules for rooftop applications and has now purchased TetraSun in order to make and sell 21 % efficient single crystal Si PV modules [16].

www.TechnicalBooksPDF.com

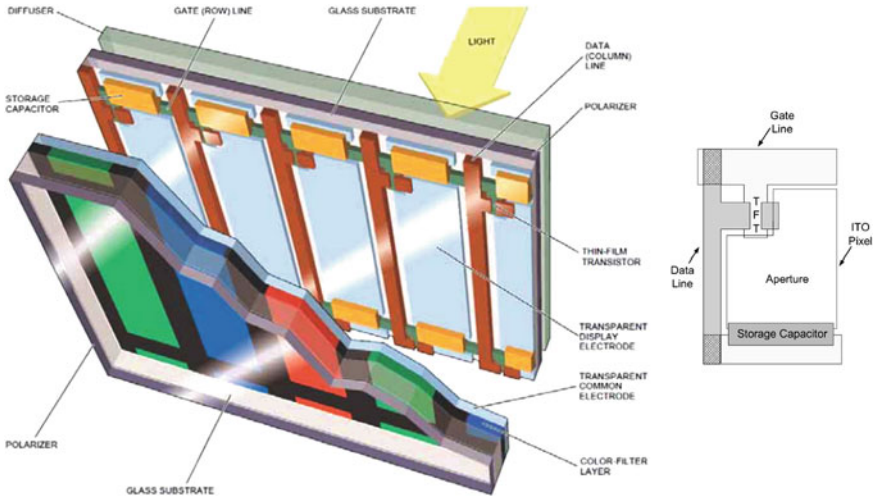
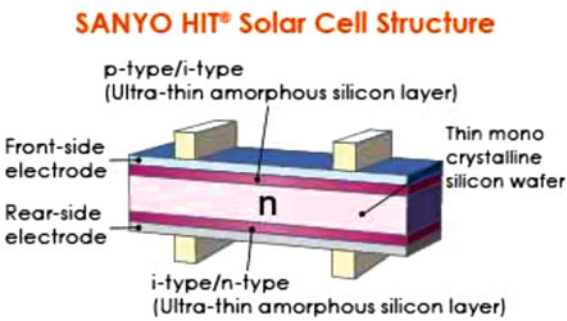


Fig. 6.8 A multicolor liquid crystal display is driven by a large area thin film a-Si transistor circuit [13]

Fig. 6.9 Liquid crystal color TV [13]



Fig. 6.10 SANYO HIT® solar cell structure



www.TechnicalBooksPDF.com

References

1. L. Fraas, L. Partain, *Solar Cells and Their Applications*, 2nd edn., Chap. 6 (Wiley, Hoboken, 2010)
2. L.M. Fraas, J. Avery, J. Gee et al., Over 35 % efficient GaAs/GaSb stacked concentrator cell assemblies for terrestrial applications, in *Proceedings of the 21st IEEE PV Specialist Conference*, Kissimmee, Florida, p. 190 (1990)
3. L.M. Fraas, R.C. Knechtli, Design of high efficiency monolithic stacked multijunction solar cells, in *Proceedings of the 13th IEEE Photovoltaic Specialist Conference*, Washington DC, p. 886 (1978)
4. http://www.pv-magazine.com/investors/module-price-index/#axzz2yzMShhzm
5. http://www.photovoltaic-production.com/5450/rise-and-fall/
6. D.E. Carlson, C.R. Wronski, Amorphous silicon solar cell. Appl. Phys. Lett. **28**, 671 (1976)
7. http://www.vintagecalculators.com/html/calculator_time-line.html
8. http://en.wikipedia.org/wiki/Eco-Drive
9. http://us.sanyo.com/Dynamic/customPages/docs/solarPower_Amorphous_PV_Product_Brochure%20_EP120B.pdf
10. J. Grinberg, A. Jacobson, W.P. Bleha, L. Miller, L. Fraas, D. Bosewell, G. Meyer, Reflective direct-view and projection displays using twisted-nematic liquid crystal cells. Opt. Eng. **14**, 217 (1975) [AIP citation]
11. P.G. LeComber, W.E. Spear, A. Ghaith, Electron. Lett. **15**, 179 (1979)
12. http://www.nature.com/nature/journal/v428/n6980/fig_tab/428269a_F1.html
13. http://www.electrochem.org/dl/interface/spr/spr13/spr13_p055_061.pdf
14. M. Tanaka et al., Development of new a-Si/c-Si heterojunction solar cells: ACJ-HIT (artificially constructed junction-heterojunction with intrinsic thin-layer). Jpn. J. Appl. Phys. **31**, 3518–3522 (1992)
15. http://www.panasonic.com/business/pesna/includes/pdf/Panasonic%20HIT%20240S%20Data%20Sheet-1.pdf
16. http://www.greentechmedia.com/articles/read/First-Solars-Quiet-Reveal-of-Its-TetraSun-High-Efficiency-Silicon

www.TechnicalBooksPDF.com

Chapter 7
Introduction to Concentrated Sunlight Solar Cell Systems

Solar electric power generation using standard silicon solar cell modules has seen major cost reductions through volume manufacturing over the last few years. According to a recent NREL study, today's system cost for an approximately 200 MWP DC fixed-axis utility-scale ground mount system is about $3.80 per WP DC. In Los Angeles without subsidies, this corresponds to an electric power price of about 18 cents/kWh. With evolutionary changes in this technology, NREL predicts that this price can drop to $1.71 per WP DC by 2020 or to about 8 cents/kWh. Herein, opportunities are discussed for introducing technical innovations that can potentially reduce this cost to about 5 cents/kWh. All of these innovations involve tracking the sun to allow the use of higher efficiency cells and in order to increase the available solar energy incident on the solar PV modules. One- and two-axis tracking concentrator systems are discussed as well as a revolutionary idea of using mirrors in space in a sun-synchronous dawn–dusk polar orbit to provide sunbeams in the early morning and evening hours for large solar farms distributed around the world extending the available sunlight hours for these production sites from 8 to 14 h/day.

Introduction

There are fundamental reasons why solar energy is attractive. The sun is going to be there for millions of years and hydrocarbon fuels are going to be depleted. Furthermore, there is the danger of climate change with increasing levels of CO_2. Nevertheless, the immediate problem for solar energy is a need for continued cost reduction. The measure of energy cost is simply cents per kilowatt hour or, technically, the levelized cost of energy or simply LCOE.

The Electric Power Research Institute created the following formula [1] for LCOE and Table 7.1 from [2] defines the various parameters in this equation.

$$L = (1 + r)(C_m + C_b)F/\eta_s Sh_a + (1 + r)C_i F \,/\, h_a + O\&M \qquad (1)$$

L. M. Fraas, *Low-Cost Solar Electric Power*, DOI: 10.1007/978-3-319-07530-3_7,
© Springer International Publishing Switzerland 2014

www.TechnicalBooksPDF.com

Table 7.1 Definition of levelized cost of electricity [2]

The 9 key variables are:
1. n_s = PV system conversion efficiency
2. C_m = PV module cost ($/m^2)
3. C_b = area-related BOS including installation ($/m^2)
4. S = Site-specific solar intensity (kW/m^2)
5. h_a = Annual solar hours for PV system (tracking)
6. C_i = Inverter cost in $/kW
7. F = Fixed charge rate (converts initial investment into annualized charge)
8. r = Indirect cost rate (permitting, NRE)
9. O&M

This equation is interesting for its complexity and because it reveals the number of disciplines that are needed for cooperation in the solar system cost reduction effort. The problem is not simply the hardware costs as for example the solar module cost, C_m, and the inverter cost, C_i. There is also the mounting hardware, C_b. These costs come down with volume production. However, there are other costs. The (1 + r) is associated with permitting and legal contracts and the F is associated with the financing institutions. Finally, it is desirable to select installation sites where there is a lot of sunlight, S, and, while maintenance may be low, there is still an O&M cost.

So what is the status today? The baseline solar cell technology today is the based on the crystalline silicon module mounted either on home rooftops or in fields at a fixed tilt facing South for the northern latitudes.

Figure 7.1a gives a representative cost analysis [3] for a baseline silicon module residential system at two different locations. As can be seen, the cost of solar electricity without subsidies is still quite high. Nevertheless, as shown in Fig. 7.1b, given subsidies in recent years, solar installed electric power capacity world wide reached 100 GW at the beginning of 2013.

Returning to Eq. (1), there are two very important terms representing major opportunities for future cost reduction at the fundamental physics level. It has been demonstrated that cell efficiencies and system efficiencies, η_s, can be dramatically increased beyond their present levels and the use of sun tracking systems also provides opportunities to increase the effective sunlight hours, h_a.

Why Track the Sun?

Figure 7.1a shows a cost analysis for a residential rooftop system. The public is most familiar with residential rooftop systems. However, larger systems, as for example commercial, industrial, and utility field systems, are cheaper because of the smaller impact of the permitting, financing, and installation costs. Today in Europe [4], residential systems account for 21 % of the solar PV market whereas these larger commercial, industrial, and utility systems account for the remaining

www.TechnicalBooksPDF.com

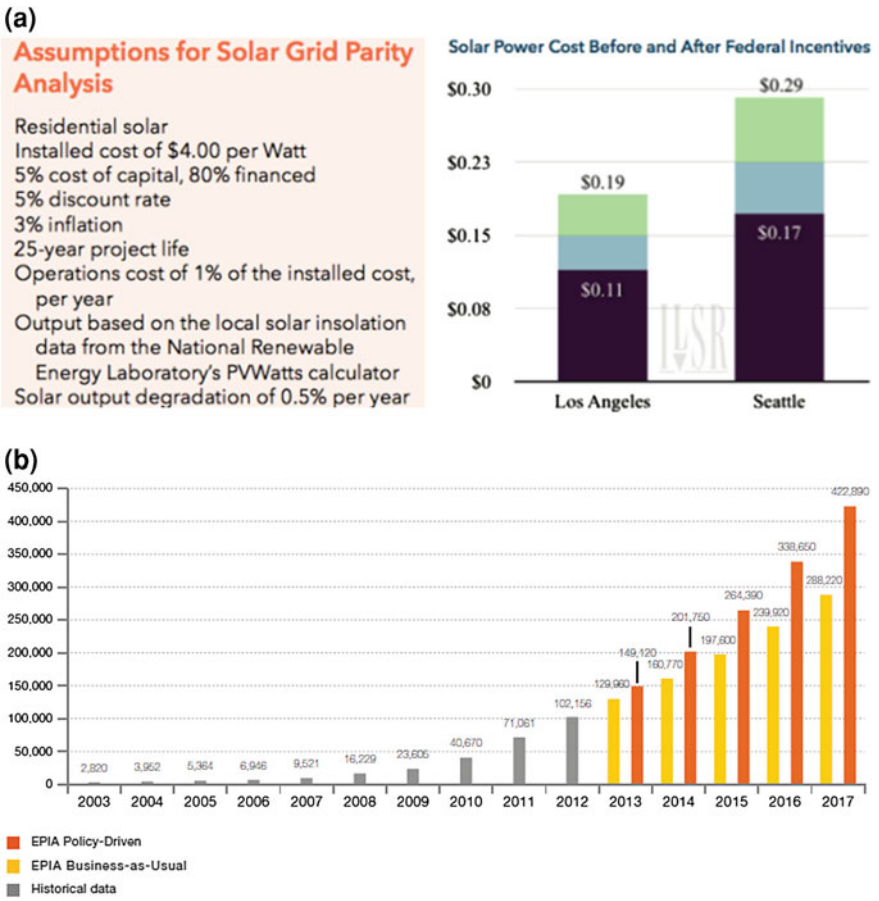


Fig. 7.1 **a** Example [3] economic assumptions relating today's residential solar installed price to LCOE given the Los Angeles and Seattle solar resource availability. The *blue* and *green* give cost reductions from federal and state subsidies. **b** Global PV cumulative scenarios until 2017 for business-as-usual and policy-driven assumptions [4]. *Vertical axis* is "cumulative global installed PV power (MW)"

79 % of the market. In the future, it is projected that the US residential and utility field markets will be approximately equal in size [4].

While smaller residential systems are mounted flat on rooftops, larger field installations can be mounted on solar trackers to follow the sun. This provides several opportunities for system improvements and potential cost reductions in LCOE. For example, by simply following the sun instead of just pointing at the sun at noon, the annual hours of sunlight, h_a, in Eq. (1) can be increased. Next, by using lower cost plastic lenses or aluminum mirrors as sunlight collectors to focus on smaller higher efficiency cells, the system efficiency, η_s, in Eq. (1) can be dramatically improved. For example, 44 % multijunction cells [5] are now

www.TechnicalBooksPDF.com



Fig. 7.2 SunPower 1-axis T20 tracker system [6]—pictured here at the Greater Sandhill Solar Farm in Mosca, CO

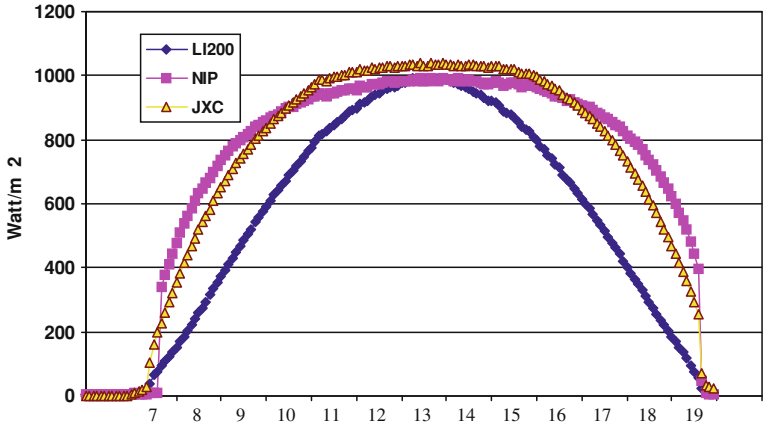


Fig. 7.3 Solar resource over a sunny day in Las Vegas for fixed tilt (*blue*) versus direct normal 2-axis tracking (*pink*) versus 1-axis tracking (*yellow*) solar modules [7]

available. These opportunities will be described in more detail in the following paragraphs and sections.

An example tracking system using planar silicon modules is shown in Fig. 7.2 and the simplest benefits of sun tracking are shown in Fig. 7.3. Figure 7.2 shows 19 % efficient SunPower modules mounted on a T20 SunPower 1-axis tracker [6]. In this figure, one can see the modules mounted on several parallel North–South-oriented beams mounted at a 20° (tilt) angle off horizontal. One can also see a drive motor mounted on a pedestal and a linked drive beam allowing the modules to follow the sun from East to West over the course of the day.

The simple benefits of tracking [7] over the course of a day in Las Vegas are shown in Fig. 7.3. According to the NREL solar resource manual [8] for Las

www.TechnicalBooksPDF.com

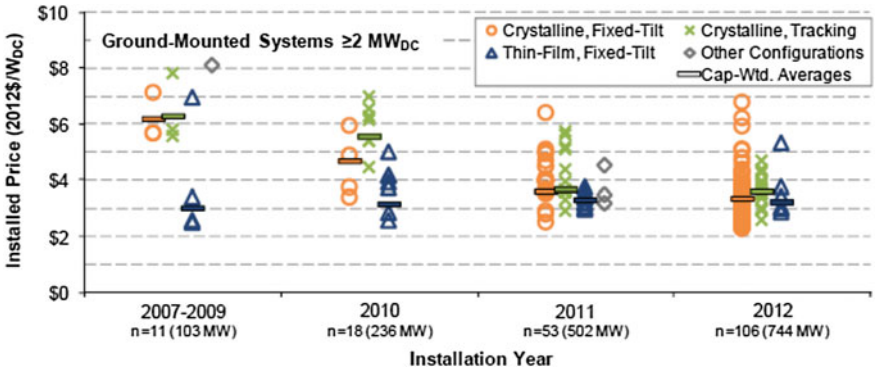


Fig. 7.4 Installed price trends for fixed tilt versus tracking 1-sun PV installations

Vegas, the annual solar hours, h_a, available for fixed tilt, 1-axis tracking, and 2-axis tracking systems are 2,372, 3,212, and 3,321 h respectively. The improvement associated with 1-axis tracking in this case is 35 %. In the future, the estimated additional cost for 1-axis tracking [9] is about 10 cents/W. According to a recent NREL study [10], today's system cost for an approximately 200 MWP DC fixed-axis utility-scale ground mount system is about $3.80 per WP DC. With evolutionary changes in this technology, NREL predicts that this price can drop to $1.71 per WP DC by 2020. Even at a future $1.71 per W, 10 cents/W is only a 6 % additional cost to gain 35 % more sunlight hours.

Sun tracking systems are already dominant today for flat plate solar panels in utility fields of greater than 2 MW. In fact, solar experts like Paula Mints, a principal analyst at Navigant Consulting (which offers technological expertise to the construction industry, among others), predict that tracking systems will find use in at least 85 % of commercial installations in 2012. Figure 7.4 supports this prediction [11].

From Fig. 7.4 in 2012, the average installed system prices for fixed tilt and tracking systems were $3.30 and $3.60 per W respectively differing by only 10 % whereas the advantage in kWh for tracking over fixed tilt will be 35 % in sunny locations.

Single-Axis Tracking Systems

In 2003, JX Crystals Inc. noted that the silicon cell efficiency could be increased by using aluminum mirrors in a low concentration (3-sun) module along with 1-axis tracking. Using SunPower cells, JX Crystals then successfully demonstrated the 100 kW installation [12] shown in Fig. 7.5. SunPower liked the idea and then proceeded to design and build the C7 low concentration system [13] shown in Fig. 7.6a, b. This C7 system now uses their 24 % efficient silicon cell. SunPower is now selling these C7 systems in multi-megawatt sizes at prices 10 % below the

www.TechnicalBooksPDF.com



Fig. 7.5 JX Crystals' 3-sun low concentration modules in operation in China in 2006 [12]

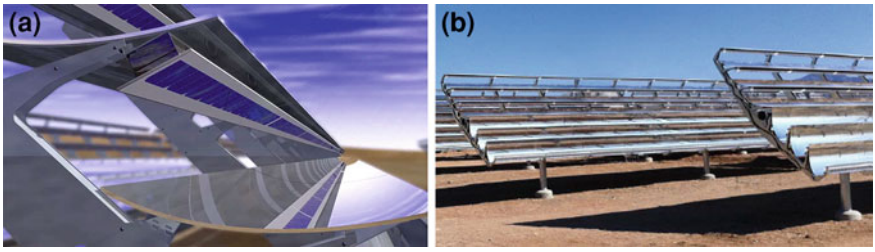


Fig. 7.6 **a** and **b**: Sun Power 1-axis C7 low concentration PV system introduced to the market in 2011 [13]

planar silicon module system prices and, in cooperation with a group in China, they are building a 1 GW plant.

So, there are opportunities still for LCOE cost reductions. However, unfortunately, solar PV systems only can produce power when sunlight is available which is only until the late afternoon. Meanwhile, electric utility peak power demands extend into the evening hours. A solution to this problem is to use parabolic trough-mirrors with linear trackers to concentrate sunlight onto pipes containing oil as shown in Fig. 7.7. The heated oil is then circulated to a central location where it is used to make steam to run a turbine generator. This concentrated solar power (CSP) system has the advantage that natural gas can be used to make the steam to run the turbine when the sun is not shining [14]. Many of these solar electric generation systems (SEGS) are in operation.

The solar power installations in Figs. 7.5, 7.6, and 7.7 all use simple single-axis trackers. However, the mirror widths are quite different. The SEGS mirrors are typically 5–6 m in aperture width while the PV mirror apertures are in the range from 0.15 to 0.35 m. The sunlight concentration ratios are also quite different with the low concentration PV (LCPV) being in the range from 3 to 7 suns, whereas the SEGS concentration ratio is much higher. This difference in aperture and

www.TechnicalBooksPDF.com

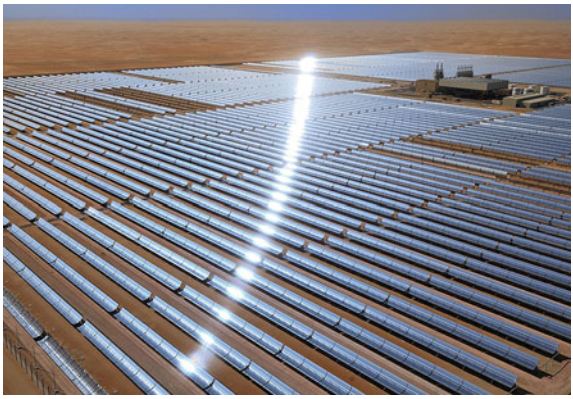


Fig. 7.7 Photograph of a 100 MW mirror trough concentrating solar power system in operation in Abu Dhabi

concentration ratio is associated with the different operating temperature requirement. The PV cells typically operate at about 50 C, whereas the SEGS systems operate at around 375 C. The system conversion efficiencies are actually similar at about 15 % for SEGS and 20 % for LCPV.

Two-Axis Tracking Systems

The system efficiency, η_s, in Eq. (1) for solar PV systems can be dramatically improved by using 44 % multijunction cells rather than the 24 % efficient silicon cells used in the LCPV system of Fig. 7.5. However, these multijunction cells are much more expensive. In order to afford these more expensive cells, much higher sunlight concentrating point focus lens or mirrors are required and this then requires two-axis solar trackers.

A module for a high concentration PV (HCPV) system is shown in Fig. 7.8a, b shows these modules arrayed on a 2-axis tracker. The module in Fig. 7.8a was designed by Fraunhofer in Germany [15] and is now being manufactured by Soitech [16]. HCPV modules and arrays are now being supplied by several companies. Amonix, an HCPV pioneering company, has installed a 30-MW field in Alamosa, CO [17] as shown in Fig. 7.9. Amonix has now demonstrated a 35 % HCPV module.

It is also possible to use mirrors in HCPV systems as demonstrated by JX Crystals and Solfocus [18]. A Sofocus module is shown in Fig. 7.10a and Solfocus modules in arrays are shown in Fig. 7.10b. The first demonstration of a 34 % HCPV module [19] was done by workers at JX Crystals in 2006 using the mirror module prototypes shown in Fig. 7.11. The performance for the modules shown in Fig. 7.11 is summarized in Table 7.2 [19].

All of these HCPV systems operate with concentration ratios in the range of 500–1,000 suns. Several HCPV manufacturers have now demonstrated multi-megawatt fields but production volumes are still well below 100 MWs/year which means that installed system prices are still higher than for planar silicon fields.

www.TechnicalBooksPDF.com

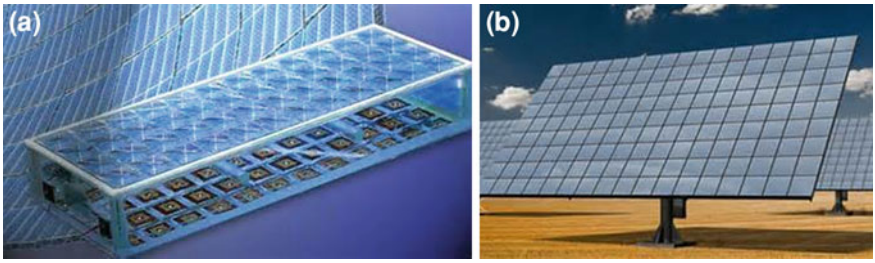


Fig. 7.8 **a** and **b**: Fresnel lens high concentration PV (HCPV) module and arrays using 40 % efficient solar cells as developed by Fraunhofer and Soitech [15, 16]



Fig. 7.9 HCPV arrays in a 30 MW field. Amonix was the pioneering developer of this technology [17]

While these systems are more complex than LCPV systems, they have great potential once they get into high volume production.

Revolutionary Space Sun Tracking Concepts

In the previous sections, the emphasis has been on the goal of reducing the cost of solar electricity, i.e., L, through the $\eta_s Sh_a$ term in Eq 1. Higher efficiency cells increase η_s and h_a increase when the hours are increased by tracking. However, there is still the problem of solar electricity in the evening. Chap. 12 will discuss a

www.TechnicalBooksPDF.com

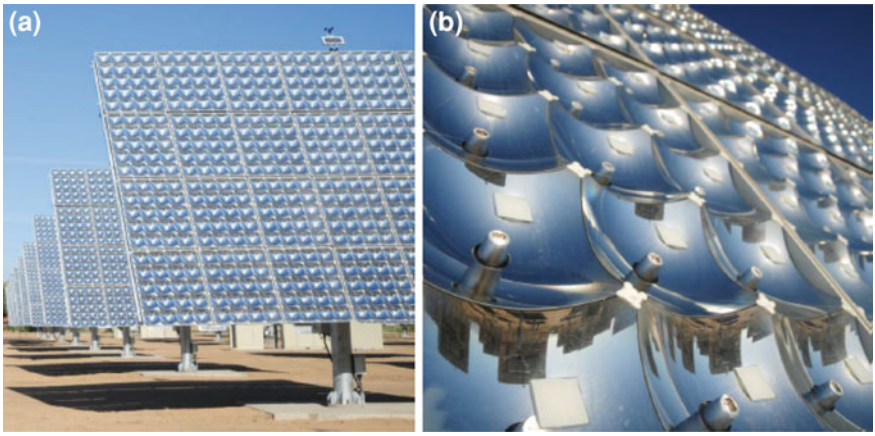


Fig. 7.10 Mirrors can also be used in HCPV systems as demonstrated here by Solfocus [18]

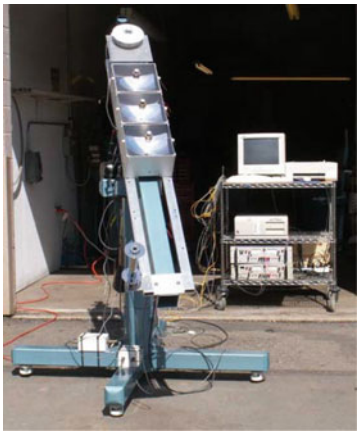


Fig. 7.11 A prototype CPV module with a 34 % efficiency under standard test conditions and with an outdoor module efficiency of 31 % at operating temperature was demonstrated by JX Crystals in 2006

Table 7.2 Performance summary for the prototype CPV modules shown in Fig. 7.11

	Packaged cells at STC	Projected STC with 90 % optical efficiency	Measure at operate temperature (April 28)	Measure module at STC (April 28)
DJ cell power (W)	17.4	15.7	14.4	15.1
DJ cell efficiency (%)	31.5	28.4	26.1	27.3
IR cell power (W)	3.64	3.28	2.6	3.1
IR cell efficiency (%)	6.6	5.9	4.7	5.6
Sum power (W)	21	19	17	18.7
Sum efficiency (%)	38.1	34.3	30.8	32.9

NIP DNI = 0.92; area = 600 cm^2; input power = 55.2 W

www.TechnicalBooksPDF.com

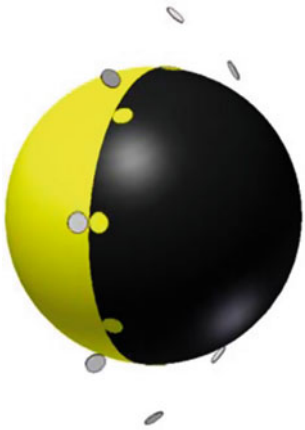


Fig. 7.12 The earth is shown schematically as a sphere with the night as *black* and the day as *yellow*. The North pole is at the top. Mirrors in a *dawn–dusk polar sun-synchronous orbit* deflect sunbeams down to solar power fields in the early morning and evening hours

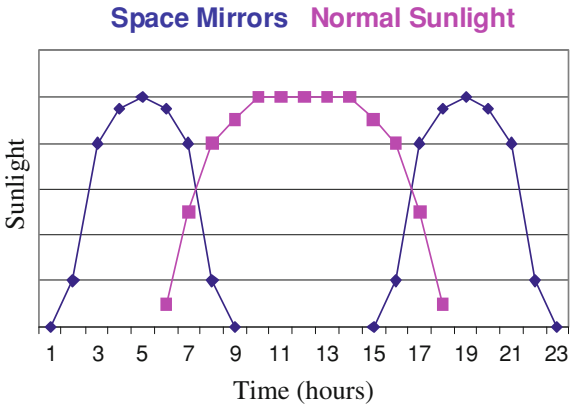


Fig. 7.13 As shown conceptually in Fig. 7.12, space mirrors in a dawn–dusk orbit add solar energy for three additional hours in morning and three more hours in the evening. Compare this with Fig. 7.3

method of increasing the sunlight hours available for large PV solar farms from typically 8–14 h/day while also providing sunlight for these fields in the evening hours. This can potentially be done by tracking the sun with mirrors in space in a dawn–dusk orbit as shown schematically in Fig. 7.12. This concept not only can reduce L with more hours but also provide sunlight to ground solar PV fields in the evening reducing the cost of solar electricity to 5 cents/kWh.

As shown in Fig. 7.13, the space mirrors provide solar energy to a solar power station for three more hours in the morning and three more hours in the evening.

The space community has dreamed of solar electricity for 24 h/day using mirrors in space that follow the sun. As shown in Fig. 7.14a, Dr. Krafft Ehricke [20] first proposed the idea of using mirrors in space to direct sunbeams down to terrestrial solar fields in 1978. NASA has studied an alternative idea, the Integrated Symmetric Concentrator Space Power Satellite (ISC-SPS) [21], as shown in Fig. 7.14b. However, there are problems with both these ideas.

www.TechnicalBooksPDF.com

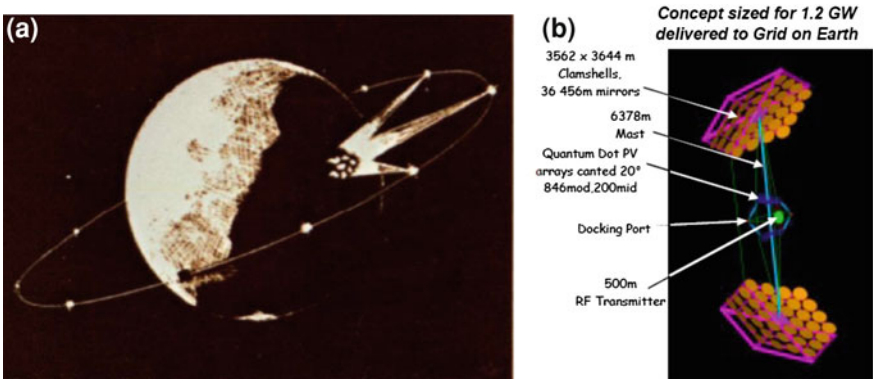


Fig. 7.14 **a** The space mirror Power Soletta concept for terrestrial solar electric power for 24 h/day was proposed by Dr. Kraft Ehricke in 1978 [20]. **b** NASA-integrated symmetric concentrator space power satellite concept [21]

In the ISC-SPS concept, sun tracking mirrors on a satellite in GEO 35,800 km above the earth capture sunlight and direct that light to solar cells on the satellite that then convert electricity into a microwave beam that is then directed to a special earth ground station to be converted again into electricity. This concept is too complex and expensive with too many energy conversion steps.

Ehriche's Power Soletta concept is attractive because of its simplicity. Ehricke proposed a constellation of mirror satellites in an orbit 4,200 km in altitude beaming power down to a 1,200 km^2 site in Western Europe. Deflecting sunlight down to earth where it is then converted to electricity is conceptually much simpler than converting it to electricity in space and then microwave beaming it down to earth and then converting it to electricity as per the Solar Power Satellite concept. The key physical limitation for this Power Soletta mirror concept relates to the size of the sun's disc as viewed from earth. The sun's disc subtends an angle of 10 mili-radians leading to beam divergence. Beam divergence for a mirror in orbit at an altitude of 4,200 km gives a sun spot diameter on earth of 42 km with a corresponding area of 1,200 km^2. Assuming that the 1,200 km^2 solar field would produce electricity at 15 % efficiency implies a 180-GW central power station. This size is much too large with enormous distribution problems.

Both the GEO and Power Soletta orbits are very high up in order to avoid the earth shadow and to stay in sunlight for 24 h/day every day all year around. Figure 7.12 represents an alternative proposal for mirrors in space deflecting sunbeams down to earth for 24 h/day all year around. This concept is based on a unique *dawn–dusk sun-synchronous polar orbit*. The idea is to place a lightweight array of mirror (heliostat) satellites in a constellation in a low earth orbits at an altitude of 1,000 km [22, 23] and at a specific inclination angle of 99° (9° off the NS plane).

As it turns out because the earth is slightly oblate, in 1958, King-Hele and Merson [24] calculated that a satellite orbit plane will rotate slowly at a rate that

www.TechnicalBooksPDF.com

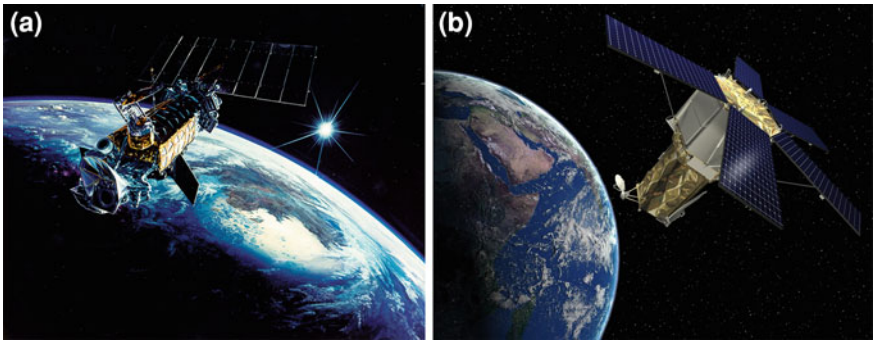


Fig. 7.15 Satellites in dawn–dusk orbit: **a** DMSP [25] satellite, **b** GeoEye [26] satellite

depends on the orbit inclination angle. This then leads to the observation that for the earth, the orbit plane for a satellite orbiting in a near polar orbit with an inclination angle of 99° will rotate nearly 1° per day so that the satellite orbit plane will always remain normal to the sun's rays day after day all year around. This is a remarkably useful sun-synchronous orbit. The US military first took advantage of this orbit in the Defense Meteorological Space Program with a first sun-synchronous satellite in 1963 [25]. There are now numerous satellites in dawn–dusk sun-synchronous orbits for weather forecasting and earth scientific surveys and as spy satellites [26]. Some example satellites in dawn–dusk orbit are shown in Fig. 7.15.

Returning to the space mirror concept for sunbeams from space for terrestrial solar fields, the concept is that mirror satellites can deflect sunbeams down to an array of solar power stations distributed near major population centers around the earth. These solar PV or trough CSP earth stations are already being built. If one assumes that there can be 40 such stations generating 5 GW each 10 years from now, then as shown in Fig. 7.13, the solar energy available to these ground sites can be increased from potentially 8 kWh/m^2/day without the space mirrors to potentially 14 kWh/m^2/day with the space mirrors. The additional 6 kWh/m^2/day would be provided in the early morning and evening hours.

There are several immediate benefits that result from this MiraSolar satellite constellation configuration. First given the lower altitude, the illuminated sunlight spot size on the earth is now only 10 km in diameter instead of the 42-km spot size associated with the Ehricke Power Soletta configuration. Furthermore, the area of each mirror array satellite now required to produce a solar intensity equivalent to daylight sunlight is now comparable in size to the 5 × 15 km ISC NASA SPS satellite size (75 km^2). The earth-based electric power station size is now approximately 5 GW instead of the Power Soletta station size of 180 GW.

Now assume this mirror satellite constellation will be available to an array of ground solar electric stations distributed around the world. Extrapolating from Fig. 7.1b, 10 years from now, there could be over 900 GW of solar in the world. All of this will not be in central power fields but if we assume that 1/3 of the 900

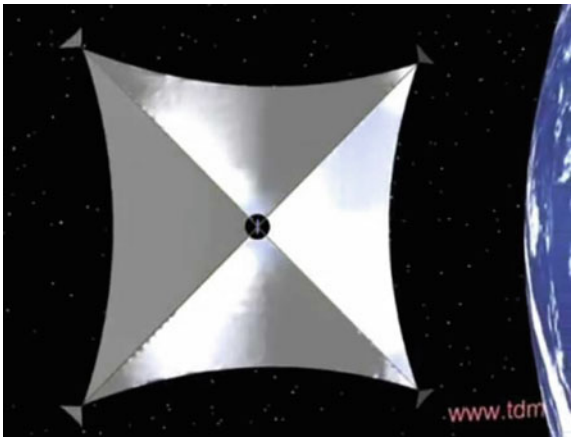


Fig. 7.16 L'Garde 10,000 m^2 Sunjammer [27] solar sail planned for launch in 2015 weighs 20 g/m^2

GW is or could be, then there will be 300/5 = 60 available solar ground stations. These stations will be located in sunny parts of the world near population centers. Here, we shall assume that over the course of 24 h as the world turns, 40 of the potential 60 future sites depending on the weather for that day will be selected to receive additional sun beam energy in the early morning and early evening hours.

The amazing thing about this concept is its attractive economics. The additional solar energy can reduce the cost of solar electricity at the ground sites to less than 6 cents/kWh. This attractive economics results from the fact that the mirrors are always in sun light and always in use and the mirrors are very lightweight reducing cost of transport into LEO.

While this concept may seem very fanciful, there are ongoing developments that are bringing it closer to realization. For example, space mirror development will be required but L'Garde and NASA are developing a solar sail for launch into space in 2015. This sail is simply a mirror as shown in Fig. 7.16. It will be necessary to rotate these mirrors to direct the deflected sun beam, but there are control moment gyros on the International Space Station and that technology can be adapted for mirror pointing. There will also be a need to reduce the launch cost for carrying the mirrors into orbit but SpaceX is working on lower cost reusable rockets [28].

This space mirror concept will be described further in Chap. 12 in this book.

Conclusions

The market for fixed tilt standard silicon modules in residential and field installations has been growing steadily. However, there are still exciting opportunities for technical improvements with still further significant cost reductions. These improvements range from the straightforward addition of simple single-axis

trackers to dramatically higher system efficiency improvements using two-axis trackers to revolutionary increases in solar energy production for large utility solar fields. It is conceivable that mirrors in space can be combined with terrestrial solar fields to expand the availability of solar energy to the early morning and evening hours producing solar electricity at below 6 cents per kWh. However, the more dramatic opportunities described here are still going to require political and financial commitments before they can become economically viable.

References

1. F.R. Goodman Jr. et al, in *Solar Cells and Their Applications*, 1st edn., Chap. 16, ed. by L. Partain (Wiley, New York, 1995)
2. L. Fraas, L. Partain, *Solar Cells and Their Applications*, 2nd edn., Chap. 26 (Wiley, New York, 2010)
3. J. Farrell, http://www.renewableenergyworld.com/rea/blog/post/2013/07/solar-costs-and-grid-prices-on-a-collision-course?cmpid=SolarNL-Thursday-July11-2013
4. Global Market Outlook for Photovoltaics 2013–2017, European Photovoltaic Industry Association, Editor Craig Winneker, http://www.epia.org/fileadmin/user_upload/Publications/GMO_2013_-_Final_PDF.pdf
5. J. Allen, V. Sabnis, M. Wiemer, H. Yuen, 44 %-Efficiency triple-junction solar cells, in *Proceedings of the 9th International Conference on Concentrator Photovoltaic Systems*, Miyazaki, Japan, 15 April 2013
6. T20 Single Axis Solar Tracker by SunPower, http://us.sunpowercorp.com/commercial/products-services/solar-trackers/T20/
7. Data collected by JX Crystals Inc in Las Vegas at UNLV
8. Solar Radiation Data Manual for Flat-Plate and Concentrating, http://rredc.nrel.gov/solar/pubs/redbook/
9. L. Fraas, L. Partain, *Solar Cells and Their Applications*, 2nd edn., Chap. 9 (Wiley, New York, 2010)
10. A. Goodrich, T. James, M. Woodhouse, Residential, Commercial, and Utility-Scale Photovoltaic (PV) System Prices in the United States: Current Drivers and Cost-Reduction Opportunities, Technical Report NREL/TP-6A20-53347, February 2012
11. G. Barbose, N. Darghouth, S. Weaver, R. Wiser, Tracking the Sun VI: An Historical Summary of the Installed Price of Photovoltaics in the United States from 1998 to 2012, July 2013, http://emp.lbl.gov/sites/all/files/lbnl-6350e.pdf
12. L. Fraas, L. Partain, *Solar Cells and Their Applications*, 2nd edn., Chap. 12 (Wiley, New York, 2010)
13. The SunPower C7 Tracker: The Power of 7 Suns, the Lowest LCOE, https://us.sunpowercorp.com/…/the-sunpower-c7-tracker-the-power-of-7-suns-t
14. https://en.wikipedia.org/wiki/Solar_Energy_Generating_Systems. Accessed 18 Oct 2011
15. L. Fraas, L. Partain, *Solar Cells and Their Applications*, 2nd edn., Chap. 14 (Wiley, New York, 2010)
16. Soitec—Soitec CPV solar technology for hot, dry regions, www.soitec.com/en/products-and-services/solar-cpv/
17. CPV Technology from Amonix, Pioneers in Multijunction Cells and …, www.amonix.com/content/cpv-technology
18. L. Fraas, L. Partain, *Solar Cells and Their Applications*, 2nd edn., Chap. 15 (Wiley, New York, 2010)

19. L. Fraas, J. Avery, H. Huang, L. Minkin, E. Shifman, Demonstration of a 33 % efficient cassegrainian solar module, in *Proceedings of the 4th World Conference on Photovoltaic Energy Conversion*, Hawaii, May 2006
20. K.A. Ehricke, The extraterrestrial imperative, www.airpower.maxwell.af.mil/airchronicles/aureview/…/ehricke.html
21. H. Feingold, C. Carrington, Evaluation and comparison of space solar power concepts, in *Proceedings of the 53rd International Astronautical Congress*, 2002
22. L.M. Fraas, Mirrors in space for low cost terrestrial solar electric power at night, in Proceedings *of the 38th IEEE Photovoltaic Specialists Conference (PVSC)*, 3–8 June 2012, http://jxcrystals.com/publications/PVSC_38_Manuscript_Fraas_5-9-12.pdf
23. L. Fraas, A. Palisoc, B. Derbes, Mirrors in dawn dusk orbit for low cost solar electric power in the evening, AIAA paper 2013–1191, in *Proceedings of the 51st Aerospace Sciences Meeting*, Grapevine TX, Jan 10 2013, http://jxcrystals.com/publications/Mirrors_in_Dawn_Dusk_Orbit_AIAA_Tech_Conf_Final_2013.pdf
24. D. King-Hele, R.H. Merson, J. Br. Interplanet. Soc., **16**, 446 (1958)
25. http://en.wikipedia.org/wiki/Defense_Meteorological_Satellite_Program
26. http://www.satimagingcorp.com/satellite-sensors/geoeye-2/
27. http://www.lgarde.com/papers/2003-4659.pdf
28. http://en.wikipedia.org/wiki/SpaceX_reusable_launch_system_development_program

Chapter 8
The Story of the 40 % Efficient Multijunction Solar Cell

This is a history of the development of the high efficiency multijunction solar cell from my perspective as one of the pioneers. The significant historical events were:

(1) First theoretical description of the InGaP/GaInAs/Ge cell predicting 40 % at 300 suns concentration by Fraas and Knetchli [1].
(2) First 35 % efficient GaAs/GaSb dual junction cell demonstrated by Fraas et al. [3].
(3) First 40 % efficient InGaP/GaInAs/Ge cell demonstrated by RR King et al. [17].
(4) First 34 % efficient concentrated sunlight PV module demonstrated by Fraas et al. [2].

Introduction

My group at the Boeing Hi Tech Center first demonstrated the 35 % efficient GaAs/GaSb two junction cell in 1989 [3]. However, there were a lot of relevant events before and after that. I have decided to tell this story in historical order and in personal terms hoping that the reader will find the way the events unfolded interesting. It is also a way to acknowledge many (although certainly not all) of the key contributors along the way. As the story unfolds, I will develop the key technical concepts necessary to understand these III–V solar cells. Over the years, the work has gone from concept to specific materials to learning how to grow the materials, and then from alternate device designs to choosing among alternate designs for different applications. Today, the issues are cost and large-scale production.

L. M. Fraas, *Low-Cost Solar Electric Power*, DOI: 10.1007/978-3-319-07530-3_8,

© Springer International Publishing Switzerland 2014

A Personal History of Multijunction or Multicolor Solar Cells

My story probably begins with the launching of Sputnik in 1957. I was a sophomore in high school and a natural in math and science. This led me to the California Institute of Technology as a college freshman in 1961 where I was fortunate to attend the first and only two-year Richard Feynman Lectures in Physics course. Feynman later won the Noble prize in physics and this Feynman Lectures on Physics three volume set is now a classic text in Physics and has been for over 30 years [4]. I received straight A's in this course and this led me to major in physics.

My next relevant memory relating to multijunction solar cells was in about 1968. I was in graduate school working on my Ph.D. in solid state physics and electrical engineering. I remember that a fellow graduate student and I were having dinner and we discussed making solar cells more efficient with two p/n junctions stacked together. I remember that we noted that if a P/N and second p/n junction were put together to make a P/N/p/n, there would be an intermediate N/p junction that would generate a voltage opposite to the other junctions and this would be a problem. We discussed increasing the impurity (called doping) concentration until the N and p layers would become metallic. This would create a $P/NN^+/p^+p/n$ structure where the intermediate junction voltage is reduced to zero. This N^+/p^+ junction is really called a tunnel junction although we knew nothing about this at the time. I believe we then conjectured that there could be difficulties for infrared to pass through this N^+/p^+ layer and there could be solid solubility problems in adding enough impurity without destroying the crystals. However, this was just a dinner conversation that probably resulted from a class we attended. It had nothing to do with either of our PH.D theses.

After I got my Ph.D., my next relevant memories date back to 1973. I was a member of the technical staff at the Hughes Research Labs. My first assignment was to work on cadmium sulfide/cadmium telluride (CdS/CdTe thin film optical display devices using liquid crystals. In these devices, a light image creates an electrical image that is then projected onto a screen via a liquid crystal. I did not know it at the time but this work with liquid crystals combined with a-Si TFT would eventually lead to liquid crystal TVs as described in Chap. 6. This display work predated the gasoline lines in the first Arab oil embargo by a year or two. With this embargo, I and many others became interested in solar cells. The CdS/CdTe pair is now the FirstSolar thin-film solar cell material.

I wrote a proposal to ERDA (the Energy Research and Development Administration later to become the Department of Energy) for work on cadmium sulfide/indium phosphide thin-film solar cells. We won a contract and started depositing these films. In about 1976, we ran some controls comparing thin film and single crystal cells made with the same materials and the single crystal devices dramatically out performed the thin film devices. I never went back.

At this same time at Hughes Research Labs, there was a group starting to work on GaAs solar cells. Workers at IBM had demonstrated GaAs cells with

efficiencies over 20 % [5]. They did this by growing a thin Aluminum Gallium Arsenide (AlGaAs) window layer on the GaAs wafer surface on top of the p/n junction. This cell is sometimes referred to as an AlGaAs/GaAs cell.

This brings me to an important technical topic called surface passivation. I did not discuss this in Chap. 4 but when minority carriers are created, they can either diffuse to the junction or to the free top surface of the cell. If one does not treat the surface properly, they can recombine at the surface returning to the valence band (or ground state) and be lost. Silicon devices work very well not just because they are single crystal but also because fortunately the oxygen ion size in silicon dioxide is just right so that a thin silicon dioxide layer forms on the silicon tying up all of the surface dangling bonds without distorting the silicon crystal. Minority carriers at the surface now reflect back toward the junction without being lost. Miraculously, this just happens when silicon is exposed to oxygen in air.

Unfortunately for GaAs, its oxide is not passivating. However, various workers in the 1970s discovered that since aluminum and gallium atoms are almost the same size, the GaAs surface could be passivated by growing a thin film of AlGaAs on its surface. The AlGaAs film was also a semiconductor with a higher bandgap so that excited carriers hitting it reflected back toward the junction. This idea was first implemented for solar cells at IBM. (Actually, after the cold war ended in the 1990s, I learned that it had been done first in Russia at the Ioffe Institute in St Petersburg [6].)

There is one more thing I need to explain about AlGaAs. Actually, for purposes of brevity, I sometimes will write a III–V material formula like this just enumerating the chemical elements involved. However, this is not really a correct formula. The correct formula for this three element III–V semiconductors should be Al(1-x)Ga(x)As. For a solar cell window layer of AlGaAs, this would be Al(0.85)Ga(0.15)As. What this means is that the group III lattice site is occupied by aluminum and gallium atoms with 85 % aluminum and 15 % gallium.

Hughes was interested in this AlGaAs/GaAs cell for space satellites because Hughes had invented the synchronous satellite and had a Space and Communication division. The group at Hughes Research Labs headed by Ron Knechli and Sanjif Kamath was the first to demonstrate that these GaAs cells would last longer in space when exposed to high-energy particle bombardment [7]. The sun emits high-energy electrons and protons that are captured by the earth's magnetic field in the Van Allen belts. These high velocity particles bombard solar cells penetrating them and knocking atoms out of place leading to current loss over time. The fact that GaAs has a shorter optical absorption length means that excited carriers are created closer to the junction and the material can tolerate more defects, in this case created by radiation exposure in space. This all follows from my discussion of the random walk problem in Chap. 4.

I began working with Ron Knechli and in 1978, we jointly published a paper pointing out that an In(0.5)Ga(0.5)P/Ga(0.9)In(0.1)As/Ge triple junction cell operated with concentrated sunlight here on earth could reach an efficiency of 40 % at 300 suns concentration (Ge = germanium) [1]. For this triple junction cell, we proposed growing successive layers of n and p GaInAs on a Ge wafer

followed by InGaP/GaInAs tunnel junction layers followed by n and p InGaP layers followed by a passivating window layer. Somehow, there would also be a n/p junction in the Ge. Today, this is called a monolithic multijunction cell. We chose this set of materials because we knew that in order to preserve single crystal properties through the structure, we needed crystal films with very similar crystal structures and atomic spacing. We also chose these particular materials because given the sun's spectrum, nearly equal currents would be generated in each active junction.

The above two points of matching atomic spacing and component cell currents are very important for monolithic multijunction cells. Because they are monolithic (grown on the same wafer), the atomic spacing for all the different materials should be almost identical. In practice this means to better than 1 %. Mismatch in atomic spacing as large as 1 % can cause crystal defects in subsequent layers destroying the whole device performance. Also, it should be noted that when solar cells are connected in series, the cell with the lowest light generated current limits the current for the whole string. In these monolithic cells, the tunnel junctions connect all of the component cells in series.

Crystal lattice matching and current matching could be achieved with these particular materials. However, this was a theoretical projection and we did not know how to grow the multiple single crystal layers in sequence. However, we did some characterization of tunnel junctions in GaAs and projected that they could be made for planar cells and concentrator cells up to about 100 suns. Above that, precipitates could be a problem. To jump ahead, In(0.5)Ga(0.5)P/GaAs/Ge triple junction cells are now used regularly on satellites. However at the time (1978), we had presented a proposal to the Air Force and it was not funded.

In 1979, Hughes decided that they were not interested in terrestrial solar cells but at that time the oil companies were, so I left Hughes to join the Chevron Research Co Alternative Energy Group. However, before going on to the years of learning how to grow single crystal III–V films at Chevron, there were some other significant events at Hughes. I relate these events because they connect to people and companies and events later in this story.

One afternoon, I was working in the lab and my department head brought by a visitor. The visitor was Bill Yerkes, the president of Spectrolab. I relate this story because 10 years later at Boeing, I was to work with Bill on the 35 % cell. Spectrolab was one of the two suppliers of space silicon solar cells. It turned out shortly after this visit that I heard that Hughes had bought Spectrolab. The story I heard was that Bill had run Spectrolab into debt trying to make terrestrial solar modules and Hughes had no choice but to buy Spectrolab because they needed space cells.

Soon after this as I was leaving for Chevron, I heard that Bill had left Hughes Spectrolab to form Solar Technology International (STI) to make terrestrial silicon panels. Over the next 10 years from 1978 to 1987, STI was bought by Arco and became Arco Solar. Arco Solar later became Siemens Solar. Today it is Solar-World. However, in the early years, STI and Arco Solar led by Bill Yerkes developed the terrestrial silicon module that I described in Chap. 5. The laminating process was based on the idea of a shower door safety glass laminant. This same module design is used today by almost all module manufacturers.

Another significant event that occurred while I was at Hughes was a visit by Paul Rappaport, one of the pioneers in silicon solar cells. He gave a lecture but I also met him privately in my department manager's office. I remember him asking if GaAs cell junctions could be made by diffusion. Our answer was that since we had to grow the AlGaAs window layer, we could simply grow the junction layers. His question still resonates today as I will describe later in this chapter.

I moved on to Chevron. When I arrived at Chevron, I soon discovered that the Chevron Solar Alternative Energy effort was focused on small grain size polycrystalline thin film solar cells. Unfortunately for me, I had been trained in solid state physics and knew about the bandgap derivation in semiconductors based on the perfect periodic lattice. Anyway, my boss Jack Duisman, was open minded and allowed me to work on III–V single crystal solar cells. This was good but the bad news was that I was by myself. Chevron Research was organized along classic lines with teams of one Ph.D. and one technician with each team having a lot of freedom. I talked Jack into allowing me to hire two technicians but I had to recruit them from the refinery, not the semiconductor industry.

History Continued: Epitaxy and Monolithic Multijunction Cells

I wanted to implement the InGaP/GaInAs/Ge cell design but I had to learn how to grow the various single crystal layers. Up until approximately this time (1979), the GaAs and AlGaAs single crystal layers were grown by a process called liquid phase epitaxy. To grow GaAs in this process for example, a wafer of GaAs is dipped into a bowl of Gallium liquid where some Arsenic is dissolved in the liquid. By controlling time and temperature as the liquid is very slowly cooled, Ga and As atoms would come out of the melt and deposit on the GaAs wafer. Since the wafer is single crystal, the new Ga and As atoms key onto the proper sites and a crystal film is grown. This process is called epitaxy. To grow AlGaAs, one adds a little Aluminum to the melt. This is liquid phase epitaxy (LPE). One could also do this epitaxy with chemicals from the vapor phase called vapor phase epitaxy (VPE) or in a vacuum chamber with chemical beams called chemical beam epitaxy (CBE). Actually at the time, chemical beam epitaxy did not exist. I was to pioneer this process at Chevron [8–11].

The problem was that one could not use LPE to grow GaAs on germanium. The germanium would dissolve in the gallium melt and contaminate the melt. Scaling up LPE for production was also a problem. Around this time, workers at Varian and Rockwell Science Center were demonstrating that AlGaAs/GaAs solar cells could be fabricated with a process called Metal-Organic Chemical Vapor Deposition or MO-CVD. In this process, the metal gallium or aluminum supply comes from compounds called metal-organics. These are vapors at room temperature. This makes them easy to transport to the heated wafer surface. Tetraethyl lead is a classic metal organic that used to be used in gasoline.

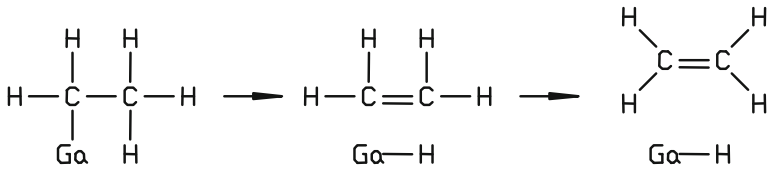


Fig. 8.1 Using Triethyl Ga instead of Trimethyl Ga removes carbon cleanly as ethylene (C_2H_4). Note that 2 vertical bonds (*left*) resonate to form 2 horizontal bonds (*middle*)

To understand metal-organics, we start with methane or natural gas. Obviously, it is volatile. A methane molecule is one carbon atom with four hydrogen atoms bonded to it, CH_4. One can remove one hydrogen atom and then bond the exposed carbon atom to gallium. CH_3 is a methyl group. Doing this three times, one obtains trimethyl gallium or TMGa or $Ga(CH_3)_3$. The gallium metal atom is now surrounded with organic groups and is volatile. To make arsenic volatile, one can add three hydrogen atoms to create arsine (AsH_3). Now one can grow a GaAs film in MO-CVD by reacting TMGa with AsH_3 as per the following reaction:

$$Ga(CH_3)_3 + AsH_3 - > GaAs + 3CH_4$$

MO-CVD works well and is now a preferred process for many III–V devices in commercial production today. The problem I had with this at the time is that arsine (AsH_3) is a very poisonous gas. If a bottle were to be released into the atmosphere, it could kill everybody in a whole neighborhood. The semiconductor community has learned to handle this gas safely but today, it should be observed that arsine was found listed as a desirable chemical weapon material in two terrorist notebooks in Afghanistan.

The advantage of using arsine in MOCVD is that the hydrogen from the arsine provides a clean way of removing carbon from the growing film creating methane and leaving a very pure semiconductor film. Anyway, I found myself at Chevron among many organic chemists. One day after I started looking at MOCVD, somebody pointed out that there is a reaction celled a beta elimination reaction that is shown in Fig. 8.1 where ethyl groups go to ethylene and hydrogen. They knew about this because of tetraethyl lead combustion experiments. This is a clean way of getting rid of carbon. (Maybe this eliminates carbon deposits in engines.)

One needs to look at the picture in Fig. 8.1. Ethane (C_2H_6) just has two carbons instead of the one in methane. The ethyl to ethylene plus hydrogen reaction occurs because of the positions of the atoms. As Fig. 8.1 shows, there is an easy resonant bond transfer [10, 11].

This meant that one could grow GaAs in a vacuum system via a reaction with Triethyl gallium and arsenic vapor without arsine toxic gas via the reaction:

$$2Ga(C_2H_5)_3 + As_2 - > 2GaAs + 6C_2H_4 + 3H_2$$

This was the beginning of what Bell Labs called chemical beam epitaxy (CBE) but what we called vacuum chemical epitaxy (VCE) [10, 11]. Their name stuck but I was the first to grow pure GaAs films using triethyl gallium in a vacuum system [8, 9].

Anyway, during my 8 years at Chevron, I grew GaAs, AlGaAs, InGaP, GaInAs, GaAsP, and GaSb III–V films. We built our own growth equipment [10, 11]. However, I was hampered by not having device fabrication process knowledge from the semiconductor community. I slowly built up an equipment and device process capability. However, being by myself was difficult. As time went on, my device designs got simpler. Initially, I tried to make the whole monolithic multijunction structure but obviously, I had to break it down into sub components. Eventually, I realized my task was monumental. I had to make three new junctions in two new materials. I had to make a top junction, a bottom junction, and a tunnel junction all working correctly together. I decided to reduce this task by stacking cells together eliminating the tunnel junction problem.

Note now that this is a new type of multijunction cell that we shall call mechanically stacked multijunction cells. Here one chip is just glued on top of another chip. This has several advantages in that more materials are possible since crystal atomic spacing need not be matched. Furthermore, currents need no longer be matched as we shall describe later.

So for a stacked cell, I decided to use an already existing silicon cell as the bottom cell and to make one new top cell. Growing GaAsP on GaP wafers could yield the top cell as this material system is commonly used in light emitting diodes. I succeeded in doing this but I just got to 26 % efficiency, no better than a single junction GaAs cell.

History Continued: New Infrared Sensitive GaSb Cell and the 35 % Efficient GaAs/GaSb Stacked Cell

I then realized that if I started with the GaAs cell as the top cell and made it transparent by putting a grid on its back side, then if I invented a new infrared bottom cell, whatever I did would have to break the world record for cell efficiencies. I looked at the periodic table and found GaSb. By this time, I appreciated the beauty in simple binary compounds as opposed to three and four element alloys. Larry Partain was a colleague at Chevron and he had calculated that the difference in bandgap energies for the top and bottom cells should be about 0.7 eV. The GaAs bandgap is 1.42 eV and the GaSb bandgap is 0.72 eV. Perfect! I then went to the literature and found that Bell Labs had made AlGaSb/GaSb photodiodes and published performance curves. Using this data, I wrote a paper projecting that the GaAs/GaSb two-color solar cell could reach an efficiency of 33.9 % under concentrated sunlight here on earth [12].

However, this was again a projection. So I started to learn how to grow GaSb films. I assumed that I would also have to grow an AlGaSb passivating window layer. This was 1986 and Chevron had lost interest in solar cells. Chevron sold the

VCE process and equipment to a Japanese Company. So I found a job at the Boeing Hi Tech Center which had just been formed. My epitaxy experience got me a position as the epitaxy group supervisor in the Materials and Devices Lab.

Before I leave the Chevron story behind, there was one more significant thing that happened at Chevron. Walt Pyle was another engineer at the Chevron Research Company and he was interested in how to use solar in the most efficient way possible. The answer is to use sunlight as light for offices to displace electricity used in florescent lights. Doing this would be like having a 100 % efficient solar cell. Since I was interested in concentrated sunlight, the idea of concentrated and piped sunlight for indoor illumination came to us in 1982 and we published a paper on this in 1983 [13]. I was excited about this idea but Chevron wasn't and this is when I decided that Chevron was just in alternative energy for public relations purposes. A memorable quote later when the alternate energy group was disbanded was that "We have paid our dues at the altar of alternative energy." I forgot about this solar lighting idea. Then in 2000, Jeff Muhs from Oak Ridge National Labs championed the idea. This concept will be described further in the Chap. 10.

Research at the Boeing Hi Tech Center was structured differently than the Chevron work had been structured. The Materials and Devices Department had about 50 researchers from the semiconductor community. There was a lot of up to date equipment for device processing and detailed knowledge for each process step used in semiconductor device fabrication. Bill Yerkes was one of the department managers there and Boeing had an ongoing solar cell effort. Jim Avery was also there working in the thin film solar cell group. Jim had been the first engineer at STI and Arco Solar and he had developed the screen-printed grid process for terrestrial silicon planar cells. He also had worked on thin film solar cells at Arco Solar and he was tired of thin film solar cells. So eventually, Jim was able to join my group and we have now worked together for 20 years.

One of my surprises at Boeing was that there were large secret solar cell defense projects for satellites. This was now 1987. I found this interesting because as I left Chevron, the annual government terrestrial-solar-cell R&D budget was about $50 million. Meanwhile, around $100 million was being spent on these secret programs. The idea was that the Russians could damage our satellites by zapping the solar cell arrays with lasers. Alternatively, what if they launched needles into orbit? We had to make our solar arrays invulnerable against attack. One of the consequences of this line of reasoning was that if sunlight concentrating-mirrors were used, the cells could only be hit with a laser from the direction of the sun, a situation difficult for an enemy to arrange.

This was the first time that I found that it is much easier to justify a multi-million dollar project for national defense than it is to justify a hundred-thousand dollar project for long term national economic benefit. Over the years since, I have seen many more examples of this but I still find this reasoning very much out of balance.

Anyway, I was given a mission to make more efficient concentrator solar cells. This allowed me to work on GaSb cells. There was one observation that I had made in the last days at Chevron. I grew a GaSb p/n junction and measured its

light generated current. I had not yet grown AlGaSb window layers but I was surprised that the current was pretty good. This suggested that perhaps by some good fortune, the *p*-type GaSb surface was passivated. As it turned out, I was also in charge of zinc diffusion in GaAs for laser fabrication. I decided that a quick path would be to try zinc diffusion in GaSb. I had a young engineer in my group, Jerry Girard, and he did a great job trying this and it worked right off, a rare occurrence, perhaps a compliment to Jerry.

Based on the above, I knew that GaSb cells would work but there was still a lot of work to do. We designed both GaAs and GaSb cell mask sets and proceeded to both refine the GaSb cells and to make good transparent GaAs cells using the MOCVD equipment in my group. Dr. Sundaram, our MOCVD expert, did the GaAs cell epitaxy and Jim supervised the cell fabrication and did the measurements. The beauty of this approach was that we could make good GaSb cells and put them away. Then we could focus on making good GaAs cells and then refocus on making stacks. Doing this brought us into 1989. We did get world record efficiencies by the end of the particular secret project but Boeing lost on the down select. Boeing's optics design used glass rather than mirrors and glass still would absorb infrared laser energy.

Dr. Edith Martin was the Vice President of the Hi Tech Center and she was always very supportive of this work. By August of 1989, I had about 6 GaAs/GaSb stacks with measured efficiencies between 33 and 37 % in time to go to a conference at Sandia National Labs where I presented these measurements. I was surprised at the resultant publicity. The solar press picked up the 37 % number and then this got reproduced in the national press. Boeing's stock went up for a day and Edith Martin got a call from her boss. He was upset that he did not know about this but Edith pointed out that she had sent him a memo. Still Boeing upper management wasn't very happy.

Actually, in retrospect, at the Sandia meeting I should have said that we had cells with efficiencies of 35 % with an uncertainty of ±2 %. However, the other problem was that the Sandia meeting was on terrestrial cells and I reported terrestrial cell efficiencies. Terrestrial efficiencies are always higher than space efficiencies by a little bit because the earth's atmosphere absorbs UV and infrared photons that are not efficiently converted by the cell. So because these UV and infrared rays are still there in space, cell efficiencies are lower for space cells. However, I don't think the efficiency was the issue. It was more that we were not supposed to be working on terrestrial solar cells, only on space cells.

But Edith kept the effort going and Bill Yerkes made a connection with the Boeing Space Station team. Meanwhile, I had three problems. First, I needed an outside confirmation. Second I needed appropriate optics for solar radiation concentration. Finally, third, the National Renewable Energy Lab (NREL) and the DOE were skeptical since they hadn't funded the work and they championed thin film solar cell approaches.

Outside confirmation was a challenge since the GaSb cell was new and responded in the infrared beyond the traditional silicon cell response range. I sent tandem cell samples to NREL, Sandia, and NASA Lewis (now NASA Glenn).

Sandia tried to make measurements under concentrated light but their probes were big and bulky and damaged the small research cells. NREL had no way of measuring with concentrated light but Keith Emery at NREL was able to confirm our quantum efficiency measurements on the GaSb cell. Meanwhile, NASA Glenn was able to confirm the current voltage curves for both cells using concentrated light. The real confirmation had to await a Lear Jet high altitude measurement on the GaSb cell which came back in time for papers published in 1990 at the IEEE Photovoltaic Specialist Conference [14]. The Lear Jet AM0 measurement and the Boeing and NREL quantum efficiency measurements were all consistent with a 32 % space cell efficiency (AM0 = air mass zero or no air = space).

So we had a space cell efficiency. What was the stack conversion efficiency here on earth? Well the problem on earth is that the sun's spectrum varies with weather conditions like humidity and time of day. The sun is redder in the morning and evening than at noon and water vapor absorbs in the infrared more or less varying with the humidity. To attack this problem, James Gee at Sandia was able to calculate solar spectra given atmospheric conditions and he had historical weather data for Albuquerque. Given the component cell data, he calculated efficiencies for component cells and the stack for various days through the year and we published this data in 1990 [3]. The bottom line is that the calculated annual average stack efficiency is 35.6 %. This was the efficiency assuming cells operating at room temperature. For operation at standard operating temperatures, this efficiency will drop to 32 % and given lens losses that will be the case for a module, this efficiency drops to 29 %. These were projections made in 1990.

Regarding the lens problem, I knew that Mark O'Neill, the president of ENTECH Inc, had a contract with NASA Glenn where he was making lightweight Fresnel lenses for space. Mark was very cooperative and we have now frequently worked together over the years. To jump ahead, mini-module efficiencies measured by ENTECH in Texas in 2001 for various multijunction cells varied between 28 and 31 %. Figure 8.2 shows a photograph of a multijunction cell circuit in outdoor testing.

In 1992, we built a mini-module using ENTECH Fresnel lenses and our tandem GaAs/GaSb cells for a Photovoltaic Advanced Space Power (PASP+) satellite. A photograph of this PASP+ module is shown in Chap. 1. This satellite was launched in 1994 with very good test results over the next year. Our mini-module performance was the highest and the degradation rate with radiation exposure was the lowest relative to all of the different types of new and baseline modules on that flight.

Unfortunately, after the mini-module was built but before the mini-module was launched, the Hi Tech Center was dismantled. Boeing decided that they would never make money on solar cell arrays. After all, they make perhaps 100 airplanes a year each costing about $100 million dollars, not millions of solar cells a year with each costing a few dollars. I left Boeing with a license to make these cells and joined JX Crystals in January of 1993.

After 1994, GaAs/GaSb stacked cells with efficiencies over 30 % were made in Germany and Russia [15]. Meanwhile, NREL has funded the InGaP/GaAs/Ge

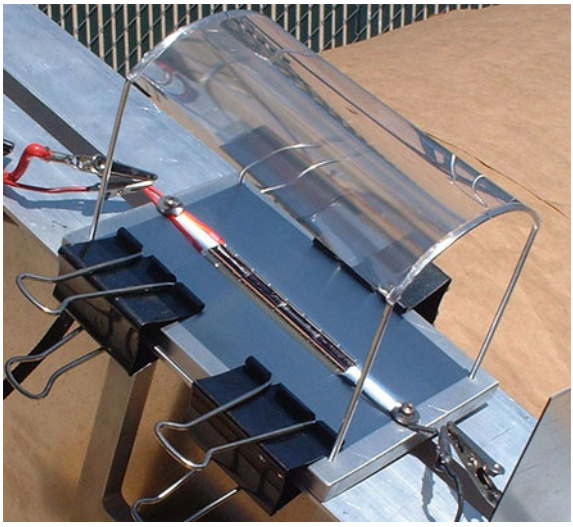


Fig. 8.2 Mini-module with linear Fresnel lens and stacked-cell circuit in outdoor testing

monolithic cell for space while, ironically, NASA has occasionally funded JX Crystals on improvements in the GaAs/GaSb stack approach. Notice the reversal of roles as NREL funds cells appropriate for space and NASA funds cells appropriate for terrestrial applications. Even more ironically, Boeing then bought Spectrolab in 2000 and eventually, Spectrolab having made InGaP/GaInAs/Ge cells for space, started making InGaP/GaInAs/Ge terrestrial concentrator cells culminating with the 40 % triple junction cell in 2006 [16, 17].

Different Designs for Different Applications

This now brings me to a technical discussion of the various approaches to making multijunction cells and the merits and disadvantages of each. Three different approaches are shown in Fig. 8.3. The center diagram in this figure shows the simple GaAs-GaSb stacked cell demonstrated for space applications at Boeing in 1989. However, as it turned out, the monolithic triple junction InGaP/GaAs/Ge cell shown on the left of this figure has been the preferred cell for space planar arrays. We refer to the structure on the right as a hybrid multijunction cell as it combines monolithic multijunction cells as components in a stacked cell. In Fig. 8.3, the hybrid InGaP/GaAs-GaSb stack cell is the cell incorporated into the 34 % efficient concentrator module shown in Chap. 7.

There are in fact a large number of issues that need to be considered in comparing various multijunction cell approaches. We begin by contrasting the GaAs-GaSb stacked cell with the pure monolithic multijunction cell. There are several significant differences. First, on the side of the monolithic approach, this cell is a single chip with two terminals just like a traditional solar cell. However, there is a

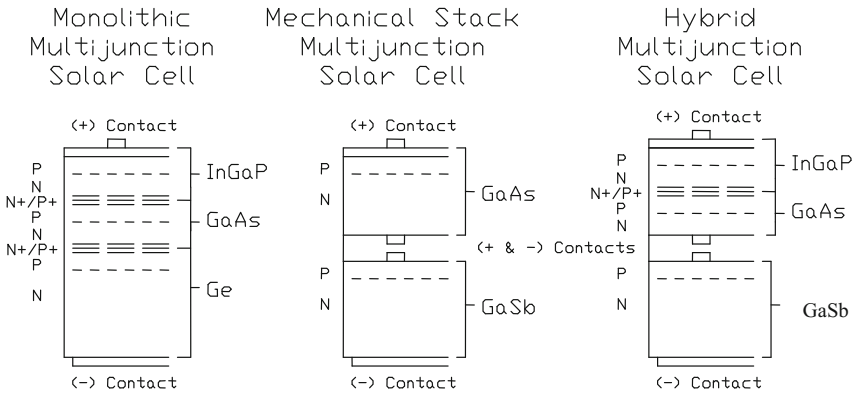


Fig. 8.3 Three different multijunction cell designs

price paid for this. Complex epitaxial structures are required. Unfortunately, they are grown using poisonous gases. Tunnel junctions are required. Local current matching of component cells is required. And lattice matched materials are required. On the side of the stacked cell, all of these constraints are removed. However, a negative for the stack is that two chips are required necessitating four terminals. For space planar arrays, the lack of space between cells and lightweight favor the monolithic cell. However, I believe that the mechanical stack approach is preferable for high concentration applications here on earth. Why?

There are several problems that arise for the monolithic approach as it is brought down to earth. The first problem is that, while the sun's spectrum is constant in space, it varies here on earth. This is a problem for the series connected cells in a monolithic multijunction cell. However, it is not a problem for the mechanically stacked cell because the 4 terminal stacked cell can be wired in a voltage-matched configuration as shown in Fig. 8.4. While the 4 terminal configuration in a stacked cell appears at first to be a problem, Fig. 8.4 shows how these 4 terminal are connected for the GaAs-GaSb stacked cell into a two terminal voltage matched triplet circuit with 3 GaSb cells in series and 3 GaAs cells in parallel. The advantage of voltage matching over current matching is that cell voltage varies very little with current variations associated with solar spectrum changes.

In order to fabricate these triplet circuits economically, improvements in stack design have been made since the Boeing days. Our latest stack design is shown in Fig. 8.5.

Notice that ribbons are bonded to the top of the top cells for the positive and negative connections. This is accomplished because the negative base layer (*N*-type GaAs wafer) is exposed by etching through the emitter layer at three edges and metal pads contact the negative base layer on the top of the cell. Notice that the GaSb and the top cell circuits are independent in this configuration. The top and bottom pads on the substrate allow testing of the GaSb cells while the left and right pads allow testing of the top cells. Notice also that the two cells will be glued

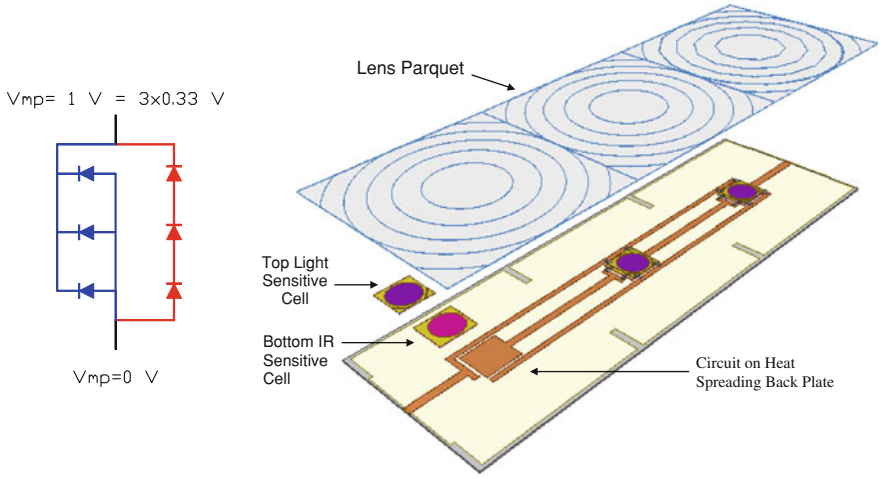


Fig. 8.4 Voltage Matched Triplet for GaAs-GaSb Stacked multijunction Cell. The diagram at the *right* shows the cells and wiring on the heat spreader plane at the lens array focal plane

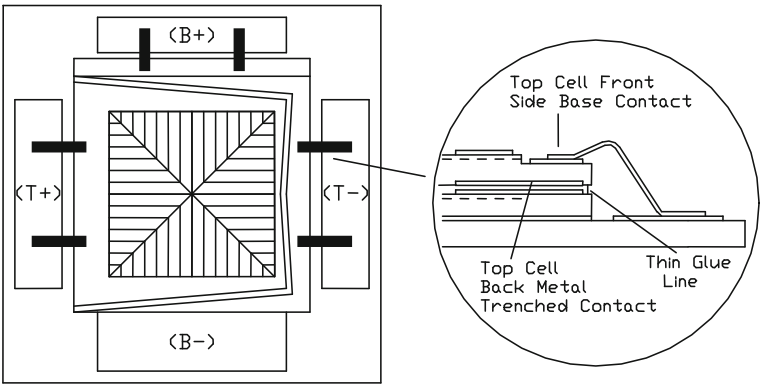


Fig. 8.5 JX Crystals 4 terminal mechanical stack receiver design with both contacts at *top* of top cell and back metal contact on top cell recessed in trench for thin low delta-T glue line

together with a thin silicone adhesive layer. Shorting of the top cell back metal contact to the bottom cell front metal contact is avoided by etching into the back of the top cell after resist patterning but before metal deposition. This puts the top cell back metal bus and grids into recessed trenches. Back side AR coating over everything follows providing another level of electrical isolation. Finally, we note that the grid density on the back of the top cell is one third of that on the fronts of both cells. This is because the *N*-type GaAs wafer is quite conductive (high mobility). This high wafer conductivity also allows the current to be passed back up through to the top etched base contact.

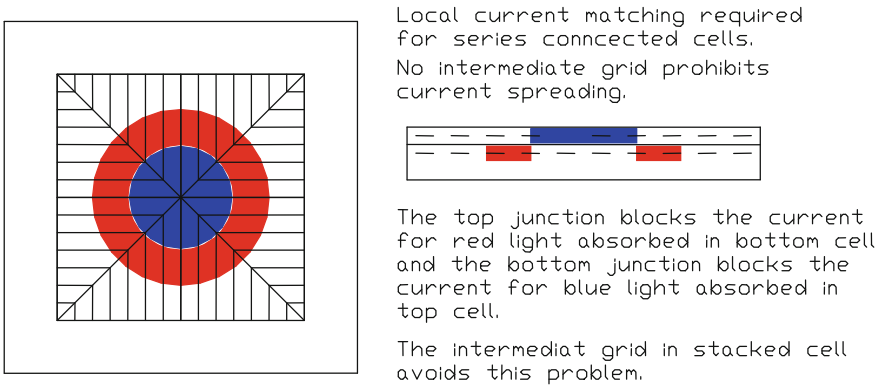


Fig. 8.6 Illustration of chromatic aberration problem for monolithic multijunction cell

Table 8.1 Monolithic vs. mechanically stacked MJ cells

Monolithic MJ cell	Mechanical Stacked MJ cell
Advantages for 1 sun space	*Disadvantages for 1 sun space*
• High efficiency and light weight for space satellites	• Two chips are heavier than one
• Two terminal device	• Four terminal device
Disadvantages for 500 sun terrestrial	*Advantages for 500 sun terrestrial*
• Series connection for 2 terminal requires tunnel junctions	• Crystal match not required giving higher efficiency
• Tunnel junctions can degrade at high currents	• Cells without tunnel junctions have proven stability
• Crystal match leads to non-optimal current matching	• Four terminals allow voltage match circuit
• Sensitive to variations in terrestrial solar spectrum	• Voltage matched circuit insensitive to variable spectrum
• Sensitive to lens chromatic aberrations	• 4 terminal device insensitive to lens chromatic aberrations
• Problems with bypass diode	• No extra bypass diode required

The second problem for the monolithic multijunction cell is associated with operation with a concentrating lens. Lenses produce color aberrations. In space, these cells are now operated without lenses at one sun. The problem for the monolithic approach is that current matching is a local requirement. If the lens produces a blue center spot with a red halo, currents are no longer matched locally and both regions will have suppressed currents dramatically reducing conversion efficiency. This problem is illustrated in Fig. 8.6. This problem can be resolved by designing a color mixing Fresnel lens or by using a homogenizing secondary.

There are other disadvantages of the monolithic approach as listed in Table 8.1. However the most significant problem in my opinion is that toxic gas use is inherent in the monolithic multijunction cell fabrication. This is much less so for

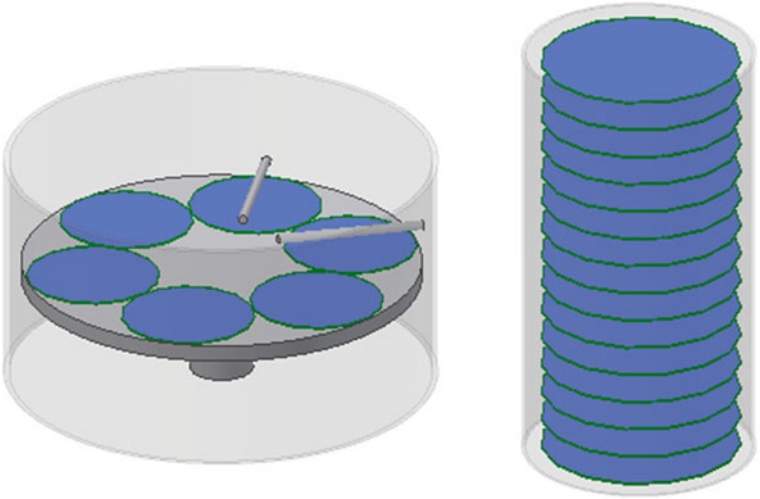


Fig. 8.7 MOCVD (*left*) versus diffusion (*right*): In the MOCVD system at the *left*, wafers are loaded face up onto a platter that spins rapidly so the wafers pass under TMGa and AsH3 injector tubes for crystal layer growth. Meanwhile, in a diffusion tube at right, wafers are stacked in pairs and a dopant vapor in the space between pairs diffuses into the wafer surface forming a junction

the mechanically stacked cell approach. This brings us back to MOCVD grown junction vs diffused junctions, the question that Paul Rappaport asked 25 years ago. Perhaps the GaAs cell surface can be passivated without the use of toxic gases and both GaAs and GaSb cells can be made with diffusions.

When it comes to production of large quantities of these cells for tens of gigawatts of electricity, the diffusion process will be much more economical as can be seen in Fig. 8.7. As is apparent in this figure, many more wafers (10 times) can be stacked like poker chips in a diffusion furnace than can be laid face up in an MOCVD machine. The capital cost of a diffusion furnace is also at least 10 times less than an MOCVD machine. This means that diffusion junction formation is at least 100 times cheaper than epitaxially grown junctions.

My dream is still that 35 % solar cells can find their way into terrestrial concentrator arrays like the Amonix array shown in the last chapter reducing the cost of solar electricity. Unfortunately, this seems to still be in the future. Are there any fundamental showstoppers (other than the funding problem)? My answer is no.

However, there are two fundamental issues that I have not yet addressed. First, arsenic is a poison. Is this a problem? No, we are talking about gallium arsenide (GaAs) cells, not arsenic. GaAs is a stable semiconductor compound. An analogy here is that chlorine (Cl_2) is a poisonous gas used in trench warfare in World War I. However, although chlorine is in sodium chloride (NaCl) which is table salt, when it occurs in a stable compound, it is not dangerous. GaAs chips are in your cell phone and GaAs solar cells are no more dangerous than your cell phone.

Second, is there enough gallium to make hundreds of gigawatts of concentrator cells? Yes, gallium is found in aluminum and zinc ores [18]. If we were to make

GaAs/GaSb stacked cells for the Amonix array, each stack would produce 5 W and weigh 1/4 gram. This is 20 W per g. Today, approximately 200,000 kg per year of gallium are used in making GaAs semiconductor devices. This means that 4 gigawatts per year can be made today with present gallium production. According to the US Geological Survey, "World resources of gallium in bauxite are estimated to exceed 1 billion kilograms, and a considerable quantity could be present in world zinc reserves." It would take 1 % of this gallium resource in bauxite to produce 200 gigawatts of electric power with these cells.

Recent Developments in Concentrator Modules: Germany and Japan Bring Multicolor Cells Down to Earth

While the US pioneered the development of multicolor cells, the US focus has been on space and military applications. Meanwhile, Sharp in Japan and the Fraunhofer Institute for Solar Energy in Germany given support from their governments, have been developing concentrator modules for use here on earth using these high efficiency cells. As shown schematically in Fig. 8.8, Sharp has used a color mixing secondary homogenizer to avoid the cell chromatic aberration problem and they have now demonstrated a 28 % efficient terrestrial concentrator module. A photograph of this module is shown in Chap. 1 of this book.

The Fraunhofer Institute for Solar Energy (ISE) has also been developing terrestrial concentrator modules using multicolor cells. Figure 8.9 shows a photograph of some of these ISE modules in outdoor testing. This module technology is now in production as shown in the Soitech HCPV array shown in the last chapter.

Recent Developments in Concentrator Modules: The Cassegrain PV Module

In September of 2004, I received a visitor at JX Crystals. Mr. Eli Shifman had purchased my first book and after reading the chapter on hybrid lighting, he observed that a cold mirror could be used as the secondary mirror in a Cassegrain module to split the spectrum as shown in Fig. 8.10.

This idea allows two simpler cells to be physically separated dividing the heat loads. As it turned out, this idea fit perfectly with a funded NREL contract where we were developing hybrid InGaP/GaAs and GaSb cells with combined efficiencies summing to 40 %.

As an historical note, the name Cassegrainian comes from a Frenchman named Cassegrain who first described in 1672 an optical telescope that used a concave primary mirror with a convex secondary mirror. The primary mirror collected starlight and bounced it to the secondary mirror that then returned the starlight

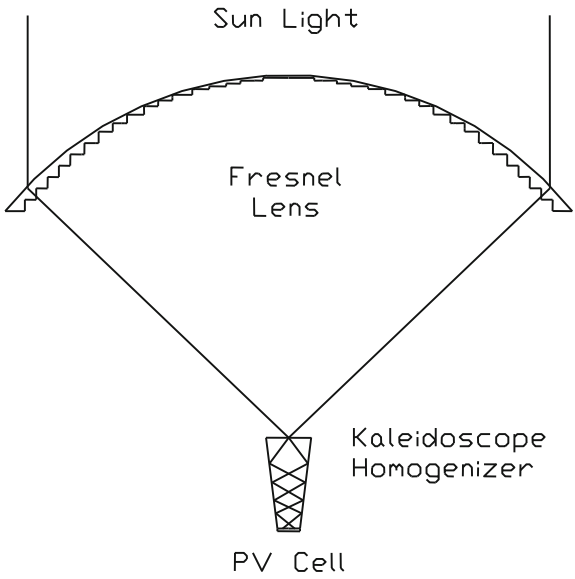


Fig. 8.8 The Sharp concentrator module uses a domed Fresnel lens to concentrate sunlight into a glass homogenizer that then mixes the rays as they bounce down to the multicolor cell at the base. The power density is uniform for each color



Fig. 8.9 Terrestrial concentrator modules using over 30 % efficient multicolor cells in outdoor testing at Fraunhofer Institute of Solar Energy

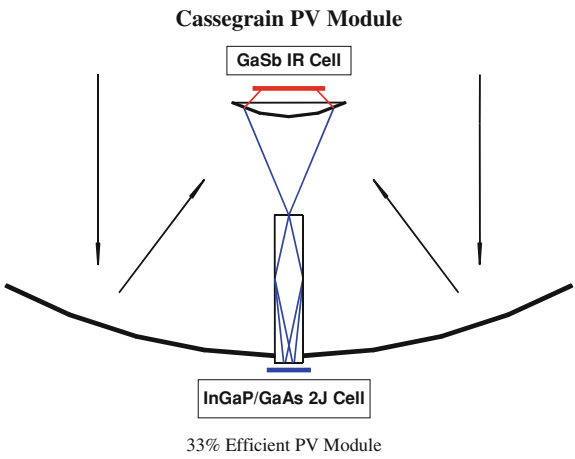


Fig. 8.10 Cassegrainian PV Module Concept uses a dichroic secondary mirror to split the spectrum into short and long wavelength bands to create two focal points

through a hole in the primary mirror to the eye of a human observer. This is now a familiar optical telescope design. The difference here is that the star is our sun, the human eye is replaced with a solar cell, and the secondary mirror is designed to split the sun's spectrum. Adding an IR cell behind the secondary then further increases the solar energy conversion efficiency.

Conclusion

In 2006, King [17] et al. at Spectrolab with a contract from NREL demonstrated the monolithisc InGaP/GaInAs/Ge triple junction cell with a 40 % efficiency at 240 suns. Meanwhile in 2006, Fraas [2] et al. demonstrated a 34 % efficient concentrator module using an InGaP/GaAs cell in combination with a GaSb IR cell as suggested in the right hand diagram in Fig. 8.3.

References

1. L.M. Fraas, R.C. Knechtli, Design of high efficiency monolithic stacked multijunction solar cells, in *13th IEEE Photovoltaic Specialist Conference*, p. 886 (1978)
2. L.M. Fraas, J. Avery, H. Huang, L. Minkin, E. Shifman, Demonstration of a 33 % efficient cassegrainian solar module", in *4th World Conference on PV*, Hawaii (2006)
3. L. Fraas, J. Avery, J. Gee, K. Emery, et al., Over 35 % efficient GaAs/GaSb stacked concentrator cell assemblies for terrestrial applications, in *21st IEEE PV Specialist Conference*, p. 190 (1990)
4. R. P. Feynman, R. B. Leighton, M. Sands, *The Feynman Lectures on Physics*, 3 Vols (Addison-Wesley, New York, 1965)
5. H.J. Hovel, J.M. Woodall, High efficiency AlGaAs-GaAs solar cells. Appl. Phys. Lett. **21**, 379–381 (1972)

6. Z.I. Alferov, V.M. Andreev, et al., Solar cells based on heterojunction p-AlGaAs-n-GaAs. Sov. Phys. Semicond. **4**(12) (1970) (Translated into English)
7. R. Loo, R. Knechtli, S. Kamath, et al., Electron and proton degradation in AlGaAs-GaAs Solar Cells, in 13th *IEEE Photovoltaic Specialist Conference*, p. 562 (1978)
8. L. Fraas, A new low temperature III-V multilayer growth technique: vacuum MOCVD. J. Appl. Phys. **52**, 6939 (1981)
9. L.M. Fraas et al., Epitaxial films grown by vacuum MOCVD. J. Crystal Growth **68**, 490 (1984)
10. L.M. Fraas et al., Epitaxial growth from organometallic sources in high vacuum. J. Vac. Sci. Technol. **B4**, 22 (1986)
11. L.M. Fraas et al., High throughput vacuum chemical epitaxy. J. Crystal Growth **105**, 35 (1990)
12. L.M. Fraas, Near Term Higher Efficiencies with Mechanically Stacked Two-Color Solar Batteries, in *Solar Cells*, vol. 19, p. 73 (1986/1987)
13. L.M. Fraas, W.R. Pyle, P.R. Ryason, Concentrated and piped sunlight for indoor illumination. Appl. Opt. **22**, 578 (1983)
14. J.E. Avery, L.M. Fraas, et. al., Lightweight concentrator module with 30 % AM0 efficient GaAs/GaSb tandem cells, in *21st IEEE PV Specialist Conference*, p. 1277 (1990)
15. A. Bett, G. Stollwerck, O. Solima, W. Wettling, Highest Efficiency Tandem Concentrator Module, in *2nd World Conference on Photovoltaic Solar Energy Conversion*, p. 268 (1998)
16. R.R. King et al., Lattice matched and metamorphic InGaP/GaInAs/Ge Concentrator Solar Cells, in *3rd World Conference of PV Energy Conversion* (2003)
17. R.R. King et al., 40 % efficient metamorphic GaInP/GaInAs/Ge multijunction solar cells. Appl. Phys. Lett. **90**, 183516 (2007)
18. Gallium, U.S. Geological Survey, Mineral Commodity Summaries (2002)

Chapter 9
Solar PV in a Larger Electric Power Context

Fuels for Electric Power

Today in early 2014, solar PV has grown to a cumulated world wide installed capacity of 135 GW. Also significantly, the US in 2013 installed a total of 5 GW of solar which is equivalent to the electric power production capacity of the Fukushima Nuclear Power Plant. But, how does solar PV fit into the larger picture for total US electric power generation? At the end of 2013, the accumulated installed capacity of PV in the US was 13 GW out of the total US installed electric power capacity of 1,100 GW. While this is small at 1.2 % relative to the total, solar PV is now growing rapidly. It grew by 41 % in 2013. As is shown in Fig. 9.1, renewable energy capacity is still very small compared to coal, natural gas, and nuclear but renewable energy and natural gas are expected to gradually displace coal and nuclear over the next several decades [1]. Figure 9.1 is a projection from the US DOE Energy Information Agency (EIA) and the reader should be warned that the EIA has tended to understate the future value of renewable energy.

Next, what about the price of solar electricity in US cents per kWh? It will obviously depend on the sunlight intensity at the installation location. In the US, the best solar locations are going to be in the pacific southwestern states. Table 9.1 gives the price of electricity in several Southwestern US states today [2]. Prices depend on the user and use.

Solar Electricity is Cost Competitive

The Fraunhofer Institute for Solar Energy in Germany has now published a study of the LCOE for solar PV installation in 2013 [3]. Their results are shown in Fig. 9.2.

Since the amount of sunlight available in a typical solar installation site in the US Pacific Southwest is between 1,800 and 2,000 kWh per square meter per year, the price of solar electricity will be between 6 and 9 Euro ¢/kWh or between

L. M. Fraas, *Low-Cost Solar Electric Power*, DOI: 10.1007/978-3-319-07530-3_9,

© Springer International Publishing Switzerland 2014

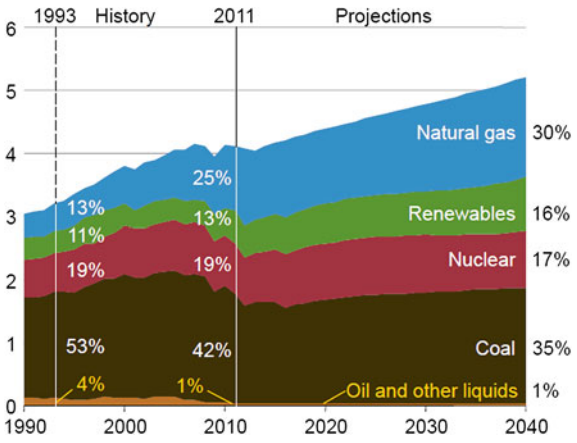


Fig. 9.1 Electricity generation by fuel, 1990–2040 [1]. (trillion kWhr per year)

Table 9.1 Jan 2014 cost of electricity [2]

	Residential	Commercial
California	16.6	13.4
Arizona	10.9	9.3
Nevada	12.5	9.6
New Mexico	11.3	9.6
Colorado	11.5	9.5

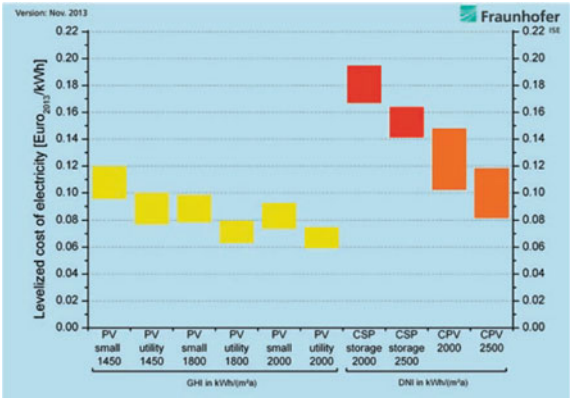


Fig. 9.2 LCOE of renewable energy technologies [3] at locations with high solar irradiation in 2013. The value under the technology refers to the solar irradiation in kWh/(m^2a): GHI for PV, DNI for CPV and CSP

8 and 12 US ¢/kWh. So, from Table 9.1, solar is now cost competitive in the US Pacific Southwest. The Fraunhofer LCOE numbers are in rough agreement with the LCOE projections [4] in Fig. 9.3 and as is seen from this figure, the LCOE is expected to continue to drop in the future.

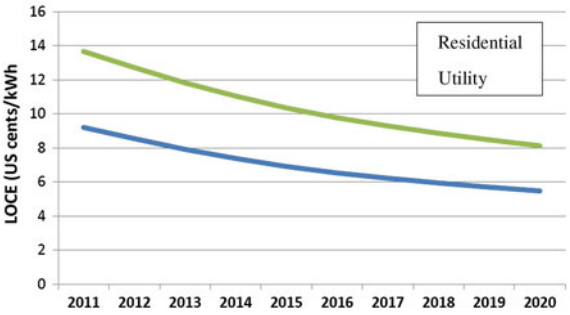


Fig. 9.3 Projections for LCOE [4]: Source Reichelstein (2012)

Intermittency and Energy Storage

The dream of the renewable energy community is that renewable energy sources can help avoid global warming and extend the use of fossil fuels for our most important needs as for example for fertilizers, plastics, and heating for our homes. Meanwhile, coal is the dirtiest fuel and the fuel that produces the most CO_2 per BTU of energy content, twice the CO_2 produced by natural gas. So, it is anticipated that natural gas and renewable energy will displace coal in the future.

Since solar and wind are intermittent resources, how far can solar and wind energy go into the electric power mix? Figure 9.4 gives a preliminary answer to this question for California [5, 6]. Since over half of the solar roofs in the US are in California, it is interesting to study California as a window into the future.

On Thursday, February 6th 2014, as a result of high demand for natural gas for heating because of the cold weather in the Eastern US, the California Independent System Operator was forced to call an emergency alert. It is surprising that there could be a gas shortage anywhere in the US continent known for "fracking" its way to an "energy independence" nirvana. But then, as pointed out by Paul Gype [5], renewable energy saved the day. There was no shortage of generation from new renewables Thursday. Geothermal, biomass, biogas, and small hydro generated a steady 1,700 MW throughout the day or nearly 6 % of peak demand. Meanwhile solar photovoltaics (solar PV) peaked at 1,800 MW around noon and wind power reached 2,700 MW during the evening peak period. Altogether, renewables generated nearly 15 % of total consumption on 6 February. Wind energy provided nearly half of all renewable generation during the 24-hour period; geothermal, nearly 25 %; solar PV, 12 %.

In the future, solar and wind are going to be combined with energy storage to resolve the intermittency problem [7–9]. This is already happening for large megawatt wind and solar plants as shown in Figs. 9.5, 9.6, and 9.7.

Experiments are also underway for community level micro grids. Figure 9.8 shows a solar village experiment at the Missouri University of Science and Technology. The buildings each have 5- to 10-kW PV systems. The buildings also have solar thermal systems for hot water. The energy storage components consist

24-Hour Renewables Production

Renewable Resources	Peak Production Time	Peak Production (MW)	Daily Production (MWh)
Solar Thermal	9:51	102	143
Solar	12:55	1,816	10,446
Wind	21:24	2,710	42,099
Small Hydro	19:16	197	3,056
Biogas	23:25	209	4,722
Biomass	16:46	350	7,897
Geothermal	10:32	902	21,488
Total Renewables			**89,851**
Total 24-Hour System Demand (MWh):			*604,018*

Fig. 9.4 This table gives numeric values related to the production from the various types of renewable resources for the reporting day, February 6th 2014. All values are hourly average unless otherwise stated. Peak production is an average over one minute. The total renewable production in megawatt-hours is compared to the total energy demand for the system for the day [6]



Fig. 9.5 Germany's Huntorf Compressed Air Energy Storage Plant [7] is the world's first and still the largest utility–scale commercial plant (as of April 2012)



Fig. 9.6 Upon completion in 2013, Abengoa Solar's Solana Generating Station [8] will be the world's largest parabolic trough solar CSP power plant and the United State's first utility-scale solar power plant to combine parabolic trough solar with molten salt energy storage (MSES) technology; able to store 6 h worth of solar thermal energy and boosting plant capacity to 41 %



Fig. 9.7 Lithium-ion Battery Energy Storage System Providing energy storage for a 98 MW wind farm, the AES Laurel Mountain Plant 32 MW lithium-ion battery storage facility [9] is the largest such energy storage facility in the United States



Fig. 9.8 Solar Village [10] at the Missouri University of Science and Technology

of two 100 kW/100 kWh lithium-ion iron nano-phosphate battery racks. There is also a fuel cell and a heat recovery unit as part of this microgrid [10].

What about intermittency and energy storage at the residential level? Here, looking at California can give us a window into the future. California is not just leading in solar and wind electric power generation but California is also leading with the number of registered new electric vehicles. This creates another opportunity with vehicle to grid electric power storage. By pioneering vehicle to grid, California can potentially replace its coal and nuclear power generation with solar and wind within the next 10 years.

Vehicle to Grid

The standard argument for electric vehicles is that EVs can reduce gasoline consumption in transportation, CO_2 emissions and the US dependence on foreign oil. However, the batteries in EVs can also serve as storage allowing renewables to cover both the day and night power needs. In this mode of operation, California



Fig. 9.9 Honda Fit EV at the 2010 LA Auto Show [13]

can displace the burning of coal and the use of nuclear for electricity generation. Recently California has announced a program to arrive at 1 million EVs over the next 10 years. It is observed here that with approximately 1.7 million EVs and 12 GW of utility solar PV/wind, California could displace coal and nuclear for electric power generation. California presently has 24 GW of utility solar PV under construction.

Normally solar photovoltaic fields are considered as sources for peak electric power generation and coal and nuclear power plants are thought to be required for base load power generation. However, coal is a dirty fuel and a major contributor to green house gases. Waste disposal and accidents from nuclear power plants are unresolved issues. Meanwhile in the transportation sector, the exhaust from vehicles burning gasoline is also a major contributor to green house gases. Electric vehicles (EV) can eliminate the green house gas CO_2 emissions from cars burning gasoline. In 2014, BMW, Honda, Ford, Fiat, Mercedes, and VW are all joining Tesla, GM, Nisan, and Toyota with the sale of EVs. This means that more than 403,000 electrified vehicles are expected to be built in 2014, up from 242,000 in 2013 [11]. Cars normally are driven on average for 2 h per day and all of these EVs will have batteries which can be used for charge/discharge cycles if connected to the grid during some fraction of the remaining 22 h every day. This means that EVs can be charged by solar and wind and hydro renewable generating plants and potentially displace coal and nuclear power plants. This concept is called "Vehicle to Grid" [12]. Figure 9.9 shows a new Honda FIT EV [13] hooked to the grid and Fig. 9.10 shows an EV being charged at an outdoor charging station [14].

Figure 9.11 shows the cumulative sales of EVs [15] up to December 2013. 30 % of these EVs are on the roads in California. The question now addressed here is: Can California utilities displace coal and nuclear power generation with solar and wind and if so when might that happen?



Fig. 9.10 Electric Vehicle at Solar Charging Station for Sustainable Urban Design [14]

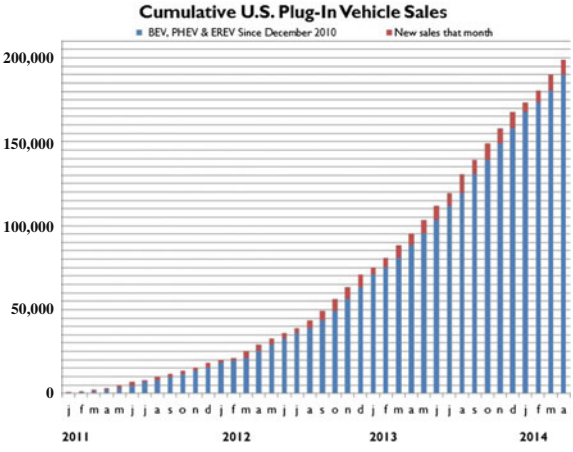


Fig. 9.11 Historical trend of US plug-in electric vehicles cumulative sales by month by type of power train from December 2010 to April 2014. Plug-in electric car sales passed the 200,000 unit mark in April 2014

The Vehicle to Grid Concept

Cory Budischak, Willett Kempton, et al. [12] from the University of Delaware have published a study of the electric vehicle to grid concept shown in Fig. 9.12 for the PJM utility district in the North East US and concluded that a combinations of wind power, solar power and electrochemical storage can power the PJM grid up to 99.9 % of the time. So, this is a very promising concept. Where might this concept first be implemented? Since California leads the world and the US in Solar installations and EV sales, California could well be first.

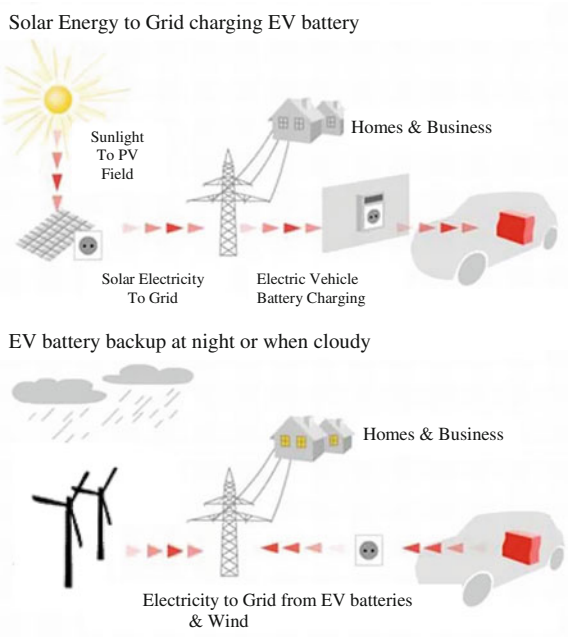


Fig. 9.12 Electric Vehicle to Grid concept

Table 9.2 California Electrical Energy Generation (Gigawatt Hours) 2012

California Generation plus Net Imports *	301,966
Total hydroelectric	27,459
Large hydroelectric	23,202
Small hydroeletric	4,257
Nuclear	18,491
In-state coal	1,580
Oil	90
Natural gas **	121,716
Direct coal imports***	9,716
Other imports****	93,149

Vehicle to Grid Opportunity in California

How many EVs and how much solar power would be required to displace coal and nuclear power production in California? Table 9.2 provides the input information required to answer this question [16].

The following calculations can now be made. The Tesla Model S has a battery capacity of 85 kWh per charge Some of this battery capacity will be used for transportaion each day. If one assume the EV battery capacity cycled to the grid will be 50 kWh and there will be a charge/dicharge cycle every day, then the starage capacity of an average EV will be 50x350 = 17,500 kWh per year. There

Table 9.3 Projected EVs in California assuming a 40 % growth rate in sales

New EVs each Year	Year	Cumulative EVs in California
50,000	2013	
70,000	2014	120,000
98,000	2015	220,000
140,000	2016	360,000
200,000	2017	560,000
280,000	2018	840,000
390,000	2019	1,230,000
550,000	2020	1,780,000

are now 50,000 EV in CA. This means that today's EV storage capacity potential is 50,000 × 17,500 = 50 × 17.5 GWh = 875 GWh.

From Table 9.2 for 2012, California In-state Coal generated 1,560 GWh. How many EVs would be required to displace CA In-State coal? The answer is $1.56 \times 10^9/1.75 \times 10^4 = 0.89 \times 10^5 = 89{,}000$ EVs. It is now interesting to compare this number with the projections in Table 9.3 for the number of EVs expected to be on the roads in California assuming a 40 % growth rate for EVs per year out until 2020. Note that it could be theoretical possible to have enough EV's to displace coal generation in California by the end of 2014.

How many EVs would be required to displace CA coal imports? The answer is $9.72 \times 10^5/1.75 = 555{,}000$ EVs. From Table 9.3, this number could be reached by 2017.

How many EVs would be required to displace CA nuclear? The answer is $18.5 \times 10^5/1.75 = 1.06$ million. EVs. This number could be reached by 2019. Since California's remaining Diablo Canyon 2.2 GW nuclear power plant is located near several earth quake fault lines and near the Pacific Ocean water's edge, this may be desirable [17].

How many EVs would be required to displace both coal and nuclear in California? The answer is 1.7 million EVs. This number could be reached by 2020. Since California now has 22 million passenger cars on the road, replacing just 1.7/22 = 8 % of these vehicles with EVs may be all that is required.

The last question is: How much solar electric power capacity would be required to displace both coal and nuclear power generation in California. From Table 9.2 and assuming base load with a 90 % capacity factor, the total 29,767 GWh for coal and nuclear equates to 4.2 GW. The Solar equivalent at 7 h per day is 29767/2500 = 11.9 GW. This agrees with the ~3X over capacity factor Kempton et al. [12] recommends for photovoltaics/wind.

According to the Mercom Solar Report 3 Feb 2014 at the end of 2013, based on annual market demand, solar PV in the US had an aggregate project pipeline of approximately 2,000 nonresidential projects. This represents almost 40 GW of potential PV capacity [18]. California dominates the 40 GW pipeline with over 60 % of capacity, firmly cementing its place as the leading US market. In fact, if California alone was compared on a global level, it would have ranked as the fourth largest global PV market in 2013. Sixty percent of 40 GW represents a solar

PV pipeline for California of 24 GW, more than enough to provide the approximately 12 GW required to displace both coal and nuclear power plants in California.

References

1. http://www.eia.gov/pressroom/presentations/sieminski_06052013.pdf
2. http://www.eia.gov/electricity/monthly/epm_table_grapher.cfm?t=epmt_5_6_a
3. http://www.ise.fraunhofer.de/en/publications/veroeffentlichungen-pdf-dateien-en/studien-und-konzeptpapiere/study-levelized-cost-of-electricity-renewable-energies.pdf
4. http://www.law.stanford.edu/sites/default/files/publication/359530/doc/slspublic/prospects_for_cost_competitive_solar_pv_power.pdf
5. http://www.renewableenergyworld.com/rea/news/article/2014/02/renewables-provide-15-of-supply-during-california-emergency-time-to-go-100-renewable
6. http://content.caiso.com/green/renewrpt/20140206_DailyRenewablesWatch.pdf
7. http://www.cleanenergyactionproject.com/CleanEnergyActionProject/Energy_Storage_Case_Studies_files/Huntorf%20Compressed%20Air%20Energy
8. http://www.cleanenergyactionproject.com/CleanEnergyActionProject/Energy_Storage_Case_Studies_files/Solana%20Solar%20Energy%20Generatin
9. http://www.cleanenergyactionproject.com/CleanEnergyActionProject/Energy_Storage_Case_Studies_files/AES%20Laurel%20Mountain%20Plant.pdf
10. http://www.renewableenergyworld.com/rea/news/article/2014/03/solar-decathlon-houses-make-up-a-solar-village-to-test-microgrid-technology
11. D. Undercoffler, *Electric-Vehicle Production Worldwide Forecast to Surge* 67 % in 2014 Los Angeles Times, 4th Feb 2014. http://www.latimes.com/business/autos/la-fi-hy-autos-electric-vehicle-global-production-forecast-201420140204,0,4398852.story#axzz2sUjsSoRm
12. C. Budischak, D. Sewell, H. Thomson, L. Mach, D.E. Veron, W. Kempton, Cost-minimized combinations of wind power, solar power and electrochemical storage, powering the grid up to 99.9 % of the time. J. Power Sources 225 (2013), p. 60e74
13. http://commons.wikimedia.org/wiki/File:Honda_Fit_EV_2010_LA_Auto_Show.jpg
14. http://en.wikipedia.org/wiki/File:Ombri%C3%A8re_SUDI_-_Sustainable_Urban_Design_%26_Innovation.jpg
15. http://en.wikipedia.org/wiki/Plug-in_electric_vehicles_in_the_United_States
16. http://energyalmanac.ca.gov/electricity/electricity_generation.html
17. http://en.wikipedia.org/wiki/Diablo_Canyon_earthquake_vulnerability
18. http://www.energianews.com/newsletter/files/16687e649ddd69d699c540e31e2eb12e.pdf

Chapter 10
Infrared Photovoltaics (IR PV) for Combined Solar Lighting and Electricity for Buildings

Concept of Concentrated and Piped Sunlight for Indoor Illumination

It is well known that solar energy can be converted into heat or electrical energy and that these forms have value. It is also well known that the sun's light energy can be used directly for illumination. However, the economic value of sunlight is not generally appreciated.

To appreciate the value of sunlight, imagine two alternative solar energy systems. In the first system, solar cells capture sunlight at a desert utility site and convert it into electricity with an efficiency of 10 %. Then the electricity is routed through electrical cables to a building. In the building, the electricity is converted back into light with an efficiency of 20 %. For this system, only 2 % of the solar energy is delivered as useful illumination energy. For the second system, imagine that sunlight is captured on a building roof and concentrated and routed with optical cables to overhead lamp fixtures with only 50 % transmission loss. The sunlight is used 25 times more efficiently in the second system. Since a solar illumination system can displace electricity, the energy in sunlight has more value as light than as electricity.

This idea of concentrated and piped sunlight is of interest here because it is an application that uses hardware to concentrate sunlight and the concentrated infrared portion of the solar radiation can be converted directly into electricity using the GaSb infrared cells invented as booster cells for the GaAs/GaSb 35 % efficient concentrated sunlight application. These IR sensitive cells can also be used in Thermophotovoltaic (TPV) systems as described in the next chapter.

The value of sunlight has been appreciated qualitatively for centuries through the use of windows and skylights. However, electric lighting is commonly used in buildings even during the day because electric lights have some special and desirable qualities not available from window lighting. Some of these features are: (1) overhead illumination, (2) illumination well into the interior of the building, (3) adequate illumination levels, (4) constant illumination levels, and (5) illumination control (on/off, high/low, portability).

Window lighting does not allow for overhead illumination or illumination well into the interior of the building. Furthermore, the illumination level supplied from

L. M. Fraas, *Low-Cost Solar Electric Power*, DOI: 10.1007/978-3-319-07530-3_10,
© Springer International Publishing Switzerland 2014

a window can vary by orders of magnitude throughout a day. For example, the direct sunbeam entering a window facing east in the morning is much more intense than the diffuse skylight entering the same window in the afternoon.

These problems with window lighting are rectified by the concept shown in Fig. 10.1, in which direct light from the sun is collected by a tracking concentrator and focused into a light guide for distribution into overhead lighting fixtures in the building interior [1]. One can install light guides in a manner analogous to installing a fire-extinguishing sprinkler system or an electrical conduit distribution system.

Referring to Fig. 10.1, note that the concentrated solar radiation is incident on a beam splitter where the visible sunlight is reflected into the light guides and the infrared portion is transmitted through to a solar photovoltaic (PV) array where it is converted to electricity.

Oak Ridge National Lab Coalition

A consortium headed by Jeff Muhs from Oak Ridge National Laboratory (ORNL) and Prof. Byard Wood from the University of Nevada started developing this concept for indoor illumination using concentrated and piped sunlight in 2000 [2]. JX Crystals is developing the IR sensitive photovoltaic array to be used in this application. The US Department of Energy funds the consortium.

The consortium refers to the concentrated and piped solar lighting concept as "hybrid lighting" because the indoor luminaire will include both provision for solar lighting and fluorescent or LED lighting with controls to accommodate night time or cloud cover lighting requirements. When the infrared PV array is added, the consortium refers to this system as a "full-spectrum solar energy" system.

In the following section, I first describe this solar lighting concept in more detail. It is shown that each Watt of visible sunlight displaces 2 W of electricity which otherwise would be used for fluorescent lighting and air conditioning. The savings from this displaced electricity can then payback the cost of the concentrator, tracker, and light guides in approximately 3 years.

In subsequent sections, the design and fabrication of an infrared sensitive GaSb cell array is described. It is shown that this array converts the free concentrated infrared energy into electricity with an electric power density of 1 W per square cm. This power density is one hundred times higher than that available from a planar silicon cell. Thus PV electric power can be produced economically at under $1/W.

ORNL Concept and Economic Potential

The ORNL system for concentrated and piped sunlight replaces the Fresnel lens in Fig. 10.1 with a dish mirror for solar concentration. Figure 10.2 shows this ORNL rooftop collector in detail. Note that the secondary mirror is a cold mirror with the

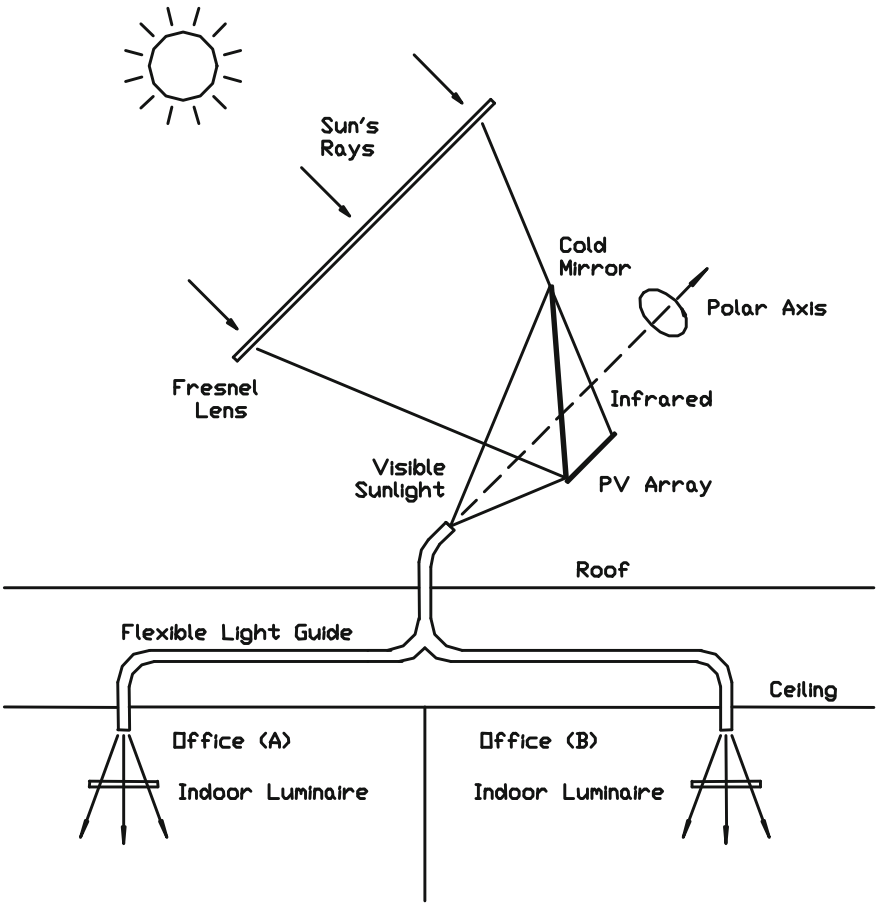


Fig. 10.1 Concept for concentrated and piped lighting for indoor illumination, with infrared energy directed to a panel of infrared-sensitive PV cells (as proposed by the author at Chevron in 1983)

infrared sensitive PV array located behind it. Figure 10.3 shows the complete ORNL system concept [2], as it would be mounted on the rooftop of an office building, including hybrid luminaries with controls.

Jeff Muhs at ORNL has previously pointed out that lighting is the single largest specific energy end-use in commercial buildings and buildings represent the largest energy end-use sector in the United States. These statements can be quantified. Conservative estimates by an independent evaluator under a DOE contract indicate that by the year 2020 in the United States alone, widespread use of full-spectrum solar energy systems will lead to:

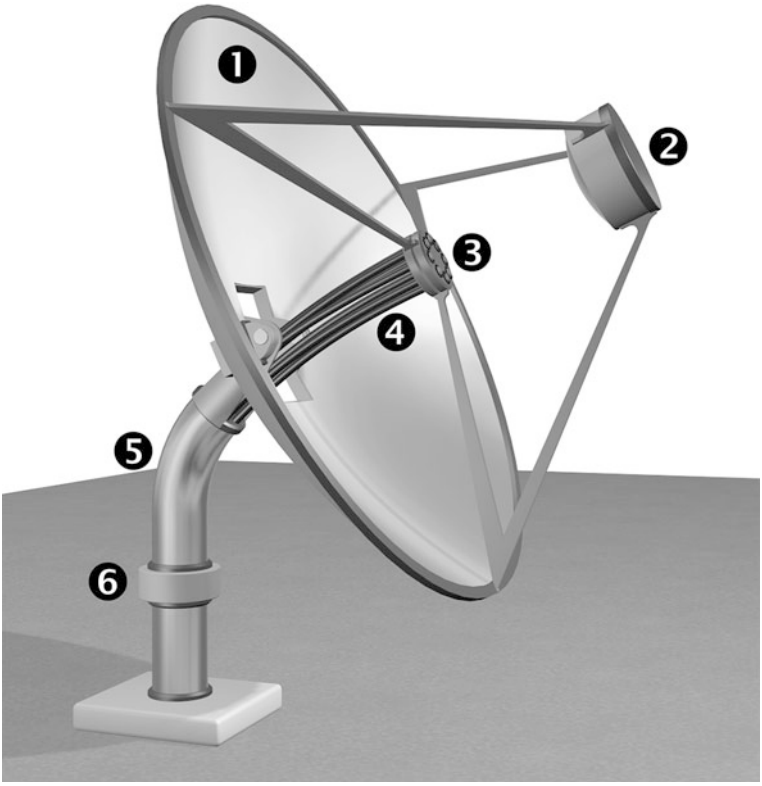


Fig. 10.2 Oak Ridge National Laboratory (ORNL) concept for a rooftop dish mirror solar concentrator, with *1* 1.8 m diameter primary mirror *2* Secondary optical element (cold mirror and concentrating PV cell array) *3* Fiber mount *4* Large-core optical fibers *5* Angled stand with altitude tracking mechanism, and 6 Azimuth tracking mechanism

- Energy savings of over 30 billion kWh (>0.3 Quads)
- Economic benefits exceeding $5 billion; and
- Reduction in carbon emissions greater than 5 MtC.

Worldwide, these impacts will likely increase by an order of magnitude.

The high economic value of solar lighting results from the fact that there are more lumens per Watt in filtered sunlight than in fluorescent lighting. Table 10.1 (extracted from a DOE study) shows how the energy in the sun's spectrum is used in a full-spectrum hybrid lighting system. Table 10.1 divides the sun's spectrum into its visible and infrared parts, as represented visually in Fig. 10.4. The sun's energy of approximately 970 W/m^2 includes approximately 490 W/m^2 of visible energy (wavelengths <0.7 microns) and 480 W/m^2 of infrared energy. In the solar lighting scheme, the sun's visible energy displaces 930 W of electrical energy for lighting and cooling. In addition, the sun's infrared energy is converted into 70 W of electric energy.

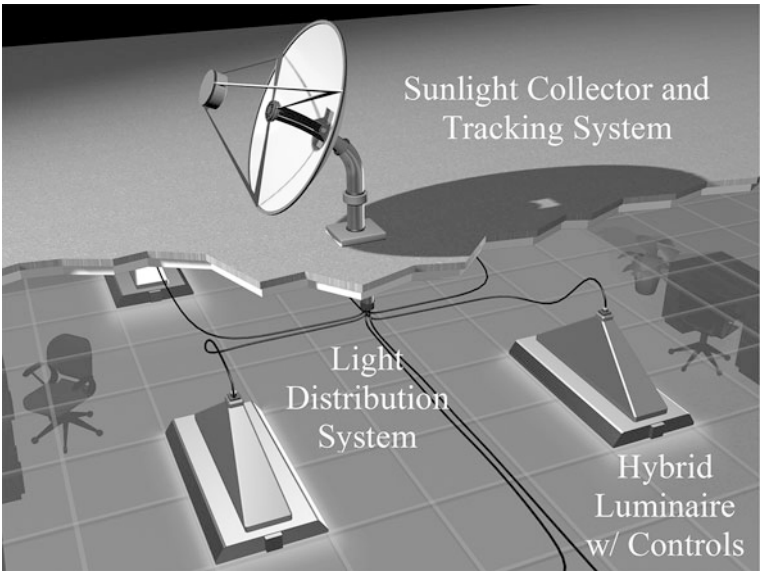


Fig. 10.3 ORNL's system concept showing visible light focal point to fiber optic light pipes, feeding into the light distribution system

Table 10.1 Energy displacement for hybrid lighting system

490 W	Visible solar energy/m^2
×200 lm/W	Luminous efficiency of filtered sunlight
=98,000 lm	Available visible light
×0.5	Passive distribution losses
=50,000 lm	Distributed light
÷63 lm/W = 800 W	Efficiency of electric lamp/ballast/luminaire
+130 W	Cooling load credit
=930 Watts	Electrical energy displaced/m^2

Conclusion #1 The sun's visible energy of 490 W/m^2 can displace 930 W of electrical energy

480 W	Infrared solar energy/m^2
−10 % = 432 W	Collection losses
×18 % = 78 W	IR energy conversion efficiency
×90 %	DC/AC conversion efficiency
=70 W	Electrical energy generated/m^2

Conclusion #2 The sun's infrared energy of 480 W/m^2 can generate 70 W of electric energy using PV cells

Final conclusion The total grid-provided electrical energy displaced = 930 + 70 = 1 kW/m^2

As Table 10.1 shows, there are more lumens per Watt in filtered sunlight (200 lm/W) than in fluorescent lights (62 lm/W), so the 490 W of filtered sunlight can displace approximately 800 W of electricity otherwise used for lighting. Also, since less heat is dissipated in the building, there is an additional credit of 130 W

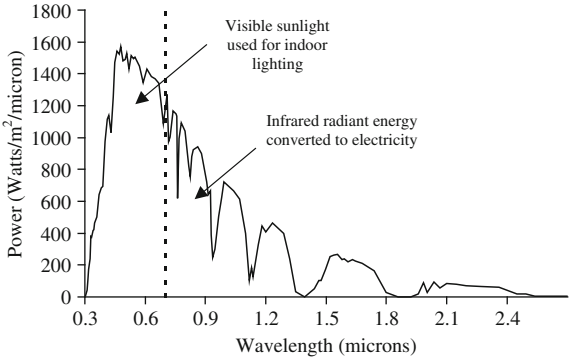


Fig. 10.4 The solar spectrum at Air Mass 1.5. The *dashed line* at 0.7 microns divides the spectrum into its visible and infrared parts

because of a reduced air conditioning load. Hence, 490 W of filtered sunlight can displace 800 + 130 = 930 W of electricity. In other words, 1 W of sunlight can displace almost 2 W of electricity. Table 8.1 also shows that the 480 W per square meter in the infrared can be used. Using a GaSb cell array, approximately 70 W of useful electric power can be generated bringing the total number of Watts displaced or produced with 1 square meter of sunlight up to approximately 1 kW.

The DOE has also sponsored a study of the potential cost of a full-spectrum hybrid lighting system. Their analysis for the future potential cost for this system assumes a 2.5 m^2 mirror collector. A 2.5 m^2 system should displace and produce 2.5 kW. It is projected that the sum of the component, installation, and maintenance cost for this system could be $2100, or 84 cents/W assuming large scale adoption, production, and installation.

ORNL Demonstration Prototype

To date, prototype components have been fabricated as shown in Fig. 10.5. This figure shows a photograph of the light-concentrating collector on the roof of a laboratory building at ORNL and a light pipe with a light diffusing end section for indoor illumination.

Design, Fabrication, and Performance for the Infrared PV Array

The focus here is on the infrared sensitive photovoltaic array for the full-spectrum hybrid solar lighting system described above. JX Crystals has designed, fabricated, and measured the performance of an array intended for use in this system [3, 4].

Referring to Fig. 10.2 and Table 10.1, the hybrid collector system's apex mounted 'cold mirror' transmits 480 W/m^2 × 2.5 m^2 × 0.9 = 1120 W of concentrated

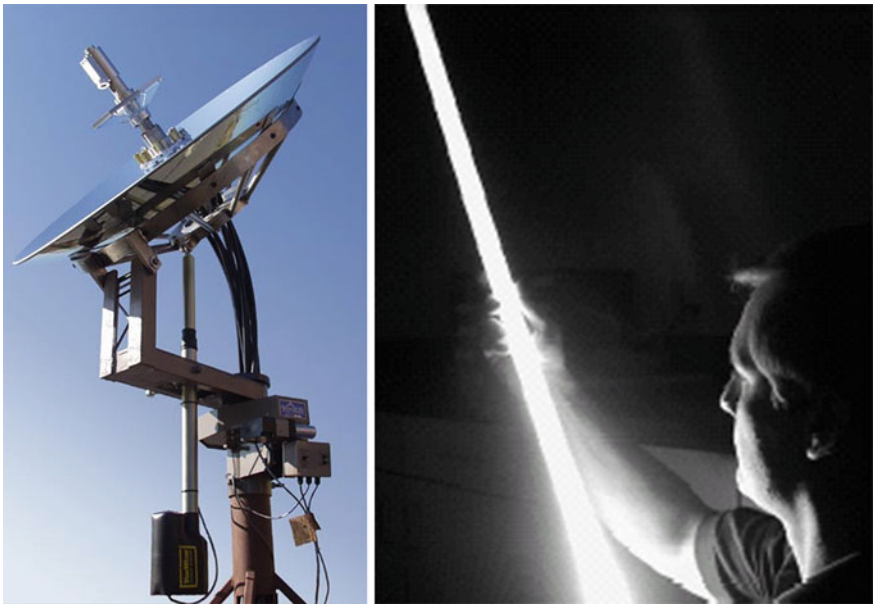


Fig. 10.5 Hybrid lighting with IR PV array from JX crystals

infrared (IR) radiation through to the PV circuit for conversion into electrical energy. An IRPV array circuit mounted in the antenna apex with a high packing density is required along with provision for high IR intensity uniformity. It is also necessary to provide cooling to keep the circuit from overheating in the intense radiation.

Figure 10.6 shows a photograph of an IRPV circuit fabricated at JX Crystals Inc. This GaSb circuit captures more of the infrared than traditional silicon solar cells. In this application, a GaSb cell will capture infrared energy over the wavelength band from 0.7 to 1.8 microns while the traditional silicon cell will only capture wavelengths over the smaller band between 0.7 and 1.1 microns. As is shown in this figure, a cell array is mounted in shingle fashion on metal pads on a thin dielectric applied to a metal substrate. The bottom of each cell is soldered to the top bus bar of the previously placed cell in that row. The rows are backside wired in series completing the IRPV circuit with 81 + % active area density.

An IR diffusing cone is used in this application to mount the IRPV receiver behind the apex mirror while its highly reflective inner surface shapes the incoming IR intensity distribution. This is necessary because, with the cells connected in series, maximum electrical power output at any illumination intensity is achieved when all cells receive equal convertible infrared energy.

The receiver circuit substrate is mounted directly on an array heat sink with an integral cooling-fan. Given a 2.5 m^2 solar collector mirror, this 100-cell array should produce approximately $2.5 \times 70 = 175$ W of electric power. The active area of this cell array is approximately 180 cm^2. The cooling fan will require approximately 5 W. While we have designed and built this shingle PV array with shaping mirror and

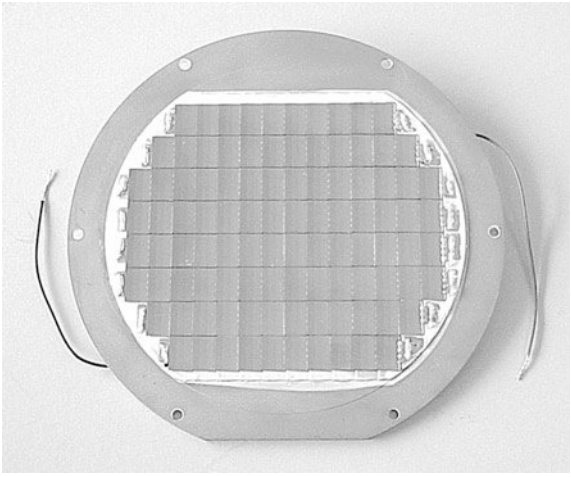


Fig. 10.6 The first IR-sensitive PV cell array for a hybrid lighting system. This 100 cell array using GaSb cells has a total active area of 180 cm^2 and generates 177 W

cooling fan using GaSb IR sensitive cells, our patent application on this receiver design notes that traditional cell types can also be used, including silicon cells.

The beauty of this hybrid lighting and PV approach is in the high power density now available to the IRPV array at the focus of the solar energy. Thus PV electric power can now be produced economically. I believe that this PV array can be made in high volume production for $100. Given an array output of 175 W, this corresponds to electric power production at 100/175 = 57 ¢/W. Fifty cents per Watt has been a dream of the solar cell community for 25 years. This cost target is now achievable because solar lighting pays the balance of system cost and the PV electric power is produced at approximately 1 W/cm^2 rather than the 0.01 W/cm^2 associated with the traditional planar solar array.

It is interesting that an innovation in one area can find a multitude of applications. In the present case, the GaSb IR PV cell that was invented as a booster cell for 35 % solar PV concentrator systems can also be used in a concentrated and piped sunlight for indoor lighting system. The next chapter points out that GaSb IR PV cells are also enabling for ThermoPV (TPV) systems that can generate electricity whenever heat is needed at night or on cold cloudy days.

References

1. L.M. Fraas, W.R. Pyle, P.R. Ryason, Concentrated and piped sunlight for indoor illumination. Appl. Opt. **22**, 578 (1983)
2. See www.ornl.gov/hybridlighting/partnership.htm
3. L.M. Fraas, W.E. Daniels, J. Muhs, *Infrared Photovoltaics for Combined Solar Lighting and Electricity for Buildings*. Proceedings of 17th European PV Solar Energy Conference, Munich, Germany, 22–26 October 2001
4. L.M. Fraas, J.E. Avery, Takashi Nakamura, *Electricity from Concentrated Solar IR in Solar Lighting Applications*. Proceedings of 29th IEEE PV Specialist Conference, p. 963 (2002)

Chapter 11
Thermophotovoltaics Using Infrared Sensitive Cells

Unfortunately here on earth, the sun doesn't always shine. This means that heat from the sun is not always available. So, it will still be desirable to occasionally burn fuels for heat. Nuclear power plants are not going to provide heat for homes and coal burned for home heating is a very dirty fuel. Consequently, natural gas, propane, and heating oil are the common fuels used for home heating today and it will be desirable to preserve these fuels for heating for as long as possible. Meanwhile, natural gas is also burned in central power plants to generate electricity. In a combined cycle gas turbine plant, approximately half of the chemical energy in the fuel is converted to electricity and the remaining half is thrown away as waste heat. However, with Thermophotovolatics (TPV), electricity could be generated in the home along with the heat for the home with a fuel utilization efficiency of over 90 %. In this case, electricity would be produced for the home with nearly twice the fuel utilization efficiency compared with the central power plant. Conceptually, by heating a ceramic element in the flame in a home furnace where it would glow in the infrared and then by placing infrared (IR) PV cells around the glowing ceramic element, one could then convert the IR into electricity thereby co-generating heat and electricity. This process is called ThermoPhoto-Voltaics or ThermoPV or TPV.

At a temperature of 6,000 K, the sun is a very hot high temperature radiation source. The peak wavelength for radiant energy from the sun is at 0.5 microns which is right in the middle of the visible light spectrum. In fact, this wavelength range is referred to as visible because the human eye has adapted to sunlight as a consequence of human evolution. Man-made heat sources are not nearly as hot or bright as the sun. As a consequence, the peak power wavelength for man-made heat sources shifts into the infrared. For example, the combustion flame temperature for a hydrocarbon fuel is at about 2,000 K. At this temperature, the peak power wavelength is at 1.5 microns. Since GaSb infrared PV cells respond out to 1.8 microns [1, 2], they are nearly perfect for generating electricity using radiant energy from man-made heat sources rather than the sun [3].

L. M. Fraas, *Low-Cost Solar Electric Power*, DOI: 10.1007/978-3-319-07530-3_11,

© Springer International Publishing Switzerland 2014

The TPV Concept

The idea of using solar cells to generate electricity from man made heat sources is not new [4]. However, until the GaSb cell was demonstrated in 1989 [1], there was no cell that responded in the required infrared range [3]. While the GaSb cell was invented as a booster cell [1] for CPV, the use of a GaSb cell is very exciting for TPV system applications [3]. The electric power densities produced by GaSb cells in TPV systems is very high just as in CPV solar systems but GaSb cells for TPV systems become the enabling component. Because the man-made "sun" is only inches away from the cells in TPV systems rather than 93 million miles away, power densities in the 2 W/cm^2 range are now readily achievable. In 1994, a first TPV fuel-fired generator demonstrated a power density of 1.6 W/cm^2 using a GaSb cell array [3].

Figure 11.1 shows the basic TPV concept. In a TPV unit, a fuel such as propane or methane is burned in a heater or furnace and a ceramic element is located in the flame. The ceramic element emits intense infrared radiation and a photovoltaic array surrounding this emitter converts this infrared energy into electric power. Thus, a TPV unit co-generates heat and electricity.

TPV Historical Background

TPV was first demonstrated by Kolm at MIT Lincoln Labs [4] in 1956 when he placed a recently demonstrated silicon solar cell next to the mantle from a Colman lantern. While TPV R&D funding was very sporadic, some significant advances followed. Werth [5] at GM realized that while silicon might be appropriate for the spectrum from the sun at 6,000 K, from Wein's Displacement Law where λ_{max} T = 2,898 μm °K, a lower bandgap photovoltaic cell would be more appropriate. Werth [5] demonstrated TPV using a propane-heated emitter and a Germanium (Ge) cell (1963). His emitter temperature (T) was 1,700 K corresponding to a peak black body wavelength of 1.7 μm. However, using a blackbody IR emitter was a problem because only 25 % of the radiation for a 1,700 K emitter falls at wavelengths below 1.7 μm in the cell response band. The remaining 75 % is wasted heat potentially just heating the TPV cell. However, then Guazzoni (1972) from the Army proposed using rare earth oxide IR emitters [6]. These rare earth oxide IR emitters have emission lines in the PV cell response band. Unfortunately, the Ge cell performance was still quite poor. Fraas et al. [1, 2] then invented and demonstrated the GaSb cell (1989) with near ideal performance and a spectral response out to 1.8 μm and with a bandgap energy of 0.72 eV.

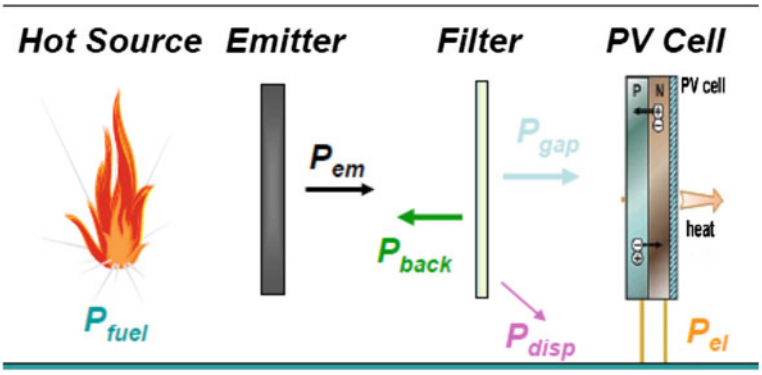


Fig. 11.1 TPV Concept: In a TPV unit, a fuel such as propane or methane is burned in a heater or furnace and a ceramic element is located in the flame. The ceramic element emits intense infrared radiation and a photovoltaic array surrounding this emitter converts this infrared energy into electric power

TPV Key Components and Requirements

JX Crystals Inc now makes GaSb cells and circuits as shown in Fig. 11.2. These cells are one of the key components in a TPV system. They can convert 30 % of the IR in the cell response band from 0.4 to 1.8 microns into electric power. However, a requirement for the use of these cells in TPV systems is to simultaneously generate a high electric power while also avoiding over heating the cells. Ideally, this can be achieved by just emitting the IR wavelength band that the cells can convert. As noted above, Guazzoni proposed using rare earth oxide IR emitters for this purpose. However, there is a problem with this as illustrated in Table 11.1.

Table 11.1 shows four cases for an emitter temperature of 1,500 K. The first row is for a black body (BB) emitter (Case 1). The problem for a BB as noted above is that only a small fraction of the total IR emitted (21 % at 1,500 K) falls in the cell convertible band. Also, while the cell electric power produced is good at 1.8 W/cm^2, the heat load on the cell at 28.1 W/cm^2 is too high. The second row in Table 11.2 shows a rare earth oxide emitter case (Case 2). As can be seen, the problem with rare earth oxides is that the emitted lines are narrow resulting in much less power in the cell convertible band (0.27 W/cm^2) [7]. So, while the long wavelength heat load is reduced, the ratio of useful electric power to heat load (TPV system efficiency) of 6.6 % is only slightly better than for the BB case at 6.2 %.

As noted by Fraas and Ferguson [8] and demonstrated by Ferguson and Dogan [9], both the cell power density and the spectral efficiency can be improved by using ceramic IR emitters containing D-level transition elements rather the F-level rare earth oxides. The resulting spectral selectivity for NiO doped Magnesia is shown in Fig. 11.3 and the improvement in TPV performance is shown in case 3 in Table 11.1. Now, the cell generated electric power increases to 1.6 W/cm^2 while the heat load is manageable at 8.5 W/cm^2. The TPV system efficiency is now

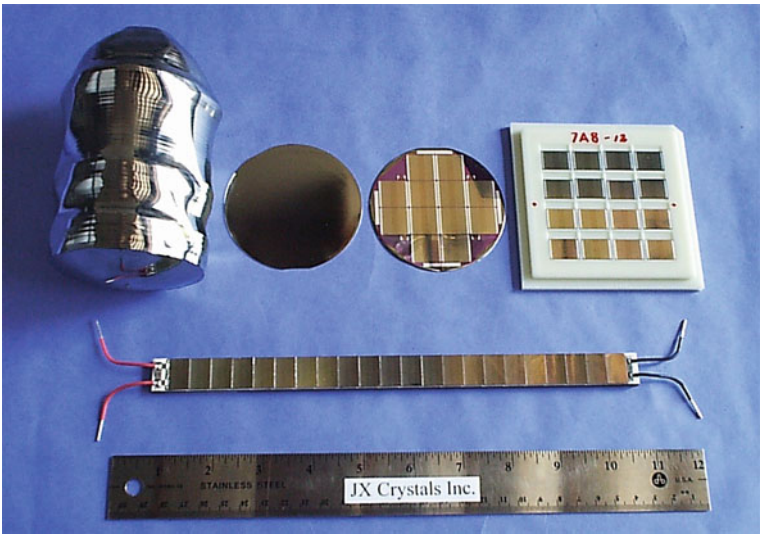


Fig. 11.2 GaSb crystal, wafers, cells, and circuit fabricated at JX Crystals Inc

Table 11.1 Radiant energy (W/cm^2) wavelength (microns) distribution 1,500 K (1,227 C)

	0.4–1.8 (W/cm^2)	1.8–4 (W/cm^2)	4–12 (W/cm^2)	0.4–12 microns (W/cm^2)	Spectral efficiency (%)	Efficiency 30 % IR cell (%)
Case 1: Blackbody	5.9	15.4	6.8	28.1	21	0.3 × 5.9/28.1 = 6.2
Case 2: Erbium (EAG) and hot glass	0.9	1.5	1.7	4.1	22	0.3 × 0.9/4.1 = 0.27/ 4.1 = 6.6
Case 3: NiO/MgO and hot glass	5.3	1.5	1.7	8.5	62	0.3 × 5.3/8.5 = 1.6/ 8.5 = 18.8
Case 4: Hi/Lo filter and hot glass	5.9	1.5	1.7	9.1	65	0.3 × 5.9/9.1 = 1.8/ 9.1 = 19.5

18.8 %. Case 4 in Table 11.1 shows another way of increasing the TPV system efficiency starting with a BB emitter using a Hi/Lo interference filter provided some additional conditions are met as will be discussed later in this chapter.

TPV Applications

Over the past several years, the GaSb cell has enabled the demonstration of a large number of TPV applications ranging from a battery charger for the Army to a home heating-stove to the cogeneration of electricity from the glowing steel billets in a steel mill. Some of the potential applications of GaSb IR cells are shown in Fig. 11.4. All of these applications depend on the availability of low cost GaSb

Table 11.2 Performance projections for TPV home combined heat and power furnaces

TPV System	Variable	Spectral efficiency (%) (C)	TPV circuit area (cm^2)	View factor	Electric system[a] efficiency (%)	Fuel thermal burn rate (kW)	TPV electric power
TPV Stove	SiC emitter	22 1250	250	0.6	1.4[b]	8.8	122 W
TPV Stove	Matched emitter	62 1250	250	0.6	2.8	4.4	122 W
TPV Boiler	Matched emitter	62 1250	500	0.7	3.9	8.8	342 W
TPV CHP	Matched emitter	62 1250	1000	0.8	4.5	15.4	695 W
TPV CHP	Matched emitter	68 1400		0.8	5.4	26	1.3 kW

[a] In all cases, cell efficiency = 30 %; Fuel chemical to radiation efficiency = 33 %
[b] *Example* 0.22 × 0.6 × 0.3 × 0.33 = 1.4 %

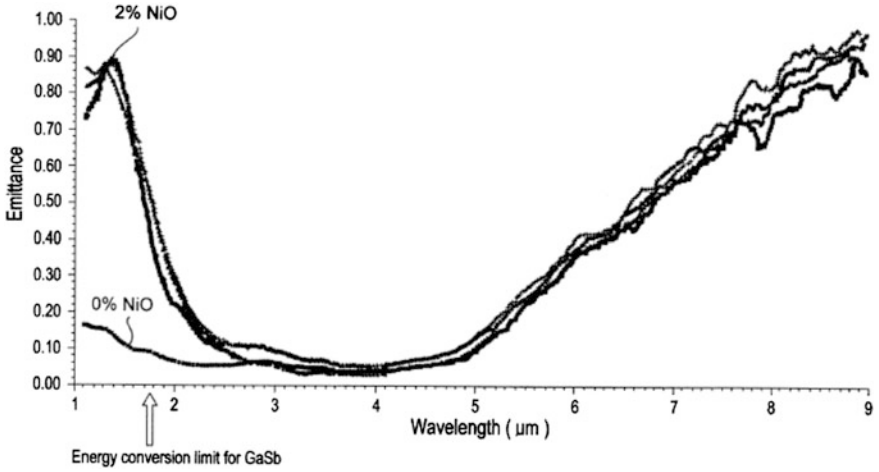


Fig. 11.3 Spectral emittance measurements [9] for a 2 wt% NiO-doped MgO tape cast ribbon at 1,268 and 1,404 °C. The emissivity of the 2 wt% NiO-doped MgO emitter appears nearly constant within this temperature range. The emittance of an 'undoped' MgO ribbon is also included for comparison. The emissivity of the NiO-doped MgO is much greater than it is for the 'undoped' MgO at wavelengths less than about 1.9 µm where radiant energy is efficiently converted by photovoltaic cells, but NiO doping has little effect on the emittance at longer wavelengths

cells and circuits (Item [1] in Fig. 11.4). Chapter 10 herein described the Piped Lighting application (Item [4] in Fig. 11.4). Several of these TPV applications will be described in more detail in the following sections.

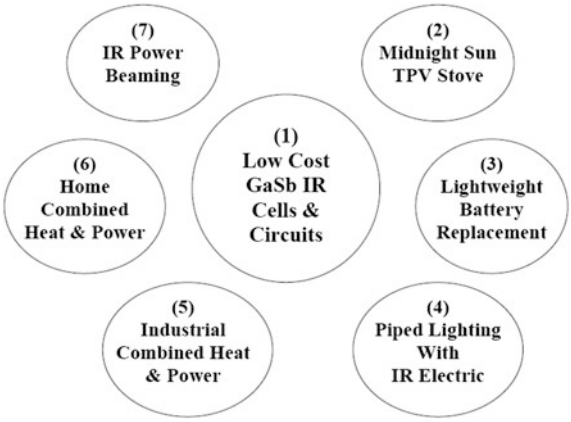


Fig. 11.4 The GaSb IR cell and circuit technology enables a large number of applications

The Midnight Sun™ TPV Stove

A dream for TPV is to cogenerate heat and electricity in the home using a modified home heating furnace (Item [6] in Fig. 11.4). As a first step along the path of realizing this dream, in the years between 1998 and 2000 using internal R&D funds, JX Crystals Inc developed the Midnight Sun™ TPV Stove shown in Fig. 11.5 (Item [2] in Fig. 11.4).

This stove was developed for off-grid cabins where the cabin owners were sympathetic to solar and wanted heat and electricity at night and in the cold winter months. The idea was that it could also be used as a fireplace insert for occasions when the power failed from ice storms in the Eastern US. In that event when the main furnace would not operate without electric power, the family could retreat to the living room where this unit would provide electricity for the refrigerator, TV, and a computer.

Figure 11.5 shows a photograph of one of these stoves along with a schematic showing how it works [10]. It burns propane. At a burn rate of 25,000–30,000 BTU/h, it will generate between 100 and 125 W of DC electricity easily converted into AC. Figure 11.6 shows the GaSb shingle circuits used in this stove and a circuit with a Hi/Lo filter attached [11]. The filter reflects back non useful wavelengths between 1.8 and 4 microns. Also shown is a current voltage trace for one of these circuits. The stove in Fig. 11.5 uses a SiC honeycomb flow-through BB emitter. There is a glass window between this emitter and the GaSb shingle circuit.

The first column in Table 11.2 summarizes the performance for the stove in Fig. 11.5. While the spectral efficiency of 22 % is similar to the value for the BB case in Table 11.1, the electrical conversion efficiency of 1.4 % is lower than simply the product of the spectral efficiency and the cell efficiency.

To understand this, one needs to also account for the fuel to IR radiation conversion efficiency. When the propane adiabatic flame temperature is 2270 K

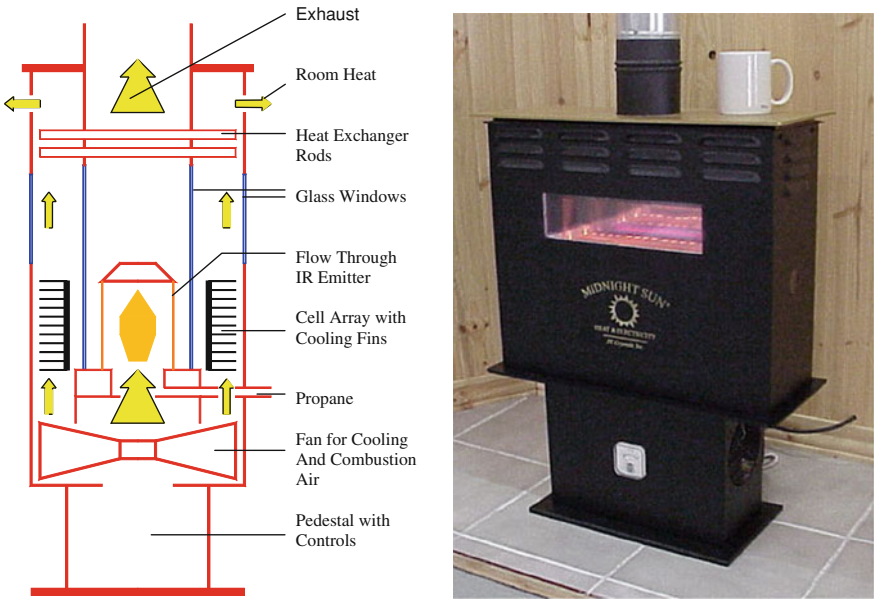


Fig. 11.5 Midnight Sun™ TPV Stove co-generates 25,000 BTU/h of heat and 100 W of electricity [10]

and the emitter temperature is 1,523 K, the radiant energy fraction extracted is (2270–1523)/2270 = 33 %. So there is an additional 67 % of the chemical energy which in this case is used for room heating. However, referring again to Table 11.1, one-third of 6.2 % is 2.1 % and this is still larger than the 1.4 % measured in row 1 in Table 11.2. The view factor between the TPV circuit and the IR emitter explains the difference. In small systems, a lot of radiant energy escapes at the edges.

But as is shown in Table 11.2, improvements are possible in the future. Table 11.2 really describes an evolutionary path from the Midnight Sun™ Stove to the combined heat and power (CHP) furnace for the home (Item [6] in Fig. 11.4). First, as is shown in Fig. 11.7, the BB IR emitter can be replaced with the NiO/MgO emitter of Fig. 11.3 with an IR radiant energy spectrum matching the response band of the TPV cells. This is the case 3 in Table 11.1. However, one still needs to account for the fuel energy to radiant energy term and the view factor term. But as is shown in Table 11.2, larger systems will have better view factors.

In Fig. 11.7, notice that the picket fence matched IR emitter consists of an array of ceramic rods simply tied together with Nichrome wire at top and bottom. This design allows for thermal gradients and rapid thermal cycles without breakage. It is also a flexible design allowing for both planar and cylindrical emitter designs. This picket fence concept will also be used in the cylindrical TPV battery replacement systems to be described in the next section. A further efficiency improvement can be made by increasing the fuel energy to radiant energy term.

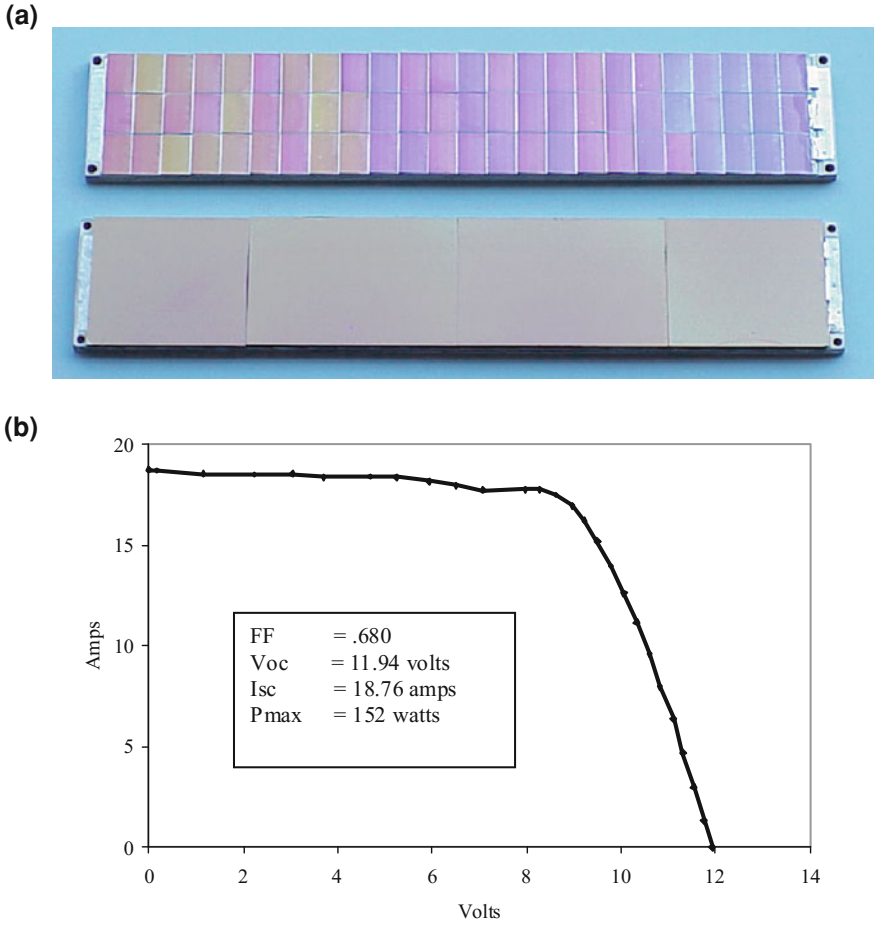


Fig. 11.6 **a** 72 GaSb cells shingle mounted on a circuit measuring 5 cm by 26 cm. *Top* circuit shows shingles with steps and cracks; *bottom* circuit is covered with planar filter covers. **b** Current versus voltage test for 72-cell circuit showing over 2 W per cell and over 1 W/cm^2

This can be done with the use of a recuperator to preheat the combustion air using energy from the exhaust gas stream. The fuel energy to radiant energy term can then be increased from 33 to 70 %. This will be the subject of the next section.

Lightweight TPV Battery Replacement

Fuel fired TPV generators have four very interesting features (Item [3] in Fig. 11.4). First, they have very high power densities and this makes the PV cells affordable. For example, with an emitter temperature at 1,200 C, the cell electric

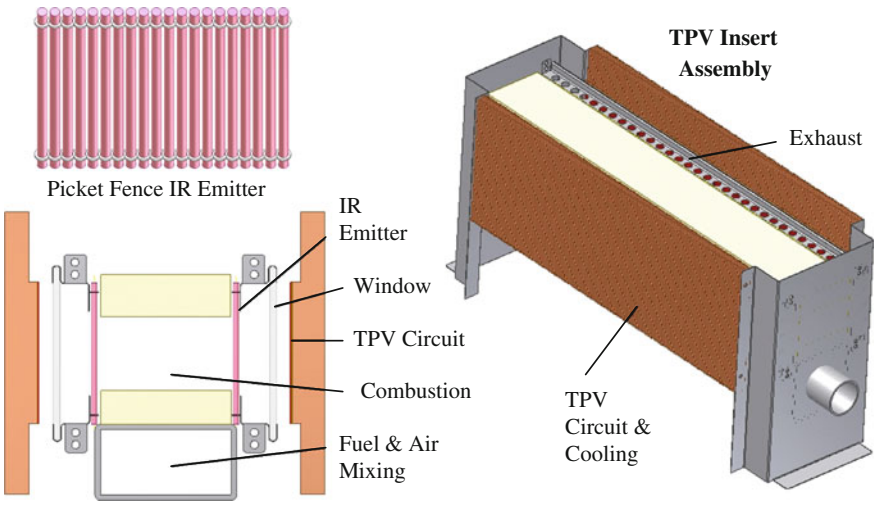


Fig. 11.7 **a** TPV insert assembly for the Midnight Sun™ TPV Stove including an NiO/MgO picket fence IR emitter for spectral control. **b** JXC GaSb TPV circuit used in Midnight Sun™ TPV Stove

power density can be over 1 W/cm^2, 100 times higher than a traditional solar cell operating in sunlight. Second, they are lightweight. For example compared to an Li-ion battery, the TPV power system described here is lighter, has much higher specific energy, operates longer, and is easily refueled. Third, these generators are quiet because the burn is continuous, and finally, fourth, a large number of hydrocarbon fuels can be used. The lightweight and quiet features make these units interesting to the military for lighter batteries for soldiers or for power and propulsion systems for unmanned aerial vehicles (UAVs). However, these applications do not use the waste heat, so electrical conversion efficiency is important.

Portable TPV Battery Concept

A lithium-ion rechargeable battery weighing 1.1 kg has a specific energy of 145 Wh/kg. Meanwhile, a hydrocarbon fuel such as Butane or Propane has a specific energy of 12,900 Wh/kg. Therefore, given a small, efficient, and lightweight chemical to electrical converter, a much higher specific energy of approximately 1,000 Wh/kg should be achievable. More generally, there is a need for a lightweight compact electric generator that can replace the use of batteries in several potential applications. For example, refueling can be much faster than battery recharging.

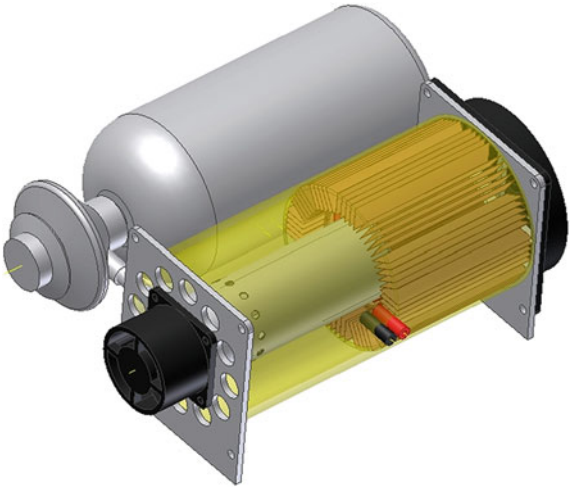


Fig. 11.8 Small portable TPV battery [12] with adjacent fuel cylinder

Figure 11.8 shows a perspective view of a portable cylindrical TPV battery charger [12]. It is a cylinder 8 cm in diameter and 15 cm long. There is a cooling air fan on one end and a combustion air fan at the other end. The length from end to end including the two fans is 18 cm. Fuel enters this TPV cylinder and DC electricity is generated.

In Fig. 11.8, a fuel cylinder is shown adjacent to this TPV cylindrical battery. TPV generators are intrinsically lightweight. In a TPV generator, any fuel such as Butane or Propane can be used to heat a small solid element until it glows in the infrared (IR) and photovoltaic cells surrounding the IR emitter simply convert the IR radiation into DC electricity.

Figure 11.9 shows a cross section drawing of the TPV cylinder shown in Fig. 11.8. Key components and subassemblies are labeled. Referring to Fig. 11.9, one can see the IR emitter subassembly in the middle on the right-hand side. It is surrounded by the GaSb TPV cells on a cylindrical circuit with fins for cooling. The power converter array subassembly is cooled via air flow around it from the cooling fan on the cylinder end at the right. The IR emitter is heated by combustion gases from its inside. Fuel and combustion air are provided through the recuperator as seen on the left-hand side.

The basic principles of operation are described next. Fuel is injected through a metering valve orifice into a Bunsen burner like center coaxial tube. Combustion air is fed into a coaxial space around the fuel tube through a finned recuperator stage and into a fuel and air mixing chamber. A fuel/air swirling mixture is then injected into a combustion chamber and ignited. An IR emitter is located around the combustion chamber. The flame heats the IR emitter to the target temperature of 1,200 C (1,473 K). The combustion byproduct gases flowing initially in one direction are then turned around and then flow back. These hot exhaust gases are confined by an outer window tube. The exhaust gases now enter the recuperator

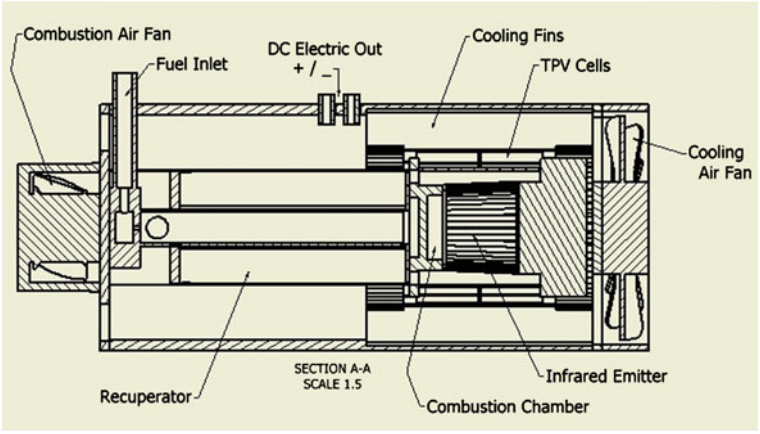


Fig. 11.9 Portable TPV generator cross-section

flowing counter to the combustion air heating the combustion air. The cooled exhaust gases exit the recuperator at the left hand side and mix with the cooling air. TPV cells in circuits surround this combustion/emitter chamber forming the TPV converter section of this compact DC electric generator.

The challenge for TPV is conversion efficiency. However, over the last several years, major improvements have been made in TPV converter components. To first order, the conversion efficiency of a TPV system is given by the product of four terms: the chemical to radiation conversion efficiency, $\eta_{CR,}$ the percent of radiation in the cell convertible band known as spectral efficiency, η_{SP}, the cell conversion efficiency, η_{PV}, and the cell to emitter view factor efficiency, VF. In recent years, JX Crystals Inc. has been making major improvements in all four of these subsystem efficiency areas.

The chemical to radiation conversion efficiency is based on the adiabatic flame temperature of approximately 2,000 C (2,273 K) and our IR emitter target temperature of approximately 1,200 C (1,473 K). Without provisions to manage the waste exhaust heat, the exhaust temperature would be 1,200 C and the system chemical to radiation conversion efficiency would only be (2,273–1,473)/2,273 or 35 %. This problem is solved by the use of a recuperator where heat from the exhaust gases is extracted and fed back into the combustion air. The recuperator design in this portable cylindrical TPV generator is novel. The goal is to extract 70 % of the chemical energy from the fuel and to convert it into radiation.

The goal is to achieve an overall TPV electric conversion efficiency of 10 %. TPV cells are now reasonably developed and cell conversion efficiencies for in-band radiation are approximately 30 %. In this chapter, the emitter subassembly and spectral efficiency will be discussed with a goal of a spectral efficiency of 60 %. Setting a goal for the VF of 80 %, then the overall TPV goal efficiency, $\eta_{TPV,}$ of 10 % can be achieved:

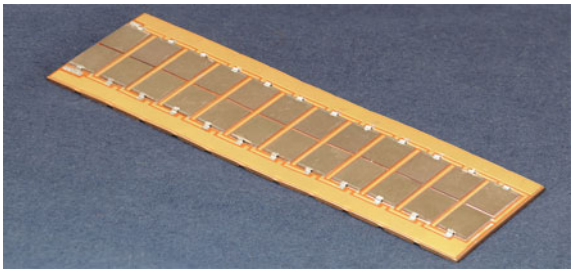


Fig. 11.10 TPV circuit in flat form

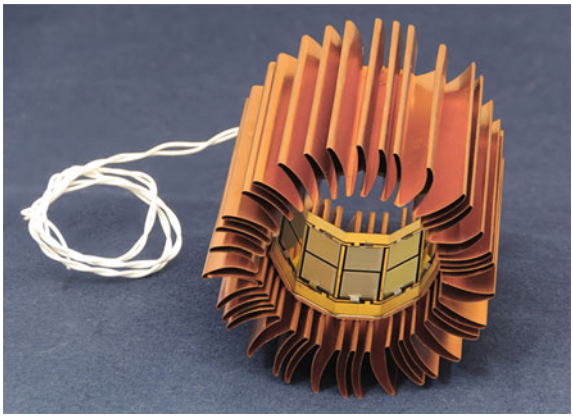


Fig. 11.11 Cylindrical TPV power converter array

$$\eta_{TPV} = \eta_{CR}\eta_{SP}\eta_{PV}VF = 0.7 \times 0.6 \times 0.3 \times 0.8 = 10\,\% \qquad (11.1)$$

The two primary subassemblies are the TPV Power Converter Array and the Burner/Emitter/Recuperator.

The TPV Power Converter Array subassembly consists of a TPV circuit, cooling fins, and a cooling fan. The GaSb TPV cells and circuits are fabricated at JX Crystals Inc. GaSb cells respond to IR radiation out to 1.8 microns. GaSb TPV cells are mounted on a circuit as shown in Fig. 11.10.

The circuit substrate base can be copper or aluminum. This metal circuit base has an insulating layer on its front side coated with a metal layer with a gold reflecting top surface. The top metal layer is etched to create cell pads, circuit traces, and reflective regions as shown. After circuit assembly, this circuit can be flash tested to verify its power conversion performance. After circuit test, convoluted fin stock is then attached to the back side of the TPV circuit. There are machined grooves on the back side of this circuit allowing the circuit to be folded into a polygonal cylinder as shown in Fig. 11.11. A circuit performance measurement is shown in Fig. 11.12.

A perspective view of the burner/emitter/recuperator subassembly is shown in Fig. 11.13. The IR emitter is shown at the top and the recuperator is shown at the

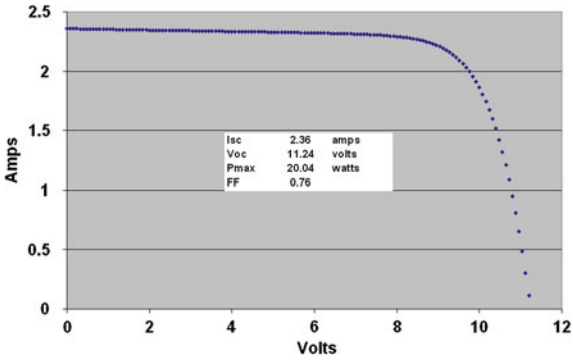


Fig. 11.12 Sample GaSb TPV circuit power curve

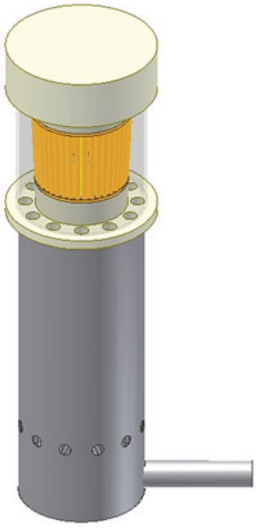


Fig. 11.13 Perspective view of the burner/emitter/ recuperator subassembly

bottom. It divides into a burner/emitter subassembly and a recuperator subassembly. The recuperator and the burner/emitter subassembly are described in more detail in the next paragraphs. The recuperator design and the IR emitter designs are novel and critical to the operation of this TPV generator.

The purpose of the recuperator is to extract energy from the exhaust and to transfer that energy into the combustion air stream. Specifically, the goal is to reduce the exhaust temperature from 800 to 300 C while increasing the combustion air temperature from 20 to 600 C. The goal is to increase the chemical to radiation efficiency to 70 % through exhaust heat recuperation.

Figure 11.14 shows front, top, and cross-section drawings of the novel Omega recuperator, and Fig. 11.15 shows a perspective view of the recuperator partially assembled. The recuperator section is novel in that it uses Omega (Ω)-shaped sheet metal heat transfer membranes as shown in Fig. 11.15. A horizontal cross-section

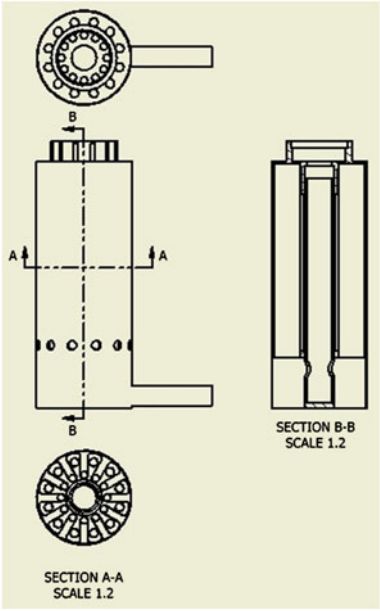


Fig. 11.14 *Front* and *top* drawings of the Omega recuperator along with *horizontal* (A–A) and *vertical* (B–B) cross sections

through this recuperator is shown in section A–A in Fig. 11.14. As shown in this cross section, 12 Omega-shaped sheet metal heat transfer elements create alternating flow cavities for the supply combustion air and for the exhaust. Heat transfers through the walls of the Omega-shaped elements as air flows in one direction and the exhaust flows in the opposite direction.

Referring to Fig. 11.15, there is a flower-shaped disk shown in the upper right. This disk fits over the fuel supply tube and the base of the burner fits over the open end of the fuel supply tube.

Figure 11.15 shows the recuperator partially assembled. As shown, the Omega-shaped sheet metal heat transfer membranes slip into the openings between the petals in the flower-shaped disk. One can now see the alternating air supply and exhaust channels. Referring to the top view drawing of the recuperator in Fig. 11.14, one can see two circular hole-patterns. The inner hole-pattern mates with the air channels and allows for the combustion air to enter the combustion chamber. The outer hole-pattern allows for the exhaust to enter the recuperator exhaust channels. Recuperator assembly is completed by placing a cylindrical sleeve around the Omega elements. This sleeve extends down and mates to the combustion air fan. There is a radial hole-pattern in this sleeve shown in Fig. 11.14 that allows the exhaust to exit and mix with the cooling air stream.

There are two requirements for a good IR emitter design in the context of a fuel fired TPV generator. These requirements are as follows:

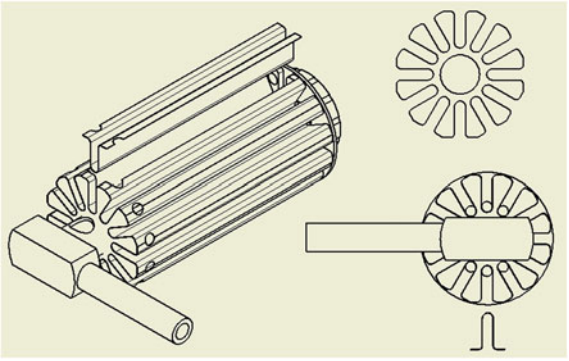


Fig. 11.15 Omega recuperator partially assembled (*left*); separate drawing of flower disk (*top right*); *bottom* view of recuperator (*middle right*); Cross section through Omega heat transfer membrane (*bottom right*)

(1) It needs to have the appropriate chemical composition such that it emits infrared radiation with wavelengths matched to the response band of the TPV cells.
(2) Its geometry must be such that it efficiently extracts energy from the combustion gases passing through and around it.

Figure 11.16 shows the side view of the infrared emitter design specifically for the cylindrical TPV generator shown in Figs. 11.8 and 11.9. Figure 11.17 shows a horizontal cross-section through this burner and IR emitter subassembly.

As shown in Fig. 11.17, the burner and IR emitter subassembly consists of a lower insulating plate with fuel and air injection holes and exhaust gas exit holes. There is a picket fence array of emitter posts on top of this insulating plate with a combustion chamber inside this array. These emitter posts are cylindrical with a diameter of approximately 1–2 mm. The hot exhaust gases exit through small slits between these IR emitter posts. The slit widths are approximately 0.1–0.2 mm. There is an insulating lid on top of this post array. A fused silica transparent window also surrounds this IR emitter post array. Because entry and exit holes for both the fuel and air and the exhaust are in the bottom plate, there is a tendency for the lower end of the emitter array to run hotter than the upper end of the emitter array unless the post array is tilted as shown. This tilt increases the slit widths between the emitter posts toward the top end enhancing the heat transfer rate at the top to promote more emitter temperature uniformity from top to bottom.

The chemical composition of the IR emitter rods is important for spectral control. The emitter rods need to have the appropriate chemical composition such that they emit infrared radiation with wavelengths matched to the response band of the TPV cells. The appropriate TPV cells are either GaSb or InGaAs/InP or Ge cells that convert radiation with wavelengths less than approximately 1.8 microns into electricity. The infrared emitter ideally should only emit radiation with wavelengths less than 1.8 microns. If infrared wavelengths longer than this wavelength are emitted, this radiation will only produce unwanted heat in the TPV cells.

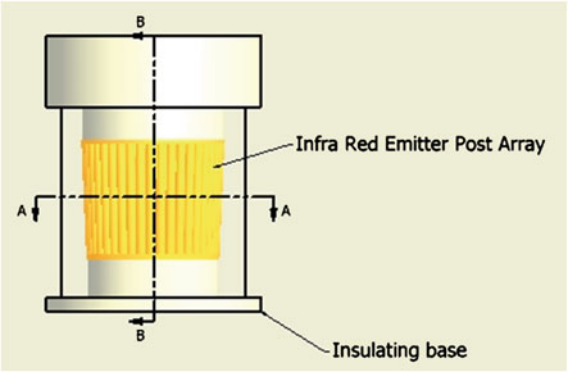


Fig. 11.16 *Side* view of the Infrared emitter assembly showing the *cylindrical array* of tilted IR emitter posts and locations of section cut for Fig. 11.17. The IR emitter rods are shown here as *yellow* hot

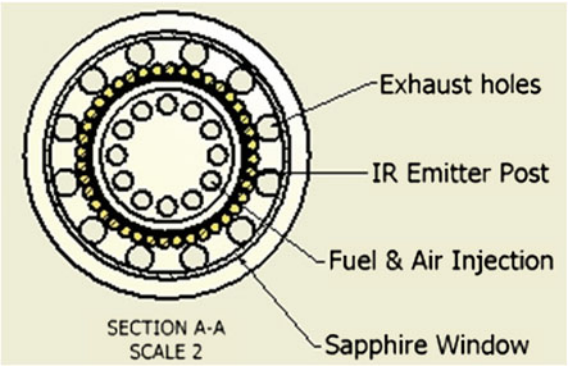


Fig. 11.17 Section A–A through emitter assembly

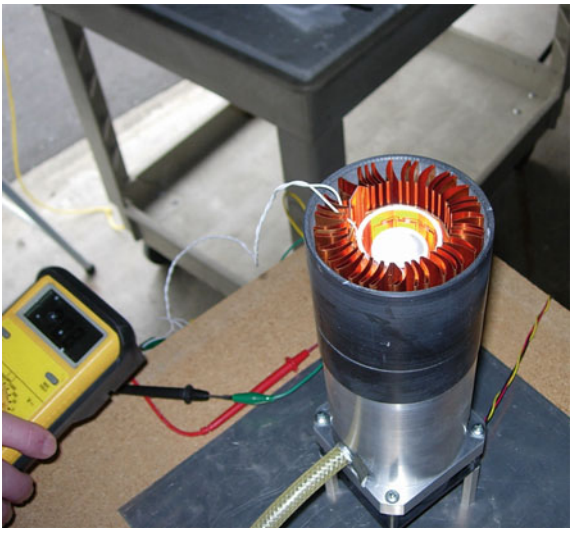


Fig. 11.18 *Early test* Pt screen emitter with emittance = 0.25 at 1.5 μm. No recuperator T = 1170 C, I_{sc} = 1.23 A, V_{oc} = 8.5 V, P_{max} = 7.6 W

In Eq. (11.1), it was noted that a target spectral efficiency for the IR emitter of 60 % would allow an overall TPV efficiency of 10 % to be achieved. It has been shown that Ni or Co ions in an oxide matrix emit radiation in the 1 to 1.8 micron wavelength range [8, 9]. Appropriate IR emitter post for this invention consists of these ions incorporated as impurities in oxide ceramics such as alumina (Al_2O_3, including sapphire), magnesia (MgO), or Spinel ($MgAl_2O_4$), Ferguson and Dogan [9] have fabricated NiO doped magnesia ribbons for use in TPV generators and measured their spectral emissivity as was already shown in Fig. 11.3.

This Ni ion spectral selectivity is explained in terms of ligand field theory and interactions between dopant ions and coordinating host atoms [9]. From the emittance data presented in Fig. 11.3, the spectral efficiency can be calculated as shown in Table 11.1. The radiance numbers presented in this table assume an emitter temperature of 1,500 K surrounded by a fused silica window shield at 1,000 K. These temperatures are consistent with the values calculated in an overall cylindrical TPV generator computational fluid dynamics (CFD) model previously published [8]. The resultant spectral efficiency is found to be 61 % consistent with the target value.

The detailed CFD study modeling the performance of the cylindrical TPV generator shown in Fig. 11.9, the omega recuperator shown in Figs. 11.14 and 11.15, and the picket fence emitter geometry shown in Figs. 11.16 and 11.17 have been performed [12]. Here, the results of these portable cylindrical TPV generator CFD simulations are simply summarized. Given a fuel burn rate of 225 W, the model predicts a cell array electrical output of 26.6 W for a gross TPV efficiency of 11.8 %. Subtracting the 2 W for the combustion and cooling air fans gives a net TPV system efficiency of 24.6/225 = 10.9 %.

JX Crystals Inc. now has a US government contract to build a prototype cylindrical TPV generator according to this design. Figure 11.18 shows an early test configuration with a burner and GaSb cell array and a platinum screen IR emitter. Work is now beginning on fabricating a recuperator and a matched emitter array. The power measured in Fig. 11.18 of 7.6 W is expected to increase with an increase in emittance (e.g. 7.6 × 0.9/0.25 = 27.4 W).

In the future, one might imagine a scale-up design of this TPV cylinder to 50 W with two of these 50 W units on the wings of a UAV as shown in Fig. 11.19.

Industrial Applications for TPV

Diffused junction Gallium Antimonide (GaSb) infrared (IR) cells are ideal for thermophotovoltaic (TPV) industrial combined heat and power (CHP) applications (Item [5] in Fig. 11.4). However, an economically attractive application is required for high volume cell production in order to reduce their cost. The steel industry represents an attractive potential high volume market for TPV. A typical steel mill produces 10 million Metric-Tons (MT) of steel a year. A typical billet has a square cross-section of 16 × 16 cm and a length of 5.6 m and weighs 1 MT. This equates

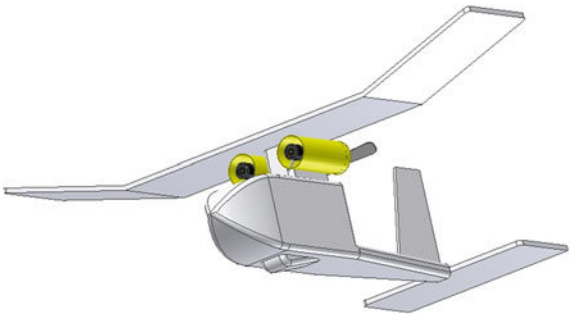


Fig. 11.19 Two JXC lightweight fuel-fired cylindrical TPV generators quietly powering a UAV

to 1,250 billets in process every hour. If TPV converter circuit arrays are placed along the two 16 cm × 5.6 m faces adjacent to each of these billets, the area of these TPV arrays would be 1,250 × 0.16 × 2 × 5.6 = 2,240 m^2. GaSb cells adjacent to a hot steel billet at 1500 K (1227 C) can potentially convert 30 % of the IR radiant energy into electricity with an electric power density of 1.8 W/cm^2 or 18 kW/m^2. At this power density, a typical steel mill could cogenerate 18 × 2,240 kW = 40 MW. A TPV power circuit design for cogeneration of electricity in a steel mill is described here. Thermal management of the heat load on these TPV circuits via IR spectral control is an important element of this design.

In a recent visit to a steel mill in Xuan Gong China, we were told that they have 2,000 m^2 of glowing steel at temperatures above 1,127 C in process 24 h/day and 7 days a week. See Fig. 11.20. A black body at 1,400 K (1,127 C) emits 3.4 W/cm^2 of infrared (IR) radiant energy at wavelengths equal or less than 1.8 microns and the JX Crystals Inc GaSb infrared sensitive thermophotovoltaic cells [1, 2] can convert 30 % of this radiant energy into electric power. This means that at least 1 W/cm^2 of electric power could be generated from the now wasted radiant energy in a steel mill. At 1 W/cm^2, this means that it is potentially possible to generate over 20 MW of electricity with TPV at this steel mill.

One can now extrapolate to worldwide TPV electric power production potential from the steel industry. In 2012, the world steel production was 1,553 million MT [13]. So, the worldwide potential for electricity production could be 6 GW. In theory, one could double this number by utilizing all four facets from the billet. Furthermore, if one notes that each billet of steel gets heated to melting twice during production, once for casting and a second time for shaping, the potential TPV electric power production could then approach 10 GW.

One might ask, at what cost will TPV be affordable? The fact that this potential TPV electric power facility would operate for 24 h/day is a distinct advantage over solar PV where the sun is only available on average for 8 h/day. One can estimate the potential value of a TPV plant from the potential annual revenues. Assuming the value of electricity to be 8 cents per kWh and noting that there are 365 C × 24 = 8760 h/year, 1 kW of TPV electric power capacity will produce 8765 × 0.08 = $700 dollars per year. If one asks for a 3 year payback, the TPV power plant might be worth $2100/kW or $2.1 per W. Figure 11.21 shows an



Fig. 11.20 **a** and **b** show photos of steel billets just after continuous casting

estimate of the cost of GaSb TPV circuits [14]. As is shown, the costs are a function of volume but will come down to affordable levels at volumes above 1 MW.

The challenge then is to design a TPV converter compatible with the steel making process. It should operate with steel at temperatures above about 1,000 C. Thermal management for cooling the TPV cells will be important and spectral management to achieve respectable conversion efficiencies will be important. Durability will also be important and it will be necessary to design to avoid contamination of the TPV cells and optical elements from deposits of iron oxide and other volatile elements.

To meet these design criteria, a planar TPV module is described here [15]. The design is shown in Figs. 11.22, 11.23. In Fig. 11.23, the modules sit adjacent to the hot surface of a hot steel plate or billet.

As shown in Fig. 11.22, each TPV module consist of a SiC ceramic plate heated by radiation from the hot steel to about 1,100 C or higher. This SiC plate serves as a BB IR emitter and it also serves to protect the TPV converter assembly from iron oxide deposits. On the side opposite to the hot steel, parallel with this SiC plate, a fused silica multi-pane window is placed as both a convection and radiation shield. Adjacent to this window in parallel and again on the opposite side from the hot steel and facing the SiC IR emitter, a TPV cell and circuit assembly is placed to receive IR radiation from the SiC emitter and convert a fraction of that radiant energy into electricity. The TPV cells in this circuit assembly are wired in series and mounted on an electrically insulating voltage stand off plate. This circuit is a shingle circuit as shown in Fig. 11.24. A TPV shingle circuit similar in size was shown in the previous chapter. The edge cells in this circuit assembly are larger than the center cells to compensate for radiant intensity falloff at the circuit edges. A glass plate is bonded to the radiation side of this cell assembly and a multilayer alternating high and low refractive index filter [11] is applied to the top surface of this glass plate. Air flows above this filter plate to cool this optical filter and this cell assembly is mounted on a water cooled plate to cool the cell circuit.

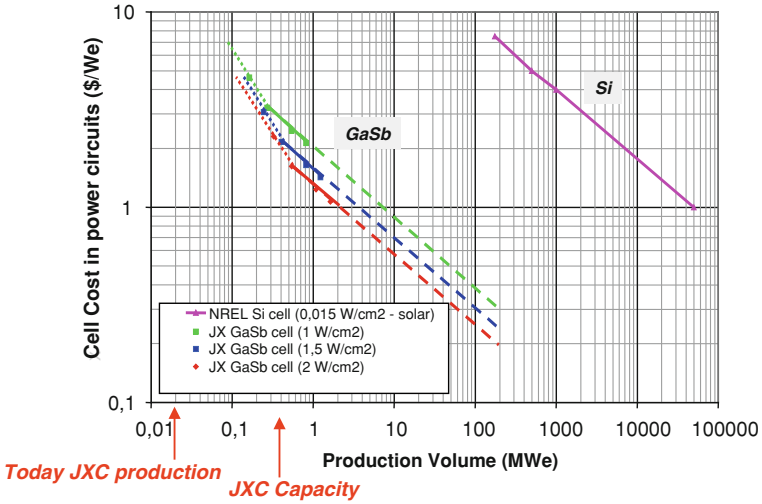
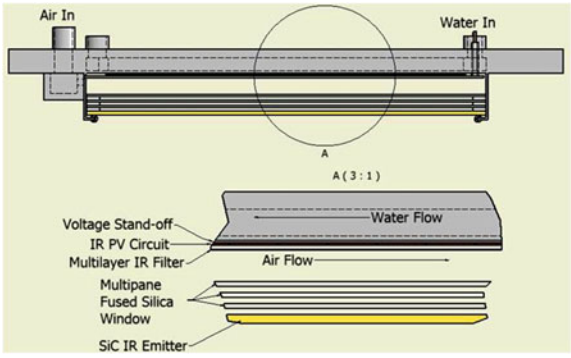


Fig. 11.21 By analogy with Si solar, the achievable GaSb Cell cost versus cumulative production volume is shown here

Fig. 11.22 Cross section of TPV planar module



From the visit to the Xuan Gong steel mill, the planar TPV module has been designed to fit with the 16 cm square billets shown in Fig. 11.20a, b. This design is merely exemplary. Specifically, the SiC and fused silica windows in Figs. 11.22, 11.23 are 18 cm square. The TPV circuit is 16 cm square and contains $10 \times 14 = 140$ GaSb TPV cells. Each cell should generate a voltage at maximum power of approximately 0.33 V. Therefore, the maximum power voltage of this circuit should be approximately 46 V. The active area of each cell is approximately 1.8 cm^2. The current and power generated by this circuit will depend on the SiC IR emitter temperature as shown in Table 11.3.

The spectral control in this design is important and also summarized in Table 11.3. It is important to suppress the non-useful IR radiation at wavelengths longer than the IR PV cell bandgap wavelength, λg. This is important both for

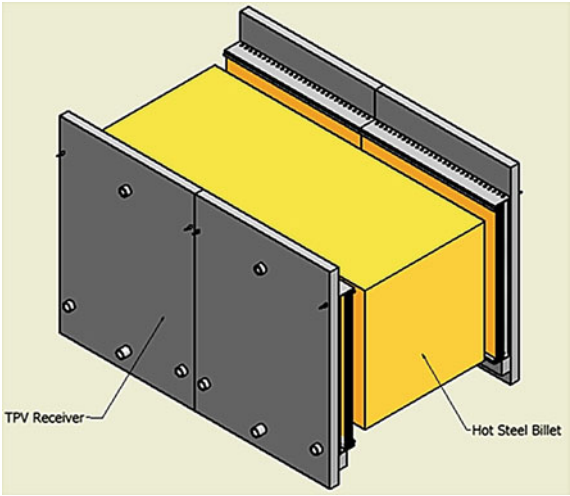


Fig. 11.23 Four planar TPV modules arrayed on both sides of glowing steel billet

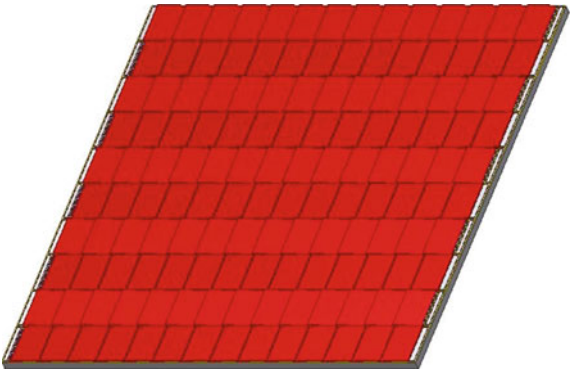


Fig. 11.24 16 × 16 cm TPV shingle circuit produces. Approximately 350 W (depending on IR emitter temperature)

conversion efficiency and for managing the cell cooling heat load. In the present embodiment, the IR PV cells are GaSb cells and the bandgap energy is 0.72 eV and corresponding bandgap wavelength, λg, is approximately 1.8 microns. However, it is possible to use alternative TPV cells which would also fall within this concept. Alternate cells might include InGaAs/InP, InGaAsSb, or Ge cells. Any cell with a bandgap between 0.75 and 0.55 eV can potentially be used with λg ranging between 1.5 microns and 2.5 microns. Table 11.3 presents efficiency and heat load calculations for the GaSb cell case and for exemplary IR emitter temperatures of 1,127 and 1,227 C corresponding to 1,400 and 1,500 K, respectively.

Note that the multi-pane fused silica window with N fused silica sheets will suppress the IR emitted radiation in the wavelength band beyond 4 microns by $E = E(SiC)/(N + 1)$. If $N = 3$, then the radiant energy from the SiC IR emitter will fall to one-quarter of its initial value. See Fig. 11.25. For example, at 1,400 K from Table 11.3, the thermal energy heat load beyond 4 microns drops from

Table 11.3 Projected TPV planar module performance

Temperature (°K)	Wavelength band (μm)	Blackbody energy (W/cm^2)	Filtered energy (W/cm^2)	Cell electric power (W/cm^2)
1,500	4–12	6.8	1.7	
	1.8–4	15.4	1.5	
	0.4–1.8	5.9		1.8 (20 % Efficiency)
1,400	4–12	5.9	1.5	
	1.8–4	11.5	1.2	
	0.4–1.8	3.4		1.1 (18 % Efficiency)

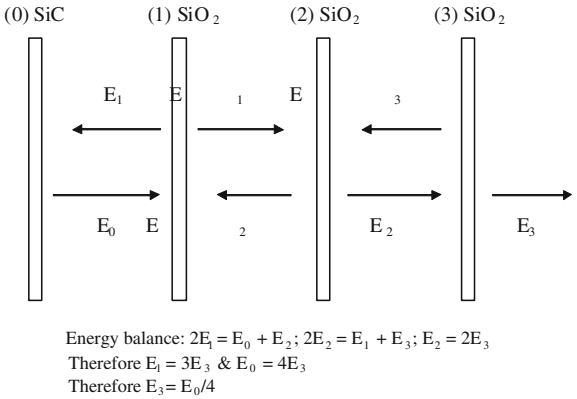


Fig. 11.25 Fused silica absorbs IR at wavelengths longer than 4 microns and then reemits half in each direction. Therefore, a 3-pane window reduces the emitted BB IR energy (E_0) beyond 4 microns to one-quarter as shown

5.9–1.5 W/cm^2. The high/low index filter efficiency is assumed to drop the radiant energy heat load in the 1.8–4 micron band at 1,400 K down from 11.5–1.2 W/cm^2. The cell efficiency for the 0.4–1.8 conversion band is assumed to be 30 %. So the electric power produced at 1,400 K will be 1.1 W/cm^2 and the worst case heat load will be $1.5 + 1.2 + 3.4 = 6.1$ W/cm^2. The worst case TPV conversion efficiency at 1,400 K would then be $1.1/6.1 = 18$ %. At 1,500 K, the electric power density, worst case heat load, and efficiency numbers all increase to 1.8, 9.1 W/cm^2, and 20 % respectively. Referring to the TPV modules in Fig. 11.24, the power output for each should be between 215 and 350 W depending on the SiC emitter temperature. There is a patent pending on this design [15].

The calculations just described in Table 11.3 assume high radiation energy view factors, F_{12}, between the multilayer dielectric filter and the IR emitter. Figure 11.26 shows the calculation of this view factor as a function of the ratio of the emitter width, W and the spacing, H between the dielectric filter 60 and the IR emitter. From Fig. 11.26, if W/H is larger than 8, the view factor will be ≥80 % [16]. A high view factor (VF) is important for high spectral efficiency. In the design discussed here, $W = 16$ and $H = 2$. This ratio is important to minimize edge losses. Another advantage for the steel application is the large TPV circuit size which then allows for a large VF.

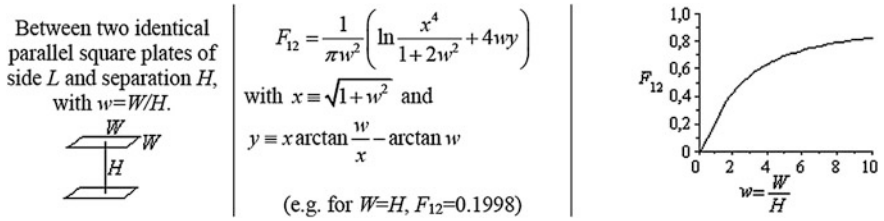


Fig. 11.26 A high view factor is also an attractive feature for the TPV steel application [16]

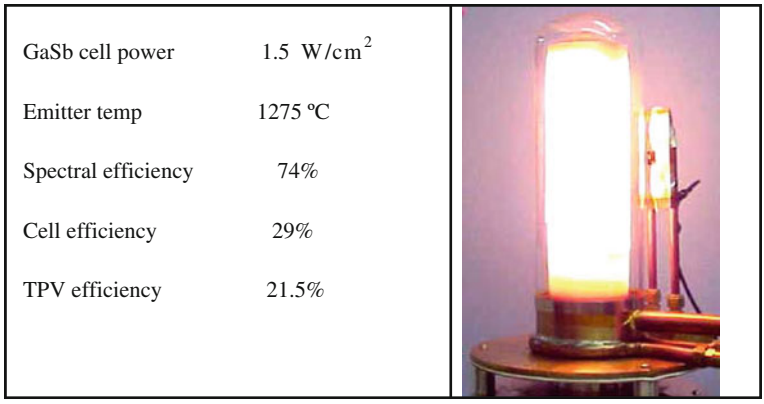


Fig. 11.27 Single cell test

Applying TPV for waste heat conversion into electricity in the steel industry is an exciting opportunity. Furthermore, since half of the world's steel is now made in China with coal as the heat source [13], TPV could reduce the amount of coal burned and reduce pollution while simultaneously cogenerating electricity economically.

Single Cell Demonstration

Figure 11.27 shows test results for a water cooled single GaSb cell adjacent to a glowing radiant tube burner operating at a temperature of 1,275 °C [3]. The cell produces 1.5 W/cm^2.

Conclusions

There are now multiple possible TPV applications. These applications are dividing into military and potential commercial and industrial CHP applications. For the military, cost is not an important criterion but weight and energy density are advantages for TPV.

The GaSb diffused junction cell and the picket fence IR emitter operating in air are potentially inexpensive enabling solutions for commercial TPV applications.

TPV for combined heat and electric power offers a path for using natural gas in distributed residential and commercial systems with over 90 % CHP energy conversion efficiency. In the recent hurricane Sandy power outages on the US east coast, it would have been more desirable to generate heat and electricity indoors with TPV CHP using natural gas than to generate just electricity with outdoor internal combustion generators burning gasoline. Furthermore, many of the east coast residents would have found the additional heat quite comforting in the snowstorm that followed hurricane Sandy.

However, volume production is still required for TPV to bring the costs down. Using TPV in a steel mill is an exciting opportunity to both reduce coal burning and pollution and to launch TPV and pull the component costs down through volume production.

References

1. L.M. Fraas, GR Girard, JE Avery, BA Arau, V.S. Sundaram, A.G. Thompson, J.M. Gee, J. Appl. Phys. 66, 3866 (1989)
2. L.M. Fraas et al, *Fundamental Characterization Studies of GaSb Solar Cells.* Proceedings of 22nd IEEE PVSC, pp. 80–84 (1991)
3. L.M. Fraas, *TPV History from 1990 to Present and Future Trends*, Proceedings of TPV7 AIP, vol 890, pp. 17–23 (2007)
4. H.H. Kohm, Quarterly Progress Report, Solid State Research, Group 35, MIT-Lincoln Laboratory, Lexington, MA, May 1, p. 13 (1956)
5. J. Werth, in *Proceedings of 3rd PV Specialist Conference Vol. II*, A-6-1 (1963)
6. G.E. Guazzoni, Appl. Spectrosc. **26**, 60 (1972)
7. D.L. Chubb, *Fundamentals of Thermophotovoltaic Energy Conversion, Chapter 3* (Elsevier, Boston, 2007)
8. L. Ferguson, L. Fraas, in *Proceedings of 3rd TPV Conference, AIP 401*, p. 169 (1997)
9. L. Ferguson, F. Dogan, Mater. Sci. Eng. **B83**, 35 (2001)
10. L.M. Fraas, R Ballantyne, S Hui, S.Z Ye et al., in *Proceedings of 4th TPV Conference, AIP 460*, p. 480 (1999)
11. L.M. Fraas et al, Spectral control for thermophotovoltaic generators, US Patent 5,403,405 (1995)
12. L. Fraas, J. Avery, H. Huang, L. Minkin, in *Proceedings of 37th Photovoltaic Specialists Conference 2050* (2011)
13. http://en.wikipedia.org/wiki/List_of_countries_by_steel_production
14. L. Fraas et al., in *Proceedings of 3rd TPV Conference, AIP 401*, pp. 33–40 (1997)
15. L.M. Fraas, Thermophotovoltaic Assembly for Electricity Production in Steel Mill (patent pending—2014)
16. http://webserver.dmt.upm.es/∼isidoro/tc3/Radiation%20View%20factors.pdf

Chapter 12
Sunbeams from Space Mirrors for Terrestrial PV

A Space Power Satellite capable of providing solar electric power economically for 24 h/day has been a dream for decades. However, the SPS concept is very complex since it assumes multiple energy conversion steps and includes specially constructed ground microwave receiver stations. The 5 km by 15 km Integrated Symmetric Concentrator SPS concept employs lightweight mirrors in a GEO orbit. Herein, it is proposed to use a constellation of 10 km diameter mirror arrays in a much lower sun synchronous orbit at an altitude of 1,000 km deflecting sunbeams down to terrestrial solar power fields at dawn and dusk. The key is that larger and larger terrestrial solar fields, photovoltaic or trough concentrated solar power, are already being built all around the world. Mirrors deflecting sunbeams down to earth is a much simpler concept. A surprising convergence of two technologies under development is now possible, i.e., lower cost access to space and the ongoing construction of numerous larger solar power fields.

The novelty here is the idea of a constellation of mirrors in a sun-synchronous dawn–dusk orbit in combination with future multiple 5-GW solar farms distributed around the world. In this scenario, the projected payback time for the mirror constellation given the additional revenues from the multiple solar fields is approximately 2 years. The key to the attractive economics for this concept is that the mirror constellation is used continuously over a 24-h period by multiple terrestrial fields as each field comes into view at dawn or dusk. However, while this idea is very intriguing, the magnitude of its implementation is daunting. Nevertheless, the idea is intriguing enough to proceed with an initial design for the required mirror satellites.

A mirror satellite design is presented here. It builds from mirror technology for solar sails as well as technology developed for the international space station. It appears that the technology is available to implement this mirror satellite design and at least go to a detailed design and test stage. Given all of the above, there is still another non-technical difference between this dawn–dusk space mirror concept and the initial SPS concept and that difference is in perspective. The dawn–dusk space mirror concept requires a global perspective and international cooperation, whereas the SPS concept is based on a traditional national perspective. In this regard, the international space station does provide hope for future international cooperation.

L. M. Fraas, *Low-Cost Solar Electric Power*, DOI: 10.1007/978-3-319-07530-3_12,
© Springer International Publishing Switzerland 2014

Introduction

The Solar Power Satellite ("SPS") concept, a proposed method of generating solar electricity for 24 h/day in space and transmitting it to earth to solve the energy needs of the earth with a clean, zero-emissions energy source has been a dream since the 1970s [1]. The proposals to do this mostly focus on microwave transmission as the means to deliver the power to earth. Due to the fundamental physics of diffraction-limited beam spread, such transmission requires apertures and receivers that are on the scale of kilometers, and hence require exceptionally large systems in space. For example, an NASA design concept, the Integrated Symmetric Concentrator Solar Power Satellite (ISC SPS) is shown in Fig. 12.1. It is 5 × 15 km in size, and requires a ground station 8 km in diameter [2]. The size, mass, and power levels of this orbital system make the proposed SPS extremely expensive.

A concept proposed in 2012, the MiraSolar array constellation [3, 4], avoids this problem. As proposed by Ehricke [5], mirrors in orbit can be used to reflect sunlight to the earth. This solution minimizes the size and mass of the space element by placing most of the complex power generation infrastructure on the ground, and using only lightweight mirror elements in space. The concept allows the ability to "ramp up" power by using a ground infrastructure that is already being built. The concept is to put a large mirror array in low earth orbit (LEO) at 1,000 km, rather than the geosynchronous orbit proposed for earlier concepts, allowing a smaller and far simpler configuration. The multiple energy conversion steps in space are eliminated. The ground stations are conventional solar fields (PV or trough CSP) already being built (See SEGS CSP in Chap.7). Thus, rather than competing with ground solar technologies, this concept is synergistic: it works with solar ground stations, not against them, and hence it can leverage a billion-plus dollar ground technology infrastructure that is already being developed.

Furthermore, while conventional concepts for SPS would require array assembly in space, the mirror elements proposed here are self-deploying and can be launched by today's launch vehicles.

This concept is crosscutting between NASA Space and terrestrial alternative energy developments. As shown in Fig. 12.2, this concept represents a convergence of two ongoing revolutions: the reduction in the cost of access to space, and a continuing remarkable growth in terrestrial solar electric power resulting in a potential cost savings of up to a factor of 10 relative to the ISC SPS concept [3, 4].

Mirror Array Constellation Concept

The mirror array concept places mirrors in "sun synchronous" orbit, in which orbital perturbations rotate the orbital plane by 360/365 of a degree per day, thus keeping the orbit at the same orientation to the sun, and hence passing over a given ground location at the same (solar) time each day. At an orbital altitude of

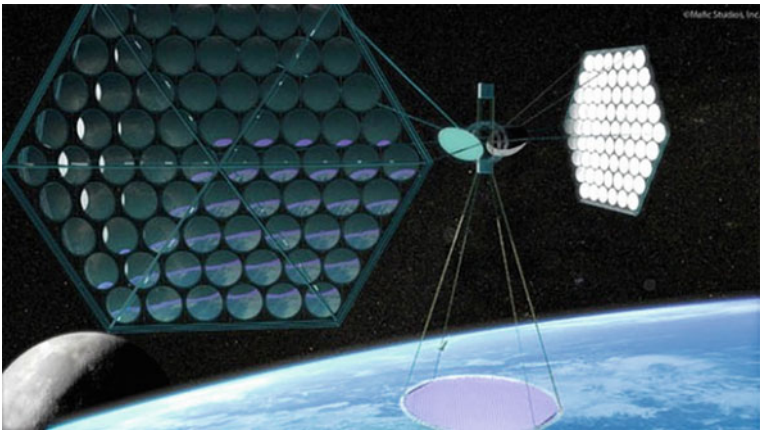


Fig. 12.1 This NASA proposed integrated symmetric concentrating Space Power Satellite uses large mirror arrays but is very complex, expensive, and in GEO [2]

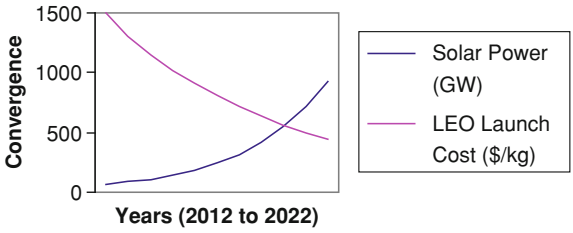


Fig. 12.2 Space and terrestrial cost convergence

1,000 km, a sun-synchronous orbit is achieved at an inclination of 99.5° (i.e., 9.5° inclined from polar) [6]. The orbital plane chosen is a "dawn–dusk" orbit, which nearly follows the earth's terminator, and thus passing overhead once in the morning and once in the evening.

A mirror satellite constellation in such a dawn–dusk orbit could harvest solar energy and reflect sunlight down to earth as shown in Figs. 12.3 and 12.4. Sunlight reflected from these mirror satellites is directed at terrestrial solar farms. In 10 years, there will be many solar farms generating electricity around the world.

This scenario has been described previously [3, 4] with an 18-mirror array satellite constellation in a dawn–dusk orbit. Because of the sun's angular diameter, the reflected spot size at the surface would be approximately 10 km in diameter [3] and the solar farm could then produce 5.5 GW of electricity. The specific scenario described assumed a constellation of 18 mirror-array satellites and 40 terrestrial solar farms generating 5.5 GW each. With these assumptions, the result was that assuming the mirror masses associated with the NASA-sponsored L'Garde solar sail (mirror), the launch cost assumed by NASA for a future Space Power Satellite, and solar electricity cost of 10 cents/kWh, the payback time for this mirror satellite

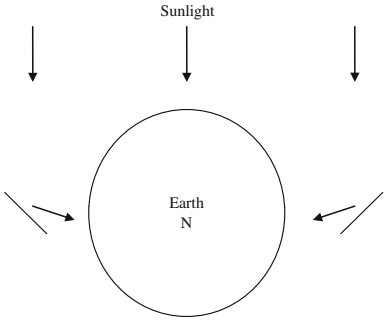


Fig. 12.3 Mirror satellites can deflect sunlight to earth

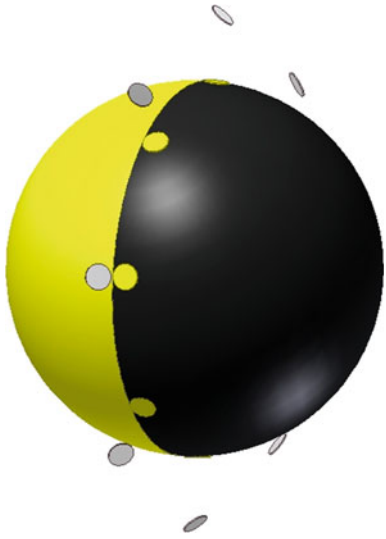


Fig. 12.4 A constellation of mirror satellites deflects sunbeams to earth solar farms to generate electricity in the evening. Here, the mirror satellites are very much exaggerated in size

constellation could be as low as 0.7 years. However, this payback time will depend on actual launch costs.

The altitude for the mirror system has not been optimized. It would most likely be chosen so that the mirror makes an integral number of orbits in a 24-h period, and thus the ground track of the orbit repeats exactly each day. Likely orbits would be either 900 km altitude, for 14 orbits per day, 1,250 km for 13 per day, or 600 km for 15 orbits per day. A 1,000-km orbital altitude, intermediate between these values, is used for representative calculations here.

Given this promising economics for an 18-mirror array satellite constellation, it was then reasoned that three 18-satellite constellations spaced in longitude as shown in Fig. 12.5 would be equally economical.

The potential impact of three longitudinally spaced planes of mirror satellites on the hours of energy production at the solar farms is shown in Fig. 12.6. As seen, at a well-chosen favorable site, the mirror satellites can add 3 h of electrical

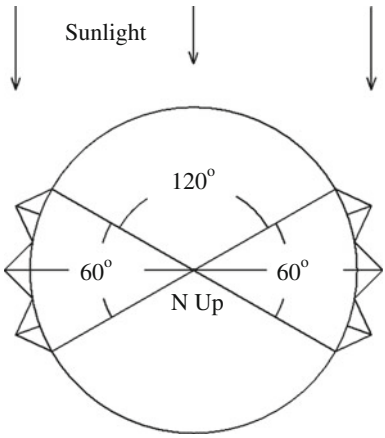


Fig. 12.5 18 mirror satellite constellations in 3 orbital planes spaced in longitude with accessible angular ranges shown

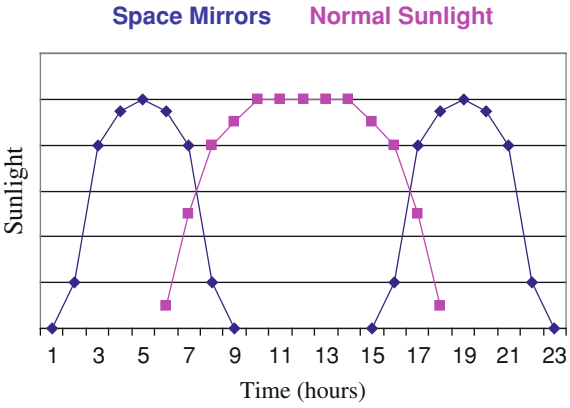


Fig. 12.6 The mirror satellite constellation can extend the hours of solar electricity production from 8 to 14 by adding 3 more hours in the morning and 3 more hours in the evening

production in the morning and 3 h in the evening, extending the solar electrical production from 8 h to 14 and thus increasing the capacity factor from 33 to 58 %.

This electrical generation profile has significant advantages over a baseline SPS design generating constant power for 24 h/day. As pointed out by Landis [7], a dawn–dusk power generation fills in ground solar generation at peak times, but does not generate power during off-peak hours centered around midnight, when very little electrical power is needed (and hence selling prices for electrical power are low).

The size of each of the mirror array satellites in this concept [3, 4] gives one pause. Even assuming ideal flatness, to produce 1-sun intensity the mirror projected area for each of the 18 (or 54) satellites in the constellation must equal the area of the 10-km diameter terrestrial solar farm. However, note that the mirror area is comparable to the size of the mirror on the proposed ISC design for a Power Satellite in GEO, 5 km by 15 km [2] and the ISC ground station would only produce 1.5 GW rather than 5 GW.

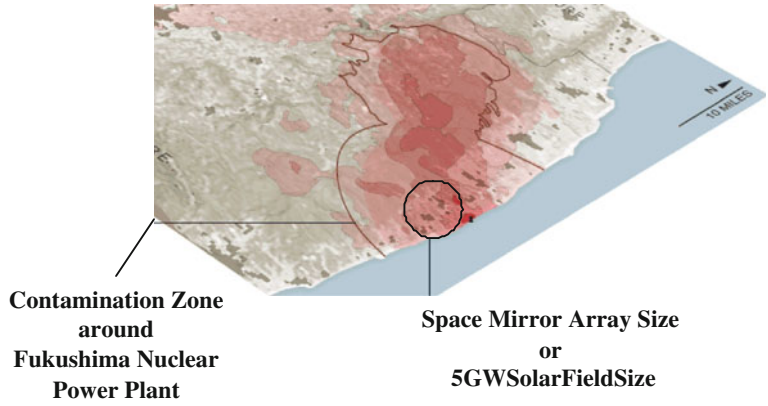


Fig. 12.7 Space mirror size relative to Fukushima nuclear contamination zone

Figure 12.5 gives some perspective on this mirror array size. Relative to the size of the earth, these mirror array satellites are really no larger than pin points. Furthermore, Fig. 12.7 gives a perspective of the size of this area relative to the size of the contamination zone around the 5-GW Fukushima nuclear power plant.

Finally, Fig. 12.8 provides still another perspective on the sunbeam from space mirror concept. Notice that the sunbeam is just directed at a solar field already dedicated to solar electric power generation.

Ground Solar Farms Around the World

The second element key for the economics for this sunbeams-from-space concept is the requirement for multiple solar farms distributed around the world. Is this a credible assumption for 10 years from now? Figure 12.9 shows the cumulative growth of solar PV from 2003 to 2012 along with a future growth projection out to 2017 [8]. In 2012, the total worldwide solar PV installed capacity reached 102 GW. Assuming a growth rate of 30 % per year, one can project $102 \times (1.3)^5 = 378$ GW by 2017 in reasonable agreement with the Fig. 12.9 projection and then $102 \times (1.3)^{10} = 1{,}400$ GW by 2022. The economic argument [3, 4] for this MiraSolar constellation assumes forty 5.5 GW ground solar power stations for a total installed capacity of 220 GW. This 220 GW power level is small compared with the projected 1,400 GW total. Figure 12.10 shows a hypothetical global distribution for these 40 ground stations. Given the same launch cost assumption made by NASA for the ISC SPS of $400 per kg, the projected mirror constellation payback time came out to be 0.7 years.

While there are many uncertainties in predicting the future, nevertheless, this concept is still very exciting. For example, if one were to assume forty 5.5 GW ground stations and a launch cost of $1,100 per kg, the payback time would change

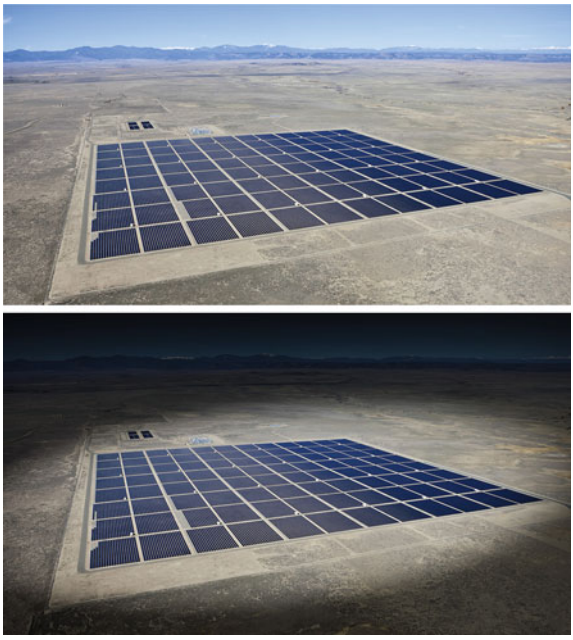


Fig. 12.8 A solar field can potentially generate power in the evening as well as during the day

to just 2 years. Alternately, with the $400 per kg launch cost and forty 2 GW ground stations, the payback time is still just 2 years.

What About Global Warming?

With mirrors in space deflecting sunbeams down to earth, is there a potential problem of global warming? The answer is no, not in the usual context of global warming. Remember that when one discusses global warming, the concern is with increased levels of CO_2 and the permanent impact of that on the earth's cooling rate. The earth's temperature is controlled by a balance between the energy input from the sun and the cooling of the earth by infrared radiation into space. Increases in the CO_2 in the atmosphere produce a green house effect, which reduces the infrared energy radiated into space for cooling. Permanent rises in CO_2 produce a permanent temperature rise. Table 12.1 summarizes the global warming effects from additional energy production versus the CO_2 green house effect.

When one produces electrical energy by using sunlight or a nuclear reaction in a nuclear power plant, the additional energy produced adds energy to the daily sunlight energy input increasing the earth's temperature very slightly. In the present case where an additional 220 GW of electrical power is produced via sunlight from space mirrors equivalent to the power from 40 nuclear power plants, the earth's temperature rise can be calculated to be 0.0018 C. However, if one

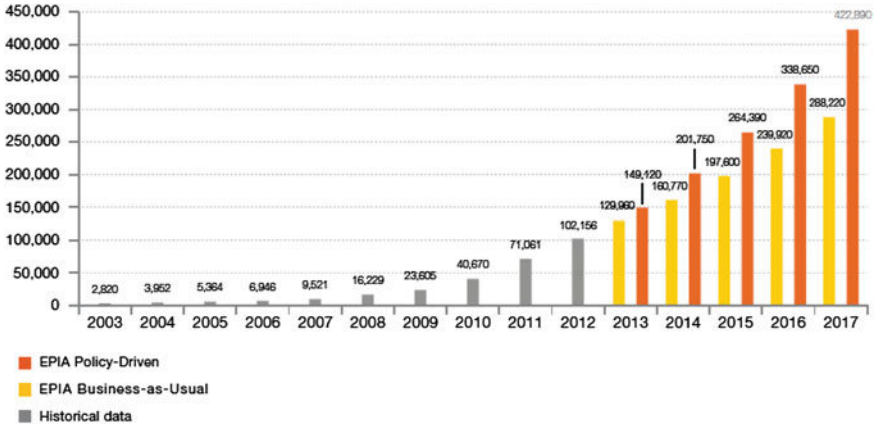


Fig. 12.9 European Photovoltaic Industry Association. Global market outlook for photovoltaics 2013–2017. Cumulative installed PV in MW [8]

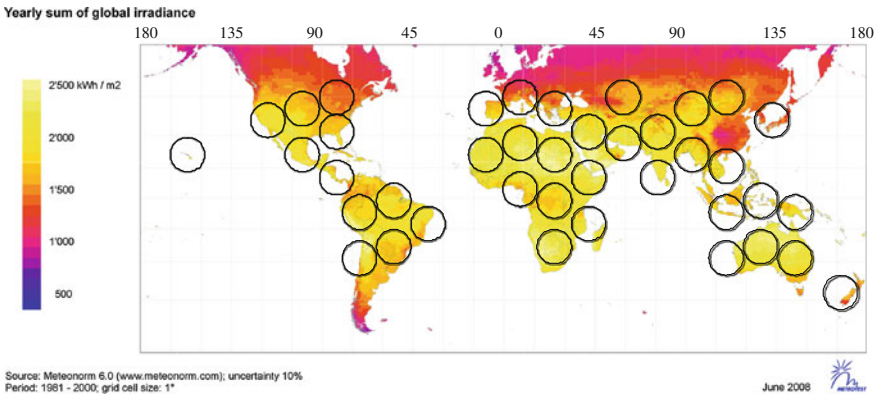


Fig. 12.10 Hypothetical 5.5 GW solar power installation global map for 2022. The *circles* note when a mirror array satellite is in range for a given solar power field. The key to the attractive economics for this concept is that the mirror constellation is used continuously over a 24-h period by multiple terrestrial fields as each field comes into view at dawn or dusk

chooses not to produce that 220 GW of electrical power by redirecting the sun beams away from the earth, the temperature rise is zero. There is no additional global warming. Meanwhile, if one chooses to produce this same amount of electrical power by burning natural gas for the next 20 years, the earth's temperature rise can be calculated to be 0.0032 C and if burning coal, the temperature rise would be 0.0057 C or 3.2 times higher. The difference is that the temperature rise from burning hydrocarbon fuels is permanent and accumulates with time. Finally, note that all of these effects associated with 220 GW of additional electric power are very small. However, in reality today, mankind consumes much more

Table 12.1 The temperature rise from burning hydrocarbon fuel is permanent

Add 220 GW new electric power	Delta T new energy (°C)	Delta T shut down no energy	Delta T from CO_2 (over first 20 yrs)
With nuclear (24 h/day)	0.002	0	0
Space mirrors (6 h/day)	0.0018	0	0
From natural Gas (24 h/day)	0.0015	0	Add 0.0032 °C Permanent[a]
From coal (24 h/day)	0.002	0	Add 0.0057 °C Permanent[a]

[a] These numbers double in second 20 years

than just 220 GW of electricity. So the effects of burning fossil fuels are much larger and the benefits of not burning fossil fuels can also be much larger (See Table 12.1 and Appendix).

Mirror Satellite Design

In a realistic system, the mirror array satellites can be composed of a larger number of smaller mirror satellites. Our thesis is that if one mirror satellite can be designed and demonstrated, then it can be replicated as needed for a constellation. What might these smaller mirror satellites look like? In a folded form, they will have to fit in the fairing of a launch vehicle, and each one will need to have attitude control that will allow the mirror sunbeam to be directed at a particular solar farm as the mirror satellite passes overhead. Figures 12.11, 12.12, 12.13 and 12.14 show a design concept.

The satellite consists of a triangular mirror with an edge dimension of 307 m. The triangular configuration was chosen because it can be supported with three booms with springs at the ends of the boom at three points then defining a plane. The springs stretch the 2.5-micron-thick mirror membranes flat. The edge dimension was chosen so that the mirror can fold up to fit in today's launch vehicles. The booms are supported by a center body containing attitude control and communication systems for the satellite.

This is a self-deploying mirror satellite design. Figures 12.12, 12.13 show the beams telescoped in and rotated 90° to fit beside the satellite body. The thin mirror membranes are folded in against the satellite body and between the beams. A fold and unfold pattern for one of the 3 mirror elements is shown in Fig. 12.14.

For deployment once in orbit as shown in Fig. 12.13, the beams rotate and telescope out and the mirror membrane unfolds and then gets stretched flat by the springs at the ends of the beams.

A significant issue for a mirror based on large-area solar-sail design using thin mirror membranes will be to design for adequate surface flatness in order to obtain the required reflected beam quality.

Being able to orient the mirror satellite so that the reflected sunlight can be directed at a given terrestrial solar farm and held in position as the satellite passes

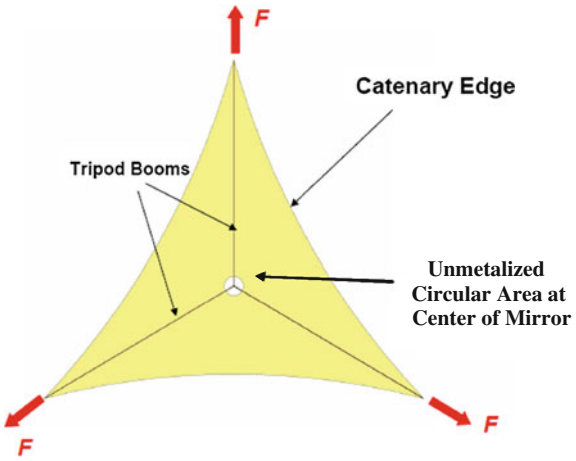


Fig. 12.11 Example deployable thin-film mirror satellite with edge dimension 307 m

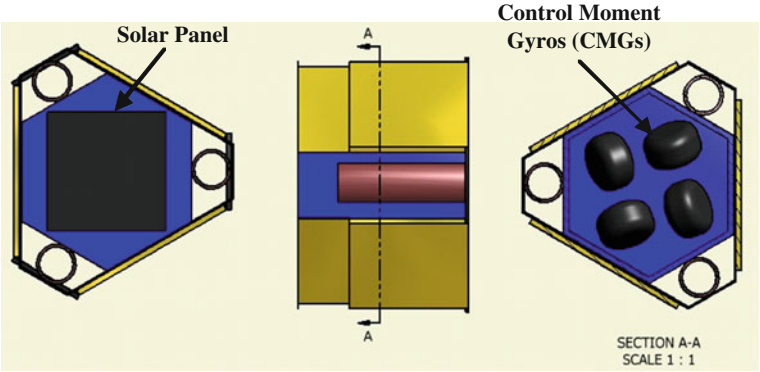


Fig. 12.12 Mirror satellite in stowed configuration (4.6 × 3 m). *Note top* solar panel for power on *left* and CMGs in body on *right*

overhead is also a key requirement. Fortunately, the control moment gyros used on the International Space Station (ISS) have the required torque. In [4], a preliminary estimate for the mass characteristics and distribution for the mirror satellite of Fig. 12.11 was given. From this, the moment of inertia, I, for this satellite can be estimated to be 4.7×10^6 kg m^2. Given the torque, T, for the CMGs on the ISS of 258 Nm, a reasonable slew rate of 5 s/degree is calculated suggesting feasibility given a more detailed system design.

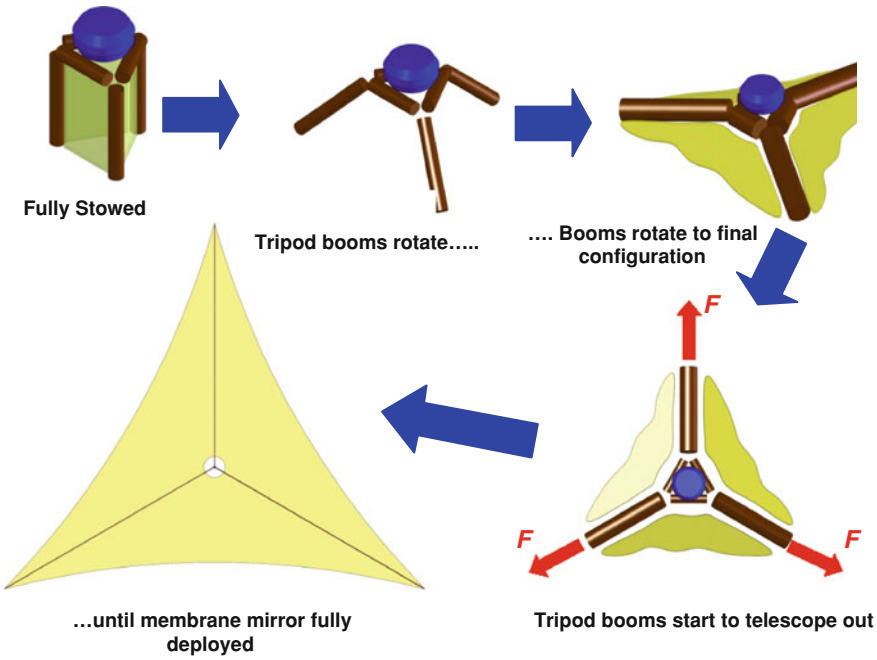


Fig. 12.13 Deployment sequence

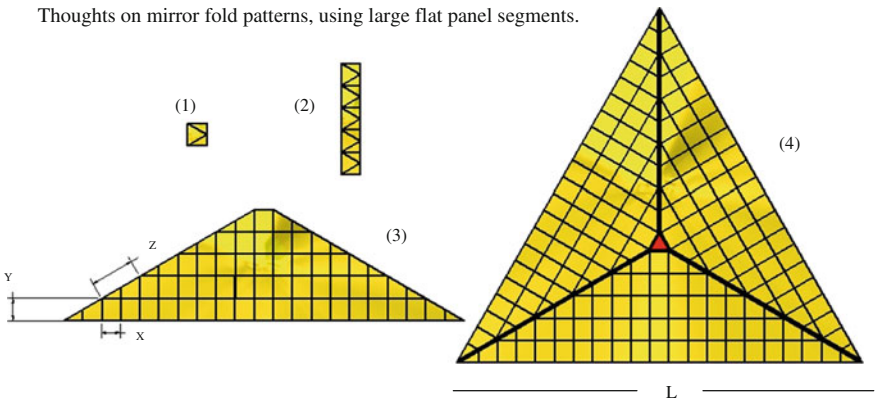


Fig. 12.14 Mirror segment pattern unfolds from *(1)* to *(2)* to *(3)*. N = # of rows (odd number), Y=2 X tan(30) = 1.16X, Z = 2X/cos(30) = 2.3 XL = (4N+1)X, A = 0.435 L^2. Example *1* A= 1200 sq m, L=53 m. Suppose X=1 m, then N = 52/4. Then N= 13. Example *2* L = 303 m, A= approx 40,000 sq m. Suppose X = 3 m, then (4N+1)3 = 303. Then N=25

Economics

From the point of view of the DOE Sun Shot program, the key question is the cost to benefit analysis. The DOE states that the current road map price for solar electricity in 2020 is $1.20 per W [9] and that the Sun Shot goal is 6.1 cents/kWh. However, an NREL bottom-up analysis states that the achievable price with evolutionary developments will be $1.71 per W [9]. This translates to 8 cents/kWh, short of the goal.

However, the DOE goal is achievable given imagination and the revolutionary space mirror concept described here. Assuming ±60° 1-axis EW tracking ground stations, then Fig. 12.5 shows 8 kWh/m^2 per day of natural sunlight and 6 kWh/m^2 per day of mirror-deflected sunlight. Now assuming good sunny sites and assuming occasional clouds, the numbers might change to 7 and 5. Mirrors then provide 12/7 = 1.71 times more energy. The next question is cost. The 220 GW of ground sites will cost 220 × $1.71 B = $376 B and assuming the first 18 satellites cost $32 B given $1,100 per kg but that the next 36 will cost 2 × $11 B because launch costs will be reduced. Then the cost penalty with added mirrors will be (376 + 54)/376 = 1.15. Now accounting for more energy but at additional cost, the net advantage is 1.5. Energy costs are then reduced to 8/1.5 = 5.3 cents/kWh. This is exciting! Also, don't forget that solar energy is now available in the evening which might be even more exciting.

Mirror Constellation Development Roadmap

In [3, 4], an 18 MiraSolar array constellation in a dawn–dusk orbit was compared with the ISC SPS [2] from both a project cost and energy production perspective. The result is shown in Table 12.2. As can be seen, assuming the same mass launch cost of $400 per kg from the NASA study [2], the deployment costs are similar but the MiraSolar can produce 18.3 GW versus 1.5 GW on a 24-h equivalent basis thanks to the assumed existence of the PV ground stations. This represents an 18.3/1.2 = 15 times cost reduction and a cost for the mirrors of only $0.6 B/GW, a potentially very economical proposition.

While this represents a major step forward, there still remain many challenges. There is still the challenge of a reduced launch cost relative to today's costs and there is the enormity of this project. Fortunately, these two problems are related through the cost reduction associated with economies of scale as suggested by Mankins [10] in Fig. 12.15.

Initially, this project will start with the development of just one mirror satellite of the type shown in Fig. 12.11. Then as is pointed out in [4], a constellation of just 18 mirror satellites providing illumination at a level comparable to the full moon could be economical for replacing street lights in the evening in city downtown areas. These projects can be handled with today's launch vehicles. But

Table 12.2 Space power system comparisons

Parameter	MiraSolar	ISC SPS
Orbit	1,000 km	36,000 km
# Satellites	18	1
Mirror area per sat	78 km^2	12.8 km^2
Total mirror area	1,404 km^2	12.8 km^2
24 h/day earth power (W[a])	220 × 2/24 = 18.3 GW[a]	1.2 GW
Cost ($400 per kg)	$11 B	$14 B
$ per 24 h GW	$0.6 B/GW[a]	$11.7 B/GW
Earth station size	5.5 GW	1.2 GW

[a] See footnote of Table 12.4

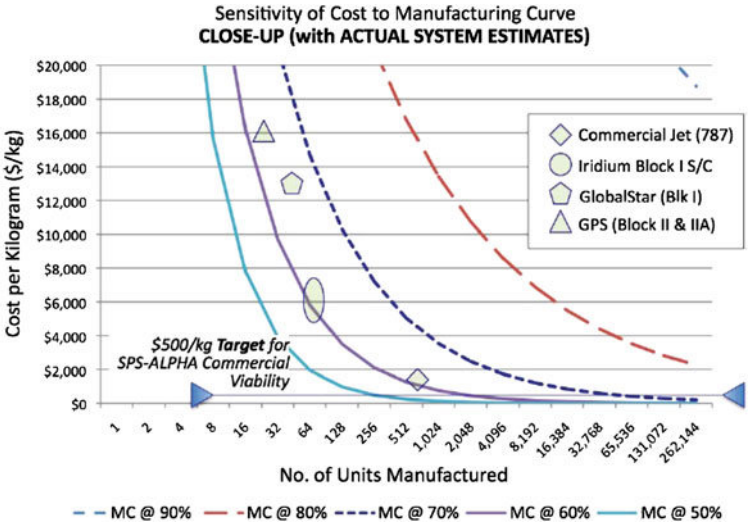


Fig. 12.15 Placement of selected aerospace examples in the context of generic learning curves [10]

then, this project will progress to the solar electric power constellation as shown in the roadmap in Table 12.3.

For the economic analysis of the project for solar electric production, the key question is: how many mirrors satellites are required and what are the launch vehicle and potential launch schedule? The 18 MiraSolar arrays would have 40 × 40 = 1,600 mirror satellites (300 m on edge, with area equivalent to 250 m diameter). This means 28,800 for the first 18 array constellation. Fortunately, large capacity launch systems are now being proposed. For example, in the NASA Space Launch System (SLS) now being worked on, each Super Heavy Lift Vehicle can carry 70 MT into orbit [11]. If each Mirror Sat weighs 1.2 MT, the first 18 MiraSolar constellation will require 28,800 × 1.2/70 = 494 launches given a launch vehicle carrying 70 MT. The first SLS test launch is scheduled in 2017.

Table 12.3 Development road map

Steps	Cost estimate
1. First mirror satellite for moonlight for 4 Disney parks	$20 Million (with R&D)
2. 18 mirror satellites for municipal street lighting	$70 Million
3. 18 mirror array constellation for ground solar farms	$32 Billion
4. 2 × 18 more mirror array constellations for solar farms	$2 × 11 Billion

Table 12.4 MiraSolar comparison with 3 Gorges Dam

Comparison	Three gorges dam	18 mirror array constellation	54 mirror array constellation
Cost	$37 B	$32 B	$54 B
Power (24 h/day)	22 GW	18 GW[a]	54 GW[a]
Electric power cost per 24 h W[a]	$1.68 per W	$1.77 per W[a]	$1 per W[a]
Land use	22 GW on 700 km^2	(5 GW on 100 km^2) × 40	(5 GW on 100 km^2) × 40

[a] Don't confuse the W here with solar peak Watts (W_p). This is corrected to 24 h equivalent

Hopefully, there will be a Super Heavy Lift Cargo Vehicle in full system operation by 2021.

Assuming the learning curves characteristic of Fig. 12.15, it is plausible to assume that a launch cost of about $1,000 per kg will occur at about 500 launches. With the 3 × 18 full orbit MiraSolar constellation giving 3 h morning and 3 h of evening power, the required launches would be about 1,500 and launch cost could drop to $500 per kg. 1,500 launches at a rate of one per day would require 1,500/365 = about 4 years, which would mean that a MiraSolar constellation could potentially be fully operational by 2025.

While the size of this project will be enormous, it is interesting to compare it with another enormous renewable energy project, the Three Gorges Dam project, now operational in China. Table 12.4 compares these two projects. Note that the MiraSolar project capital cost for electric power is lower than for the Three Gorges dam project, the land use ratio is better, and finally, from Table 12.3, the start-up costs are lower.

Conclusions

In order to appreciate the simplicity of the concept described here, one needs to compare it with the earlier Integrated Symmetric Concentrator Space Power Satellite (ICS SPS) shown in Fig. 12.1 and described by Feingold and Carrington [2]. That concept has 2 × 42 large mirror arrays focusing sunlight onto a center satellite body where there are solar cell arrays that receive the sunlight and convert it

into electricity and then into a microwave beam. Then the SPS sends energy to a special earth ground station to be converted into electricity. This ICS SPS concept is 5 × 15 km in size and the ground station is 8 km in diameter and this satellite is in GEO 36,000 km above the earth.

By comparison, the concept described here also consists of a large mirror array but the array is in LEO at 1,000-km altitude, and the multiple energy conversion steps in space are eliminated and the ground stations are conventional solar cell fields already being built.

Furthermore, while the array proposed for the conventional SPS concept requires assembly in space, mirror elements that are self-deploying and can be launched by today's launch vehicles have been described here.

The NASA Mars rover curiosity project was a spectacular success. However, it costs $2.5 billion. This chapter has outlined a more down-to-earth NASA development project that would also be revolutionary and could contribute to solving the future world's energy needs.

References

1. P.E. Glaser, Power from the Sun: its future. Science **162** (3856), 857–861 (1968)
2. H. Feingold and C. Carrington, Evaluation and comparison of space solar power concepts, 53rd IAF Congress. Acta Astronautica **53** (4–10), 547–559 (2003)
3. L.M. Fraas, Mirrors in space for low cost terrestrial solar electric power at night, *38th IEEE Photovoltaic Specialists Conference (PVSC), 2012*, 3–8 June 2012
4. L. Fraas, A. Palisoc, B. Derbes, Mirrors in dawn dusk orbit for low cost solar electric power in the evening, *AIAA paper 2013-1191, 51st Aerospace Sciences Meeting, TX*, 10 Jan 2013
5. K.A. Ehricke, Space light: space industrial enhancement of the solar option. Acta Astronaut. **6**(12), 1515–1633 (1979)
6. V.A. Chobotov, Sun synchronous orbits, in *Orbital Mechanics*, 2nd edn. (AIAA, New York, 1996), p. 218
7. G.A. Landis, Reinventing the solar power satellite, *NASA Tech Memo TM-2004-212743* (2004)
8. Global Market Outlook for Photovoltaics 2013–2017, European Photovoltaic Industry Association http://www.epia.org/fileadmin/user_upload/Publications/GMO_2013_-_Final_PDF.pdf
9. A. Goodrich, T. James, M. Woodhouse, Residential, commercial, and utility-scale photovoltaic (PV) system prices in the United States: current drivers and cost-reduction opportunities, Technical Report NREL/TP-6A20-53347, Feb 2012
10. J.C. Mankins, 2011–2012 NASA NIAC Project Report. SPS-ALPHA: the first practical solar power satellite via arbitrarily large phased array, 15 Sept 2012
11. NASA Space Launch System, www.nasa.gov/sls/ Accessed 1 June 2013

Appendix
Calculations Related to Table 12.1 and Global Warming

Assume forty 10 km diameter ground sites being illuminated 6 h per day. This ground area is 40×78 km^2 = 3,120 km^2. Assume that the mirrors are pointed away from the earth unless being directed at these ground sites. So the energy collected by the mirrors beamed down to earth is 1.37 kW $\times$ $3.12 \times 10^9 \times 6$ h/day.

The above can be compared with the solar energy arriving on the earth in a day which is 1.37 kW $(6.4 \times 10^6)^2 \times 3.14$ m^2 $\times$ 24 h/day = 1.37 kW $\times$ $128 \times 10^{12} \times 24$ h/day.

The ratio of these two energies is $3.12 \times 6 \times 10^9/128 \times 24 \times 10^{12} = 0.006 \times 10^{-3}$ or 6 ppm. Relative to the earth's T of 300 K, this would be a T rise of $1.8 \times 10^{-3} = 0.0018$ °C.

Next, let's explore the alternative of generating 220 GW of energy for 14 h per day with natural gas for a period of 20 years. From the Table A.1, NG will generate $1.2 \times 10^5 \times 453$ g per 10^6 BTU. Assume 50 % efficiency from heat to electricity and 1 BTU = 3×10^{-4} kWh, then $2 \times 1.2 \times 453 \times 10^5$ g/300 kWh = 109 g/300 kWh = 1.1 g/3 kWh = 0.35 g/kWh

How much CO_2 will be generated by a 220 GW 14 h per day plant in 20 years? $220 \times 14 \times 365 \times 20$ GWh = 2.25×10^7 GWh = 2.25×10^{13} kWh. CO_2 displaced is then $2.25 \times 0.35 \times 10^{13}$ g = 8×10^{12} g = 8 Tg.

From Figs. A.1, A.2, one can see that 10,000 Tg of CO_2 has led to about 0.4 °C of global warming. So, the displaced CO_2 from burning natural gas would reduce global warming by $8 \times 0.4/1000$ C = 0.0032 C. If instead, coal is burned, the CO_2 rise would be 0.0057 C.

Both effects are very small but there is a net benefit for space mirrors of a factor of 3.2 compared to coal burning. Finally, note that the space mirror effect is a single event whereas the CO_2 effect is permanent and cumulative.

L. M. Fraas, *Low-Cost Solar Electric Power*, DOI: 10.1007/978-3-319-07530-3,

© Springer International Publishing Switzerland 2014

Table A.1 Fossil fuel emission levels—pounds per billion BTU of energy input

Pollutant	Natural gas	Oil	Coal
Carbon dioxide	117,000	164,000	208,000
Carbon monoxide	40	33	208
Nitrogen oxides	92	448	457
Sulfur dioxide	1	1,122	2,591
Particulates	7	84	2,744
Mercury	0.000	0.007	0.016

Source EIA Natural gas issues and trends 1998

Trends in Global Emissions

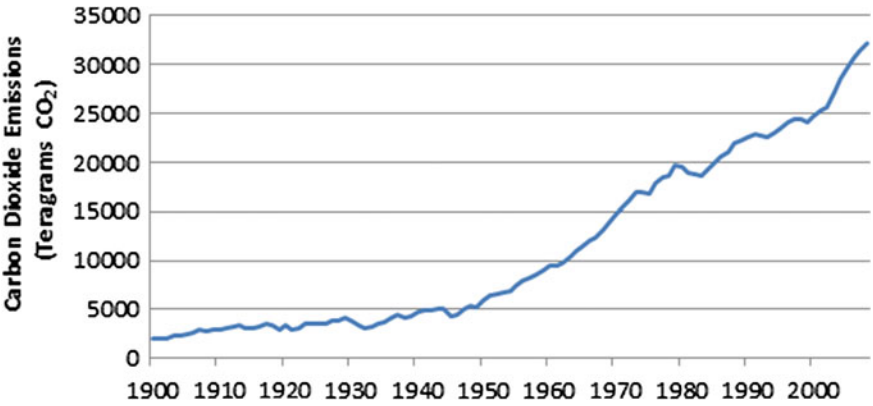


Fig. A.1 Global carbon dioxide (CO_2) emissions from fossil fuels 1900–2008

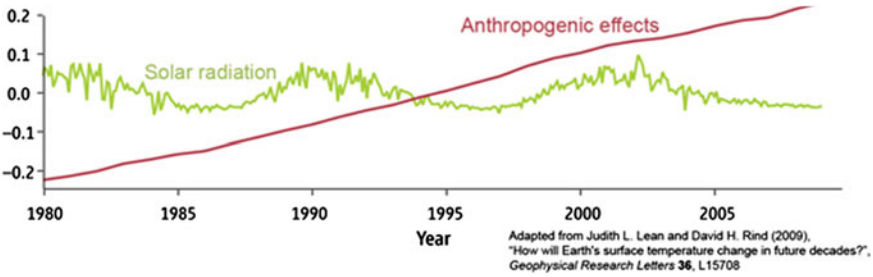


Fig. A.2 Temperature rise in °C

Author Biography



Dr. Fraas has been active in the development of Solar Cells and Solar Electric Power Systems for space and terrestrial applications since 1975. He led the research team at Boeing that demonstrated the first GaAs/GaSb tandem concentrator solar cell in 1989 with a world record energy conversion efficiency of 35 %. He received awards from Boeing and NASA for this work. He has over 30 years of experience at Hughes Research Labs, Chevron Research Co, and the Boeing High Technology Center working with advanced semiconductor devices.

Dr. Fraas joined JX Crystals in 1993, where he has led the development of advanced solar cells and concentrated sunlight systems. At JX Crystals, he pioneered the development of various thermophotovoltaic (TPV) systems based on the new GaSb infrared sensitive PV cell. In 1978 while at Hughes Research Labs, he published a pioneering paper proposing the InGaP/GaInAs/Ge triple junction solar cell predicting a cell terrestrial conversion efficiency of 40 % at 300 suns concentration. This 40 % efficiency has now been achieved and this cell is the predominant cell today for space satellites. It is now entering high volume production for terrestrial Concentrated Photovoltaic (CPV) systems.

Dr Fraas holds degrees from Caltech (B.Sc. Physics), Harvard (M. A. Applied Physics), and USC (Ph.D. EE). At Caltech, he studied Physics with Prof. Richard P. Feynman. Dr. Fraas has written over 350 technical papers, over 60 patents, and a book entitled *Path to Affordable Solar Electric Power and The 35 % Efficient Solar Cell* (2005). He is co-editor and co-author of a Wiley book entitled *Solar Cells and Their Applications (2nd Edition)* published in 2010.

L. M. Fraas, *Low-Cost Solar Electric Power*, DOI: 10.1007/978-3-319-07530-3,

© Springer International Publishing Switzerland 2014

Index

A
1-axis trackers, 86, 94
Air Mass 1.5, 132
Alexandre Edmond Becquerel, 1, 2
AlGaAs/GaAs solar cell, 3, 4
AM0 = air mass zero or no air = space, 106
Amonix, 87, 88
Amorphous silicon (a-Si), 32, 73, 75
Amorphous silicon (a-Si) solar cell, 3, 4
Arab oil embargo, 2
Arctic Sea Ice, 16

B
Balance-of-system (BoS), 77
Bell labs silicon cell, 2
Black body IR emitter, 136, 137, 152
Boeing hi-tech center, 104

C
Cadmium telluride (CdTe), 32
California Valley Solar Ranch, 11
Carbon capture and sequestration, 15
Cassegrain PV module, 112
Chemical beam epitaxy (CBE), 101, 102
Chevron Research Co, 100, 104
Chinese bank solar subsidies, 1
CHP TPV for steel industry, 152, 157
CO_2 levels, 17
Combined heat and power (CHP), 31, 40, 141, 158
Concentrated PV (CPV), 28, 34, 40
Concentrated solar power (CSP), 120
Concentrator photovoltaics (CPV), 3–5, 9, 118
Control moment gyros, 170
Copper and copper oxide cell, 1, 2
Copper indium gallium di-sellenide (CIGS), 31, 32, 34, 35
Crystalline silicon (c-Si), 1, 6
Czochralski crystal growth, 1

D
Dawn–dusk polar orbit, 90, 92, 159, 161, 164, 170
Diode, 45, 51
Direct normal irradiance (DNI), 118

E
Eco-drive solar watch, 74
Einstein's photon theory, 1
Electric vehicle (EV), 121–123
Energy band diagram, 45
Energy gap, 47
Energy information agency (EIA), 13
Energy storage, 119, 121
ENTECH mini-module outdoor test, 106

F
First solar, 73, 74, 77
Fracking shale gas, 19
Fraunhofer Institute for Solar Energy (ISE), 87, 117
Fresnel lens, 88
Fukushima nuclear contamination zone, 164

G
GaAs/GaSb dual junction cell, 103, 105, 106, 112
GaAs/GaSb stacked Cell, 5, 105, 106, 112
GaAs/GaSb two junction cell, 39
GaAs/GaSb two junction stacked cell, 5, 6
GaSb infrared cells, 6
GaSb IR cell, 41, 134, 138

L. M. Fraas, *Low-Cost Solar Electric Power*, DOI: 10.1007/978-3-319-07530-3,

© Springer International Publishing Switzerland 2014

GaSb shingle mounted circuit, 140
Generic learning curves, 171
Geosynchronous orbit (GEO), 159, 164, 173
Global horizontal irradiance (GHI), 118
Global horizontal irradiation US map, 14
Global solar irradiance (World), 166
Global warming, 16, 18, 22, 165–167
Group III–V semiconductor, 50

H
High concentration PV (HCPV), 40
Hot steel billets, 152
Hubbert's peak, 15
Hughes Research Lab, 98, 99
Hybrid lighting, 128, 130, 132, 134

I
InfraRed PhotoVoltaics (IR PV), 133, 134
InGaP/GaAs two junction cell, 4
InGaP/GaInAs/Ge cell, 101, 107, 114
InGaP/GaInAs/Ge multi junction cell, 9, 31, 38
InGaP/GaInAs/Ge triple junction cell, 3, 4
Interdigitated back contact Si cell, 70
Intermittency, 119, 121
International space station, 32, 159, 170
IR emitter, 136, 137, 141, 144, 146, 149, 151
IR PV single circuit, 133

L
L'Garde Sunjammer solar sail, 93
LCOE roadmap, 71
Levelized cost of electricity (LCOE), 13, 25, 26, 81, 117–119
Levelized cost of energy or simply LCOE, 81
Liquid crystal color TV, 78
Liquid crystal display (LCD), 74, 76
Liquid fuels supply, 16
Liquid phase epitaxy (LPE), 101
Lithium-ion battery energy storage, 121
Low conceentration PV (LCPV), 8

M
Matched IR emitter, 141
Metal-organic chemical vapor deposition (MO-CVD), 101, 102
Midnight Sun^{TM} TPV stove, 41, 140, 141
Mirror array constellation, 160, 163, 166, 167, 173
Mirrors in space, 90, 91, 94
Molten salt energy storage, 120
Multi-crystalline silicon cell, 36
Multijunction solar cell, 53, 98

N
N/P junction solar cell, 34
NASA Glen GaSb cell calibration, 105–107
NASA space launch system (SLS), 172
National Renewable Energy Lab (NREL), 4, 5
NiO/MgO matched emitter, 141, 143

O
Oak Ridge National Lab coalition, 128

P
P/N junction diode, 51, 52
Parabolic trough concentrated solar power (CSP), 120
PASP+ module, 106
Peak oil, 15
Periodic table of the elements, 45
Photons, 45
Photovoltaic advanced space power (PASP+) flight, 5
Photovoltaics (PV), 1–7, 9
Portable TPV battery, 143, 144
Price learning curve, 33
Public Utility Regulation Act (PURPA), 4
PV module production by region, 65
PV system price, 27

Q
Quantum mechanics, 45

R
Representative carbon pathways (RCP), 18

S
3-sun low concentration modules, 86
Sanyo HIT solar cell, 77, 78
Selenium cell, 2
Semiconductor junction, 47
Silicon cell and module fabrication, 1
Single crystal semiconductors, 45
Soitech, 87, 88
Solar cell band diagram, 52
Solar cell efficiencies, 53, 56, 58, 77
Solar cell power curve, 52

Solar lighting for buildings, 128, 130, 134
Solar module efficiencies, 58
Solar powered calculator, 74
Solar sail, 159, 161
Solar Technology International (STI), 1
Solar village, 119, 121
SolarWorld, 1, 2
Solfocus, 87, 89
SOLYNDRA CIGS failure, 60
Space mirror deployment, 168–170
Space mirrors, 159, 164, 167, 170
Space power satellite, 90, 91, 161, 173
SpaceX reusable launch vehicle, 93
Spectral control, 143, 149, 152, 155
Spectrolab, 100, 107, 114
Sun power 1-axis C7 low concentration PV system, 86
Sun synchronous orbit, 90–92, 160
SunPower 1-axis T20 tracker system, 84
SunPower C7 field installation, 70
SunPower Corp, 1, 2, 4, 8, 10, 11
SunPower Oasis power block, 11

T
Telstar communication satellite, 2, 3
Terrestrial PV, 159–161, 169
Terrestrial solar field (CSP), 159, 160
Terrestrial solar field (PV), 90, 159
TetraSun, 77
Thermophotovoltaics (TPV), 31, 40, 135–138, 141, 144–147, 149, 151–153, 156–158
Thin film cells, 31
Thin film PV, 73, 74
Thin film transistor (TFT), 74
TPV battery replacement, 142
TPV generators quietly powering a UAV, 152
TPV view factor, 141, 145, 156
Tracking the sun, 81, 90
Trough concentrating solar power (CSP) system, 87
Twisted-nematic liquid crystal, 74
Two-axis tracking systems, 87
Typhoon Haiyan, 17, 18

U
Unmanned aerial vehicle (UAV), 143, 151
US Department of Energy (DOE), 13, 23

V
Vehicle to grid, 121–124

W
Wind power, 119, 123

Y
Yingli solar, 1